PB80-197569

Supercritical Fluid Regeneration of Activated Carbon for Adsorption of Pesticides

Arthur D. Little, Inc.
Cambridge, MA

Prepared for

Industrial Environmental Research Lab.
Research Triangle Park, NC

Mar 80

U.S. Department of Commerce
National Technical Information Service
NTIS

United States
Environmental Protection
Agency

Industrial Environmental Research
Laboratory
Research Triangle Park NC 27711

EPA-600/2-80-054
March 1980

PB80-197569

Research and Development

EPA

Supercritical Fluid Regeneration of Activated Carbon for Adsorption of Pesticides

REPRODUCED BY
NATIONAL TECHNICAL
INFORMATION SERVICE
U. S. DEPARTMENT OF COMMERCE
SPRINGFIELD, VA. 22161

RESEARCH REPORTING SERIES

Research reports of the Office of Research and Development, U.S. Environmental Protection Agency, have been grouped into nine series. These nine broad categories were established to facilitate further development and application of environmental technology. Elimination of traditional grouping was consciously planned to foster technology transfer and a maximum interface in related fields. The nine series are:

1. Environmental Health Effects Research
2. Environmental Protection Technology
3. Ecological Research
4. Environmental Monitoring
5. Socioeconomic Environmental Studies
6. Scientific and Technical Assessment Reports (STAR)
7. Interagency Energy-Environment Research and Development
8. "Special" Reports
9. Miscellaneous Reports

This report has been assigned to the ENVIRONMENTAL PROTECTION TECHNOLOGY series. This series describes research performed to develop and demonstrate instrumentation, equipment, and methodology to repair or prevent environmental degradation from point and non-point sources of pollution. This work provides the new or improved technology required for the control and treatment of pollution sources to meet environmental quality standards.

EPA REVIEW NOTICE

This report has been reviewed by the U.S. Environmental Protection Agency, and approved for publication. Approval does not signify that the contents necessarily reflect the views and policy of the Agency, nor does mention of trade names or commercial products constitute endorsement or recommendation for use.

This document is available to the public through the National Technical Information Service, Springfield, Virginia 22161.

TECHNICAL REPORT DATA
(Please read Instructions on the reverse before completing)

1. REPORT NO. EPA-600/2-80-054	2.	3. RECIPIENT'S ACCESSION NO. PB 80 197569
4. TITLE AND SUBTITLE Supercritical Fluid Regeneration of Activated Carbon for Adsorption of Pesticides		5. REPORT DATE March 1980
		6. PERFORMING ORGANIZATION CODE
7. AUTHOR(S) R. P. DeFilippi, V. J. Kyukonis, R. J. Robey, and M. Modell		8. PERFORMING ORGANIZATION REPORT NO.
9. PERFORMING ORGANIZATION NAME AND ADDRESS Arthur D. Little, Inc. 20 Acorn Park Cambridge, Massachusetts 02140		10. PROGRAM ELEMENT NO. 1BB610
		11. CONTRACT/GRANT NO. Grant R804554
12. SPONSORING AGENCY NAME AND ADDRESS EPA, Office of Research and Development Industrial Environmental Research Laboratory Research Triangle Park, NC 27711		13. TYPE OF REPORT AND PERIOD COVERED Task Final; 1/77-5/79
		14. SPONSORING AGENCY CODE EPA/600/13

15. SUPPLEMENTARY NOTES IERL-RTP project officer is Max Samfield, Mail Drop 62, 919/541-2547.

16. ABSTRACT

The reportdescribes the development of a new process for regenerating activated carbon, using supercritical CO2 as a desorbent. Supercritical CO2 in the range of 30-250 C and at pressures $>$80 atm. is a good solvent for organics. A series of pesticides was tested for treatment by carbon adsorption and supercritical CO2 regeneration. Alachlor and atrazine, selected for further study, both permitted regeneration over multiple cycles with a low average loss per cycle. All pesticides tested showed a substantial capacity decline (30-plus%) after one generation, but after several cycles both alachlor and atrazine exhibited a stable working capacity. Regeneration is rapid. Water in the carbon pores is not detrimental, at least not at 120 C. Shorter exposure time of carbon to adsorbent resulted in less first-cycle decline. Desorption rates increased with temperature, and higher regeneration pressures (150-275 atm.) gave improved regenerability. Treatability studies on a plant sample of atrazine manufacturing wastewater indicated a stable but low working capacity of carbon. Working capacities of 0.05 to 0.08 g TOC per g carbon were obtained at regeneration pressures of 150-275 atm. at 120 C.

17. KEY WORDS AND DOCUMENT ANALYSIS

a. DESCRIPTORS		b. IDENTIFIERS/OPEN ENDED TERMS	c. COSATI Field/Group	
Pollution	Carbon Dioxide	Pollution Control	13B	07B
Pesticides	Supercritical Flow	Stationary Sources	06F	20D
Adsorption	Waste Water	Supercritical CO2	14B	
Activated Carbon	Water Treatment	Alachlor	11G	
Regeneration		Atrazine		
Desorption			07D,07A	

18. DISTRIBUTION STATEMENT Release to Public	19. SECURITY CLASS *(This Report)* Unclassified	21. NO. OF PAGES
	20. SECURITY CLASS *(This page)* Unclassified	22. PRICE

EPA Form 2220-1 (9-73)

EPA-600/2-80-054
March 1980

Supercritical Fluid Regeneration of Activated Carbon for Adsorption of Pesticides

by

R.P. DeFilippi, V.J. Kyukonis,
R.J. Robey, and M. Modell

Arthur D. Little, Inc.
20 Acorn Park
Cambridge, Massachusetts 02140

Grant No. R804554
Program Element No. 1BB610

EPA Project Officer: Max Samfield

Industrial Environmental Research Laboratory
Office of Environmental Engineering and Technology
Research Triangle Park, NC 27711

Prepared for

U.S. ENVIRONMENTAL PROTECTION AGENCY
Office of Research and Development
Washington, DC 20460

18

ABSTRACT

The objective of this program was to perform laboratory-based studies directed toward development of a new process for activated carbon regeneration based on supercritical carbon dioxide as a desorbing solvent. Supercritical CO_2 at temperatures in the range of 30-250°C, and pressures above about 80 atm, is a good solvent for organics, with mass-transfer properties superior to ordinary liquids.

A series of pesticides was screened for suitability for treatment by carbon adsorption and supercritical CO_2 regeneration: Alachlor, Atrazine, Carbaryl, Pentachlorophenol, Trifluralin, and Diazinon. Alachlor and Atrazine were selected as candidates for further study. Both pesticide solutions permitted repeated regeneration over multiple cycles with a low average capacity loss per cycle. Alachlor-loaded carbon was regenerated 31 times. All pesticide candidates showed a substantial capacity decline after the first regeneration (30+%); after several cycles, both Alachlor and Atrazine exhibited a stable working capacity.

Process studies showed that regeneration is rapid: a 30-minute regeneration cycle is feasible. At least at a temperature of 120°C, regenerability and rate of desorption was unaffected by the presence of water in the carbon pores. Time of exposure of GAC to adsorbent influenced regenerability: initial-cycle decline was less for shorter exposure times, even when saturation of the GAC was achieved. Desorption rate increased with temperature; higher regeneration pressure (275 atm vs. 150 atm) gave improved regenerability.

Through seven cycles, regeneration in a closed-loop recycle-CO_2 system gave Alachlor effluent levels of 0.2 ppm or less. Regeneration of 4-ft (120-cm) long columns in desorption gave concentration-time traces similar or slightly better (faster regeneration) than those from 1-ft (28-cm) long columns. Treatability studies carried out with a plant sample of Atrazine manufacturing wastewater showed that a stable but low working capacity of GAC was achievable. Depending on regeneration pressure, working capacities of 0.05 to 0.08 g TOC/g GAC were obtained for the pressure range of 150 to 275 atm, at 120°C.

This report was submitted in fulfillment of Grant No. 804554010 by Arthur D. Little, Inc. under the sponsorship of the U.S.-Environmental Protection Agency. This report covers the period January 31, 1977, to May 31, 1979.

TABLE OF CONTENTS

Page

ABSTRACT ii

TABLE OF CONTENTS iii

LIST OF FIGURES iv

LIST OF TABLES vii

NOTATION ix

I. INTRODUCTION 1

II. CONCLUSIONS 3

III. RECOMMENDATIONS 5

IV. BACKGROUND 6

V. PESTICIDE SCREENING STUDIES 27

VI. MODEL SYSTEM STUDIES 59

VII. PROCESS DEVELOPMENT STUDIES 88

VIII. PLANT WASTEWATER TREATABILITY STUDY 122

IX. PROCESS DESIGN AND ECONOMIC ANALYSIS 136

X. REFERENCES 152

XI. APPENDICES

A. LOCAL EQUILIBRIUM THEORY 156

B. PHYSICAL PROPERTIES & DESIGN CALCULATIONS 170

FIGURES

Page

IV-1 Reduced Pressure-Density Diagram 11
IV-2 Solubility Map of Naphthalene in SCF and NCL Carbon Dioxide 13
IV-3 Solubility of SiO_2 in Water 15
IV-4 P-T Projections of the Phase Diagrams and Critical Locus of Binary CO_2 + Alkane Mixtures 16
IV-5 Diffusivity of Carbon Dioxide in the Near Critical Region 18
IV-6 Chromatographic Separation of n-Alkanes with Supercritical CO_2 23
IV-7 Chromatographic Separation of Polynuclear Aromatic Hydrocarbons with Supercritical CO_2 24
IV-8 Chromatographic Separation of Some Oxygenated Compounds with Supercritical CO_2 25

V-1 Experimental Apparatus for Supercritical Fluid Extractions 31
V-2 Adsorption Isotherm 34
V-3 Batch Adsorption Rate Curves 36
V-4 Schematic Diagram of Adsorption Apparatus 37
V-5 Adsorption Breakthrough Curve, High Flow Rate Q_H 39
V-6 Adsorption Breakthrough Curve, Low Flow Rate Q_L 40
V-7 Solubility of Pesticides in SCF 42
V-8 Solubility of Alachlor and Carbaryl at Low Pressures 43
V-9 Adsorption Isotherm of Four Pesticides 45
V-10 Adsorption from Carbaryl Solution (Series C-1) 46
V-11 Adsorption from Carbaryl Solution (Series C-2) 47
V-12 Diazinon Adsorption Breakthrough Curves 50
V-13 Atrazine Adsorption Breakthrough Curves 51
V-14 Alachlor Adsorption Breakthrough Curves 52
V-15 Comparison of Virgin Alachlor Adsorption Breakthrough for AL-1 and AL-2 Series 54
V-16 Series Al-1 Alachlor Adsorption Breakthrough Curves 55
V-17 Series Al-2 Alachlor Adsorption Breakthrough Curves 56
V-18 Effect of Regeneration Pressure on Alachlor Breakthrough Curves: Al-1 Series 57
V-19 Effect of Regeneration Pressure on Alachlor Breakthrough Curves: Al-2 Series 58

FIGURES (continued)

		Page
VI-1	Adsorption and Desorption Apparatus	60
VI-2	Desorption of Phenol from GAC with Supercritical CO_2	63
VI-3	Adsorption of Phenol on Filtrasorb 300	64
VI-4	Adsorption of Phenol on CC-1230	65
VI-5	Adsorption of Phenol on GX-31	66
VI-6	Adsorption of Phenol on XE-348	67
VI-7	Prolonged Adsorption Breakthrough of Phenol on F-300: 2500 ppm Feed.	71
VI-8	Loading as a Function of Time During Prolonged Adsorption: 2500-ppm Phenol on F-300	72
VI-9	Prolonged Adsorption Breakthrough of Phenol on F-300: 120 ppm	73
VI-10	Loading as a Function of Time During Prolonged Adsorption: 120 ppm Phenol on F-300	74
VI-11	Phenol Loading as a Function of Time x Concentration	76
VI-11A	Phenol Loading After 2-Day Adsorption	77
VI-12	Adsorption Breakthrough Curve for Acetic Acid on F-300	82
VI-13A	Desorption Curves for Alachlor Following 1 Day of Adsorption	85
VI-13B	Desorption Curves for Alachlor Following 3 Days of Adsorption	86
VI-13C	Desorption Curves for Alachlor Following 10 Days of Adsorption	87
VII-1	Alachlor Adsorption Breakthrough Curves	90
VII-2	Alachlor Adsorption Breakthrough Curves: Comparison of Slow and Rapid Loading	90
VII-3	Alachlor Adsorption Breakthrough Curves with F-300	92
VII-4	Alachlor Adsorption Breakthrough Curves with F-400	93
VII-5	Alachlor Adsorption Breakthrough Curves: Effect of GAC Mesh Size on Effluent Quality	95
VII-6	Solubility of Alachlor	96
VII-7	Schematic Diagram of Desorption and Separation Apparatus	98
VII-8	Schematic Diagram of Recycle Test Apparatus	99
VII-9	Comparison of Complete Breakthrough Curves for Alachlor Adsorption	101
VII-10	Adsorption of Alachlor: Closed-Loop Regeneration Series	102
VII-11	Adsorption of Alachlor: Four-Foot Column	105
VII-12	Desorption Curves for Small and Large Columns	106
VII-13	Reproducibility of First-Cycle Desorption Curves	110

FIGURES (continued)

		Page
VII-14	Regeneration Curves for Small and Large Columns: First Cycle	112
VII-15	Regeneration Curves for Successive Cycles, 380-g Columns	114
VII-16	Breakthrough Histories at Various R Values	117
VII-17	Desorption Curve for 2500 ppm Phenol	118
VII-18	Variation of Desorption Curve with Number of Transfer Units	120
VII-19	Variation of Regeneration Curve with Number of Transfer Units	121
VIII-1	Atrazine Wastewater Adsorption Apparatus	124
VIII-2	Total Organic Carbon Analyzer (TOCA)	126
VIII-3	Adsorption Breakthrough Curve in Atrazine Wastewater	128
VIII-4	Atrazine Wastewater Regeneration Apparatus	129
VIII-5	Regeneration Apparatus with High-Pressure UV Detector	133
VIII-6	High Pressure UV Desorption Trace of Atrazine	134
IX-1	Schematic of a SCF Adsorbent Regeneration System	137
IX-2	Number of Transfer Units vs Throughput	140
IX-3	Process Flow Diagram	145
IX-4	Piping and Instrumentation Diagram	146
A-1	Cylindrical Volume Element	156
A-2	Column Profile as a Function of Time	158
A-3	L.E.T. Desorption Curve	160
A-4	L.E.T. Regeneration Curve	160
A-5	Alachlor Desorption Curve	163
A-6	Best-Fit Regeneration and Desorption Curves	164
A-7	Best-Fit for 10-Day Alachlor Adsorption	166
A-8	Best-Fit for 3-Day Alachlor Adsorption	168
A-9	Best-Fit for 1-Day Alachlor Adsorption	169

TABLES

		Page
IV-1	Critical Conditions of Common Fluids	12
IV-2	Solubility of Organic Compounds in Liquid CO_2	19
V-1	Characteristics of Selected Pesticides	28
V-2	Molecular Structure of Selcted Pesticides	29
V-3	Components of Solubility Test Apparatus	32
V-4	Characteristics of Granular Activated Carbon	33
V-5	Components of Dynamic Adsorption Apparatus	38
V-6	Adsorption Data of Carbaryl, Alachlor, Atrazine, and Diazinon	49
VI-1	Phenol: Summary of Operating Conditions and Results	62
VI-2	Prolonged Adsorption of Phenol	69
VI-3	Effect of Adsorption Period on Working Capacity	78
VI-4	Regeneration of High CO_2 Flow Rate	80
VI-5	Adsorption Data for Acetic Acid	83
VII-1	Size Characteristics of F-300 and F-400	94
VII-2	Alachlor Regeneration Results	100
VII-3	Loading Data for Alachlor Closed Loop Series	103
VII-4	Regeneration Results, Three 380-g Columns	111
VIII-1	Properties of Atrazine	123
VIII-2	Adsorption Conditions and Results	130
IX-1	Design Calculations, Small Column Case	141
IX-2	Design Calculations, Large Column Case	142
IX-3	Summary of Desorber Analysis	143
IX-4	Plant Component List	148
IX-5	Estimated Processing Costs	151

TABLES (continued)

Page

B-1 Physical Properties of CO_2 170

B-2 Properties of F-300 GAC 171

B-3 Operating Parameters 172

B-4 Adsorption Conditions 173

B-5 Mass Transfer Coefficients; Pore Diffusion 174

B-6 Mass Transfer; Film Coefficients 176

B-7 Pressure Drop in Packed Beds 180

B-8 Analysis of Breakthrough Curve 184

B-9 Analysis of R Based on 120 ppm and 2500 ppm Results 186

NOTATION

a	Interfacial area of solid phase per volume of bed, cm^2/cc
b	Correction factor for kinetic coefficient
c	Concentration of solute in fluid phase, γ/cm^3
c_o	Fluid phase concentration of solute at equilibrium with initial solid loading, γ/cm^3
c_F	Fluid-phase concentration of solute in regenerant fed to column inlet, g/cm^3
$c(L,t)$	Concentration of solute in regenerant at column outlet, g/cm^3
$c_{w,sat}$	Solubility of solute in water, g/cm^3
c_{sat}	Solubility of solute in regenerant, g/cm^3
K	Adsorption equilibrium constant, $cm^3/$
k_f	Mass transfer coefficient for fluid phase
k_p	Mass transfer coefficient for solid phase
k_w	Langmuir adsorption constant for aqueous solutions fo solute, ppm^{-1}
L	Length of adsorbent bed, cm
N	Number of transfer units
q	Solute loading per weight of adsorbent, gr/gr
q_{ir}	Solid-phase concentration of irreversibly adsorbed solute, g/g reversibly adsorbed
q_m	Maximum solid loading corresponding to a monolayer gr/gr
q_o	Initial solid-phase concentration at the start of regeneration, g/g
q_{total}	Total solid-phase concentration of solute, g/g
R	Dimensionless adsorption constant, $1 + Kc_o$
T	Dimensionless throughput, $UC_o\hat{t}/q_o\rho_B L$
t	Time, min.
$\hat{t}$	Time following the arrival of the fluid front at the column exit, min.
t_o	Residence time for non-adsorbing fluid to elute bed, min.
tr	Reduced time (t/t_o), bed volumes of regenerant
tr_1	Reduced time for $t = t$, bed volumes
tr_2	Reduced time to complete regeneration, bed volumes
t_1	Time for plateau at c_o to elute bed, min.
t_2	Time to completion of regeneration, min.

Notation (continued)

U	Superficial velocity
v	Average fluid intersticial velocity, cm/min
v_c	Characteristic velocity of a given fluid concentration
X	Dimensionless concentration, c/c_o
x	Solute mole fraction
x(L,tr)	Concentration solute in regenerant at column exit, rt. fr.
$X_\circ$	Fluid-phase concentration in equilibrium with qo, rt. fr.
Z	Distance from column inlet, cm

Greek Symbols

ε	Interstitial void fraction
κ	Kinetic mass-transfer coefficient in the Thomas equation, (1)
ρ_B	Adsorbent bulk density

I. INTRODUCTION

Granular activated carbon treatment is presently in limited use for industrial wastewaters from the manufacture of pesticides and other hazardous chemicals. The major factor constraining expanded use is cost, and much of the cost is associated with carbon regeneration for reuse. The existing thermal regeneration process for granular carbon using the multiple-hearth furnace is capital and energy intensive, and responsible for losses that lead to high cost for make-up carbon. The production of corrosive gases such as HCl is also a problem in any thermal process. Other regeneration methods under development appear to have drawbacks also. For example, liquid solvent extractive regeneration is expensive because of the requirements for removal of all solvent from regenerated carbon and for purifying spent solvent for recycle.

A novel extractive regeneration process employing supercritical fluids (dense gases) as the extracting agent has been under development at Arthur D. Little. A supercritical fluid is any fluid at pressures and temperatures above the critical point. Supercritical carbon dioxide has high solubilities for organic compounds. Moreover, solubility changes rapidly with pressure, so that the solvent can be freed of solute by pressure changes much like pumping and expanding a liquid. Diffusion coefficients for solutes in supercritical fluids are about an order of magnitude higher than in liquids; thus, the desorption rate of adsorbate from activated carbon into supercritical CO_2 is much more rapid than the corresponding liquid extraction.

Early tests in our laboratory using different organics adsorbed on activated carbon confirmed that there is relatively rapid and effective regeneration using supercritical CO_2. A comparative engineering and cost analysis indicated that both capital and operating costs for the process could be significantly less than those for multiple-hearth furnace regeneration. Based on these results, research and development of the supercritical CO_2 regeneration process were continued under funding by the Chemical Process Branch of the Industrial Environmental Research Laboratory, EPA/RTP.

Because of the importance of effective treatment of pesticides manufacturing wastewater, this industry segment was chosen as the focus of the development program. Pesticides play a major role in modern life. They are essential to the production of food and natural fibers, the preservation of wood as a structural material, and the control of disease. They are, however, toxic by definition, and that toxicity can extend to man and other mammalian species.

Control of pesticide discharges into the environment represents a difficult problem. An important step towards the solution is the control of pesticides discharged by point sources. These sources fall into two categories: technical pesticides manufacture, and pesticides preparations and formulations production. Greater emphasis is placed on the reduction of wastes from pesticides manufacture, because much higher tonnage of hazardous wastes is produced in manufacturing compared to preparation and formulation. (Gruber, 1975).

The severity of the problem of pesticides residues is underlined by EPA action in banning the use of several of the more persistent and toxic pesticides. While needed to eliminate the most hazardous materials, these bans place the burden on substitute materials which are considered more acceptable, but also have at least some degree of toxicity. The total need for pesticides will not diminish; indeed, projections indicate that the total pesticides growth rate is on the order of 10% per year (Anon., 1975). The great majority of pesticides are manufactured by processes which release contaminated wastewaters. These wastewaters are successfully treated in many cases, but in other cases they are dealt with using methods which may not be permissable in the future, such as deep well disposal. Additionally, the effectiveness of wastewater treatment methods presently used for adequate reduction of hazardous effluents may be questionable in some cases. Thus, the need exists for alternate treatment processes which will be effective in eliminating these hazardous wastes. One treatment process which has been successful in a number of industrial plants is activated carbon adsorption. Wider study of adsorbent treatment of pesticide manufacturing wastewaters is on-going, much under the sponsorship of EPA, and it shows promise of extended applications.

Many pesticides are expensive chemicals, the average price being of the order of $1.00/lb. Raw-material chemicals are also expensive, as indicated by the fact that starting materials are a major cost in the manufacture of pesticides. Manufacturing wastewaters can contain as much as several percent of starting or product chemicals, and thereby represent an economic loss as well as a serious pollution problem. A wastewater treatment process which would allow recovery of chemicals from these aqueous wastes would have obvious benefit. In addition to removing hazardous organic solutes from the wastewater, the process would recover chemicals for recycle; in some cases, process water may be recycled as well. Thus, the ideal of closed loop operation may be approached, with the costs of pollution control at least partly covered by chemicals recovery.

This rationale has been a major factor in considering an activated carbon process which is nondestructive of the adsorbate. The ability of activated carbon or other adsorbents to remove hazardous chemicals from wastewaters may be combined with an adsorbent regeneration process which would permit chemicals recovery. The development of this capability was a basic objective of this program.

The program approach included two major initial phases carried out in parallel: screening of a series of pesticides to aid in the selection of candidates suitable for further study; and model system studies to develop a better understanding of the fundamental operations controlling the process. These were followed by process development studies to determine optimum conditions and mode of operation; treatability studies using plant samples of pesticide manufacturing wastewater; and engineering-design and economic evaluations.

II. CONCLUSIONS

A. PESTICIDE SCREENING

1. The following pesticides were screened as aqueous solutions for their suitability for treatment by carbon adsorption and supercritical CO_2 regeneration: Alachlor, Atrazine, Carbaryl, Pentachlorophenol, Trifluralin, and Diazinon. Alachlor was selected as the candidate for further study, and Atrazine was selected as a backup candidate. Both pesticide solutions permitted repeated regeneration over multiple cycles with a low average capacity loss per cycle. Alachlor-loaded carbon was regenerated 31 times.

2. All pesticide candidates showed a substantial capacity decline after the first regeneration (30+%). After several cycles, both Alachlor and Atrazine exhibited a stable working capacity.

3. While solubility of pesticide in SCF CO_2 of at least several tenths of a percent was observed in all cases, there was no correlation between solubility level and regenerability.

B. MODEL SYSTEM STUDIES

1. Phenol as a model compound exhibited regeneration behavior similar to the selected pesticides: an initial drop in capacity on the first cycle, followed by constancy of working capacity over additional cycles.

2. Regeneration was rapid, as predicted. Rates depended on conditions; a 30-minute regeneration cycle is feasible.

3. At least at a temperature of 120°C, regenerability and rate of desorption was unaffected by the presence of water in the carbon pores. It was removed rapidly by SCF CO_2.

4. Time of exposure of GAC to adsorbent influenced regenerability. Initial-cycle decline was less for shorter exposure times (even when saturation of the GAC was achieved). This may be caused by a slow irreversible adsorption or chemical reaction occurring on the carbon surface.

5. Desorption rate increased with temperature. At 250°C and 15 min of regeneration, a working capacity was obtained which was roughly equivalent to that at 120°C for 60 min.

6. Higher regeneration pressure (275 atm vs 150 atm) gave improved regenerability, as well as consistently higher solubility in SCF CO_2.

7. Acetic acid is a weakly adsorbed solute (one-third the working capacity of phenol) which could be completely desorbed from GAC, as tested in an eight-cycle series.

C. PROCESS DEVELOPMENT

1. The Alachlor content of 100 ppm snythetic solutions could be reduced to an effluent level below 0.2 ppm by virgin and SCF-regenerated carbon.

2. Regeneration in a closed-loop recycle CO_2 system gave regenerability results similar to once-through CO_2. Effluent levels after GAC treatment with recycle-CO_2-regenerated carbon could be reduced to 0.2 ppm.

3. Regeneration of 4-ft (120-cm) long columns gave desorption concentration-time traces similar or slightly better (faster regeneration) than those from 1-ft (28-cm) long columns.

4. Local equilibrium theory was effective in modeling desorption behavior over almost the entire desorption run length. Tailing, probably due to mass transfer resistances, was longer than predicted by local equilibrium. Batch adsorption isotherms measured in SCF CO_2 were not effective in predicting column dynamic behavior using local equilibrium assumptions.

5. The contribution of mass-transfer kinetics to SCF CO_2 desorption appears to be predictable, based on known relationships such as those used in the Thomas model. Differences in one-foot and four-foot column behavior appeared to be rationalized on this basis.

D. PLANT-SAMPLE TREATABILITY

Treatability studies carried out with a plant sample of Atrazine manufacturing wastewater showed that a low, stable working capacity of GAC was achievable. Depending on regeneration pressure, working capacities of 0.05 to 0.08 g TOC/gGAC were obtained for the pressure range of 150 to 275 atm, at 120°C.

E. PROCESS ECONOMICS

An example case of phenol treatment was used to design and cost a system for regenerating 10,000 lbs per day of spent GAC. The capital cost was estimated at $800,000, and the operating cost at $0.085 per lb of regenerated carbon. No credit for recovered adsorbate was taken in these costs.

III. RECOMMENDATIONS

1. The SCF regeneration process should be tested at larger scale. This could be done at a carbon regeneration capacity in the range of 1-5000 lbs per day.

2. The process concept of adsorption and regeneration in the same small-volume vessels should be developed and tested. This provides less operating complexity, and eliminates losses of carbon due to transfer. It may require small particle-size carbon to improve adsorption kinetics, but the attendant increased pressure drop in the bed may be a worthwhile trade-off.

3. A mobile pilot plant should be built and used for treatability studies on site. Usually, excessive sample volumes rule out testing at a location away from the manufacturing operation producing the wastewater.

4. Bench-scale studies should be expanded to a broader range of adsorbates and plant samples.

5. Further model studies should be performed to help verify the present understanding of both physical and chemical processes that occur in adsorption and desorption. These should include tests to help clarify the time-dependent effects observed in this program.

IV. BACKGROUND

The purpose of this section is to provide adequate background information in three areas directly related to this program: current regeneration processes for activated carbon applied to wastewater treatment; desorption of adsorbates from activated carbon using liquid solvents; and other work in supercritical fluid extractions.

A. CURRENT REGENERATION PROCESSES FOR ACTIVATED CARBON

1. Thermal Processes

By far the predominant methods for activated carbon regeneration are thermal processes which destroy the adsorbate. For granular carbon, the multiple hearth furnace is in widespread use, and the rotary kiln has been used to a limited extent. Recently, fluid-bed and radiative furnaces have been reported to be under development. For powdered carbon, a commercial thermal transport process has been described.

In each thermal system, the same basic steps occur. The spent carbon, superficially drained of free water, is introduced into the furnace where the remaining water is removed by evaporation. This water, largely occupying the pore volume, is of the order of 40 to 50 percent by weight of wet granular carbon, and 75% of wet powdered carbon. After drying, the temperature of the carbon is then raised to about 1500°F which causes volatilization of lower molecular weight organics, followed by pyrolysis of the heavier adsorbed components and volatilization of the pyrolyzed fragments. The third step involves gasification of the carbon residue by carbon dioxide and steam reforming reactions at temperatures up to about 1700°F. In addition, there is some oxidation of the carbonized residue and the gaseous volatile components.

Added fuel is required for the entire process. Evaporation of water accounts for about 25 percent of the heat requirement; the balance goes into sensible heat in elevating both carbon and gaseous constituents to reaction temperature, and a small amount is needed to provide for the net endothermic pyrolysis and gasification reactions involved. A large excess of steam is employed to favor the steam-carbon reaction, and oxygen content is kept low to minimize combustion of the activated carbon adsorbent.

2. Non-Thermal Processes

a) Wet-Air Oxidation for Powdered Carbon

Because of the problem with losses in thermal regeneration of powdered activated carbon, attempts have been made to apply the Zimpro wet-air oxidation process to powdered carbon regeneration. In this process, an aqueous slurry of spent carbon is contacted with air at temperatures between 390° and 470°F, and pressures above 225 to 500 psi (Zimpro 1974). A 0.8 MGPD municipal system has been tested over a period of about 50 days (Burant, 1973). In spite of carbon losses from several sources, the make-up carbon cost was estimated to be only about 1.2¢ per thousand gallons, which is a favorably low figure.

b) Alkaline Regeneration for Acid Adsorbates

In some industrial wastewaters, the major organic constituent is acidic, and capable of being adsorbed by granular activated carbon. In these cases, the adsorption equilibrium may be shifted by desorbing with an aqueous solution at alkaline pH. This process has been applied by Dow Chemical in Midland, Michigan, to phenol in wastewater (Himmelstein, 1974). A similar process has been used in a large-scale plant by Sherwin Williams with p-cresol (Minor, 1974). The economic prospect for such a process depends strongly on the relative recovery values for any given application. An additional benefit is the ability to regenerate _in situ_, avoiding the need to transport carbon from the contacting vessel to the regeneration system.

c) Solvent Regeneration

The use of organic solvents to regenerate carbon has been considered, although no commercial applications are presently known. There have been pilot-scale studies on organics adsorbed from coke plant flushing liquor, regenerated with hot benzene solution (Lovens, 1974). Process costs may be high, at least in cases where the solvent and adsorbate cannot be reused without some separation and/or refining step.

Because supercritical fluid desorption is a special case of solvent regeneration, a more detailed review of past research in this area is presented in Section IV-B.

d) Biological Regeneration

Attempts have been made to utilize the biological activity of micro-organism cultures to regenerate carbon (Lovens, 1974; Perrotti, 1974). Among other factors, its effectiveness depends on the degree of biodegradability of the adsorbed organics. While some restoration of carbon adsorptive properties is possible, nothing approaching complete regeneration has been observed. Since a significant amount of biological activity exists in a carbon bed treating municipal wastes, it is probably more appropriate to view this as combined biological and physical-chemical treatment (as in the PACT powdered activated carbon treatment process), rather than a regeneration method. Renewed interest in biological regeneration has accompanied recent research on activated carbon for drinking-water treatment (Suffit, 1980).

3. Comparative Process Analysis

The multiple-hearth furnace is by far the most prevalent process equipment in use. While the great majority of operating experience has been in regeneration of carbon in industrial process use, its use for wastewater treatment is growing. However, based on published information, the multiple hearth furnace is still considered to be costly and difficult to operate.

Costs reported over the last few years for furnace regeneration of activated carbon show that operation of high-capacity systems run on the order of 11-19¢ per pound regenerated (Remirez, 1977). According to data from the Lake Tahoe activated carbon plant (EPA, 1973), the regeneration operating costs are about 70% of the total operating costs, exclusive of amortization. For regeneration capacities ranging from 5,000 to 60,000 lbs/day, capital costs are reported as $0.85 to $4.20 million for multiple hearth furnace systems (Remirez, 1977). A figure for systems costs of $1.0 million for minimum capacity furnaces have also been published (Shuckrow, 1977).

Other thermal processes for regenerating granular carbon presently offer no apparent advantage. Reactive regeneration systems, such as alkaline regeneration of carbon after adsorption of organic acids, may be economical, but only in special cases. They have the advantage of avoiding the thermal degradation of carbon, and provide the opportunity for recovery of the adsorbed species where desirable. However, they do not have a broad range of application.

In contrast, solvent regeneration processes may hold substantial promise, in that they could be capable of handling a broad spectrum of adsorbates. At present, however, this potential advantage is outweighed by problems such as the difficulty of solvent removal from carbon and the attendant loss of adsorptive capacity if solvent removal is incomplete; the cost of solvent losses in the carbon bed; the cost of solvent processing in a separation step for recovering the solvent for recycle; and the creation of secondary problems such as the formation of an oily condensate if steam stripping is used.

Powdered carbon may become attractive in the future because of its low unit cost. At present, however, the problems of handling the fine powder and the high losses in thermal regeneration are difficult to overcome. The latter may be solved by the Zimpro process, but there are unknowns associated with hidden losses, such as residual carbon in the ash blowdown, and oxidation of the adsorbent.

B. DESORPTION FROM ACTIVATED CARBON USING LIQUID SOLVENTS

Although very few carefully defined experiments have been made, there is sufficient data to conclude that organic adsorbates can be desorbed from activated carbon by extraction with conventional liquid solvents. The extraction is, in general, a slow and tedious process. Whether or not adsorbates can be removed completely by liquid solvents is open to question. The ease of desorption and the extent to which desorption is complete appears to depend upon the nature of the carbon, solute and solvent.

The major fraction of the carbon surface area is relatively uniform and non-polar, with graphitic-like character. On this part of the surface, solutes are held predominantly by physical adsorption; London dispersion forces act as relatively weak bonds between solute and surface. A small but significant fraction of the surface is heterogeneous and polar. These sites have been attributed to inorganic impurities and 'surface oxides' (carboxyl, hydroxyl and carbonyl groups) that are formed during the oxidative activation of the carbon during preparation (Coughlin, 1968; Mattson, 1969; Snoeyink, 1967).

The number and nature of these sites vary from one carbon to another, depending upon the procedure used for activation. On such sites, adsorption of polar compounds may occur by chemisorption or by chemical reaction of solutes with surface oxides. Thus, adsorption on activated carbon ranges from weak to very strong.

The degree to which adsorbates can be removed by a liquid solvent depend on the type of adsorption. At one extreme, physically adsorbed solutes can be removed readily by solvent extraction; indeed, some low molecular weight, volatile solutes can be removed by heating or steam-stripping. At the other extreme, chemisorbed or chemically bound solutes cannot be removed by solvents; they can only be removed by chemically reacting them off the carbon (e.g., by oxidation during thermal regeneration).

While solvent extraction of many organics is technically feasible, liquid solvent regeneration has not attained commercial viability. There are a number of serious drawbacks to scaling up the analytical methods to an industrial process for carbon regeneration. In particular, the rate of desorption is very slow and the degree of removal of solutes is far from complete. In addition, commercial solvents are relatively expensive and must be recovered for reuse. Consequently, solutes must be removed from the solvent after desorption. For moderately volatile solutes, recycle of solvent will require extensive distillation. Furthermore, many conventional solvents are health hazards in themselves; thus, they must be completely removed from the carbon before the adsorbent is reused. If the solvent is air- or steam-stripped from the carbon, the stripping agent may require further processing to avoid emission of an air pollutant.

For efficient and economic regeneration of activated carbon, the desired solvent characteristics are (i) high solubility for the adsorbates, (ii) favorable mass transfer properties for rapid desorption and (iii) high volatility for subsequent separation of solutes. Liquid solvents exhibit high solubility but slow diffusion. In the gas phase, mass transfer is rapid but solubilities are very low. Fluids in the region of their critical temperatures and pressures, called supercritical fluids (SCF), represent a good compromise. The density is typically a third that of the normal liquid: high enough to provide for good solubility, yet low enough to permit high diffusivity and rapid mass transfer. We have found that activated carbon and other adsorbents can be regenerated efficiently by desorbing adsorbates with supercritical fluids.

C. SUPERCRITICAL FLUIDS AS EXTRACTING AGENTS

The supercritical fluid region can best be visualized with the aid of a reduced pressure-density diagram, shown in Fig. IV-1. The dashed curve is the focus of liquid-vapor equilibrium, which terminates at the critical point (C.P.). In terms of reduced density,p/pCP the density of the normal liquid is about 2.6: in other words, the critical density is about 40% of that of the normal liquid. The critical conditions of common materials are given in Table IV-1.

The SCF region, as we use the term, refers to reduced temperatures in the range of 1 to 1.4 and reduced pressures from 1 to 6. We shall also make reference by the near-critical liquid (NCL) state, which refers to the region bounded by $.95 < T_r < 1$. In the SCF and NCL regions, fluids still have high enough density to exhibit liquid-like solubility behavior, yet the densities are low enough so that diffusivities are appreciably higher than those of normal liquids.

Although there is sufficient evidence to show that solid and liquid solutes have unusually high solubilities in supercritical fluids (Paul, 1971), very few systems have been extensively investigated. One system which has been studied in some dpeth is naphthalene (m.p. 58°C) in CO_2 (T_c = 31.0°C, P_c = 72.9 atm). From the data of Tsekhanskaya, (1964) and Quinn (1936), we have been able to interpolate and extrapolate a 'map' of solubility over a wide range of conditions, as shown in Fig. IV-2. The dashed curve represents the solubility in saturated liquid and vapor. At the critical point, the solubility is 0.23 mole-% naphthalene; at 300 atm and 55°C, it is over 5 mole-%, which is equivalent to 15 wt-%. At high pressures (150-300 atm), the solubility increases with increasing temperature. This conventional solubility behavior is the result of increasing activity (or vapor pressure) of the solute with increasing temperature. On the other hand, at pressures near the critical (70-80 atm), there is an inverse solubility relationship; solubility decrease dramatically with increasing temperature because the density of the solvent is decreasing rapidly with small change in temperature (see Fig. IV-1).

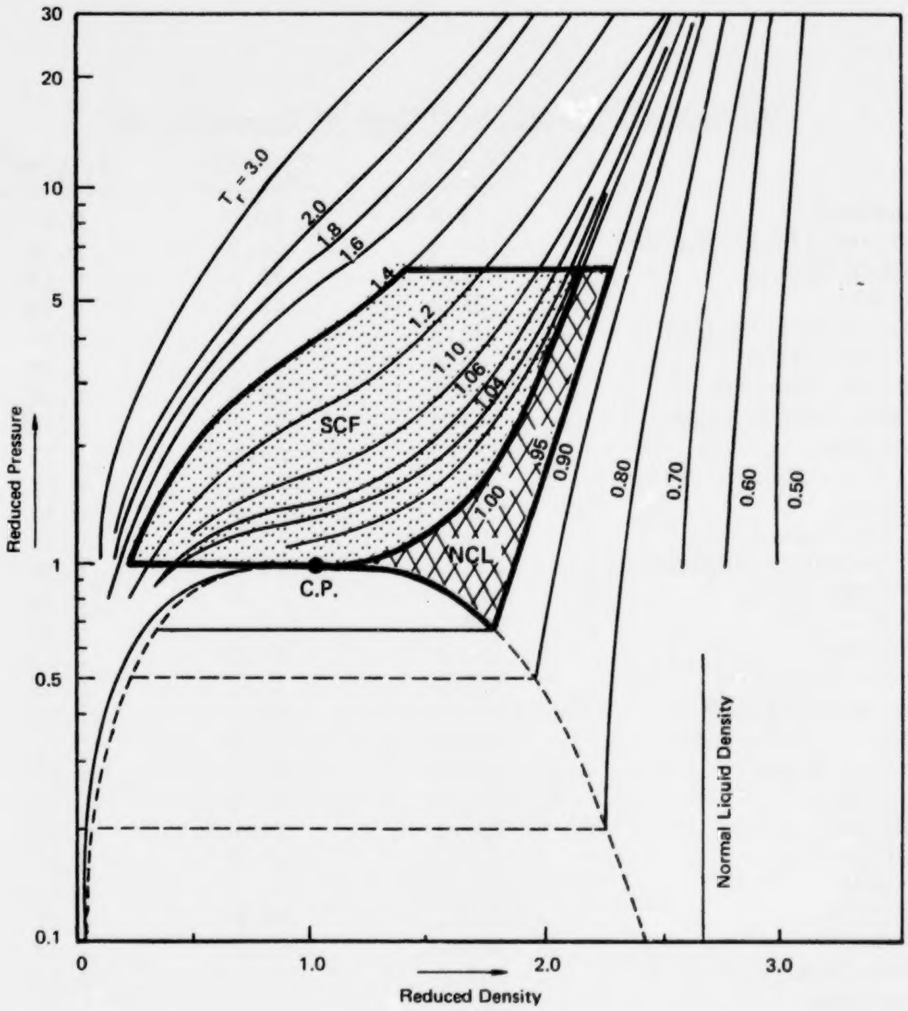

FIGURE IV-1 REDUCED PRESSURE-DENSITY DIAGRAM. SUPERCRITICAL FLUID (SCF) AND NEAR-CRITICAL LIQUID (NCL) REGIONS, AS INDICATED (After Giddings, et al., 1968)

Table IV-1 Critical Conditions of Common Fluids

	T_c(°C)	P_c(atm)	ρ_c(g/cm^3)
Ethylene	9.9	50.5	0.23
Chlorotrifluoromethane	28.8	38.2	0.58
Carbon dioxide	31.0	72.9	0.47
Ethane	32.2	48.2	0.20
Tetrafluoroethylene	33.3	38.9	0.58
Nitrous oxide	36.5	71.7	0.46
Methyl fluoride	44.6	58.0	0.31
Sulfur hexafluoride	45.6	37.1	0.75
Propylene	91.9	45.4	0.23
Chlorodifluoromethane	96.4	48.5	0.52
Propane	96.7	42.0	0.22
Carbon disulfide	104.8	65.	0.45
Dichlorodifluoromethane	111.7	39.4	0.56
Dimethyl ether	126.9	52.6	0.26
Ammonia	132.3	111.3	0.24
n-Butane	152.0	37.5	0.23
Sulfur dioxide	157.5	77.7	0.53
Nitrogen dioxide	157.8	100.	0.56
Methyl ethyl ether	164.7	43.4	0.27
Diethyl ether	193.6	36.3	0.27
n-Pentane	196.6	33.3	0.23
n-Hexane	234.2	29.6	0.23
Isopropanol	235.3	47.0	0.27
Acetone	235.9	47.	0.28
Methanol	240.3	78.9	0.27
Ethanol	243.4	63.0	0.28
Chloroform	263.4	54.	0.50
n-Heptane	267.0	27.0	0.24
Benzene	288.9	48.3	0.30
Water	374.	218.	0.32

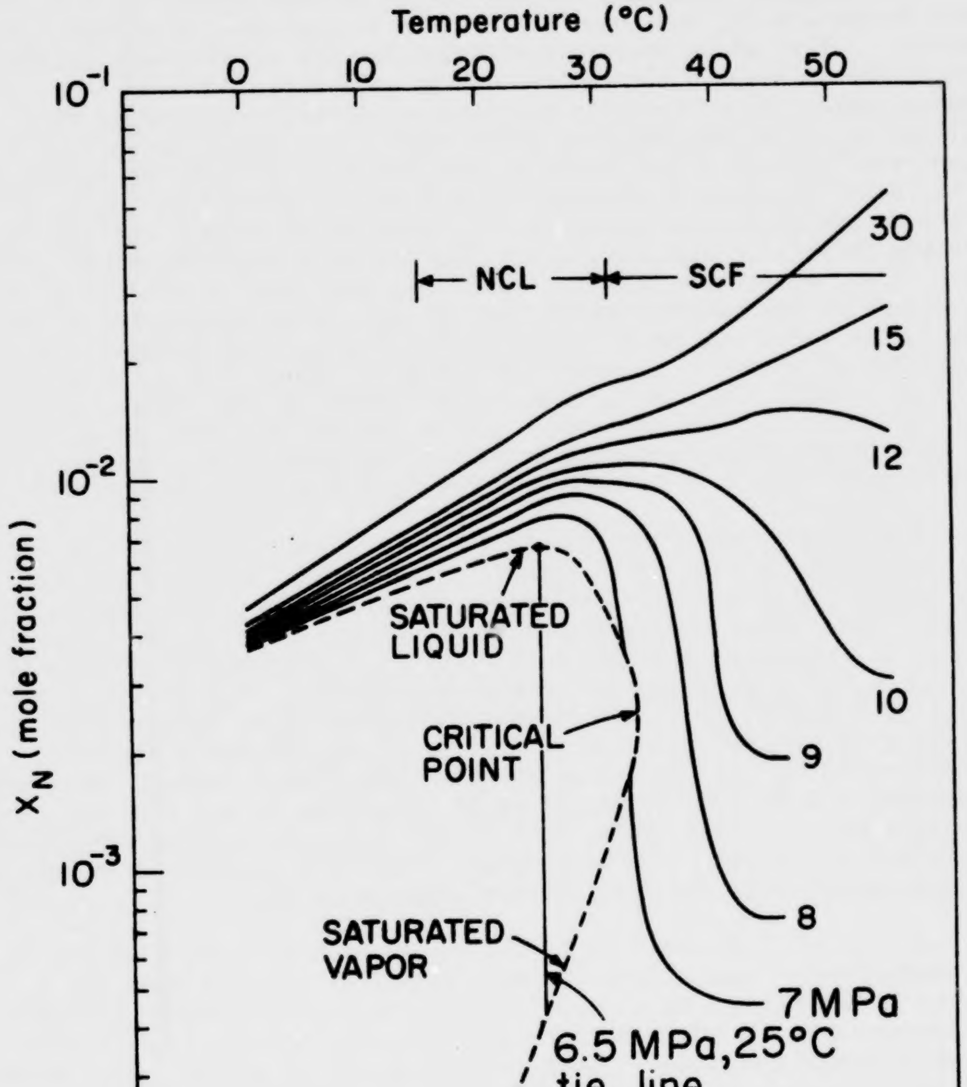

FIGURE IV-2 SOLUBILITY MAP OF NAPHTHALENE IN SCF AND NCL CARBON DIOXIDE

We have reason to believe that the solubility map shown in Fig. IV-2 is representative of a broad range of solid solutes in supercritical fluids. The solubility behavior shown in Fig. IV-2 results from the usual interplay of secondary valence forces between molecules in solution. These forces are the same ones that result in departure from ideal gas behavior. If accurate equations of state for the mixture were available, then it should be possible to predict the solubility behavior from chemical potential or fugacity equality, which is the criterion of equilibrium. The Peng-Robinson (P-R) equation of state, which is a recent modification of the Redlich-Kwong equation of state is reported to be fairly accurate in the sub- and supercritical regions (Peng, 1976). We are in the process of using the P-R equation to predict the naphthalene-CO_2 solubility map; results to date indicate that the method works well. Thus, we believe that the solubility map shown in Fig. IV-2 is not unique to the naphthalene-CO_2 system, but is representative of the behavior of solid solutes in supercritical fluids. For example, the solubility of silica in supercritical water is shown in Fig. IV-3 (Kennedy, 1950). The similarities in the shapes of the isobars in Figs. IV-2 and IV-3 are striking. In the SCF region, water is not hydrogen-bonded to any appreciable extent; it behaves as a moderately polar liquid solvent with dielectric constant of 2.5-10 (Franck, 1970).

Although there is scant data in the literature on solubilities of organic solids and liquids in supercritical fluids, there is a large body of data on solubilities in near-critical liquids. For example, Francis (1954) reported the mutual solubilities of NCL CO_2 at 25°C with each of 261 organic substances (Table IV-2). Each of these solubilities represents a single data point on a solubility map. For example, Francis reports the solubility of naphthalene in liquid CO_2 at 25°C as 2 wt-%. In Fig. IV-2 the corresponding point lies on the saturated liquid curve at 25°C, which is 0.62 mole-% or about 2 wt-%. Thus, Francis' data can be used as a guide for the magnitude of solubility in the critical region. It should be noted that nearly half of the compounds studied were completely miscible with NCL CO_2. The naphthalene solubility behavior discussed above is representative of the less soluble organics in CO_2.

From Fig. IV-2 we see that solubility at high pressure (150-300 atm) and supercritical temperature can be substantially higher than the solubility in saturated liquid at 25°C. At some point of higher pressures and temperatures, solutes that are only slightly soluble at 25°C will become completely miscible. That is, the system of solute + CO_2 reaches a mixture critical point beyond which only a single, homogeneous phase exists. Such critical loci have been reported for a number of organics with CO_2 (Schneider, 1970). The pressure-temperature projections of the critical loci for mixtures of CO_2 and several alkalenes is shown in Fig. IV-4 (Liphard, 1975). For octane, there exists a continuous vapor-liquid

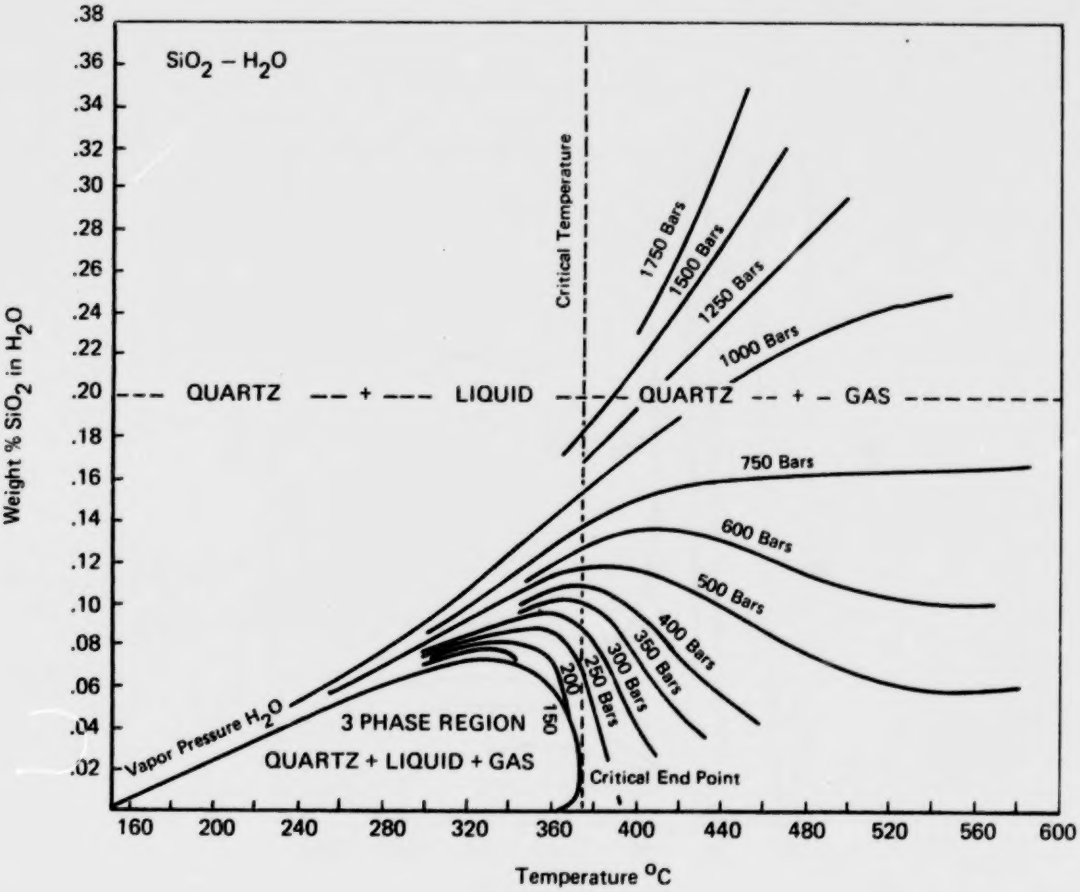

Fiqure IV-3 Solubility of SiO_2 in H_2O (Kennedy, 1950)

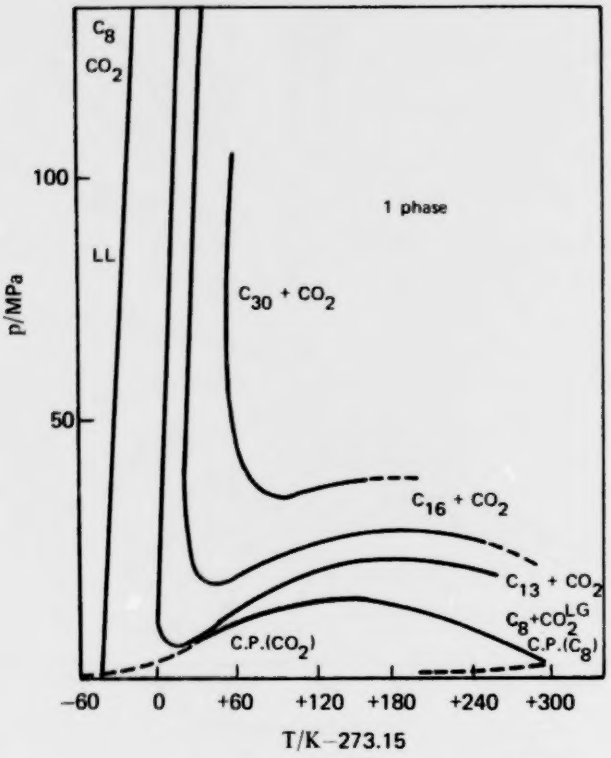

FIGURE IV-4 P–T PROJECTIONS OF THE PHASE DIAGRAMS AND CRITICAL LOCI OF BINARY CO_2 + ALKANE MIXTURES. FULL LINES, CRITICAL CURVES; BATCHED LINES, VAPOR PRESSURE CURVES OF CARBON DIOXIDE AND OCTANE, RESPECTIVELY.
(Liphard and Schneider, 1975)

critical locus connecting the critical points of the pure materials. There is also a liquid-liquid critical locus that exists at low temperatures. To the right of the L-L critical and above the L-G critical, only one phase exists; in that region, octane and CO_2 are completely miscible. Note from Table IV-2 that both heptane and dodecane are completely miscible with liquid CO_2 at 25^oC; thus, octane would also be completely miscible at 25^oC, which is corroborated by Fig. IV-4 . For tridecane and higher molecular weight alkanes, the L-G and L-L critical loci merge into a single, continuous critical locus. To the upper right side of the critical locus, the system is completely miscible; below it and to the left, the system exhibits two or more phases of limited miscibility. Note that for hexadecane at 25^oC, the critical point occurs at around 250 atm. At 25^oC and pressures below 250 atm, the hexadecane-CO_2 system exists as two phases. At 25^oC and 65 atm, Table IV- 2 lists a solubility of 8 wt-% hexadecane in the CO_2-rich phase. Reasoning in the converse manner, it might be anticipated that those substances exhibiting limited solubility in liquid CO_2 at 25^oC would be completely miscible with CO_2 at higher pressures and temperatures.

This brief discussion of solubility phenomena in the critical region illustrates several important generalities:

(1) Enhanced solubility in the critical region is a general phenomenon that arises from the normal interplay of secondary valance forces.

(2) A large number and variety of organic compounds are partially or completely miscible with CO_2 in the near critical liquid region.

(3) Partially miscible systems at NCL conditions tend to complete miscibility at supercritical conditions.

In addition to high solubility, a good extracting agent must exhibit high diffusivity for rapid mass transfer. There is relatively little direct data on diffusivities in supercritical fluids, but there is a growing body of indirect evidence for rapid mass transfer.

Several investigators have measured self-diffusivity of CO_2 in the sub- and supercritical region (for a compilation, see Vargaftik, 1975). We have correlated these data and developed a map of self-diffusivity, as given in Fig. IV-5 . In liquid CO_2 at 25^oC, the diffusivity is about an order of magnitude higher than that of conventional liquid solvents. The vapor diffusivity at 25^oC is another factor of 10 higher. At supercritical temperatures, the diffusivities vary between 10^{-3} and 10^{-4} cm^2/sec; decreasing from the higher to lower values with increasing density.

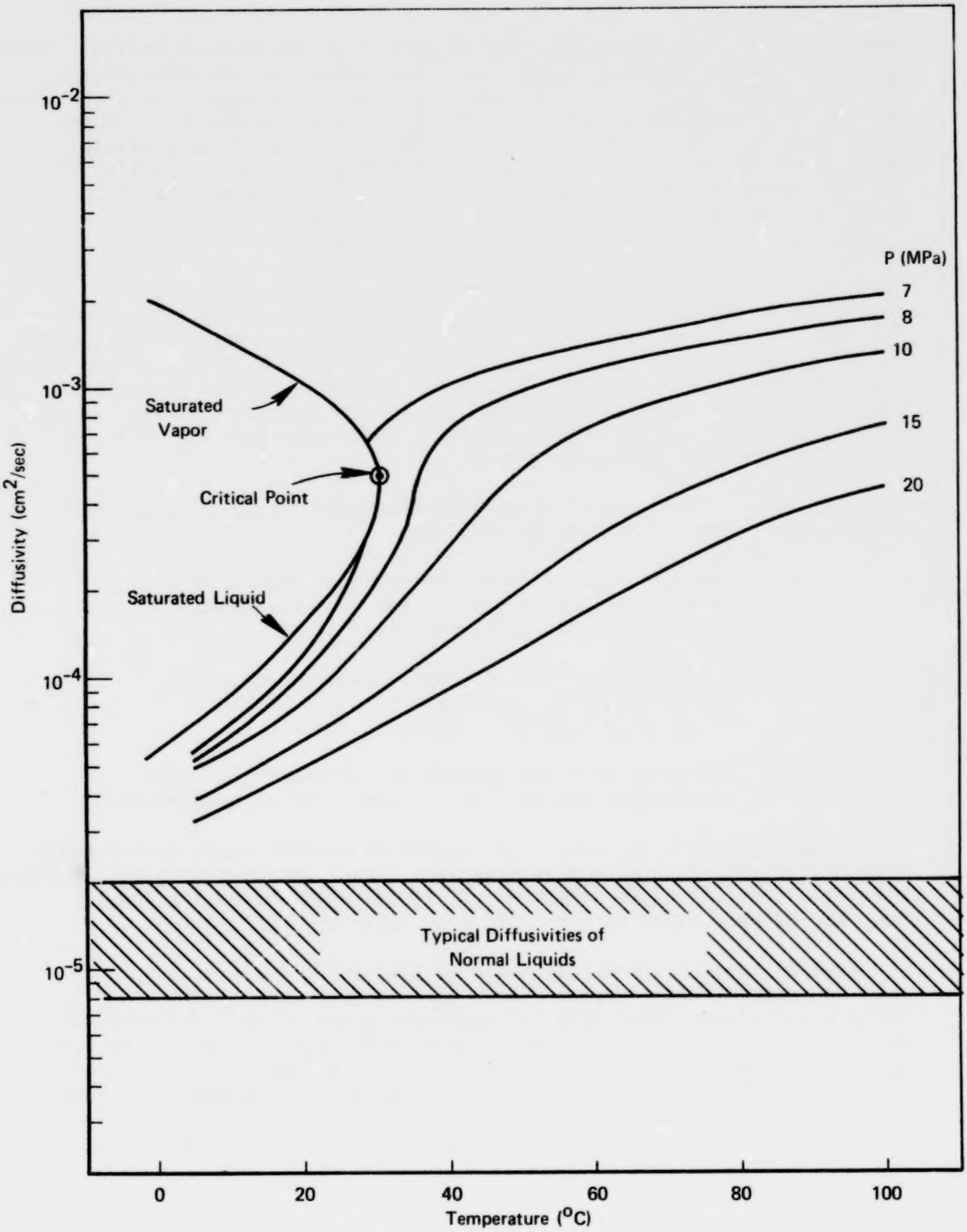

FIGURE IV-5 **DIFFUSIVITY OF CARBON DIOXIDE IN THE SCF AND NCL REGIONS**

TABLE IV-2

SOLUBILITIES IN LIQUID CO_2 AT 25°C AND ITS SATURATION PRESSURE

(Solubilities in Weight Percent)

M = Complete Miscibility

Paraffins and Naphthenes

n-Butane	M
Cyclohexane	M
Decahydronaphthalene (decalin)	22
2,2-Dimethylpentane	M
n-Dodecane	M
Ethane	M
n-Heptane	M
n-Hexadecane	8
Methylcyclobexane	M
n-Octadecane (mp 28°C)	3
Paraffin wax (mp 52°C)	.1
Propane	M
n-Tetradecane	16
2,2,3-Trimethylbutane (triptane)	M

Olefins

1-Decene	M
1-Octadecene	10
Propylene	M

Aldehydes

Acetaldehyde	M
Benzaldehyde	M
n-Butyraldehyde	M
Cinnamaldehyde	4
Crotonaldehyde	M
1-Heptaldehyde	M
Hydrocinnamaldehyde	17
Paraldehyde	M
Proprionaldehyde	M
Salicylaldehyde	M
Valeraldehyde	M

Aromatic

Benzene	M
Bibenzyl (mp 52.5°C)	1
Biphenyl (mp 71°C)	2
Chlorobenzene	M
α-Chloronaphthalene	1
Di-sec-butylbenzene	M
p-Dichlorobenzene (mp 53°C)	M
α,α-Dichlorotoluene	M
p-Dimethoxybenzene (mp 53°C)	M
Dimethylnaphthalenes (mixed)	2
2,4-Dinitrochlorobenzene (mp 62°C)	1
Diphenylmethane (mp 27°C)	4
o-Hydroxybiphenyl (mp 56°C)	1
2-Methoxybiphenyl (mp 29°C)	5
α-Methoxynaphthalene	1
α-Methylnaphthalene	6
β-Methylnaphthalene (mp 35°C)	9
Naphthalene (mp 52°C)	2
Nitrobenzene	M
o-Nitrobiphenyl (mp 37°C)	2
o-Nitrochlorobenzene (mp 32°C)	21
α-Nitronaphthalene (mp 58°C)	1
o-Nitrotoluene	M
p-Nitrotoluene (mp 51°C)	20
Phenylcyclohexane	8
Tetrahydonaphthalene (tetralin)	12
Toluene	M
Tri-sec-butylbenzene	M
α,α,α-Trichlorotoluene	2

Ketones

Acetone	M
Acetophenone	M
Benzalacetone (mp = 42°C) (4-Phenyl-3-butane-2-one)	5
Benzophenone (mp = 48°C)	4
2-Butanone (methyl ethyl ketone)	M
Chloroacetone	M
Cyclohexanone	M
2,5-Hexanedione	M
4-Hydroxy-4-methyl-2-pentanone (diacetone alcohol)	M
2-Octanone	M

TABLE IV-2 (continued)

SOLUBILITIES IN LIQUID CO_2 AT 25°C AND ITS SATURATION PRESSURE

(Solubilities in Weight Percent)

Alcohols

t-Amyl alcohol	M
Benzyl alcohol	8
sec-Butyl alcohol	M
t-Butyl alcohol	M
β-chloroethanol	10
Cinnamyl alcohol (mp 30°C)	5
Cyclohexanol	4
1-Decyl alcohol	1
Methanol	M
β-Ethoxyethanol (Cellosolve)	M
Ethyl alcohol	M
2-Ethylhexanol	17
Furfuryl alcohol	4
Heptyl alcohol	6.2
Hexyl alcohol	M
Isopropyl alcohol	M

Esters

Benzyl benzoate	10
Butyl oxalate	M
Butyl phthalate	8
Butyl stearate	3
β-Chloroethyl acetate	M
Ethyl acetate	M
Ethyl acetoacetate	M
Ethyl benzoate	M
Ethyl chloroacetate	M
Ethyl chloroformate	M
Ethylene diformate	M
Ethyl formate	M
Ethyl lactate	M
Ethyl maleate	M
Ethyl oxalate	M
Ethyl phenylacetate	M
Ethyl phthalate	10
Ethyl salicylate	M
Ethyl succinate	M
β-Hydroxyethyl acetate	17
Methyl acetate	M
Methyl benzoate	M
Methyl formate	M
Methyl phthalate	6
Methyl salicylate	M
Phenyl phthalate (mp 70°C)	1
Phenyl salicylate (mp 43)	9

Phenols

o-Chlorophenol	M
p-Chlorophenol (mp 43°C)	8
2-Chloro-G-phenyl phenol	1
o-Cresol (mp 30°C)	2
m-Cresol	4
p-Cresol (mp 36°C)	2
2,4 Dichlorophenol (mp 45°C)	14
p-Ethylphenol (mp 46°C)	1
o-Nitrophenol (mp 45°C)	M
Phenol (mp 41°C)	3
β-Methoxyethanol	M
p-Methylcyclohexanol	4
Phenylethanol	3
Tetrahydrofurfuryl alcohol	3

Carboxylic Acids

Acetic acid	M
Caproic acid	M
Caprylic acid	M
Chloroacetic acid (mp 61°C)	10
α-Chloroproprionic acid	26
Formic acid	M
Isocaproic acid	M
Lactic acid	0.5
Lauric acid	1
Oleic acid	2
Phenylacetic acid (mp 77°C)	0

Amides

Acetamide (mp = 82°C)	1
N,N-Diethylacetamide	M
N,N-Diethylformamide	M
N,N-Dimethylacetamide	M
N,N-Dimethylformamide	M
Formamide	0.5

TABLE IV-2 (continued)

SOLUBILITIES IN LIQUID CO_2 AT 25°C AND ITS SATURATION PRESSURE

(Solubilities in Weight Percent)

Amines and Nitrogen Heterocyclics	
Aniline	3
o-Chloroaniline	5
m-Chloroaniline	1
N,N-Diethylaniline	17
N,N-Dimethylaniline	M
Diphenylamine (mp 53°C)	1
N,N′-Diphenylethylene diamine (mp 62°C)	1
N-Ethylaniline	13
N-Ethyl-N-benzylaniline	4
N-Methylaniline	20
α-Naphthylamine (mp 52°C)	1
Phenylethanolamine	1
2,5-Dimethylpyrrole	5
Pyridine	M
o-Toluidine	7
m-Toluidine	15
p-Toluidine (mp 45°C)	7

Nitriles	
Acetonitrile	M
Acrylonitrile	M
Benzonitrile	M
β-Hydroxypropionitrile	1
Phenylacetonitrile	13
Succinonitrile (mp 54.5°C)	2
Tolunitriles (mixed)	M

By comparison of Figs. IV-2 and IV-5 it can be seen that the decrease in diffusivity with density is less than the increase in solubility with density: at 40^oC, the diffusivity decreases from 80 atm ($8x10^{-4}$ cm^2/sec) to 120 atm ($1.5x10^{-4}$) by a factor of 5.3, while the solubility increases from 80 atm (0.1 mole-%) to 120 atm (1.2 mole-%) by a factor of 12. Thus, we see that the gain in solubility at higher density more than outweighs the decrease in diffusivity. Furthermore, the diffusivities in the SCF range are at least an order of magnitude higher than that of conventional liquid solvents.

Indirect evidence for rapid mass transfer can be gleaned from the field of supercritical fluid chromatography, where the SCF is used as the mobile phase for column elution with liquid or solid stationary phases (Gouw, 1975; Rijnders, 1969). The conventional technique of discrete peak column chromatography is closely aligned to frontal chromatography which, in turn, is equivalent to extraction of solutes from adsorbents. In other words, the retention time in SCF chromatography depends on the combination of solubility and mass transfer characteristics in much the same manner as does extraction.

An example of the decrease in retention obtainable by increasing density of the mobile phase is shown in Fig. IV-6 (Sie, 1966). The chromatograms were obtained with CO_2 as the carrier at 40^oC with a squalane stationary phase. The three curves show the effect of increasing pressure from 1 atm (gas) to 50 atm (expanded supercritical fluid; reduced density = 0.2) to 80 atm (supercritical fluid; reduced density = 1.2). The retention time for octane decreases by a factor of 10 in going from 1 to 50 atm and by another factor of 3 at 80 atm. One of the technical inconveniences in SCF chromatography is that the SCF mobile phase can extract the stationary liquid phase. The squalane stationary phase used in Fig. IV-6 is the C_{30} solute shown in Fig. IV-4. Although the conditions used in the SCF chromatography lie below the squalane critical locus, there is a finite solubility of squalane in the carrier at high pressure, resulting in migration of the stationary phase.

A striking example of the ability of SCF CO_2 to extract non-volatile hydrocarbons is shown in Fig. IV-7 (Jentoft, 1976). This separation was carried out at 39^oC and 122 atm. Within 40 min, methyl-substituted benzanthracenes are eluted. Fig. IV-8 illustrates the separation of a variety of oxygenated hydrocarbons using pressure programming of supercritical CO_2 from 55 to 117 atm. The Carbowax 400 stationary phase shows significant migration under these conditions; carbowax 4000 has a solubility of 1.7 wt-% in SCF CO_2 (Giddings, 1968).

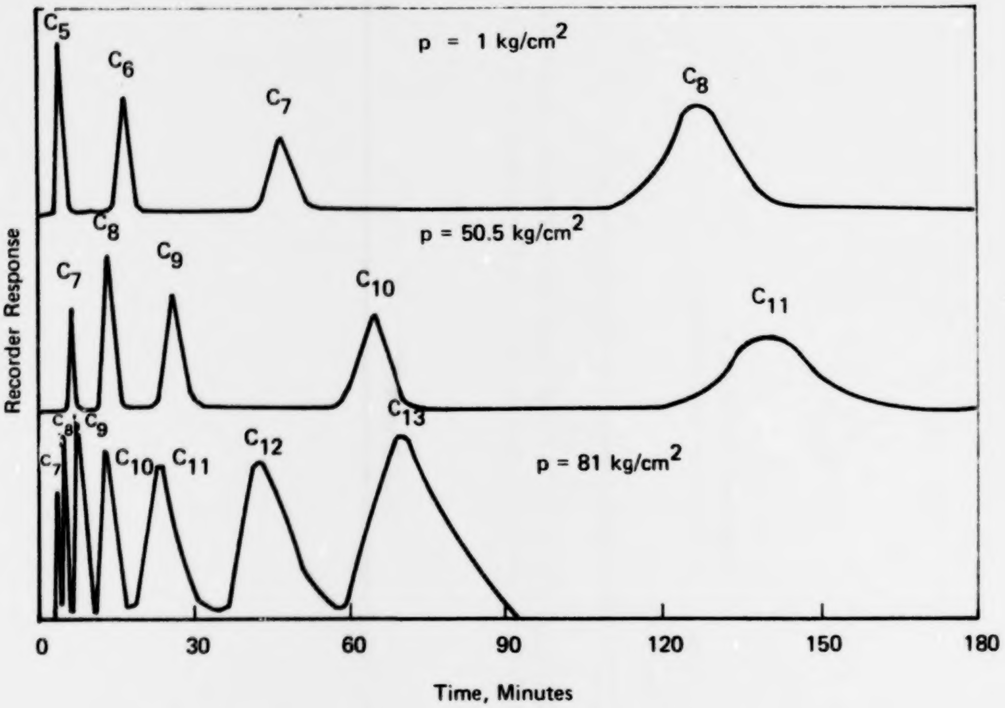

FIGURE IV–6 SEPARATIONS OF N–ALKANES ON A SQUALANE COLUMN AT 40°C WITH CO_2 AS A CARRIER AT DIFFERENT PRESSURES AND COMPARABLE LINEAR RATES OF MOBILE PHASE.
(Sie, et al., 1966)

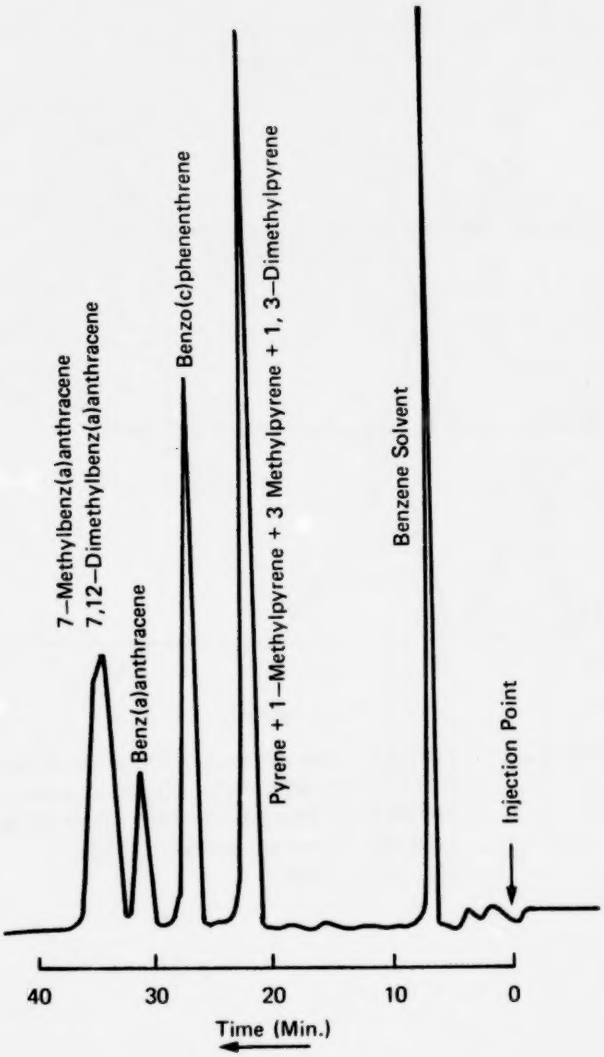

FIGURE IV–7 SEPARATION OF POLYNUCLEAR AROMATIC HYDROCARBONS ON "PERM PHASE" ETH: CO_2 MOBILE PHASE AT 39°C AND 120 atm (Jentoft and Gouw, 1976)

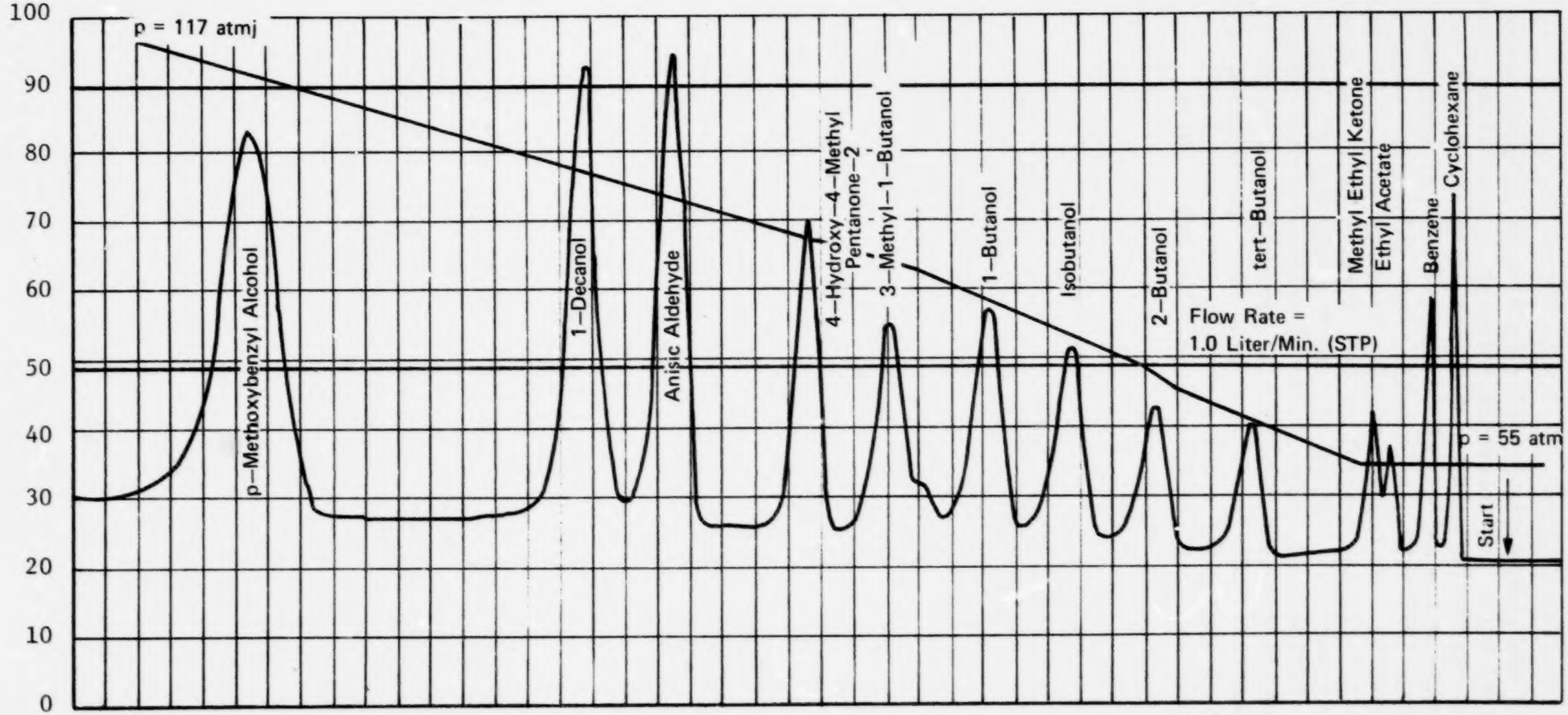

FIGURE IV- 8 CHROMATOGRAM OF SOME OXYGENATED COMPOUNDS. COLUMN: CARBOWAX 400 ON PORASIL. MOBILE PHASE: CO_2 AT 40°C. PRESSURE PROGRAMMED FROM 5 TO 115 atm. (Gouw amd Jentoft, 1975)

As a result of the unique characteristics of high solubility and rapid mass transfer, there is increasing interest in exploiting supercritical fluids as extracting agents. A number of recent French and German patents describe the use of SCF CO_2 to extract caffeine from coffee and tea (Hag, 1973 a,b), cocoa butter from pulverized kernels (c), aroma constituents from pepper, cloves, cinnamon and vanilla beans (d) and selective extraction of nicotine from tobacco (e). The extracts are free of trace impurities that would stem from the use of organic liquid solvents. Furthermore, degradation of heat-sensitive solutes is avoided because the processes employ mild temperatures, in the range of 30 to $60^{o}C$. Supercritical fluids have also been investigated as potential extracting agents for crude petroleum and residual oil (Zhuze, 1957), coal tar (Wise, 1970) and coal (Maddocks, 1979).

V. PESTICIDE SCREENING STUDIES

A. INTRODUCTION

Six pesticides were selected for initial screening based upon considerations such as large production volume, inclusion of a variety of organic classes in the screening, and reasonable safety in handling in laboratory tests. The pesticides selected for laboratory testing were Carbaryl, Alachlor, Pentachlorophenol, Atrazine, Trifluralin and Diazinon. Technical and commercial information about each one is given in Table V-1. The molecular structure of the species is given in Table V-2 in order to give a graphic illustration of the complexity of the molecules; as was related previously, not only do organic moledules such as simple alcohols and carboxylic acids dissolve in SCF CO_2, but complex polynuclear aromatic and heterocyclics as well.

In the screening phase, the following tests were carried out:

1. Measurement of pesticide solubility in supercritical CO_2 at several temperature and pressure levels.
2. Determination of the adsorption isotherm on GAC of a solution of pesticide in water.
3. Measurement of dynamic adsorption breakthrough using a solution of pesticide in water.
4. Measurement of the extent of regeneration by subsequent re-adsorption tests to determine capacity and capacity recovery of GAC.

B. APPARATUS AND TEST PROCEDURES

The apparatus for the four general classes of tests stated above, the experimental methods of obtaining data, and the calculational methods for reducing the data to solubility and capacity values are described below. Other tests requiring apparatus and procedures not previously seen in the literature are presented in subsequent sections as they arise.

1. Determination of Pesticide Solubility

Before carrying out adsorption and regeneration tests on GAC which had been loaded with a pesticide, it was necessary to determine the solubility of the pesticide in SCF CO_2; clearly, if the pesticide were not soluble in SCF, it could not be removed from spent GAC.

TABLE V-1

PESTICIDES SELECTED FOR SCREENING STUDIES

Pesticide	Class	Trade Name	Production Volume in 10^6 lbs/yr	Toxicity LD_{50} (Mg/Kg)
Carbaryl	Alkyl carbamate, insecticide	Sevin, Hexavin	50	560
Alachlor	Acetanilide herbicide	Lasso	30	3,000
Atrazine	Triazine, herbicide	AA tram, Fenamine	200	3,080
Pentachlorophenol	Wood preservative, Molluscicide	Dowicide, Pentachlor	70	125-210
Trifluralin	Nitroaromatic, herbicide	Treflan	35	3,700
Diazinon	Organophosphate, Insecticide	Spectracide, Diazide	15	100-150

TABLE V-2 **PESTICIDES (AND CLASS) TESTED FOR SOLUBILITY IN CARBON DIOXIDE**

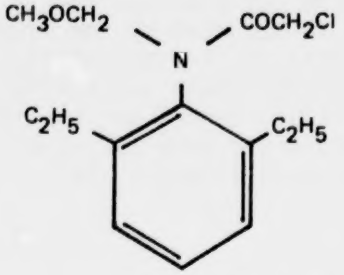

ALACHLOR (Acetanilide)

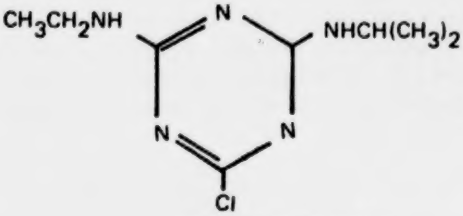

ATRAZINE (Triazine)

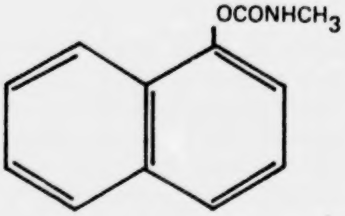

CARBARYL (Carbamate)

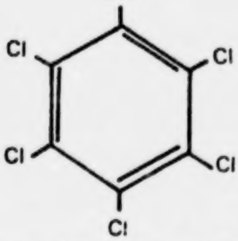

PENTACHLOROPHENOL (Chlorophenol)

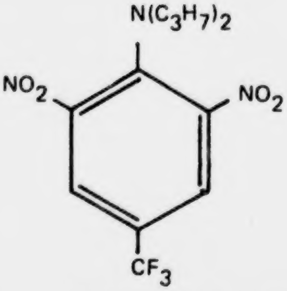

TRIFLURALIN (Nitroaromatic)

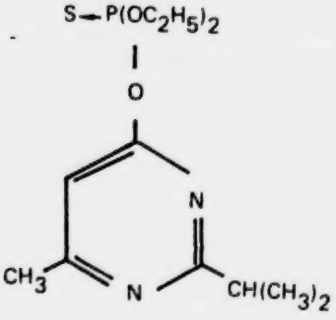

DIAZINON (Organophosphate)

A schematic diagram of the laboratory apparatus used for solubility measurements is shown in Figure V-1; details of the size and rating of the individual components are given in Table V-3. In carrying out a solubility determination, a given amount of material is loaded into the extraction vessel, the system pressurized to a given level by compressing CO_2 from the supply SCF CO_2 flow rate through the sample collector, and is measured by the rotameter and dry test meter. The CO_2 flow rate for[*] almost all the solubility measurements was in the range of about 5-10 SLM. For a single solubility determination, the flow of SCF CO_2 through the extraction vessel was continued for several minutes, stopped, and the collector removed and weighed. The increase in wieght represented the amount of pesticide collected. The solubility, in weight percent, was calculated as

$$C = \left(\frac{\text{weight of pesticide}}{\text{weight of } CO_2 \text{ passed through + weight of pesticide}}\right) \times 100$$

2. Granular Activated Carbon

The characteristics of the granular activated carbons used are summarized in Table V-4. The standard carbon used was Filtrasorb®-300, which is in wide application in industry today; unless otherwise indicated, all tests were run with Filtrasorb®-300.

3. Adsorption Isotherm in Water

Standard methods of obtaining adsorption isotherms were used. In the experimental procedure, a Wrist Action Shaker Table was normally used to agitate flasks which contain a given volume of pesticide solution (either synthetic or real wastewater) to which has been added a given amount of GAC. Measurement of the concentration change over the duration of the test allows the loading, X, in grams pesticide/gram GAC to be calculated from the experimental data as

$$X = \frac{\text{ppm}_{\text{initial}} - \text{ppm}_{\text{final}}}{\text{ppm GAC}}$$

Results are usually plotted logarithmically to give a Freundlich isotherm, as shown schematically in Figure V-2. The concentration was measured by ultraviolet spectrophotometry using a Perkin Elmer 550 doublebeam spectrophotometer. The UV spectrophotometer was calibrated by preparing solutions of various concentrations and determining the calibration curve at that wavelength as

$$\text{Response} = k \text{ (concentration)}$$

where k is the slope of the line (millivolts/ppm)

---

[*] Standard liters per minutes, referenced to 25°C and 1 atm pressure.

FIGURE V-1

EXPERIMENTAL APPARATUS FOR SUPERCRITICAL FLUID EXTRACTION

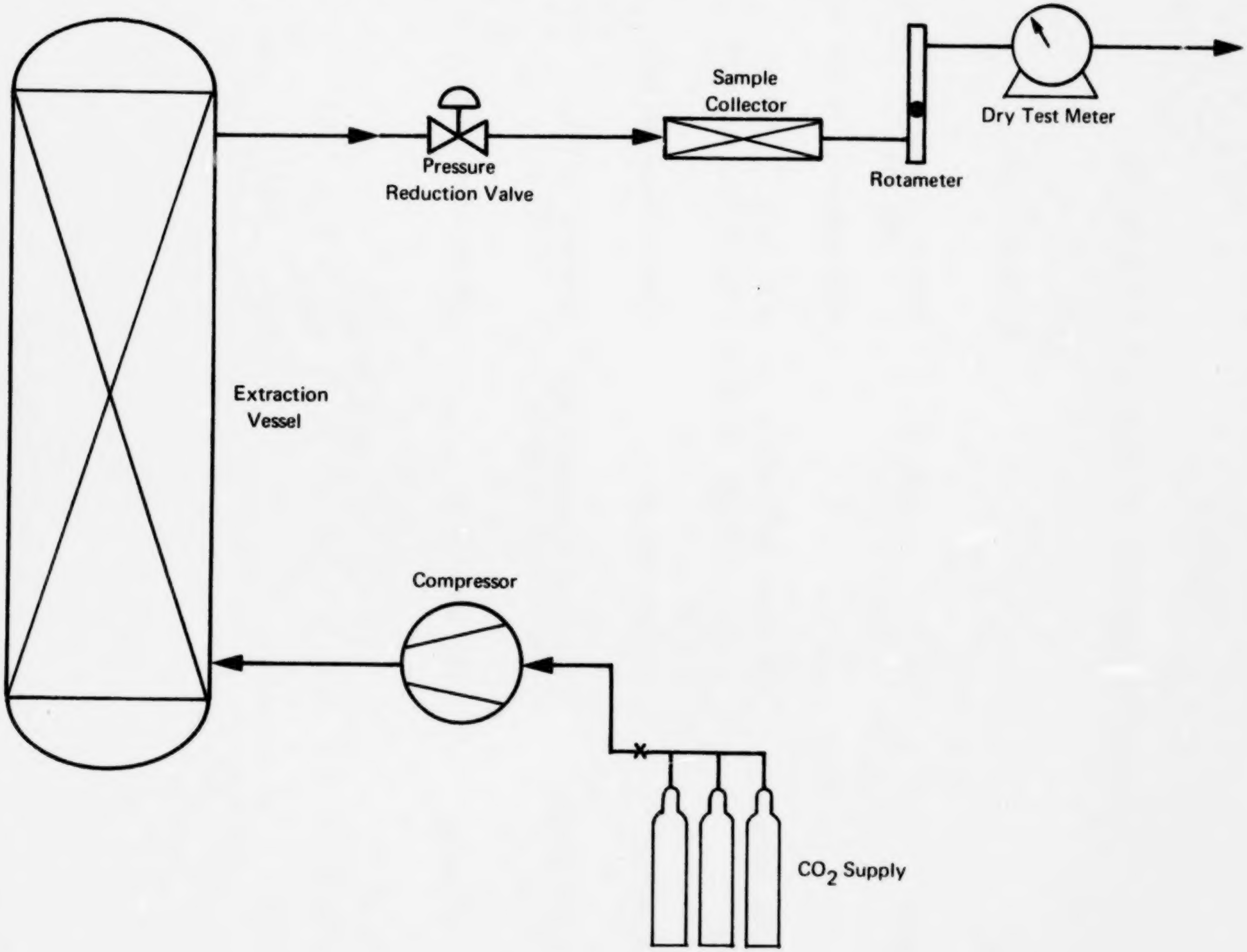
Sample Collector
Dry Test Meter
Pressure Reduction Valve
Rotameter
Extraction Vessel
Compressor
CO_2 Supply

TABLE V-3

EXPERIMENTAL APPARATUS FOR SOLUBILITY DETERMINATION

Item	Make	Characteristics
Compressor	American Instruments, Model 46-13427	Working pressure, 30,000 psi Displacement, 120 cc/min
Extraction Vessel	American Instruments	3/8" ID x 11" tubing
Rotameter	Fisher & Porter, 10A3565Y	Flow rating, 100 SLPM
Dry Test Meter	Singer, DTM 200	Flow rating, 200 SCFH
Valving and Piping	American Instrument and Autoclave Engineers	Pressure rating, 10,000 psi
Sample Collector	SGA Scientific	200 mm Drying Tube

TABLE V-4

CHARACTERISTICS OF ACTIVATED CARBON USED

Type	Manufacturer	Mesh Size	Surface Area M^2/g
F-300	Calgon	8-30	950-1050
F-400	Calgon	12-40	1050-1200
GX-31	Amoco	16-30	2300-2500
XE-348	Rohm & Haas	20-50	500

FIGURE V-2 **ADSORPTION ISOTHERM**

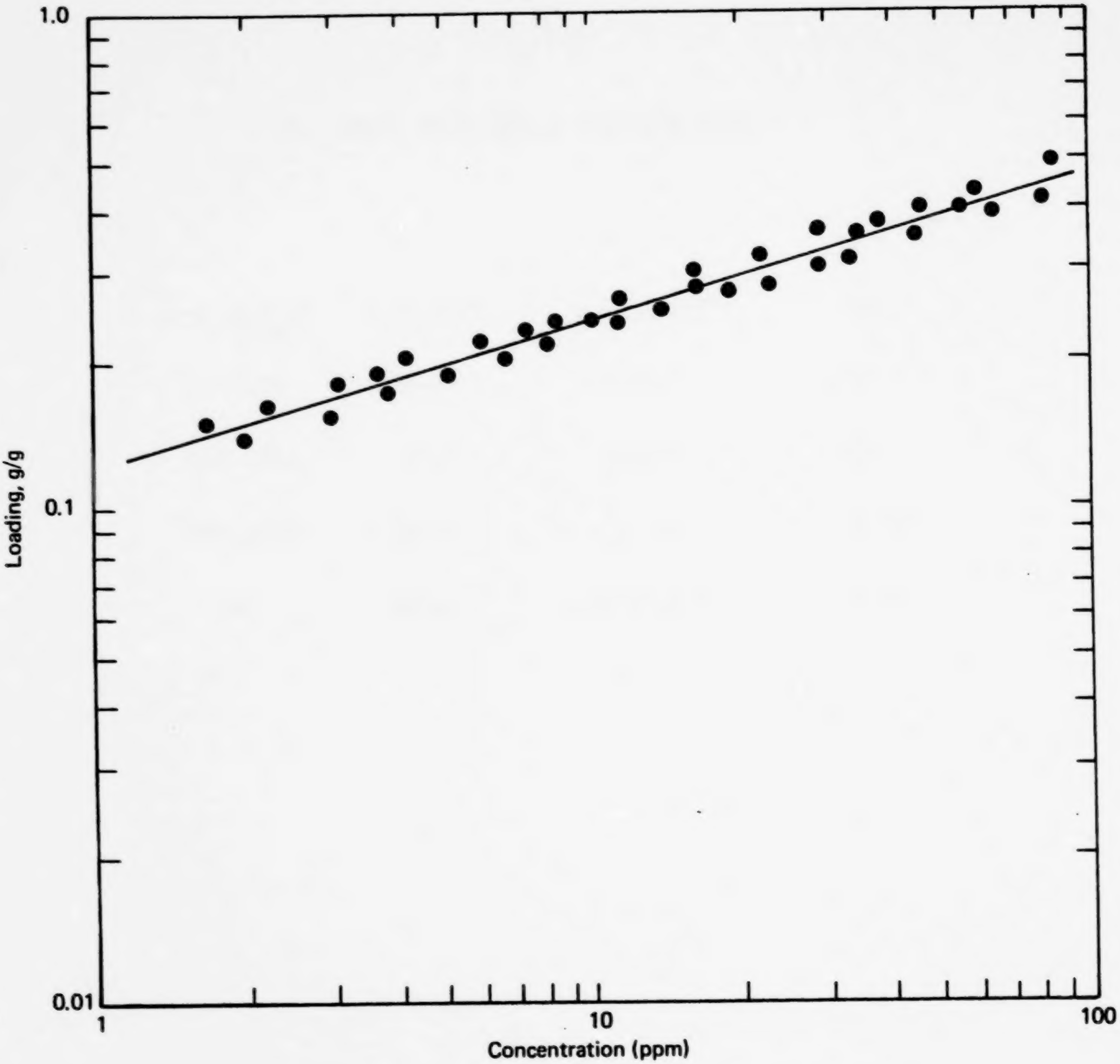

During the determination of the adsorption isotherms, the solution concentrations were determined periodically. A sample of about 2 ml from each flask was pipetted into a quartz UV cell, the response obtained, and the 2 ml aliquot returned to the flask. These periodic concentration measurements were plotted and used to determine the approach to equilibrium and ultimately the equilibrium loading on GAC; a plot of the measurements shows the rate of concentration change (i.e., and adsorption rate curve), and a representation of two such rate curves for two different GAC concentrations is shown in Figure V-3.

4. Dynamic Adsorption Breakthrough Curves

The schematic diagrams of the adsorption apparatus is shown in Figure V-4, and the details of the individual components are listed in Table V-5.

The breakthrough concentration-vs-time curve was obtained either by continuous on-line UV monitoring of the column effluent in a flow-through cell or by measuring individual grab samples obtained with a fraction collector.

Two different flow rates were used in the adsorption tests, 7.5 gpm/ft^2 (0.51 cm/sec) and 1.1 gpm/ft^2 (0.075 cm sec); the high flow rate resulted in a faster breakthrough and was used in the initial screening tests in order to assess in a reasonably short period of time the multicycle regeneration behavior of GAC loaded with a given pesticide. Later in the Process Development portion of the program, adsorption tests were carried out at a flow rate of 1.1 gpm/ft^2 which more nearly approximates the flow rate used in many industrial and municipal GAC installations. Representative examples of breakthrough curves are shown in Figures V-5 and V-6 for high and low flow rates, respectively. In almost all adsorption tests the synthetic solution was prepared at about 80-85% of the solubility limit of pesticide in water.

Determination of the amount of pesticide adsorbed on GAC was carried out in several parallel ways: in integration of the breakthrough curve as indicated in Figures V-5 and V-6; by measurement of the average concentration of the total effluent collected from which the loading value is calculated as

$$X = \frac{(\text{Total volume})\ (C_{in} - C_{off})}{\text{g GAC}}$$

and in some cases by determining the actual amount loaded by gravimetric means

$$X = \frac{\text{Change in weight of the GAC}}{\text{Weight of GAC}}$$

For the gravimetric determination the GAC was dried with CO_2 at 1 atm and 55°C, conditions which were found to remove only water and no pesticide.

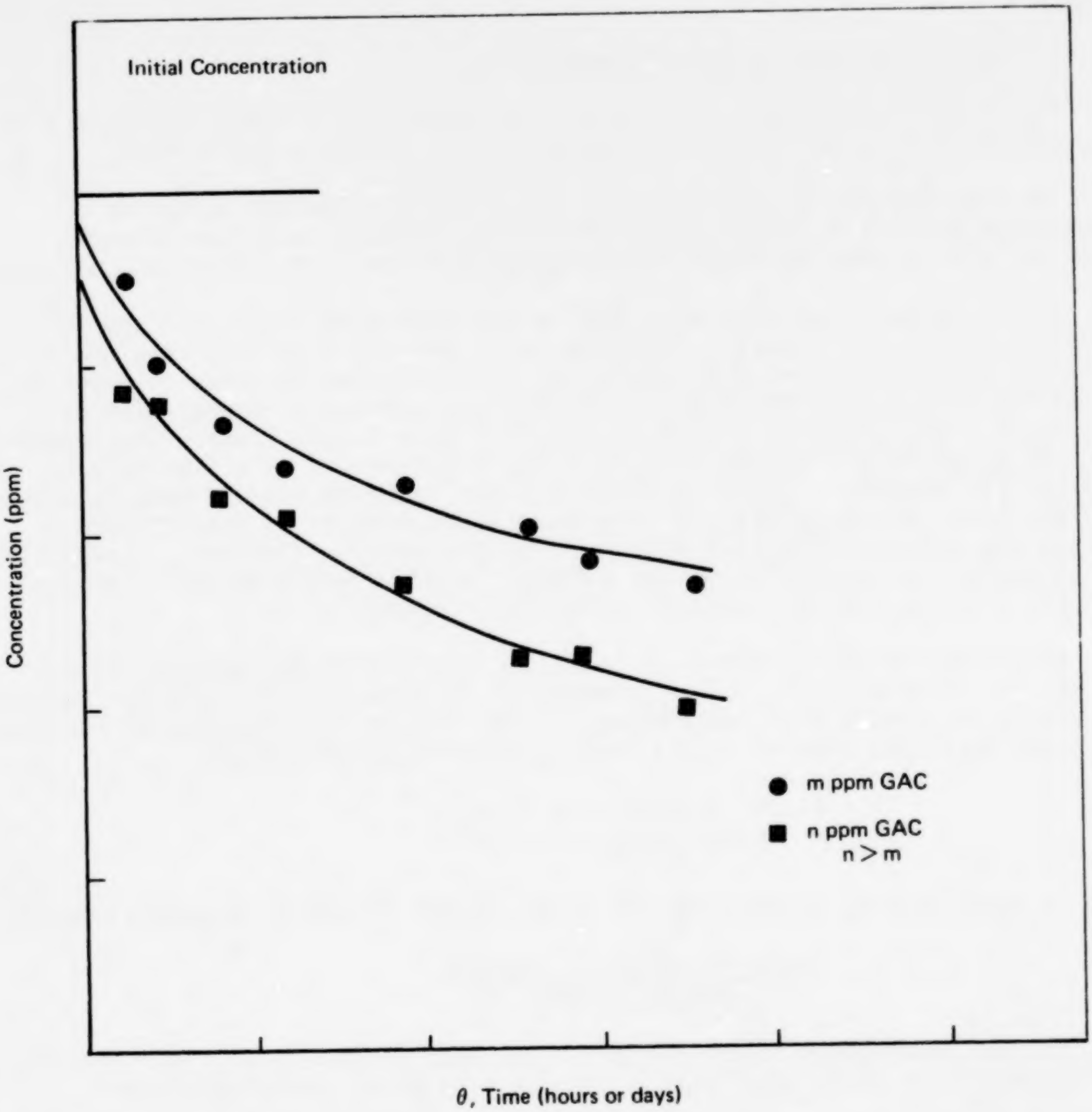

FIGURE V–3 BATCH ADSORPTION RATE CURVES

FIGURE V-4

SCHEMATIC DIAGRAM OF ADSORPTION APPARATUS

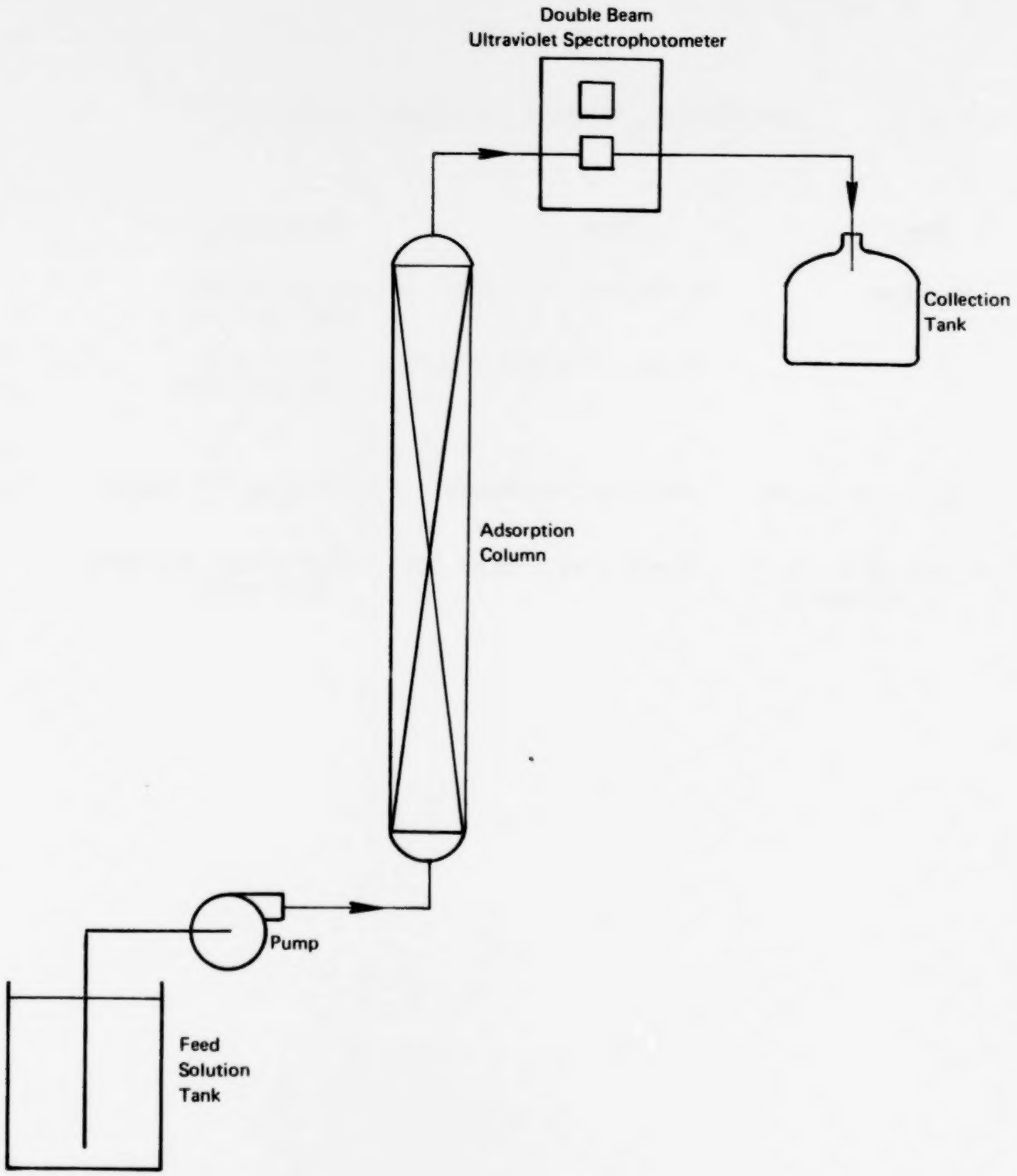
Double Beam
Ultraviolet Spectrophotometer
Collection
Tank
Adsorption
Column
Pump
Feed
Solution
Tank

TABLE V-5

EXPERIMENTAL APPARATUS FOR DYNAMIC ADSORPTION

Item	Make	Characteristics
Feed Pump	Milton Roy, Mini Pump	0.2-3.2 ml/min (for low flow)
	Gilson, HP 4/HF Minipuls	0-100 ml/min (for high flow)
Adsorption Column	American Instruments	3/8" ID x 11" Tubing
Ultraviolet Spectrophotometer	Perkin-Elmer, Model 550	Double Beam, Variable Wavelength

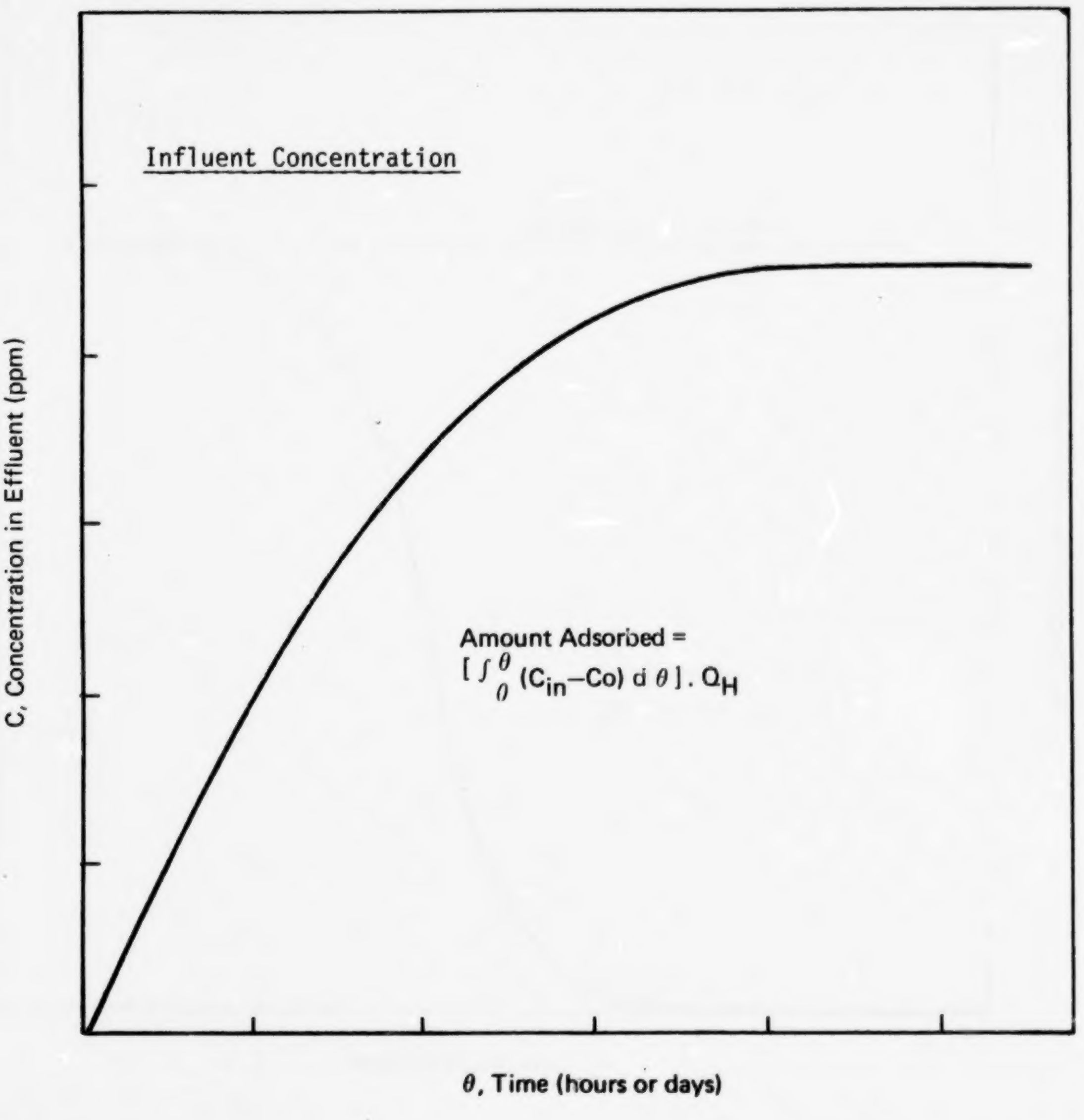

FIGURE V-5 ADSORPTION BREAKTHROUGH CURVE, HIGH FLOW RATE Q_H

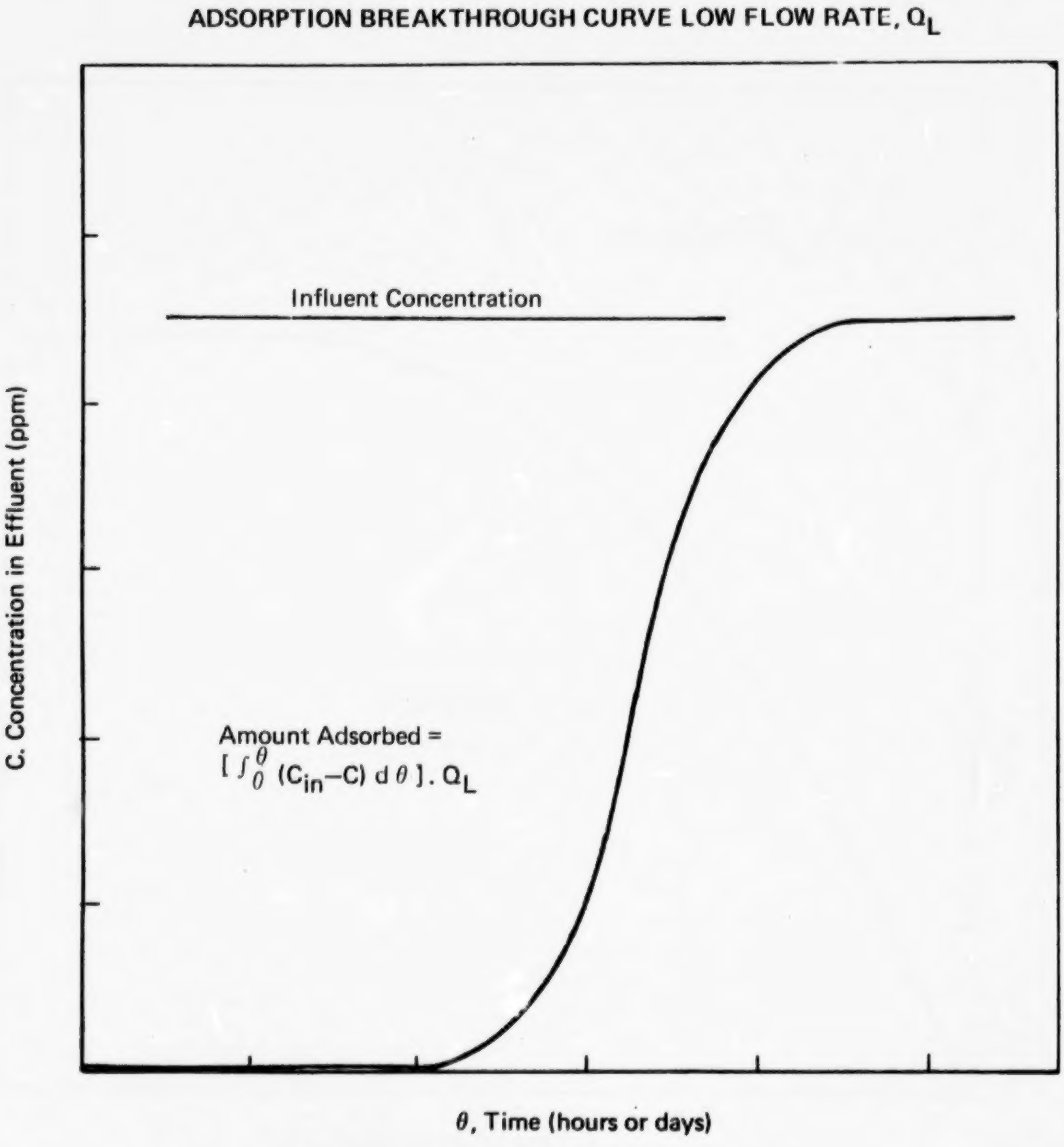

FIGURE V-6 ADSORPTION BREAKTHROUGH CURVE, LOW FLOW RATE Q_L

5. Regeneration With Supercritical CO_2

The regeneration apparatus was essentially identical to the solubility apparatus shown in Figure V-1, the extraction vessel replaced with a GAC-filled column of the same size. Regeneration tests were carried out in situ on a pesticide-spent GAC column in the same manner as a solubility test; a given amount of CO_2 at a given pressure was passed through the column, regulated by the flow control valve, and expanded to 1 atm. The reduction in pressure caused the pesticide to precipitate from the CO_2 in the sample collector and the total CO_2 passing through the collector was measured by the rotameter and dry test meter. The amount of pesticide precipitated in the collector was weighed and compared to the residual weight remaining on the GAC to assess the closure of the material balance. In almost all cases, material balances closed to within 90-95%.

After each regeneration, a re-adsorption test was made with the GAC column, again in situ, the breakthrough curve measured, and the loading obtained as described earlier for the virgin GAC tests. The ratio of the loadings, X, for the second and first cycle adsorption is the percent capacity recovery after one cycle

$$\text{Recovery (\%)} = \frac{X_2}{X_1} \quad (100)$$

The average capacity recovery after n cycles is given by the expression

$$\text{Average Capacity Recovery (\%)} = \sqrt[n-1]{\frac{X_n}{X_1}} \cdot 100$$

Other apparatus and test procedures are presented as they relate to specific tests.

C. RESULTS OF SCREENING TESTS

1. Solubility in Supercritical Carbon Dioxide

The solubility of the pesticide in supercritical CO_2 was a primary criterion for pesticide selection. Solubilities of each pesticide were measured at 275 atm's (4000 psia) and two temperature levels: 70°C and 120°C. These data are summarized in Figure V-7.

As shown, the solubilities vary over a range of more than two orders of magnitude. Trifluralin is soluble to the extent of about 20 wt. %; Alachlor and Diazinon have solubilities in the range of 5% to 10%; Pentachlorophenol on the order of 1%; Atrazine and Carbaryl on the order of .1 to .4 wt. %.

Because it is desirable to run the regeneration at as low a pressure as possible, some additional testing was done for solubilities at 150 atm's, and the results are shown in Figure V-8. Both Alachlor and Carbaryl were tested, and both showed solubility decreases of about an order of magnitude.

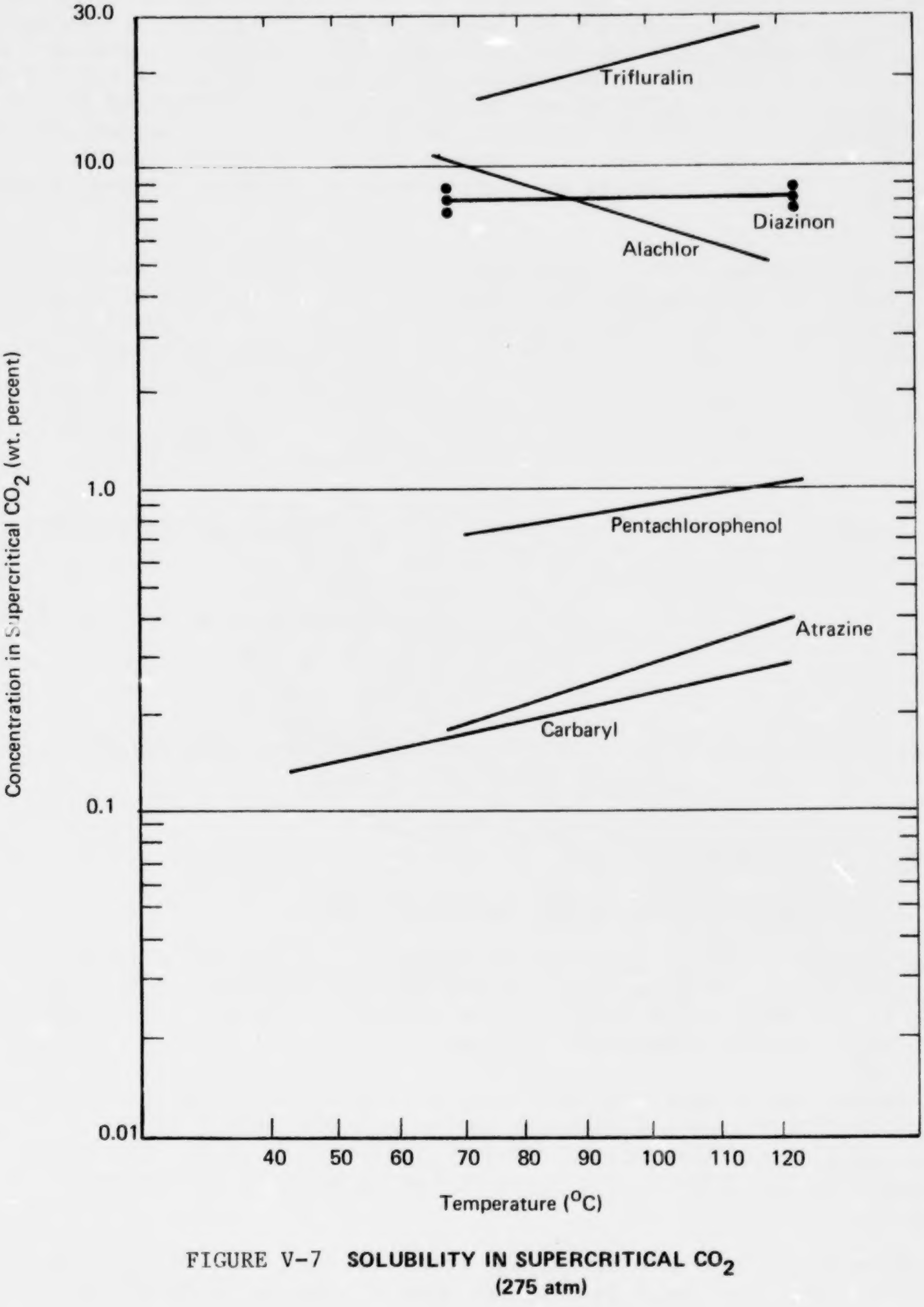

FIGURE V-7 **SOLUBILITY IN SUPERCRITICAL CO_2**
(275 atm)

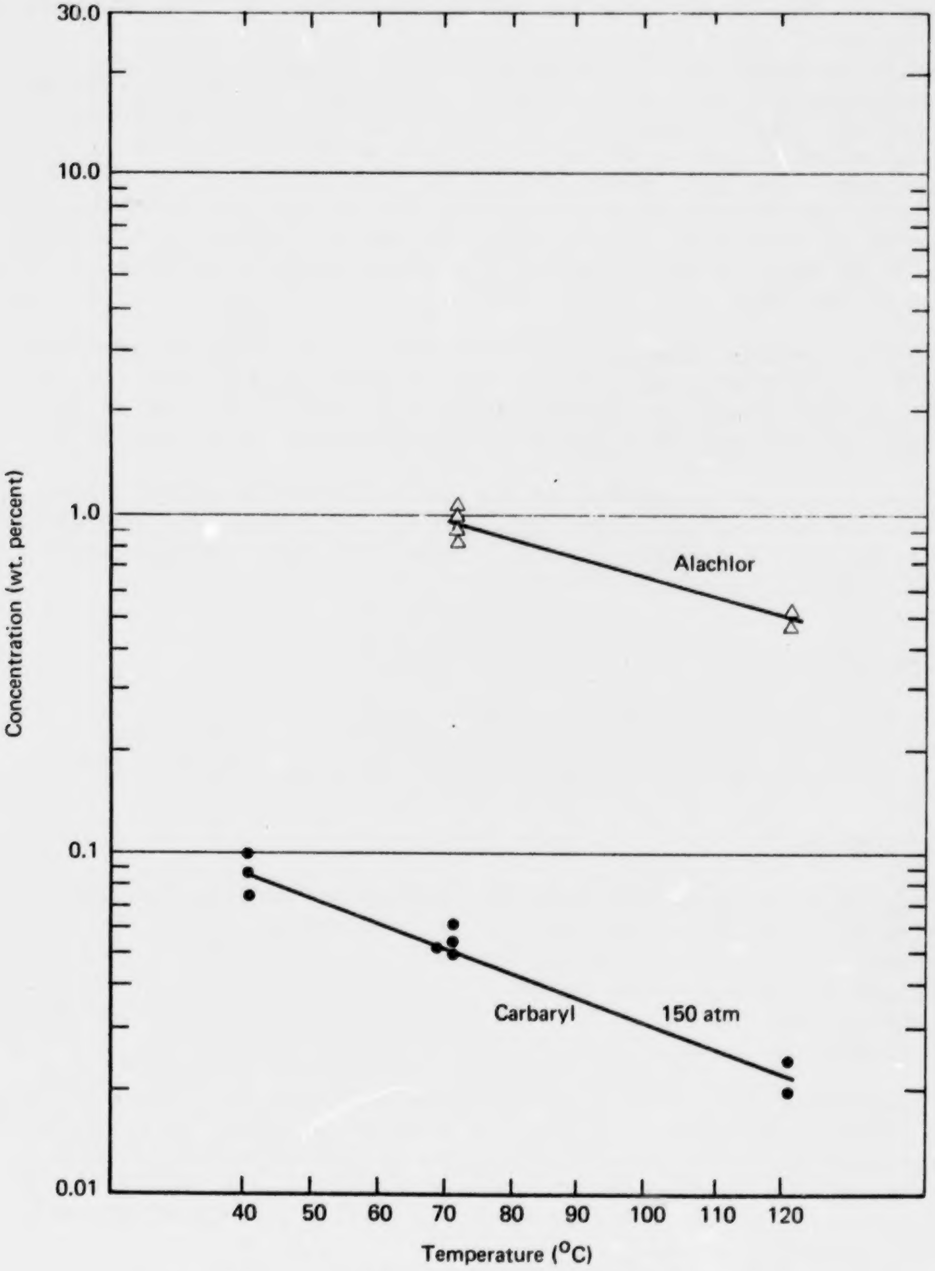

FIGURE V-8 **SOLUBILITY IN SUPERCRITICAL CO_2**

2. Adsorption Isotherms

Adsorption isotherms for Alachlor, Atrazine Carbaryl, and Diazinon are given in Figure V-9. In each case, loadings were greater than 0.1 weight of adsorbate per weight of granular activated carbon; in fact, with the exception of Atrazine, these pesticides showed adsorptions in excess of 0.2 grams per gram of GAC over the entire concentration range studied.

It should be noted that the organic content of wastewaters from pesticide manufacturing will often contain only a small proportion of the pesticide product itself. However, the pesticide is usually difficult to treat biologically, and is often selectively adsorbed relative to the organics present. For this reason, it is important to determine the suitability of GAC for the pesticide alone, even though the total organic carbon removed by adsorption treatment may be small. Selective adsorption of the pesticide would allow biological treatment to effect removal of the balance of the TOC.

Adsorption isotherm studies were attempted for Trifluralin and Pentachlorophenol. Trifluralin was discontinued because, at the very low Trifluralin concentrations in aqueous solution (about 1 ppm) the weight of adsorption was too low for adsorption in a practical time period.

Preliminary column adsorption studies with Pentachlorophenol showed that breakthrough was very diffuse, and thus GAC adsorption did not appear to be effective as a treatment process. Because of this, further study of Pentachlorophenol was discontinued.

3. Regenerability

Repeated adsorption/regeneration cycles were performed for four pesticides: Carbaryl, Diazinon, Atrazine and Alachlor. Performance in these tests were judged as the final citerion for pesticide selection.

a. Carbaryl

Two separate series of Carbaryl adsorption/regeneration tests were carried out. Rapid loading adsorption breakthrough curves for Series C-1 are given in Figure V-10 and for Series C-2 in Figure V-11. C-1-A1 and C-2-A1 are the breakthrough curves forCarbaryl adsorption on virgin GAC, and the -A2 and -A3 curves are the breakthrough curves for the second and third adsorption tests after previous regeneration.

The conditions for regeneration of Carbaryl-loaded GAC were 275 atm at either 120°C or 70°C and at a CO_2 flow rate of 10 SLM. The duration of the regeneration period was chosen on the basis of the solubility measurements and the loading of pesticide on the GAC. The amount of CO_2 required to remove the pesticide based on solubility considerations was calculated from the relation

$$\text{Solubility (wt \%)} - \left(\frac{\text{grams pesticide on GAC}}{\text{grams CO passed through column}}\right) \times 100$$

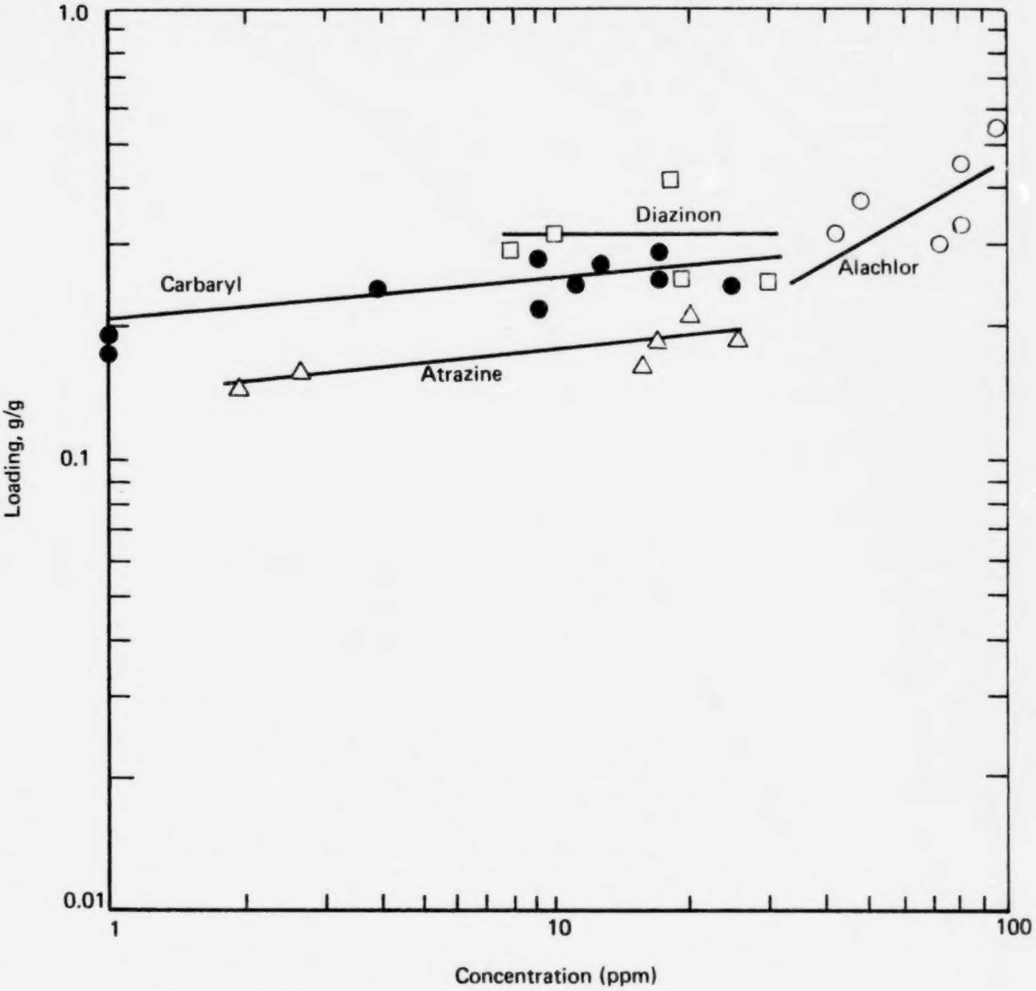

FIGURE V-9 **ADSORPTION ISOTHERMS FROM AQUEOUS SOLUTIONS**

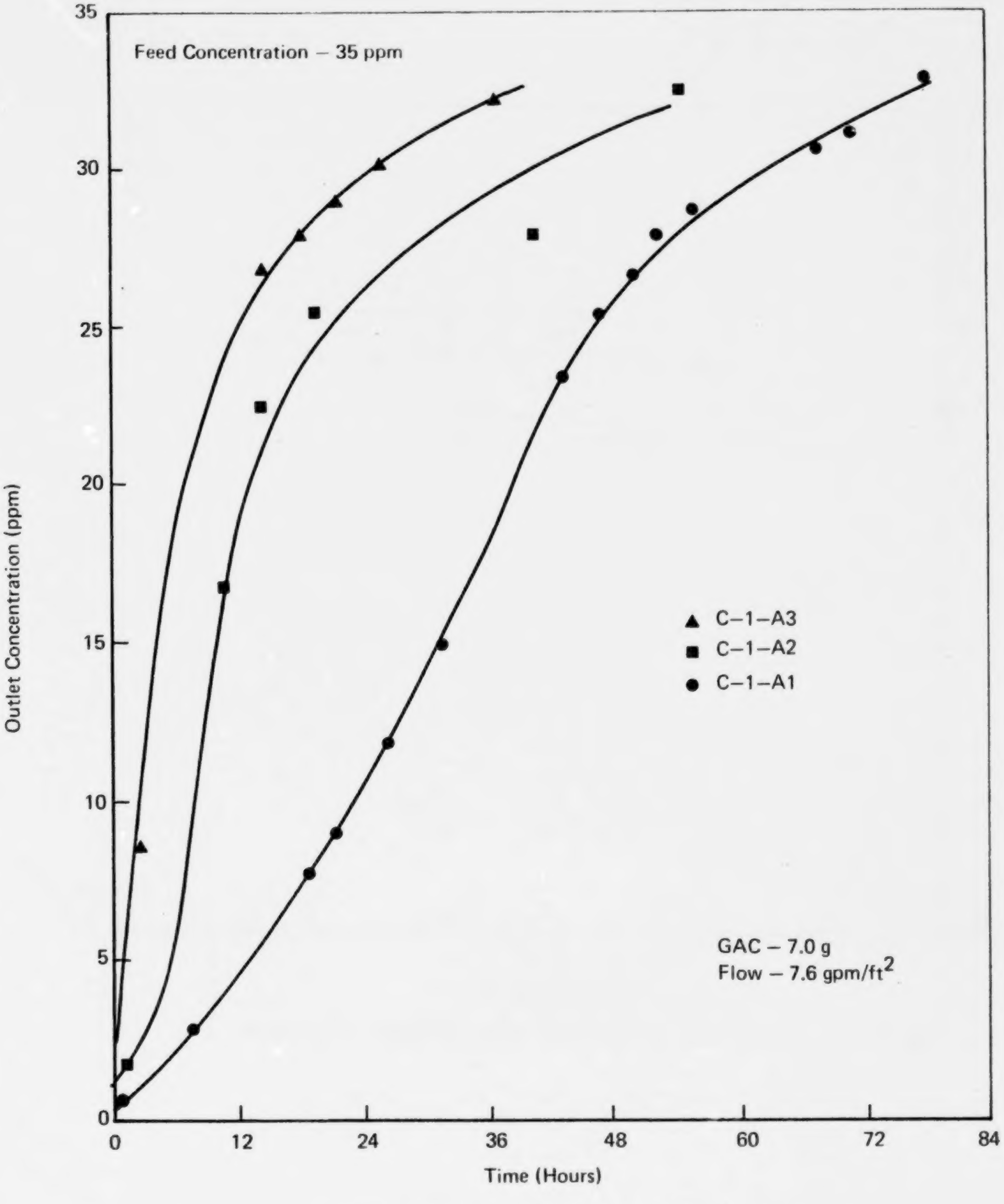

FIGURE V-10 **ADSORPTION FROM CARBARYL SOLUTION (SERIES C–1)**

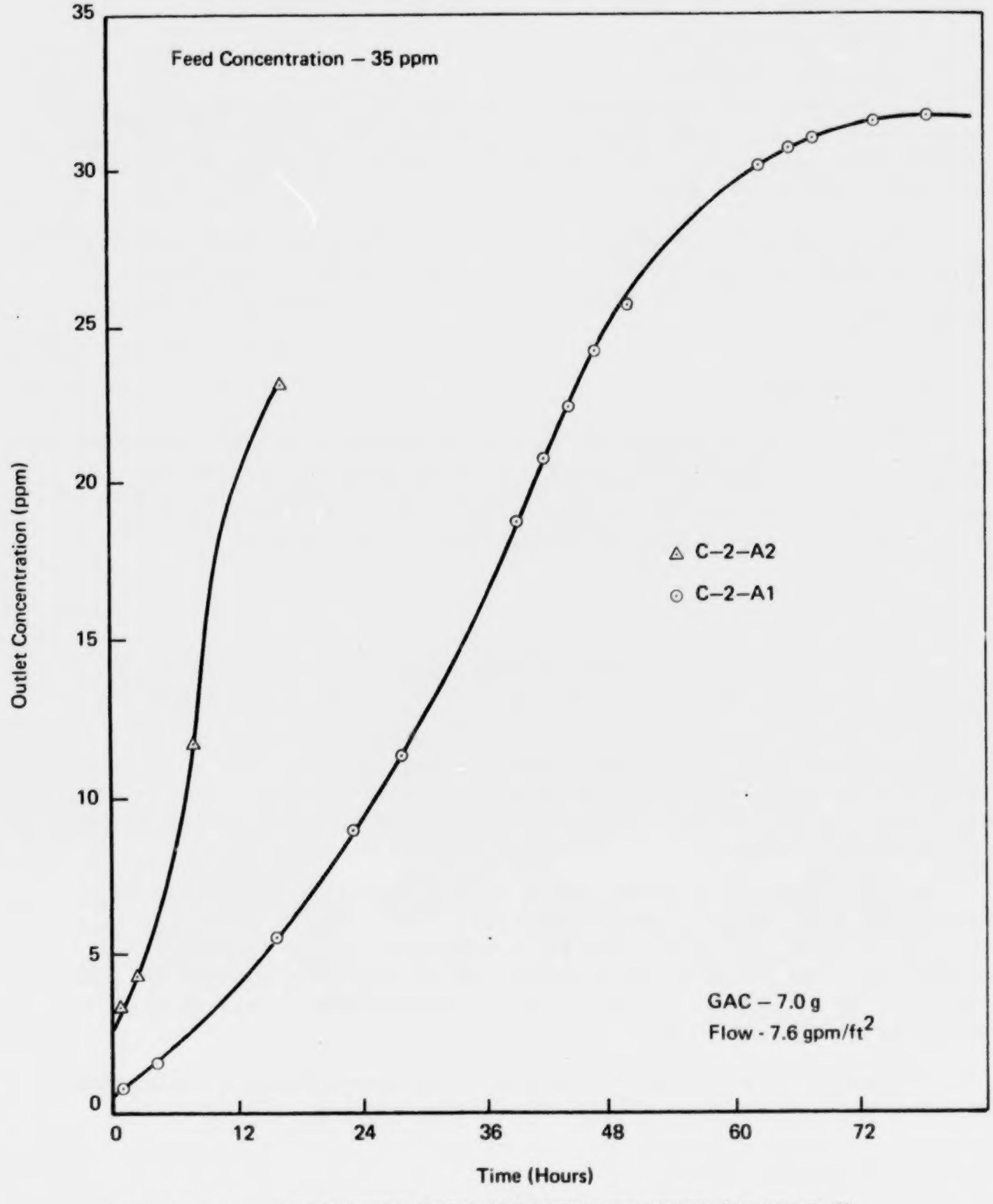

FIGURE V-11 **ADSORPTION FROM CARBARYL SOLUTION (SERIES C–2)**

Specifically, with a loading of 0.2 g/g and a solubility of 0.2 wt at 275 atm and 120°C, the minimum volume of CO_2 in standard liters required is

$$\text{Volume of } CO_2 \text{ (SL)} \;-\; \frac{1.4 \times 100 \times 1}{0.2 \times 1.8} \;=\; 390$$

For the initial regeneration tests, the CO_2 flow for regeneration was about three to five times that calculated from the solubility and loading values given previously. For example, in regenerating C-1-R1 a total flow of about 1800 SL was used.

Adsorption data are given in Table V-6. The adsorptive capacity decreased by about 50% per cycle; no effort was directed to the determination of the reason for the capacity decrease with Carbaryl in the screening phase.

b. Diazinon

Adsorption breakthrough curves for three Diazinon tests are shown in Figure V-12. As in the Carbaryl series, a large capacity drop was experienced after each regeneration using the standard regeneration conditions of 275 atm, 120°C, and 1800 SL or CO_2. Loading data are tabulated in Table V-6. The Diazinon series was stopped after three cycles.

c. Atrazine

Figure V-13 gives the breakthrough curves for seven adsorption/regeneration cycles using an Atrazine solution of 28 ppm. Corresponding loading data are given in Table V-6. The loading of Atrazine on regenerated GAC is lower than that on virgin GAC; however, the capacity value reaches a constant level after about three or four cycles. The breakthrough and regeneration tests in the series were carried forward for three more cycles to verify the finding. The average capacity recovery on the seventh adsorption test was 93%.

Despite comparable solubilities in CO_2, Atrazine-loaded GAC could be regenerated well while Carbaryl could not. This finding indicated that the solubility level per se was not the predominant factor influencing regenerability. The equilibrium distribution of pesticide between GAC and the CO_2 solution influences the duration of regeneration. This is discussed in detail in Section VII.

Because of its favorable regenerability characteristics, Atrazine was selected as a possible candidate for further process studies.

d. Alachlor

Initial dynamic adsorption breakthrough curves with synthetic Alachlor solution at a flow rate of 7.5 gpm/ft^2 are shown in Figure V-14 and a tabulation of the loading data is given in Table V-6. The capacity recovery for Alachlor-loaded GAC after regeneration is much higher than for Carbaryl; whereas the capacity for Carbaryl decreased about 50% per cycle, adsorptive capacity for Alachlor was still about 70% of virgin GAC after ten cycles.

TABLE V-6

GAC LOADING AND REGENERATION DATA

(Figures in gr/gr GAC)

	CARBARYL		ALACHLOR		ATRAZINE		DIAZINON	
Cycle #	Loaded	Removed	Loaded	Removed	Loaded	Removed	Loaded	Removed
1	0.24	0.09	0.20	0.18	0.11	0.07	0.23	0.09
2	0.13	0.08	0.17	0.15			0.14	0.07
3	0.07		0.17	0.23	0.07	0.04	0.04	
4			0.13	0.12		0.06		
5			0.15	0.14	0.06	0.06		
6				0.18	0.06	0.04		
7				0.14	0.06			
8			0.13	0.17				
9			0.12	0.15				
10			0.14	0.20				
11			0.15	0.14				
12			0.12	0.14				
13			0.15	0.15				
14			0.15	0.14				
15								
16			0.14	0.11				
17			0.13	0.14				
18				0.12				
19								
20			0.10	0.12				
21			0.12	0.12				
22			0.11	0.06				
23								
24				0.17				
25			0.11	0.20				
26			0.11	0.20				
27			0.09	0.22				
28			0.10	0.21				
29			0.11	0.20				
30			0.10	0.22				
31			0.11	0.20				

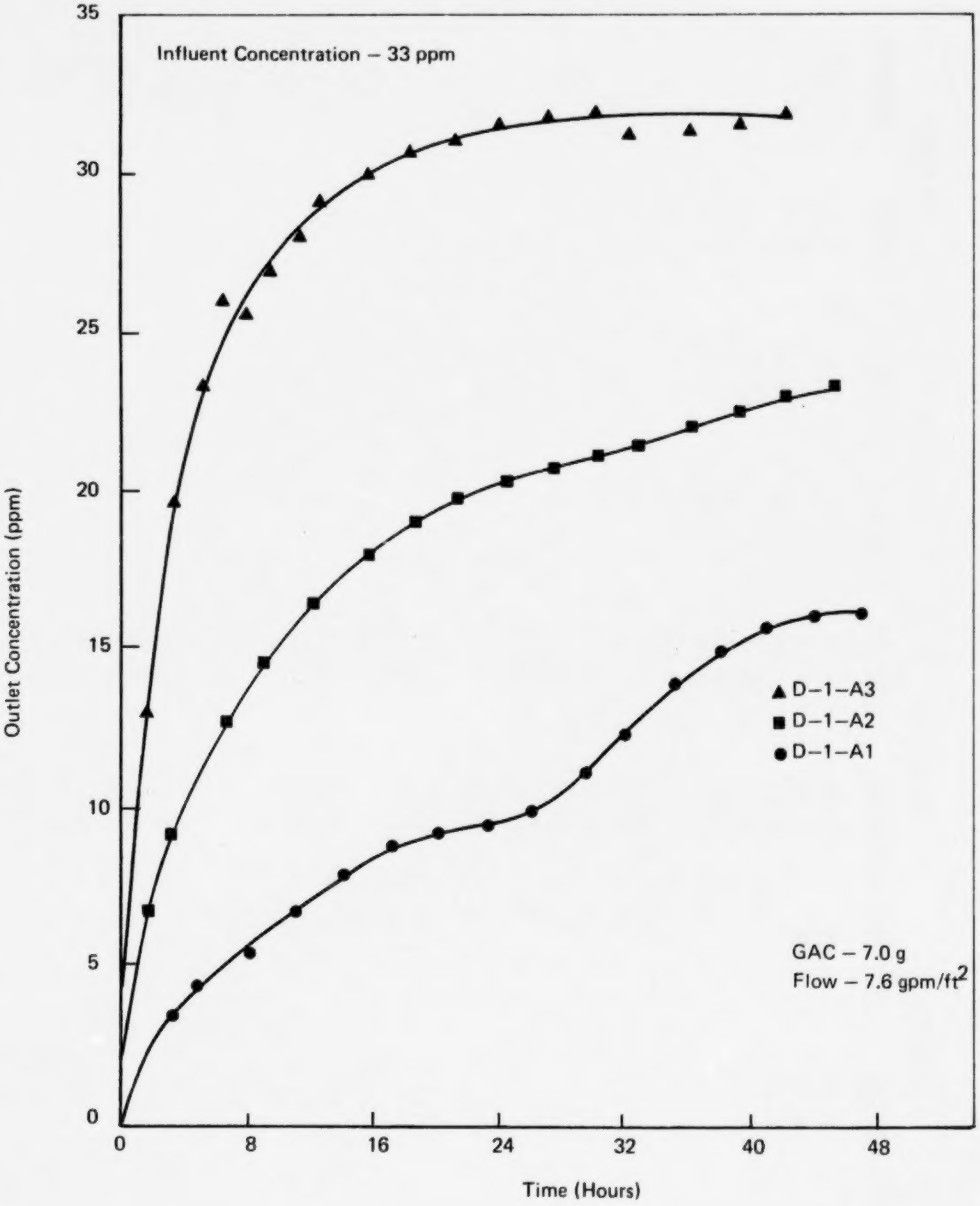

FIGURE V-12 **ADSOPRTION FROM DIAZINON SOLUTION**

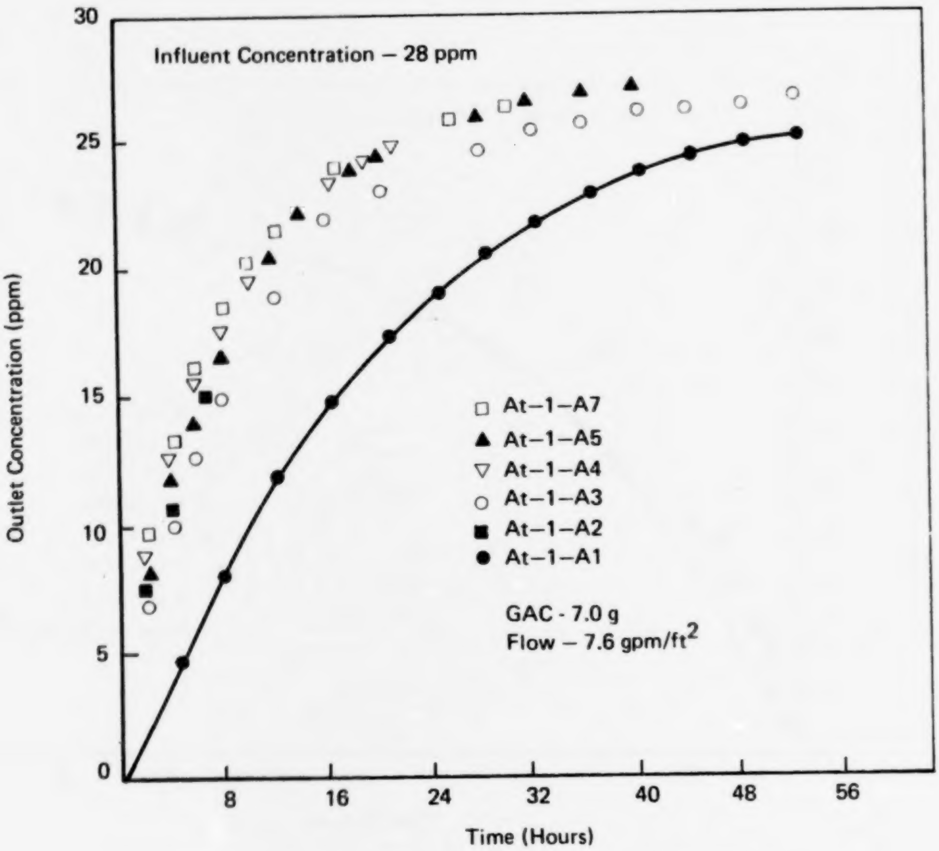

Figure V-13 **ADSORPTION FROM ATRAZINE SOLUTION**

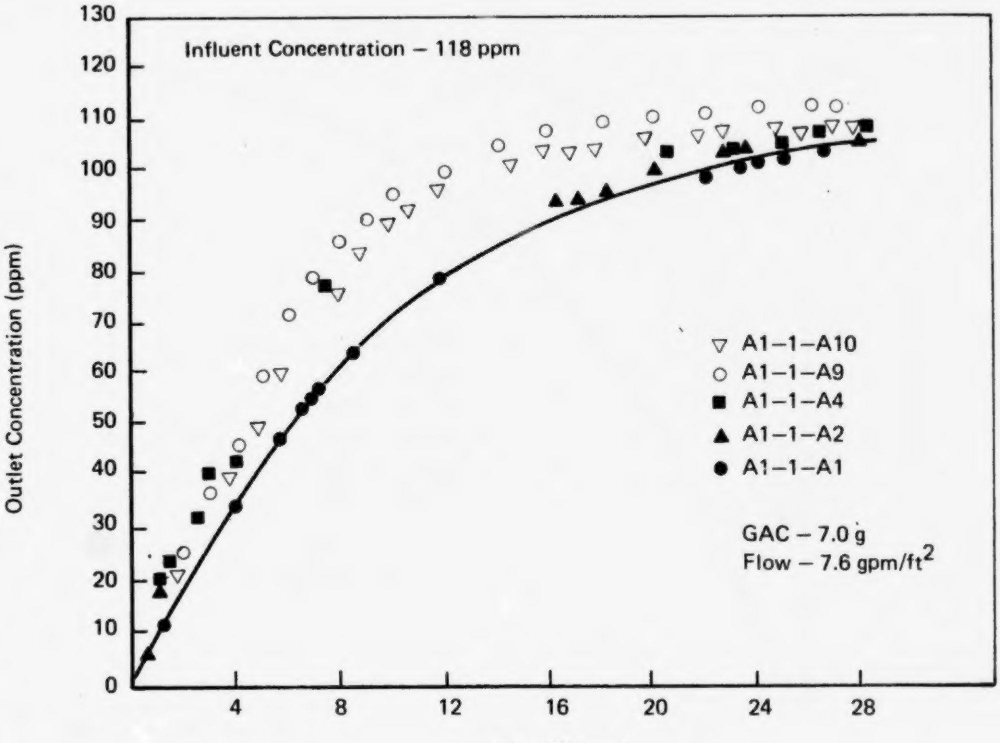

Figure V-14 **ADSORPTION FROM ALACHLOR SOLUTIONS (SERIES AI–1)**

The dynamic adsorption tests were continued with the Series Al-1 column and another series, Al-2 was started in parallel. The first adsorption cycle of each series is compared in Figure V-15 in order to given an indication of the experimental accuracy of the adsorption breakthrough determinations; the two breakthrough curves for virgin GAC are in good agreement.

Both of the Alchlor series were continued; a total of 31 cycles for Al-1 and 18 cycles for Al-2 were carried out. Figure V-16 is a composite of the 31 cycles for the Al-1 series, and Figure V-17 for the Al-2 series.

Within each Alachlor series some tests with variations in regeneration pressure were carried out. Figure V-18 shows three breakthrough curves for adsorption carried out on GAC regenerated at two different pressure levels., 1950 and 275 atm in the Al-1-series. Figure V-19 shows three adsorption curves for similar tests in the Al-2 series. The curves given in Figrues V-16 and V-19 show that a CO_2 volume of 1800 SL at 150 atm did not regenerated Alachlor-loaded GAC to as great an extent as did the same total flow at 275 atm; however, as the figures show, a subsequent 275-atm regeneration of the adsorption which followed the 150 atm regeneration returned the capacity to its previous 275-atm level.

The average capacity recovery for the Al-1 series was 98%.

Because of the demonstration of a reasonable capacity recovery after 31 regeneration cycles, Alachlor was selected for concerted effort in the Process Development phases; these studies are described in Section VII.

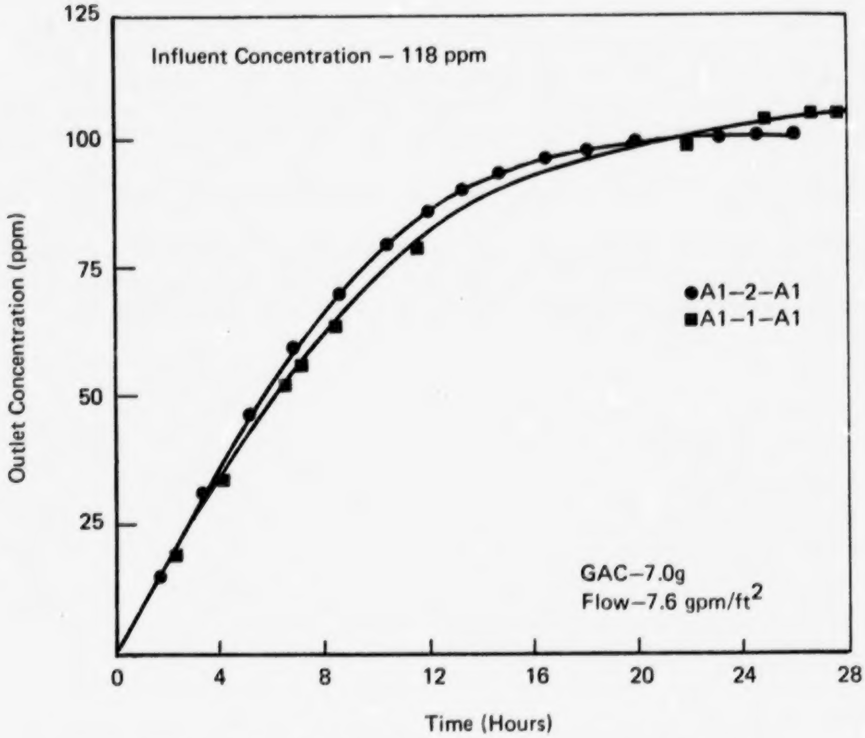

Figure V-15 **COMPARISON OF VIRGIN ALACHLOR ADSORPTION BREAKTHROUGH FOR AI–1 AND AI–2 SERIES**

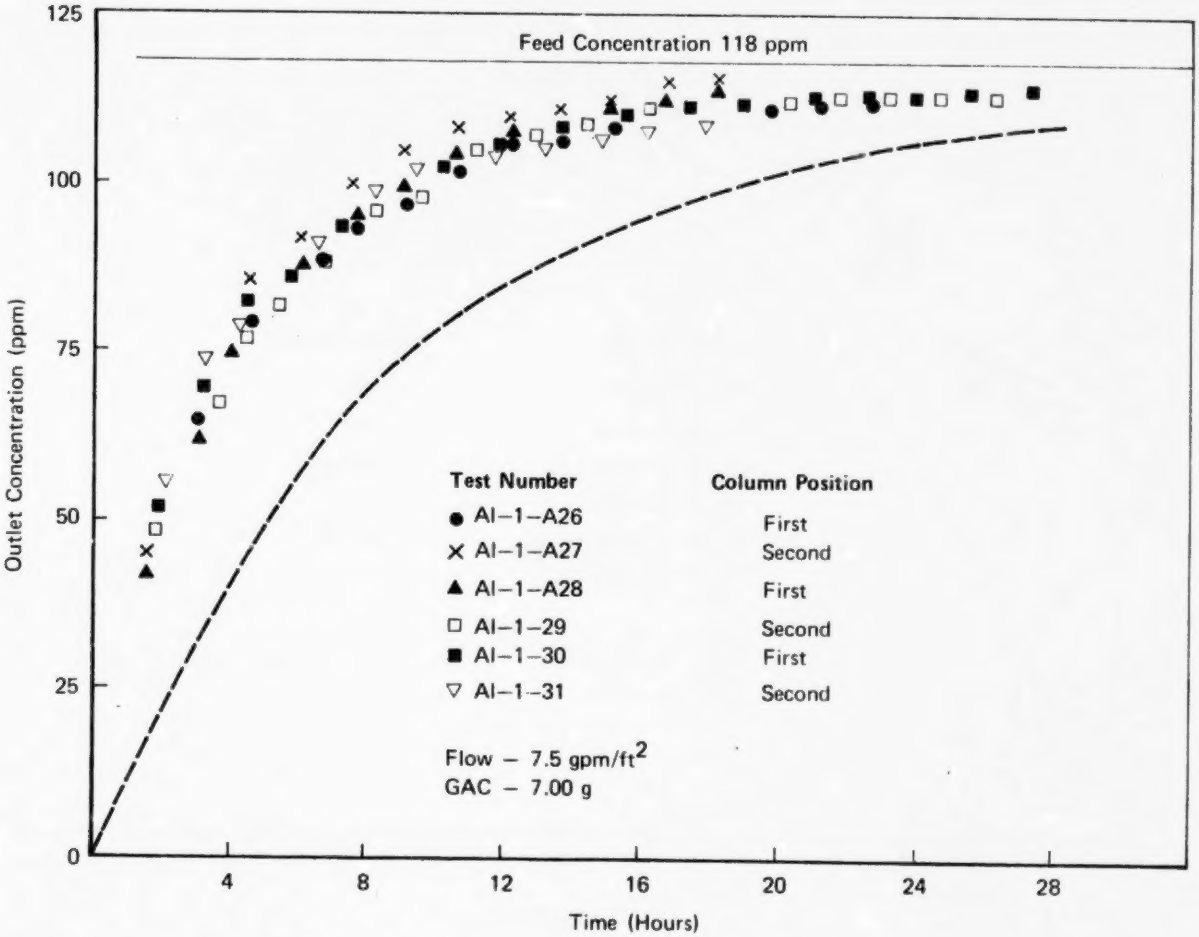

Figure V-16 **ADSORPTION CURVES FOR ALACHLOR (SERIES 1)**

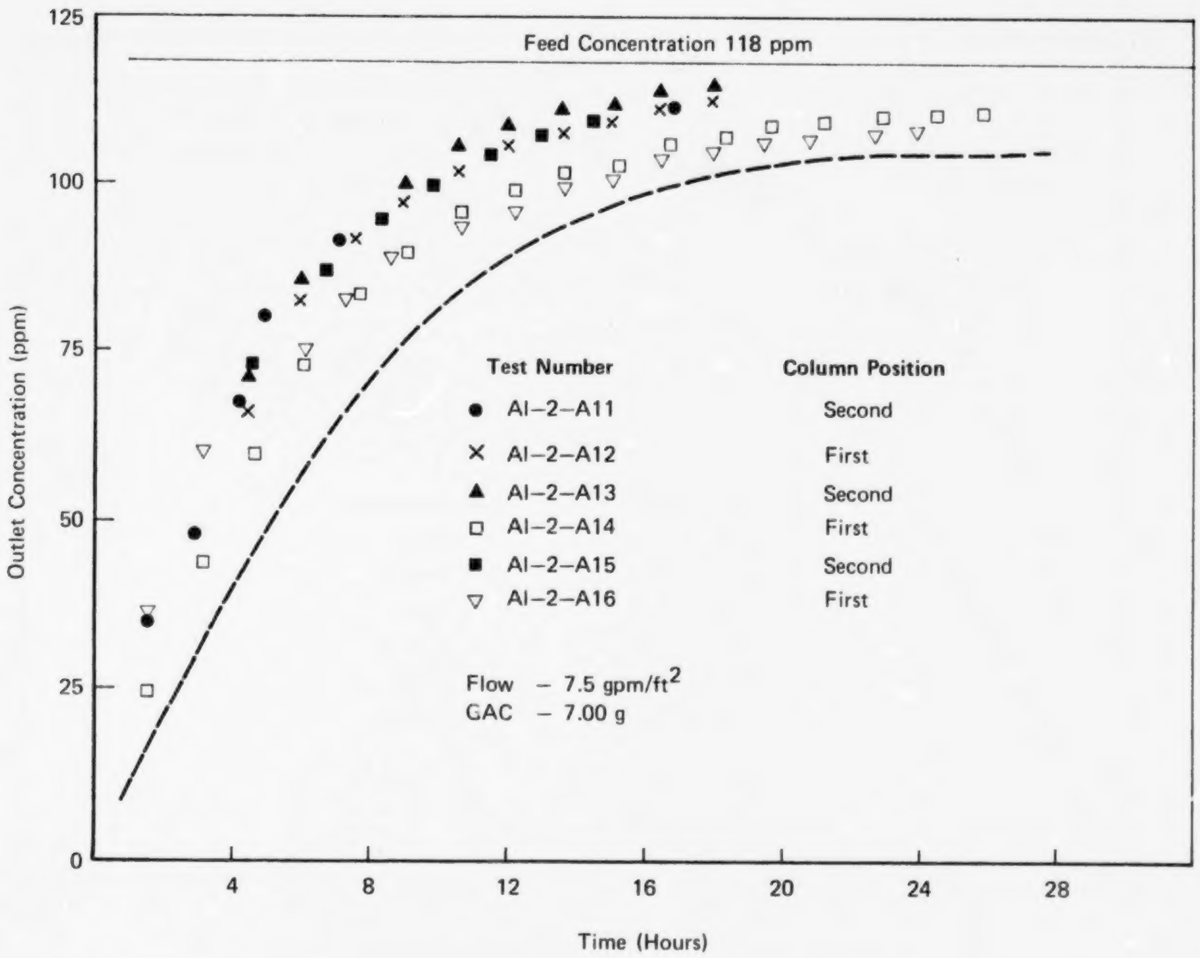

Figure V-17 **ADSORPTION CURVES FOR ALACHLOR (SERIES 2)**

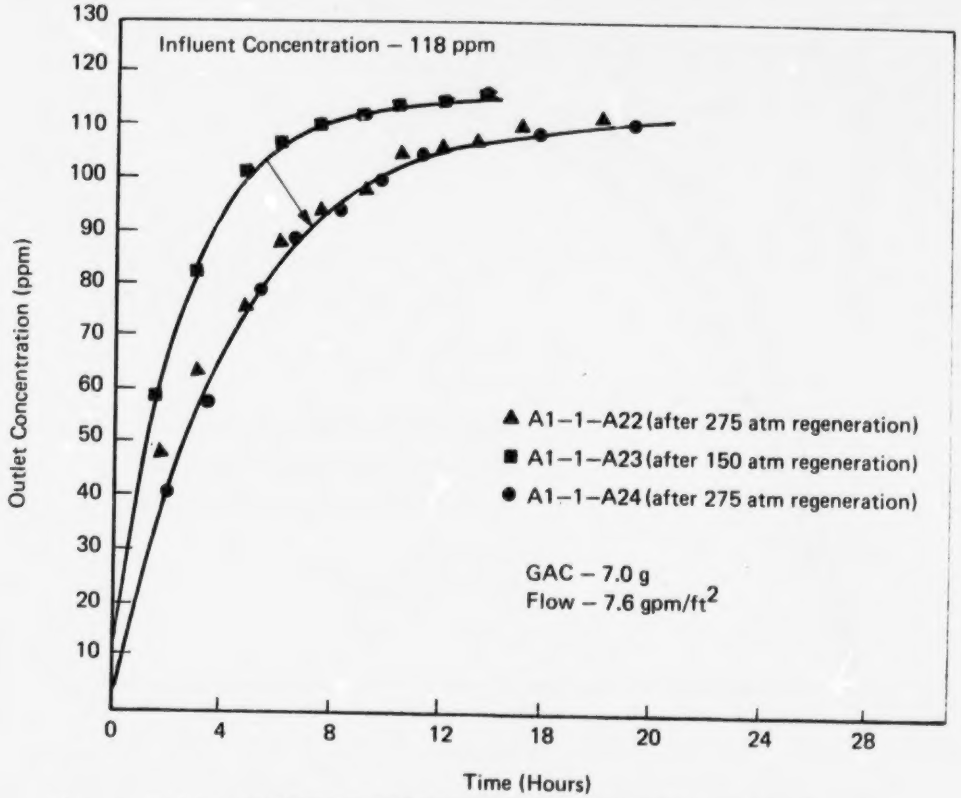

Figure V-18 **ALACHLOR ADSORPTION BREAKTHROUGH CURVES: EFFECT OF REGENERATION PRESSURE (AI–1)**

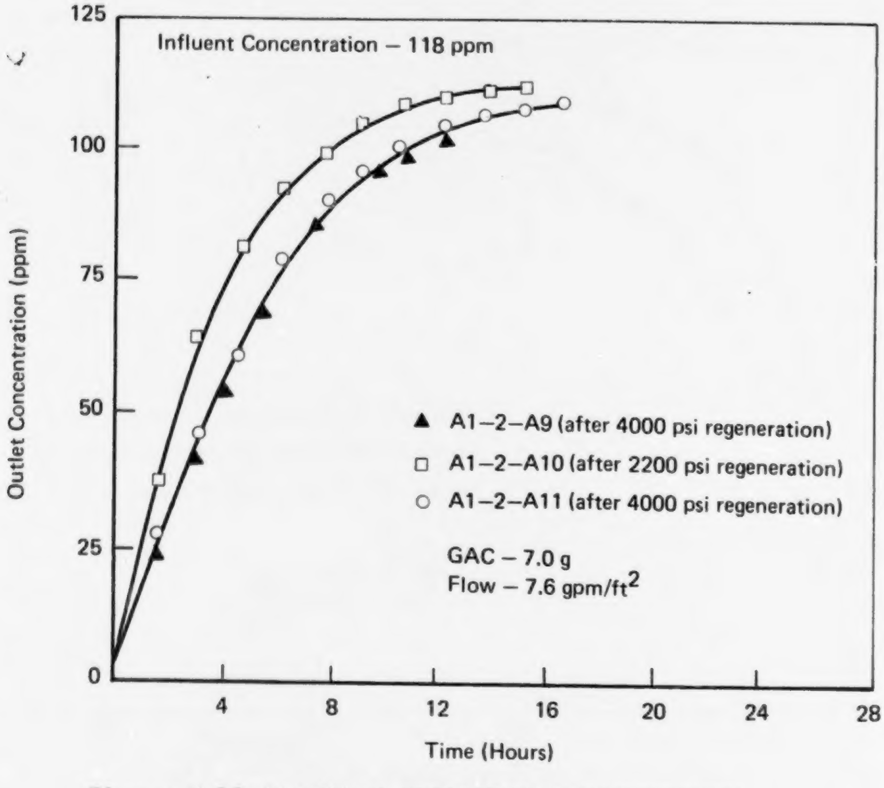

Figure V-19 **ALACHLOR ADSORPTION BREAKTHROUGH: CURVES EFFECT OF REGENERATION PRESSURE (AI–2)**

VI. MODEL SYSTEM STUDIES

A. INTRODUCTION AND PROCEDURES.

The purpose of the model system studies was to obtain fundamental information about the supercritical CO_2 regeneration process using known well-characterized adsorbates. The studies were initiated in parallel with pesticide screening, using phenol as a model adsorbate. When Alachlor was selected from the screening studies, it was used for further work in this phase also.

The degree to which SCF CO_2 can regenerate adsorbents was determined by subjecting GAC columns to repetitive adsorption and desorption cycles. The apparatus for these tests is shown in Fig. VI-1, and is similar to that used in the screening studies. The adsorbents were packed into 304-stainless steel columns and maintained at ambient temperature during adsorption. Aqueous solutions of solute were fed at constant flow rate with a minipump (Milton Roy, model 396-31). The column effluent was monitored with an on-line UV spectrophotometer (Perkin-Elmer, model 550) and the total effluent was collected. The loading on adsorption was determined by one or more of the following methods: (i) integration of the breakthrough curves; (ii) the change in concentration between feed and total effluent collected; (iii) the change in weight of the column if the column was dried prior to desorption.

Prior to desorption, the column was drained of interstitial water. In some runs, the column was dried with low pressure CO_2 at 55°C. Liquid CO_2 (siphon grade, min. purity 99.5%) was pumped to operating pressure (Aminco diaphragm-type compressor, model 46-13427) and brought to operating temperature in a preheater, passed through the column, and then to a pressure let-down valve. Solute was collected in a cooled U-tube. The instantaneous flow rate was measured by a rotameter and the total CO_2 flow by a dry test meter.

Results reported herein were obtained with three column sizes. The minicolumn dimensions were 0.42 cm i.d. x 5 cm and contained 0.37 g activated carbon. The small columns were 0.95 cm i.d. x 28 cm and contained 7.0 g carbon, unless otherwise stated. The large columns were 3.3 cm i.d. x 120 cm and contained 380 g carbon. Three commercially available granular activated carbons (Calgon Filtrasorb 300, National Coal Board Anthrasorb CC1230EH and Amoco GX-31) and a carbonized synthetic resin (Rohm and Haas Ambersorb XE-348) were used. The standard carbon for most tests was F-300, screened to -12 + 30 mesh; when not otherwise stated, the standard carbon was used. Table V-4 (Section V) gives properties of these carbons.

At the outset of the program, six variables were identified as the key parameters to be studied in column regeneration tests: type of carbon, regeneration temperature, pressure, flow rate of regenerant, total

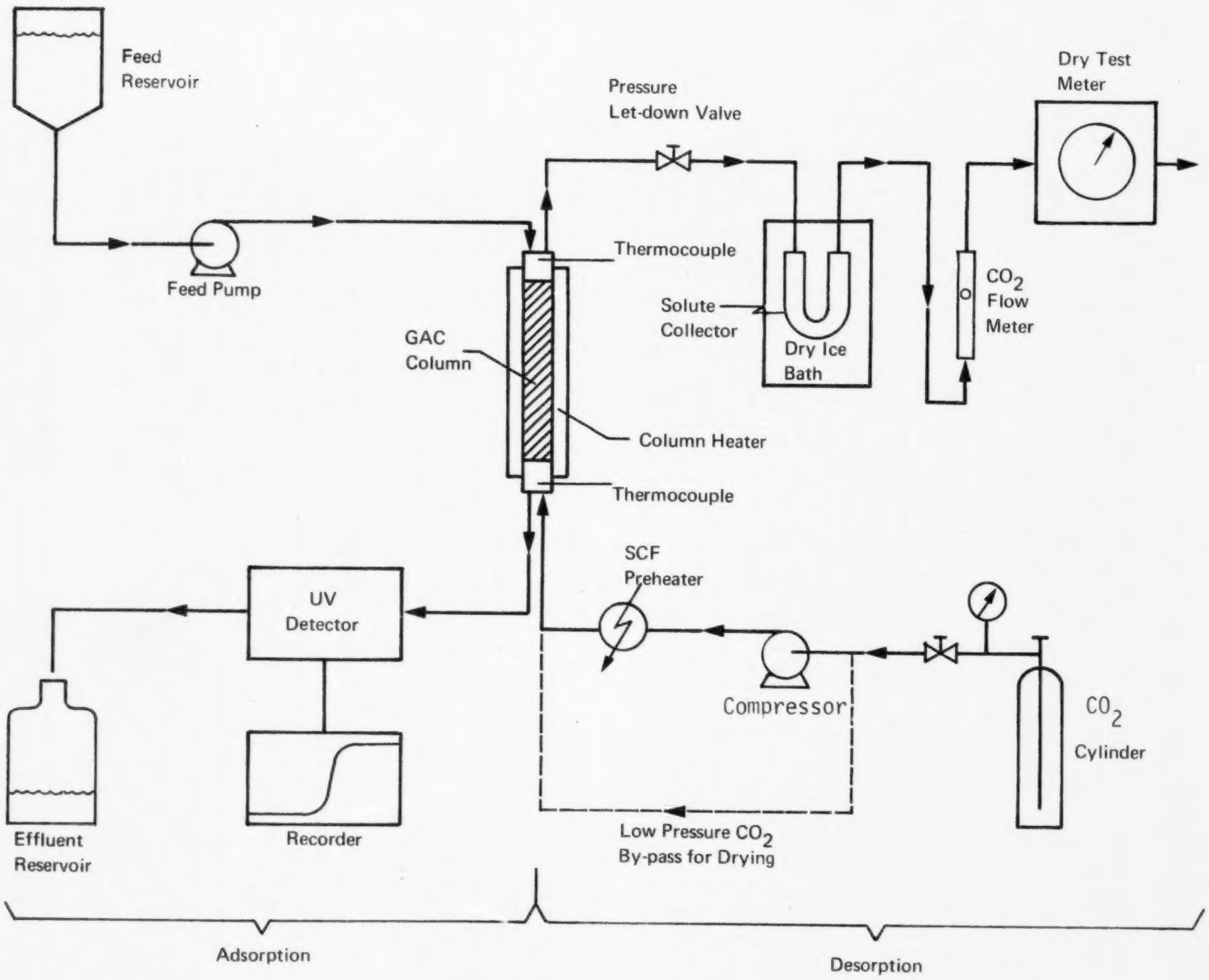
Feed
Reservoir
Feed Pump
Pressure
Let-down Valve
Dry Test
Meter
Thermocouple
Solute
Collector
Dry Ice
Bath
CO_2
Flow
Meter
GAC
Column
Column Heater
Thermocouple
SCF
Preheater
UV
Detector
Compressor
CO_2
Cylinder
Effluent
Reservoir
Recorder
Low Pressure CO_2
By-pass for Drying
Adsorption
Desorption

FIGURE VI-1 **ADSORPTION AND DESORPTION APPARATUS**

quantity of regenerant and water content (i.e., regenerating wet or dry). During the course of this program, an additional parameter was found to have significant impact on the regeneration process; time of exposure of the column to aqueous feed during adsorption.

B. PHENOL REGENERATION

1. Regenerability Studies

To demonstrate the ability of SCF CO_2 to regenerate activated carbon, a series of adsorption-desorption cycles was conducted using a mini-column of Filtrasorb 300, screened to -100 + 120 mesh. Rapid adsorption and sharp breakthroughs were attained by using relatively low flow rates (.2 to .5 ml/min) of concentrated phenol solution (10,000 ppm). After adsorption breakthrough occurred (15 to 25 min) the column was dried with low pressure CO_2. Desorption was conducted at 150 to 190 atm and 55°C. In some runs, the desorption curve was obtained by flame ionization detection of the effluent.

A series of eight adsorption-desorption cycles was run on a single carbon column. The results are shown in Table VI-1 as experiment 1. The loading of the virgin carbon was 0.35 g/g, which is higher than that commonly reported for phenol owing to the high feed concentration. The loading after the first regeneration is 0.25 g/g and is relatively steady (within experimental error) thereafter. The drop in loading after the first regeneration has been observed in a number of cases, as will be discussed later.

The rate of desorption of phenol as a function of time is shown in Fig. VI-2. This desorption curve, which was observed during the regeneration following the fourth adsorption cycle, is typical. The concentration of solute in the regenerant fluid peaks soon after the onset of regeneration, decreases rapidly until 80 to 90% of the solute has been removed and then decreases slowly until regeneration is complete. Note that the bulk of the desorption is very rapid; 50% of the adsorbate is removed within 20 min and 90% within 1 h. Desorption is complete within 3 h. Unlike desorption in liquid solvents, the desorption of phenol from activated carbon using supercritical CO_2 is very rapid.

A series of experiments was made with 0.95 cm i.d. columns containing three different carbons and a carbonized synthetic resin. The F-300 carbon was screened to +20 mesh; the other adsorbents were used as received. A phenol concentration of 2380 ppm was used at a moderate flow rate of 3.2 ml/min (1.1 gpm/ft^2). During adsorption, effluent concentration was monitored with an on-line UV spectrophotometer. When the effluent concentration reached 90% or more of the feed concentration, adsorption was terminated and the GAC was regenerated using SCF CO_2 at 120°C and 150 atm for 3 h at a flow rate of 8-9 standard liters per minute (SLM). Note that the columns were not dried prior to desorption.

The conditions and results are shown in Table VI-1 as experiments 2-5; the adsorption breakthrough curves for the repetitive cycles are shown in Figs. VI-3 through VI-6. Note that the loadings reported in the first adsorptions are less than the equilibrium loadings because the adsorptions were terminated after 5 to 7 h. The higher loading of GX-31 is due to a surface area of about 2 to 2-1/2 times that of standard GAC.

Table VI-1. Summary of Operating Conditions and Results

Experiment No.	1	2	3	4	5
Type of carbon	F-300	F-300	CC-1230	GX-31	XE-348
Solute	phenol	phenol	phenol	phenol	phenol
Weight of adsorbent(g)	0.37	7.0	7.0	4.0	7.9
Mesh size	-100+120	+20	N/A	-16+30	-20+50
Adsorption					
Feed conc. (ppm)	10,000	2,380	2,380	2,380	2,380
Flow rate (gpm/ft^2)	0.3-1.0	1.1	1.1	1.1	1.1
Desorption					
Temp. (°C)	55	120	120	120	70
Pressure (psig)	2200-2800	2200	2200	2200	2200
Capacity (g/g) Cycle No.					
1	0.35	0.19	0.21	0.50	0.17
2	0.25	0.16	0.18	0.44	0.15
3	0.24	0.15	0.18		0.12
4	0.24	0.16			0.13
5	0.25				0.14
6	0.26				
7	0.23				
8	0.22				

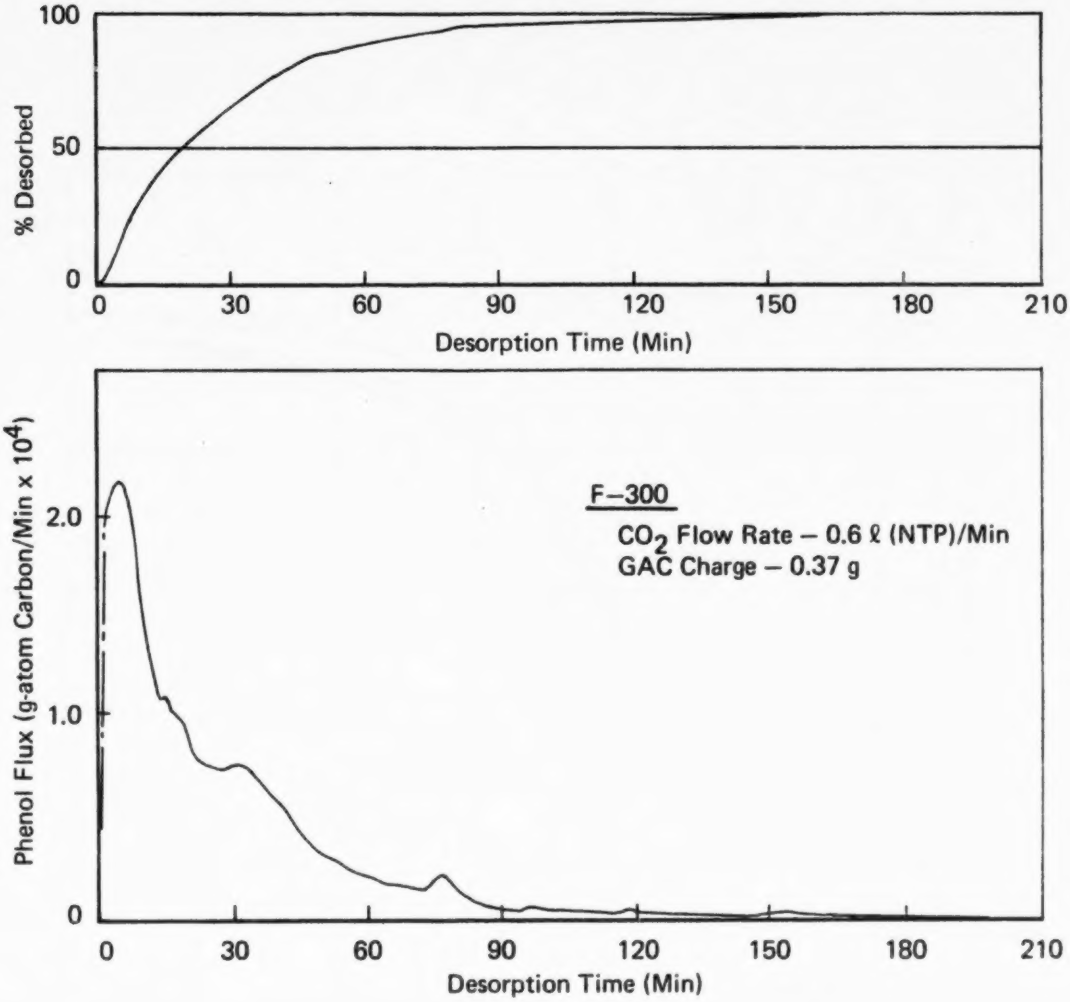

FIGURE VI–2 DESORPTION OF PHENOL FROM GAC WITH SUPERCRITICAL CO_2

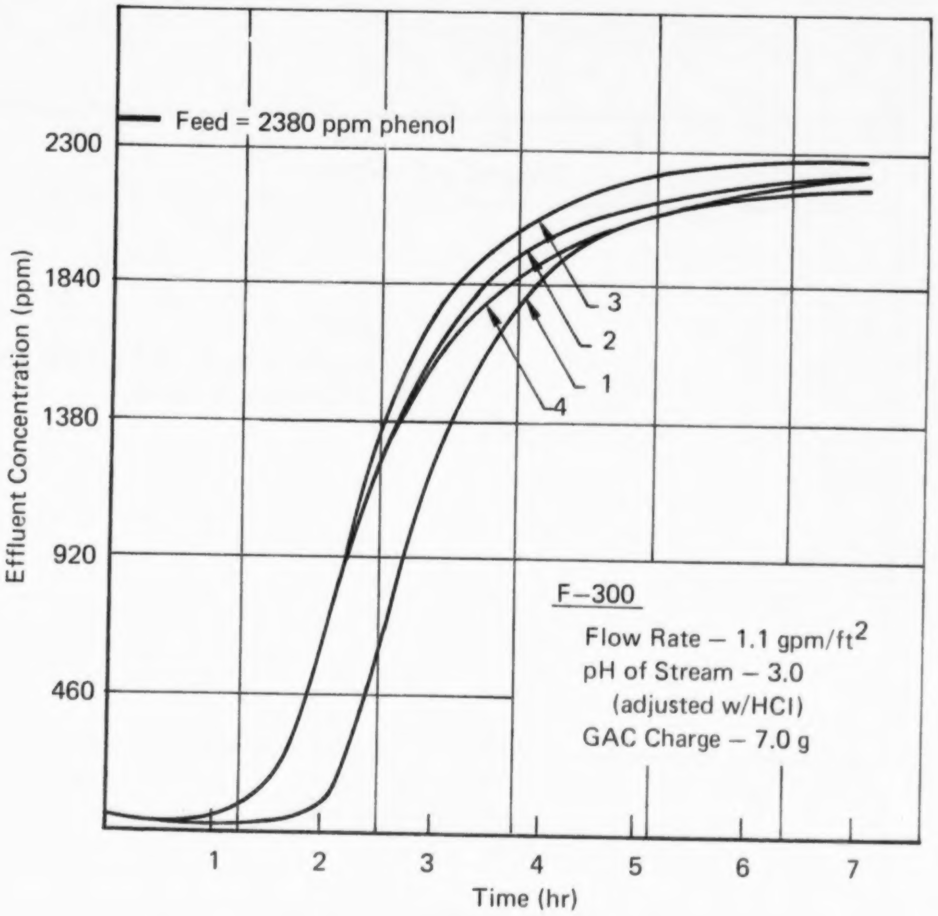

FIGURE VI-3 **ADSORPTION OF PHENOL ON F–300 (NUMBERS ON CURVES REFER TO ADSORPTION CYCLE)**

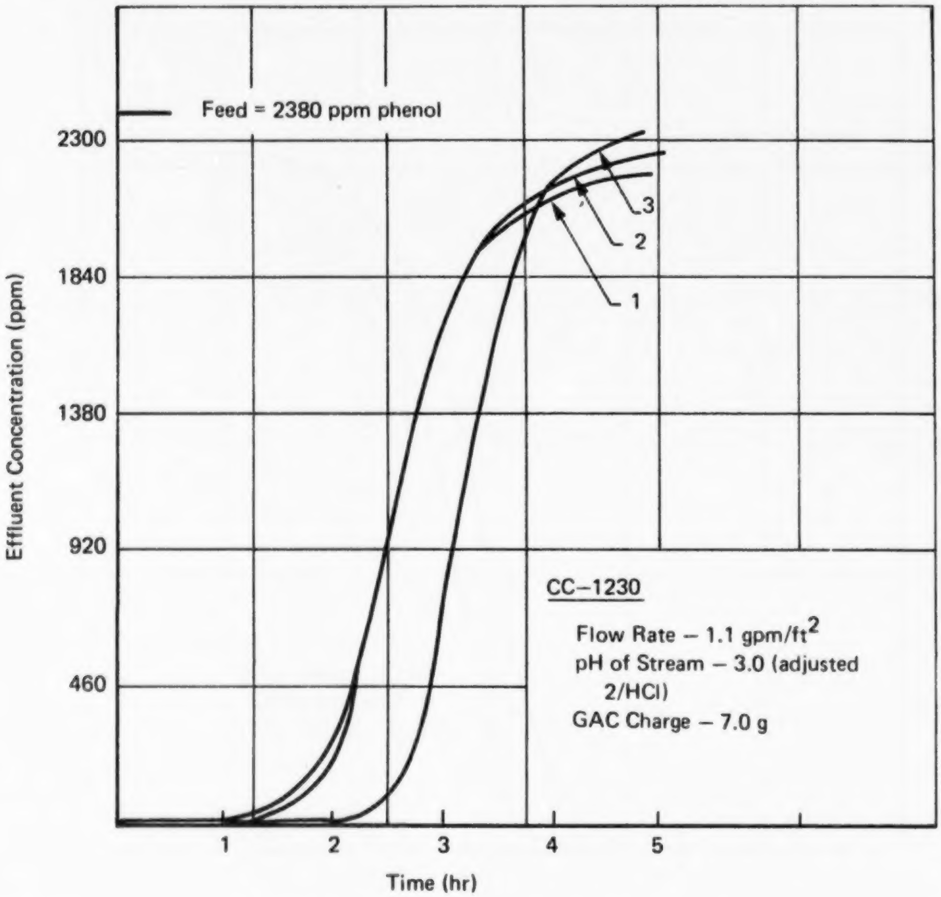

FIGURE VI–4 ADSORPTION OF PHENOL ON CC–1230 (NUMBERS ON CURVES REFER TO ADSORPTION CYCLE)

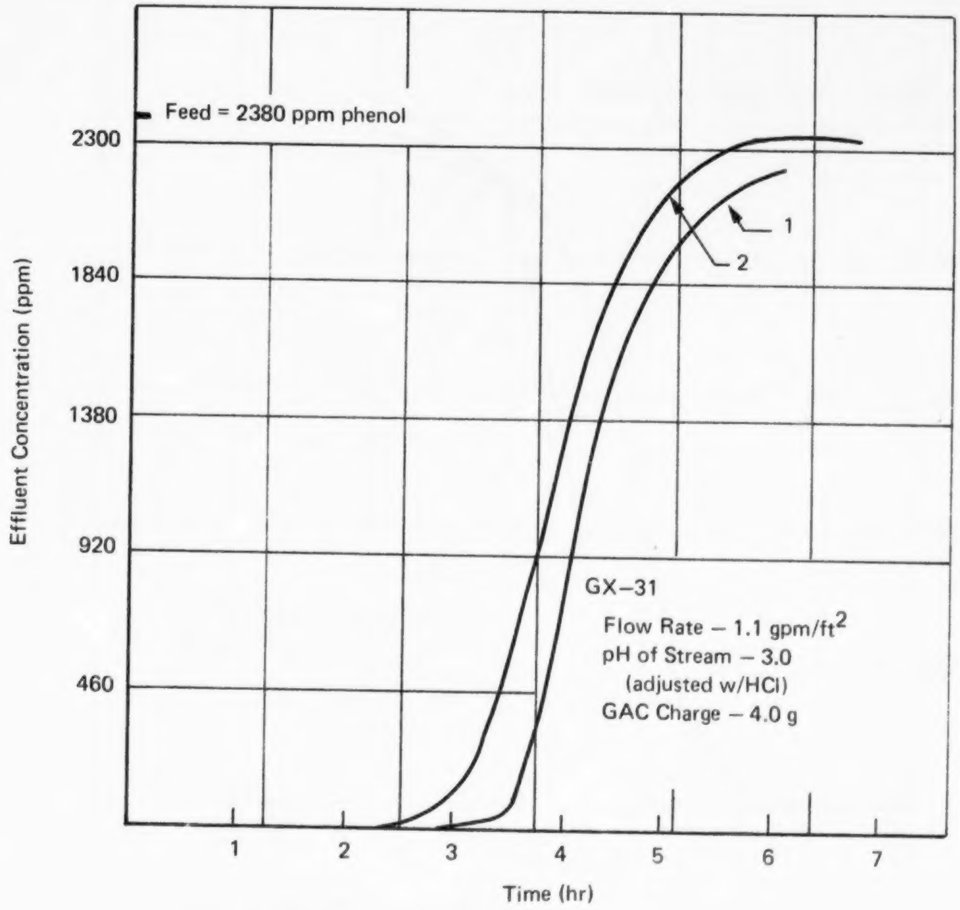

FIGURE VI–5 ADSORPTION OF PHENOL ON GX–31 (NUMBERS ON CURVES REFER TO ADSORPTION CYCLE)

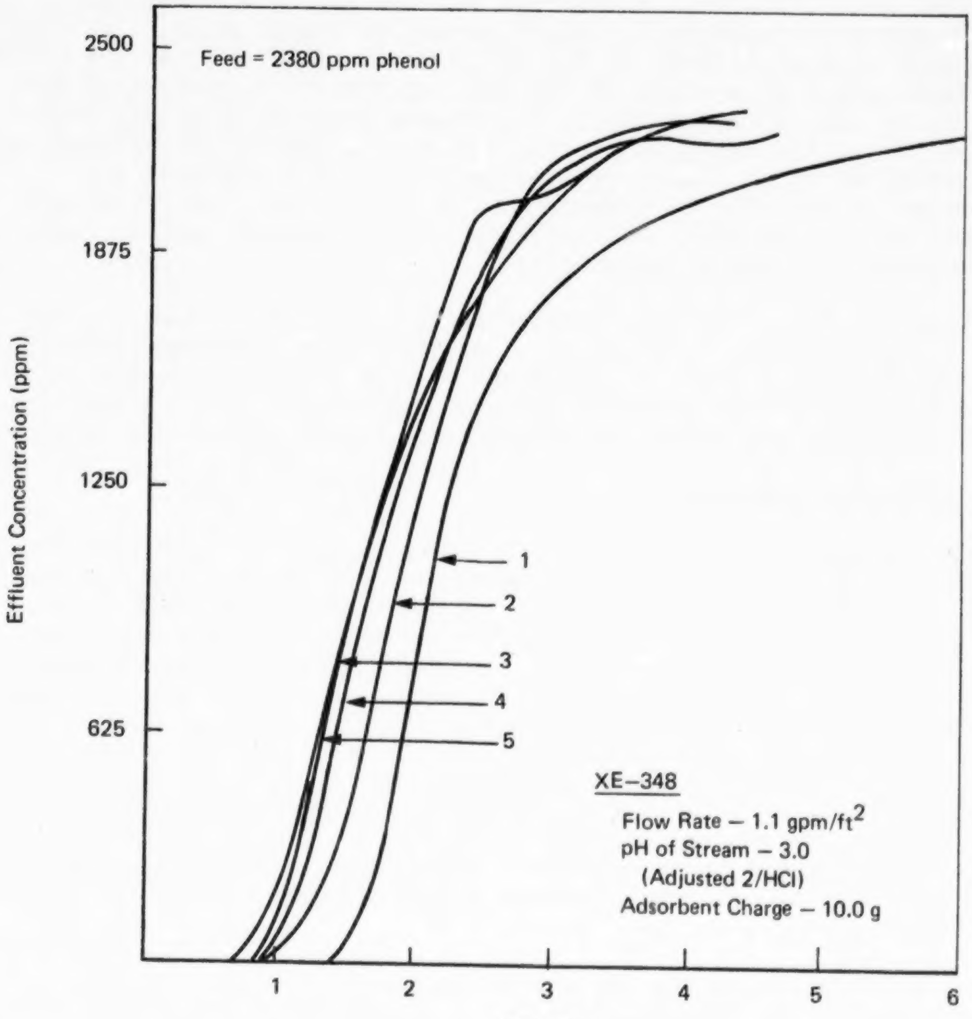

FIGURE VI–6 ADSORPTION OF PHENOL ON XE–348 (NUMBERS ON CURVES REFER TO ADSORPTION CYCLE)

All four adsorbents responded similarly to SCF CO_2 regeneration. Over 80% of the virgin carbon capacity could be attained in the second adsorption cycle. Where more than two cycles were run (experiments 2, 3 and 5), the loading was essentially constant at that measured during the second cycle. Thus, all of the carbons employed in these tests could be regenerated with SCF CO_2.

This set of experiments illustrates a phenomenon that has been observed in a number of tests. The drop in capacity observed after the first regeneration of phenol cannot be recovered by longer periods of regeneration using more CO_2. The decrease in capacity might be due to the formation of immobilized species; either chemi-sorbed or products of chemical reaction. Since the time for adsorption and desorption was short, the process involved is probably non-activated. Since the formation of this immobilized species is rapid and only occurs during the first adsorption, the surface sites involved in its formation are unavailable in subsequent adsorptions. Thus, we tentatively have attributed this irreversible adsorption to chemisorption or complex-formation of phenol with high-energy surface sites.

It is also to be noted that in experiments 2 to 5, the column was not dried prior to desorption with SCF CO_2. At 120° C and pressures above 15 MPa, the solubility of water in regenerant is high enough to provide for drying and solute desorption within the same time frame. Thus, a separate drying step between adsorption and regeneration is not necessarily required.

2. Prolonged Adsorption of Phenol

In conventional industrial practice, GAC columns remain on-stream for weeks or months. In laboratory studies of phenol, adsorption isotherms, it has been reported that several weeks are required to reach adsorption equilibrium (Snoeyink, et al., 1969). In the phenol experiments reported above, the adsorption step was terminated after 7 h. If additional adsorption were to occur beyond 7 h, it would be important to establish whether the additional uptake is reversible or irreversible with respect to SCF regeneration. Thus, two series of adsorption-desorption tests were conducted with prolonged duration of the adsorption step. Feed concentrations were 120 and 2500 ppm phenol with - 12 + 30 mesh F-300. After each adsorption, the column was dried with low-pressure CO_2 at 55°C and then weighed to determine the total loading. Conditions for regeneration were 55°C and 150 atm. After regeneration, the column was again weighed to determine the amount of solute desorbed. These results are given in Table VI-2.

The behavior[*] of column P-1 is similar to that shown previously for experiment 2 in Table VI-1. The loading after 6 h of adsorption amounted to 0.21 g/g, of which over 80% could be desorbed by SCF CO_2.

---

[*] When comparing the results of Tables VI-1and VI-2, it must be kept in mind that column weights were not measured in the earlier tests. The loadings given in Table VI-1 are the amounts adsorbed in the i-th cycle, as determined by integration of breakthrough curves. Those values should be compared to the sixth column of Table VI-2.

TABLE VI-2. PROLONGED ADSORPTION OF PHENOL

Loadings determined by weight of dried column (g solute/g GAC)

Column No.	Feed Conc. (ppm)	Cycle No.	Adsorption Time (h)	Loading (g/g) After Adsorption	Loading (g/g) After Regeneration	Adsorbed in ith Cycle (g/g)	Desorbed in ith Cycle (g/g)
P-1	2500	1	6.1	.209	.025	.209	.184
P-B	2500	1	48	.261	.106	.261	.155
		2	96	.274	.146	.168	.128
		3	96	.294	.154	.148	.140
		4	168	.300	.190	.146	.110
		5	96	.327	.200	.137	.127
		6	192	.331	.217	.131	.114
		7	192	.334	.230	.117	.104
P-A	120	1	96	.137	.069	.137	.068
		2	192	.176	.099	.107	.077
		3	168	.174	.111	.075	.063
		4	264	.194	.126	.086	.071
		5	408	.199	.140	.073	.059
		6	360	.200	.141	.060	.059
P-C	120	1	504	.210	.140	.210	.070
		2	96	.210	.150	.070	.060

The adsorption breakthrough curves for column P-B are shown in Fig. VI-7 The first 6 h of the first cycle of P-B was identical to that of P-1. By 6 h, the effluent concentration is very nearly identical to the feed concentration; since the total adsorption after 48 h increases to 0.26 g/g, there is an additional up-take of 0.05 g/g between 6 and 48 h. This slow, continuing adsorption upon prolonged exposure is consistent with results of others cited previously.

As shown in Fig. VI-7 for column P-B, there is a decline in capacity with successive cycles, the decline being most pronounced in the first three cycles. The per-cycle adsorption (Table VI-2, column 6) decreases faster than the per-cycle desorption (column 7). By the sixth or seventh cycle, the gap between the per-cycle adsorption and desorption has narrowed considerably, indicating that we are approaching a steady state of constant working capacity.

The difference between per-cycle adsorption and desorption is the residual remaining after regeneration (column 5). Although this residual builds up substantially over the 7 cycles, we note that the total adsorption (column 4) also increases. In other words, the build-up of residual does not impact the reversible adsorption on a one-to-one basis. This phenomenon is seen more clearly in Fig. VI-8, wherein the results of Table VI-2for the 2500 ppm feed are plotted as a function of total time of exposure of the GAC column to aqueous feed. Over the 7 cycles, the column was in contact with aqueous solution for more than 35 h. From Fig. VI-8, we see the total loading increasing monotonically with exposure, the rate of build-up decreasing with increasing time. After 2 h, the residual loading nearly parallels the total loading so that the fraction desorbed shows a mild decrease with increasing time.

The results of a series of prolonged adsorption at 120 ppm is given in Table VI-2 for column P-A. The adsorption breakthrough curves are given in Fig. VI-9and loadings as a function of exposure time in Fig. VI-10. The trends are similar to those observed from column P-B at 120 ppm feed.

When all of these results for phenol are viewed in perspective, it appears that there are two forms of irreversibly adsorbed species (i.e., species not desorbed by SCF CO_2 under the regeneration conditions). First, there is an irreversible species that forms rapidly during the first cycle, resulting in a residual even when the adsorption exposure is of the order of 20 min (Table VI-1 experiment 1). Second, there is an irreversible species that builds up gradually over prolonged exposure and undoubtedly forms by an activated process. The presence of the second irreversible species decreases the amount of the reversibly adsorbed species (i.e., the solute that is desorbed during SCF CO_2 regeneration), but the decrease is not in proportion to the increase in activated irreversible species. Thus, it appears that the activated species does not compete directly for the surface sites upon which the reversible species adsorbs.

The activated irreversible species could result from a slow chemisorption or from a chemical reaction which might be catalyzed by impurities in the carbon pores (e.g., inorganics that might have been introduced during the

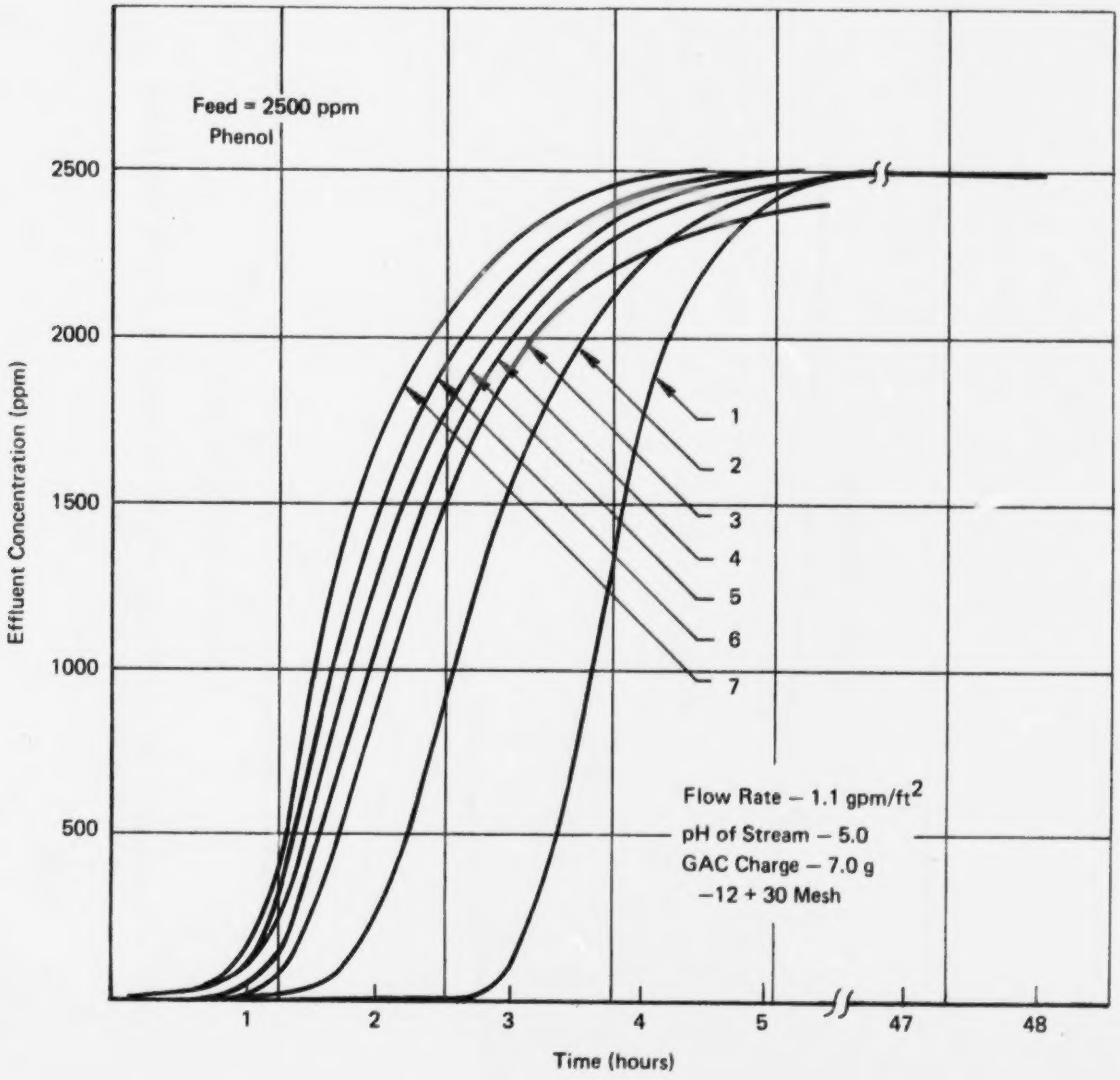

FIGURE VI-7 **PROLONGED ADSORPTION OF PHENOL ON F–300 (NUMBERS ON CURVES REFER TO ADSORPTION CYCLE)**

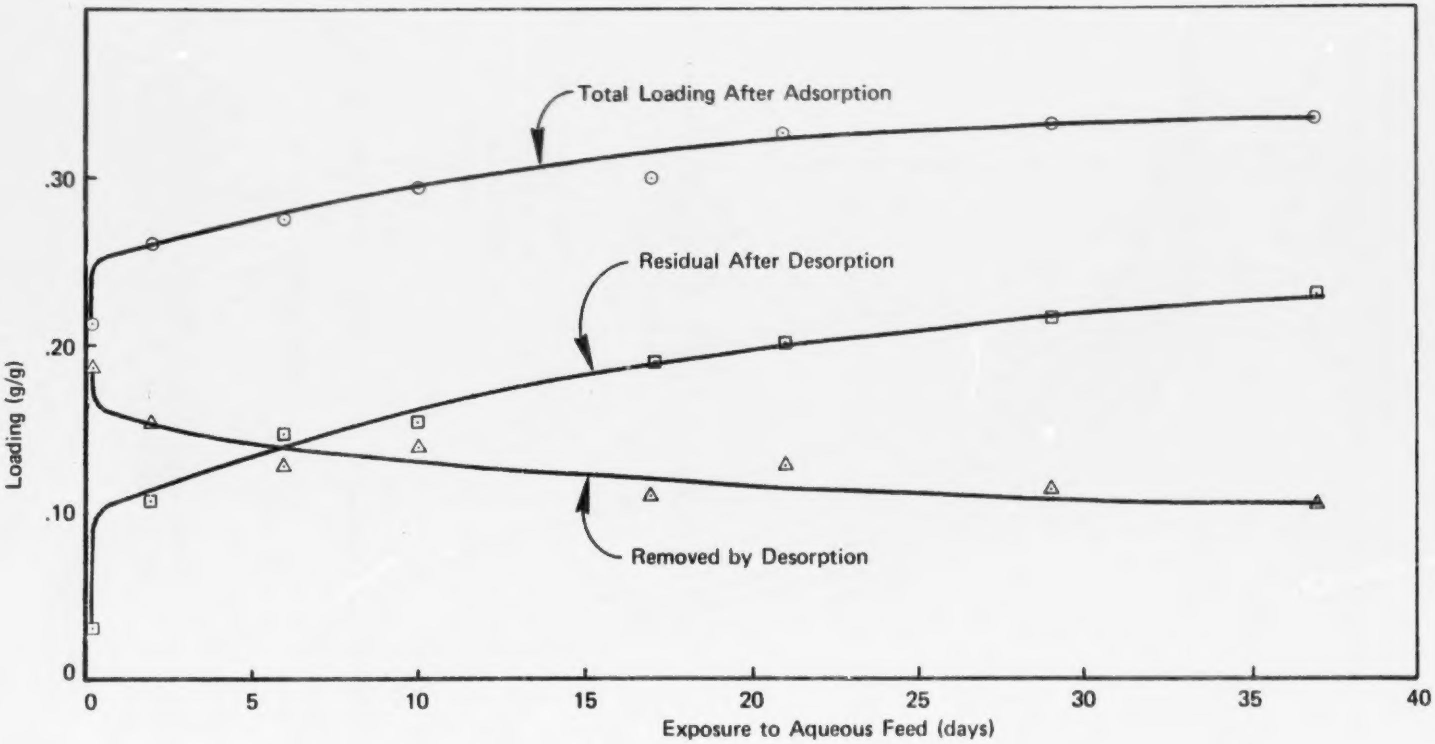

FIGURE VI-8 **LOADING AS A FUNCTION OF TIME OF EXPOSURE DURING PROLONGED ADSORPTION; PHENOL ON F–300**

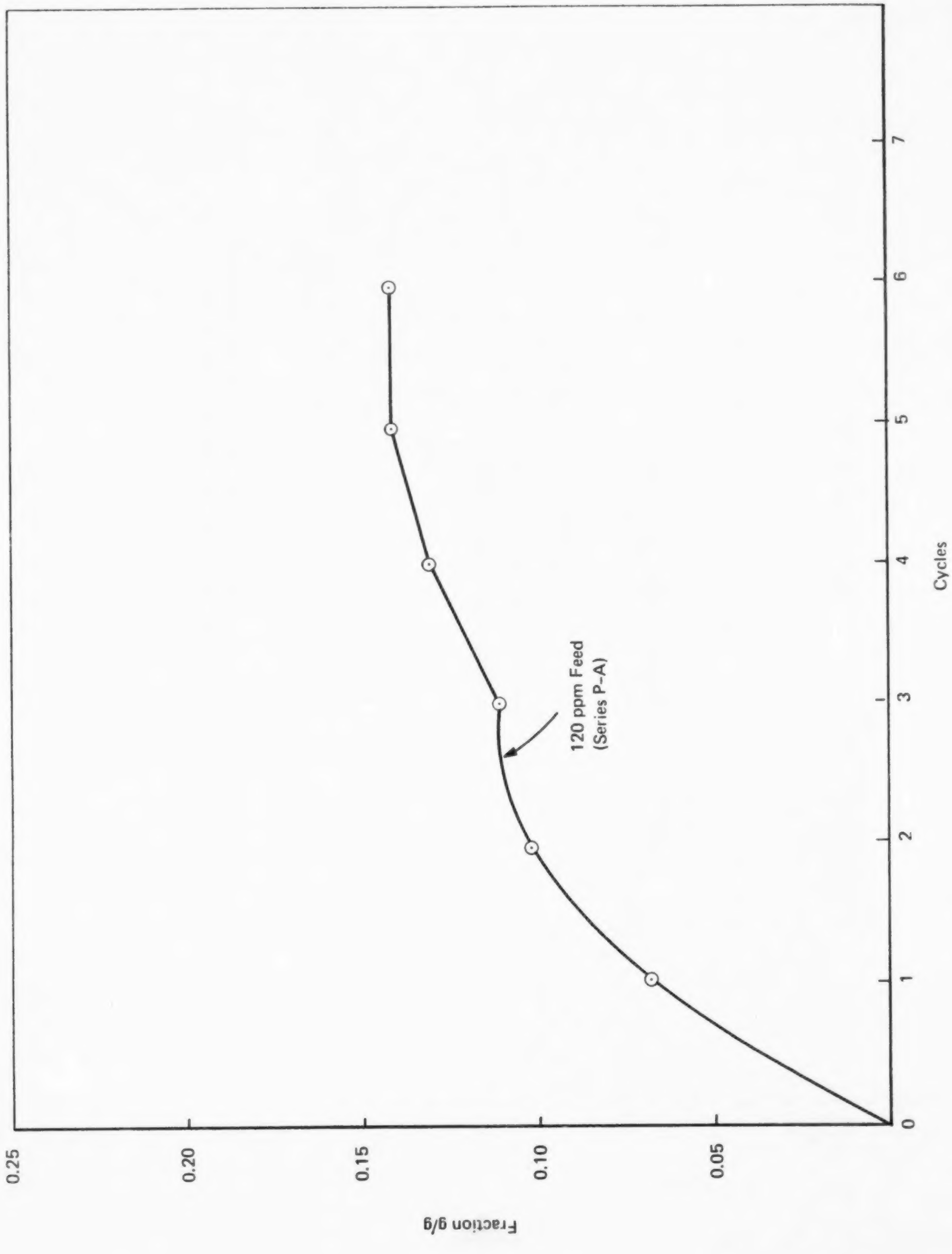

FIGURE VI-9 PROLONGED ADSORPTION BREAKTHROUGH OF PHENOL ON F-300: 120 ppm FEED (NUMBERS ON CURVES REFER TO ADSORPTION CYCLE)

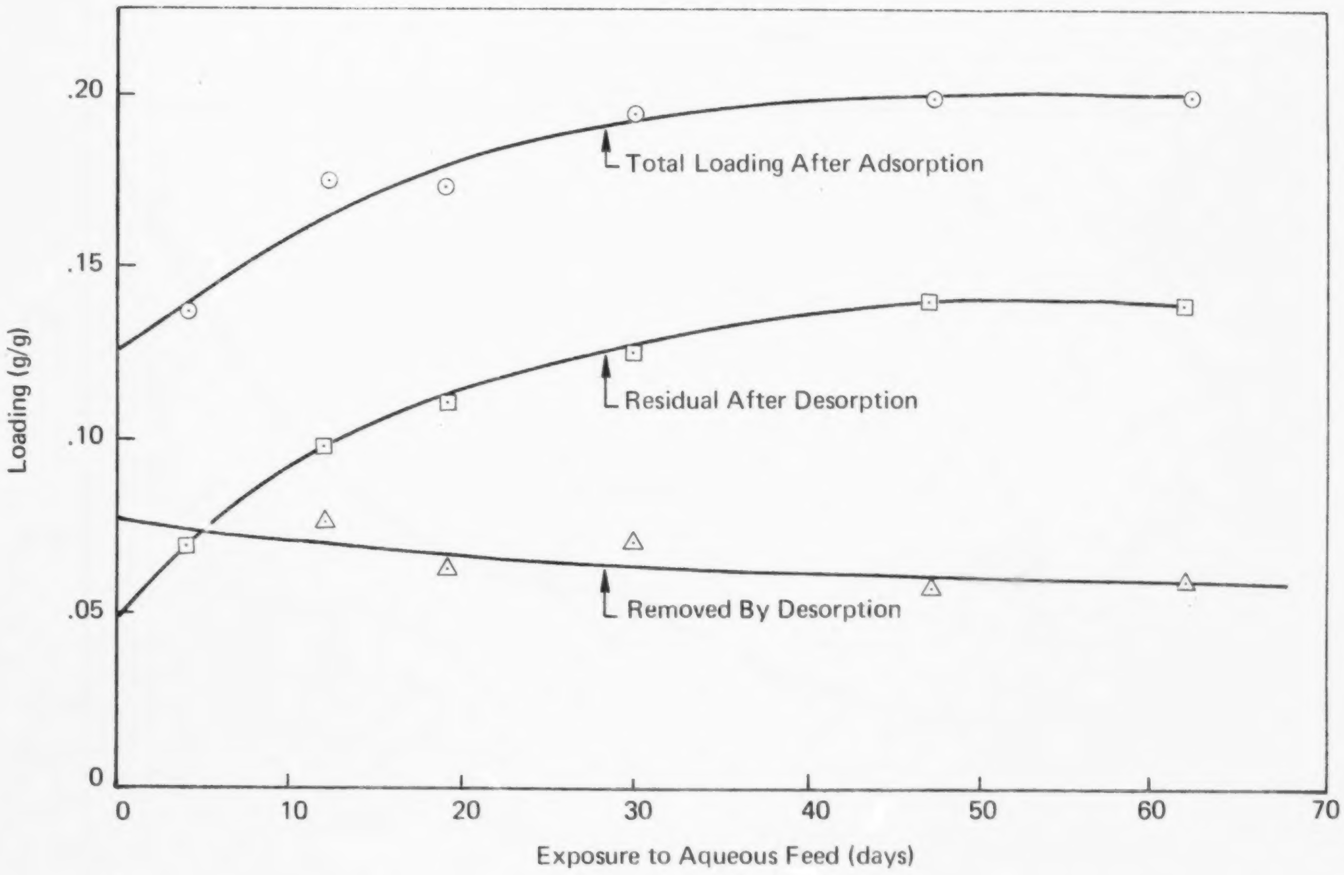

FIGURE VI-10 LOADING AS A FUNCTION OF TIME OF EXPOSURE DURING PROLONGED ADSORPTION; 120 PPM PHENOL ON F-300

original activation of the carbon). In either case, we might expect the build up of residual to be proportional to the phenol concentration in solution. To test this hypothesis, loadings for both 120 and 2500 ppm feed were plotted as a function of "equivalent exposure," defined as the product of concentration and time. As shown in Fig. VI-11, the residual for both feed concentrations fall close to a single curve, while the total loadings are clearly different. The difference between total loading and residual is the reversible portion, which is naturally much higher for the 2500 ppm feed. In retrospect, we see that the high concentration, prolonged adsorption series, P-B, accentuated the build up of residual. For example, at 120 ppm, it would take an exposure of 2 years to reach the residual level of 0.23 g/g, which was found after 37 days at the 2500 ppm feed level.

As a further test of the hypothesis that the time of exposure during adsorption is the key variable in determining the build up of residual, column P-C was exposed to 120 ppm phenol for 21 days. It was then regenerated and reloaded for a second cycle of four-days duration. The results are given in Table VI-2 and Fig. VI-11A(●,■,▲). The results, as seen in Fig. VI-11A, are in relatively good agreement with the proposed hypothesis; the residual build up in the first cycle of column P-C is consistent with the build up over 3 to 4 cycles of column P-A, for which the combined adsorption exposure was 20-30 days.

It appears that the residual is due to a product of chemical reaction of phenol on activated carbon. Subsequent experiments have shown that part of the residual can be desorbed at higher temperatures. The solute recovered is an orange solid, the identity of which has not yet been established. The high-temperature desorption of residual is consistent with the results of Seewald and Juntgen (1977), who used temperature-programmed desorption of phenol from activated carbon. They found a broad peak of moderate surface concentration that desorbed in the range of 100 to 200°C.

The results of the prolonged adsorption tests provide a number of important implications for the optimal design of a SCF regeneration process. For a feed of 2500 ppm phenol on Filtrasorb 300, the pertinent results are summarized in Table VI-3. If SCF regeneration were used with a conventional adsorber design, relatively large adsorption columns would be used and typically left on-stream for days to weeks. The working capacity for SCF-regenerated GAC would be 40% of the virgin carbon capacity. On the other hand, if short adsorption cycles were used, then the SCF working capacity would be 65% of that of virgin carbon. Short adsorption cycles would dictate small adsorber bed volume, with a significant reduction in carbon inventory.

In conventional adsorber design the bed volume is much larger than the volume of the active adsorption zone (i.e., the zone in which rapid adsorption occurs). Carbon is inactive for most of the adsorption period, either having reached saturation or awaiting the arrival of the adsorption zone. Large columns are preferred mainly to minimize the frequency of carbon transfer into and out of the bed. On the other hand, with SCF regeneration, the bed can be

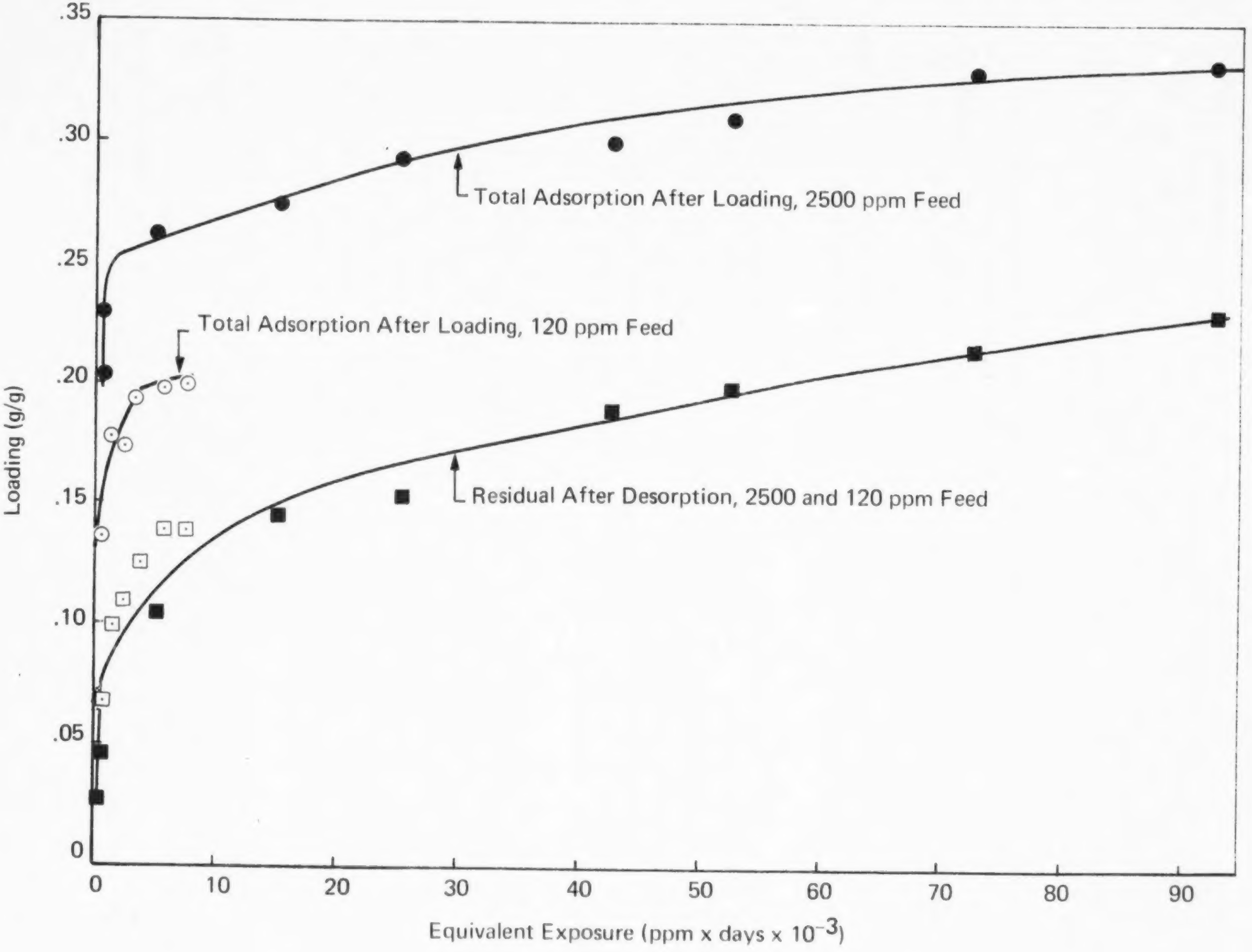

FIGURE VI–11 LOADING AS A FUNCTION OF THE PRODUCT OF TIME AND FEED CONCENTRATION

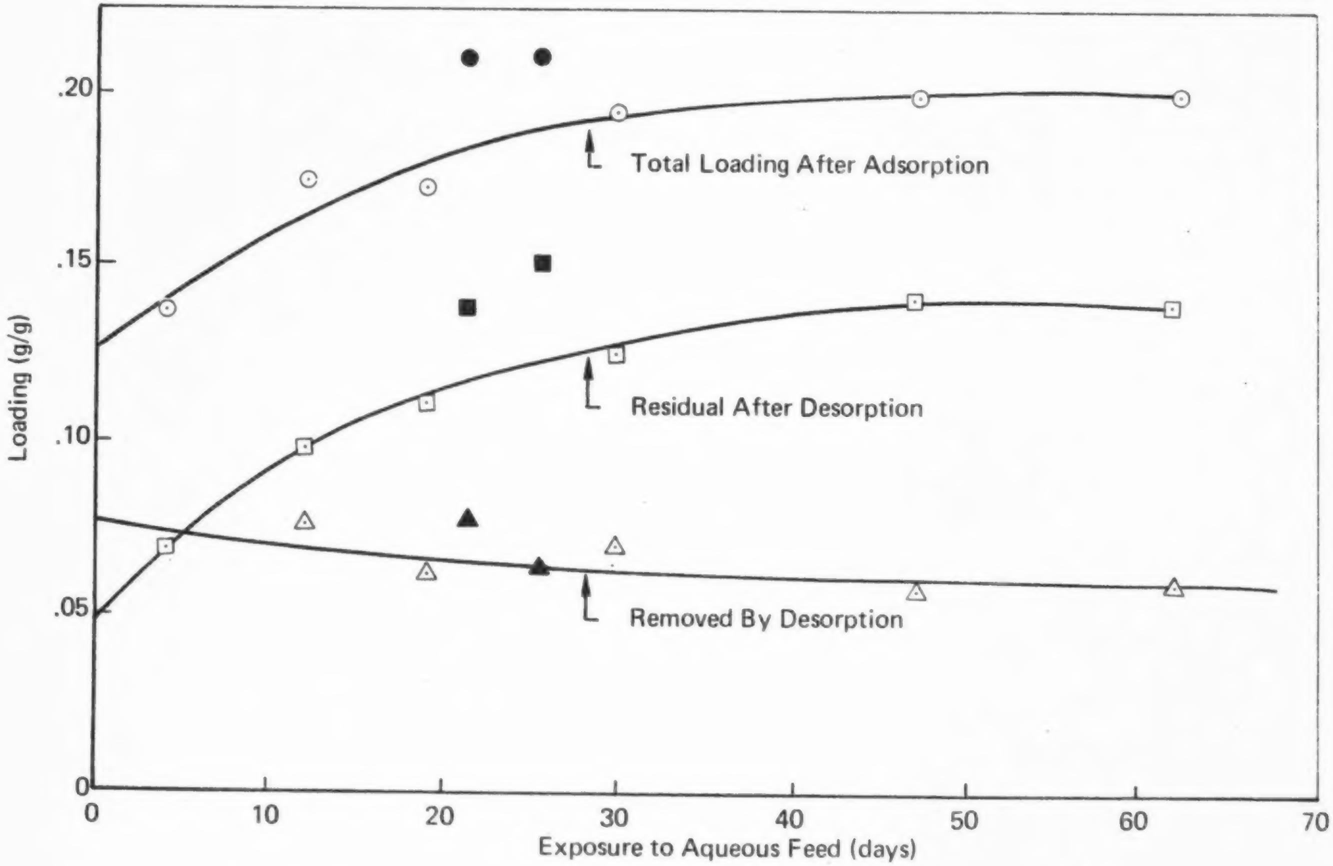

FIGURE VI–11A LOADING AS A FUNCTION OF TIME OF EXPOSURE DURING PROLONGED ADSORPTION; 120 PPM PHENOL ON F-300

TABLE VI-3 EFFECT OF ADSORPTION PERIOD ON WORKING CAPACITY

(2500 ppm phenol on F-300; regenerated at 55°C, 150 ATM)

	Virgin GAC Capacity (g/g)	Steady-State Working Capacity (g/g)	Percent of Virgin Long Cycle
Long adsorption cycle	0.26	0.10-0.11	40
Short adsorption cycle	0.21	0.16-0.18	65

regenerated in situ if the column is designed to withstand high pressure. If the adsorption period is made relatively short, then the cost of small high-pressure vessels for adsorption and in situ desorption can be traded off for the cost of large, low-pressure adsorbers and large carbon inventory.

3. Effect of Temperature on SCF Desorption of Phenol

A series of experiments was conducted to determine the effect of temperature on SCF regeneration of phenol. Three 7-g columns of F-300 were loaded with 2500 ppm phenol during 7 h adsorption cycles. The columns were dried and weighed prior to regeneration. Desorption was conducted at 150 atm and at two temperatures; 120 and 250°C. In these tests, the regenerant flow rate was 50 SLM, which is a factor of 6 higher than those used previously. The results are given in Table VI-4 .*

Column PH-3 was regenerated to 3 h. The per-cycle adsorption dropped by 10% from the first cycle loading of 0.25 g/g to subsequent cycles at 0.22 - 0.23 g/g. This result is comparable or slightly better than that observed for 120°C without prior drying (Table VI-1, experiment 2). After the first cycle, the per-cycle desorption is slightly less than the per-cycle adsorption, indicating at most a slight build-up of residual.

Column PH-4 was regenerated under the same conditions as PH-3, except that the desorption was terminated after 15 min. The fact that the first cycle desorption of 0.16 g/g was less than that of PH-3 (0.22 g/g) does not necessarily imply more irreversible adsorption; rather, we believe that 15 min desorption was not quite sufficient to remove all of the solute that is capable of being desorbed at 120°C. This interpretation is supported by the higher per-cycle desorption and gradual decrease in residual in subsequent cycles of the PH-4 series.

Column PH-5 was regenerated for 15 min at 250°C. Although three cycles of desorption is barely sufficient to identify any trends, it appears that 15 min at 250°C is long enough to attain a working capacity comparable to 60 min at 120°C (PH-3).

C. ACETIC ACID REGENERATION

The ease of desorption is a function of the strength of adsorption. All solutes adsorbing from the aqueous phase must compete with water for surface sites. Thus, weakly adsorbed species generally exhibit relatively low loadings. Acetic acid is a typical case of weakly adsorbed solutes.

---

*For all three columns, the virgin, first cycle adsorption is 0.25 to 0.26 g/g, which is somewhat higher than that of column P-1 (see Table B). The - VI-2 difference is believed to be due to the fact that another batch of GAC was used for these tests; such differences from batch-to-batch are not uncommon.

TABLE VI-4. REGENERATION AT HIGH CO_2 FLOW RATE

(Adsorption at 2500 ppm for 7 hrs;
Desorption at 150 ATM)

	Cycle No.	Loading (g/g)		Adsorbed in i^{th} Cycle (g/g)	Desorbed in i^{th} Cycle (g/g)
		After Adsorption	After Regeneration		
Series PH-3 desorption at 120°C; 50 SLM; 3000 SL	1	.25	.03	.25	.22
	2	.26	.03	.23	.23
	3	.26	.06	.23	.20
	4	.28	.06	.22	.21
Series PH-4 desorption at 120°C; 50 SLM; 750 SL	1	.25	.09	.25	.16
	2	.27	.08	.18	.19
	3	.26	.05	.18	.21
	4	.23	.05	.18	.18
Series PH-5 desorption at 250°C 50 SLM; 750 SL	1	.26	.02	.26	.24
	2	.24	.05	.22	.19
	3	.29	.06	.24	.23
	4	.30		.24	

A series of adsorption-desorption cycles were made with acetic acid of F-300 GAC screened to + 20 mesh. The results are shown in Fig. VI-12 For the high feed concentration used, the adsorption front broke through almost immediately and the effluent concentration gradually rose to the level of the feed. On the 7-g carbon column, the effluent reached the feed concentration within 2 hr and the loading obtained on virgin carbon is 0.048 g/g.

The column was regenerated, without drying, with SCF CO_2 at 120°C and 150 atm. The desorption was essentially complete within 30 min. As seen in Table VI-5 the loadings obtained upon readsorption were within experimental error of that obtained on virgin GAC. Only one curve is shown in Fig. VI-12 because the breakthrough curves were essentially identical for all eight adsorption cycles. Thus, for this weakly adsorbed solute, capacity recovery is complete and the rate of regeneration is extremely rapid.

D. ALACHLOR REGENERATION

As discussed in the preceding section, Alachlor was chosen as the pesticide for further study. In the pesticide screening studies, Alachlor was regenerated for more than 30 cycles. The working capacity declined gradually from 0.20 to 0.10 g/g over the first 19 cycles and then remained constant from the twentieth cycle to the conclusion of the series at the thirty-second cycle.

The behavior of Alachlor is similar in kind to that observed for prolonged loading of phenol at low concentration (i.e., 120 ppm). In both cases, the loading declined most during the first cycle and then declined more gradually in subsequent cycles. On the other hand, the rate of adsorption of phenol is significantly faster than that of Alachlor. This herbicide has a low water solubility (140 ppm at 25°C) and relatively low diffusivity due to its high molecular weight (MW = 269) and somewhat bulky structure. During the course of determining the Alachlor adsorption isotherm, the rate of adsorption was measured. The results, shown in Fig. V-13 (Section V), indicate that over the first 5 days, adsorption is still proceeding at a modest rate.

The question arises as to whether the build up of adsorbed Alachlor over the prolonged adsorption period is primarily irreversible species, as was the case with phenol. If reversibly adsorbed Alachlor is taken up rapidly and irreversible adsorption occurring slowly, then we would expect to find no more solute desorbed after prolonged exposure than that obtained after short exposure.

To further elucidate the nature of Alachlor adsorption a series of experiments were conducted in which the desorption curves were measured after several different times of exposure. The desorption curves were obtained by trapping solute during regeneration in the apparatus of Fig. VI-1. The procedure for regeneration was as follows:

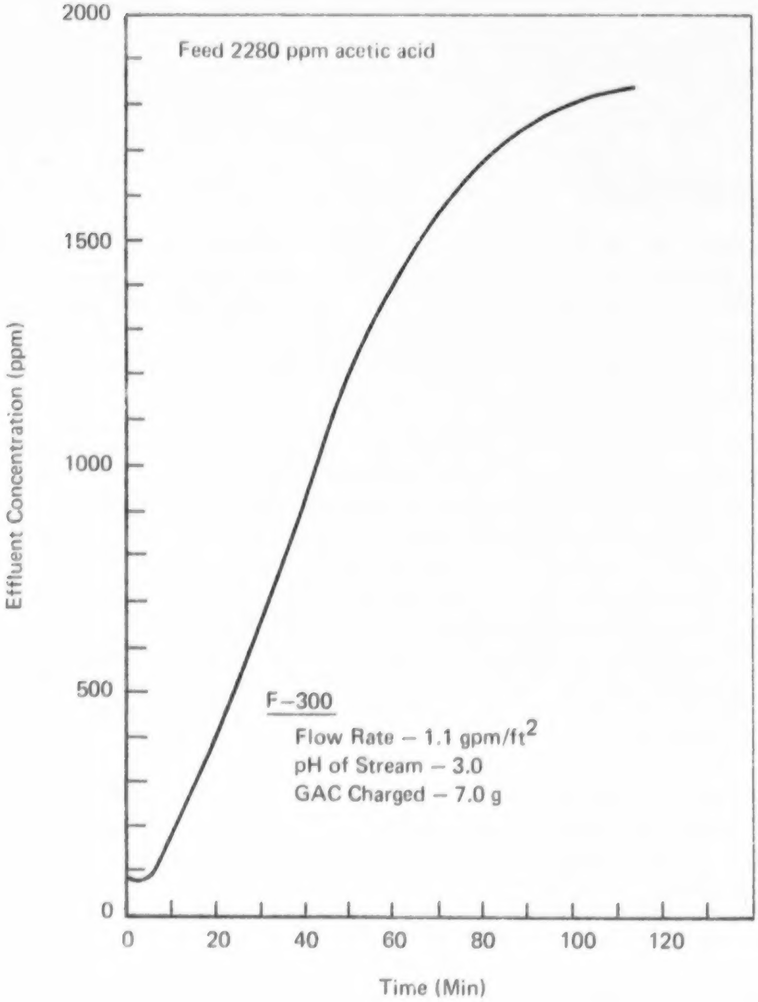

FIGURE VI–12 ADSORPTION OF ACETIC ACID ON F–300

TABLE VI-5

ACETIC ACID REGENERATION

$120^{o}C$, 150 atm CO_2

Cycle No.	GAC Capacity, g/g
1 (virgin)	0.048
2	0.043
3	0.044
4	0.045
5	0.046
6	0.044
7	0.045
8	0.050

a. The column, containing spent GAC, was dried at 1 atm and 55°C and then pressurized to the desired level (typically 275 atm for the majority of the Alachlor regeneration tests).

b. A given amount of CO_2 was passed through the column, as measured with the dry test meter.

c. The amount of Alachlor removed from the column and collected in the cold trap was weighed and the average concentration calculated; that concentration value is plotted as a "bar" in the desorption curve.

The desorption curves obtained after one, three and ten days of adsorption are shown in Fig. VI-13. The corresponding amounts of solute collected were 0.105 g/g (1 day), 0.131 g/g (3 days) and 0.185 g/g (10 days). The increase in desorbable solute with longer adsorption period is evidence that the adsorption of the reversible Alachlor species occurs by a relatively slow process. The increase in initial concentration of the effluent (i.e., at the onset of regeneration) in Fig. VI-13 as adsorption period increases is consistent with a higher loading of reversibly adsorbed solute.

The slow build up of irreversibly adsorbed Alachlor does not necessarily imply that the rate is controlled by a highly activated process. Since Alachlor feed concentration was only 120 ppm (vs. 2,000 to 10,000 ppm for phenol) and Alachlor diffusion is relatively slow, the rate of formation of an irreversible Alachlor species may be controlled by mass transfer and not reaction kinetics. During each adsorption cycle, the major fraction of Alachlor adsorbed can be desorbed. The reversibly adsorbed species is undoubtedly physically adsorbed, the rate of which should not be appreciably activated in the adsorption kinetics. Since a sharp break in adsorption rate was not observed during the 28-h adsorption period, it is likely that the rate of adsorption was controlled by mass transfer. As the build-up of irreversibly adsorbed species occurred in parallel with the reversible adsorption, the rate of irreversible adsorption of Alachlor could well have been also diffusion-controlled. Thus, we cannot distinguish between activated and non-activated kinetics for adsorption of the irreversible Alachlor species.

As discussed previously (Section VI-B, Phenol Regeneration), it may be advantageous in commercial practice to use the same column for adsorption and in situ regeneration (i.e., no transfer of GAC between adsorption and regeneration). When reversible adsorption is slow, as in the case of Alachlor, in situ regeneration is not feasible. On the other hand, if the rate of adsorption is diffusion-controlled, then the rate can be increased by using a narrow cut of smaller particles. Since this represents a departure from commercially available GAC, the cost of the adsorbent would undoubtedly require a premium. However, a higher cost of adsorbent would not have a significant impact on the economics of the SCF regeneration process because GAC is not lost during regeneration. Thus, it may be desirable to use GAC that is tailored to the SCF regeneration process. In this manner, bulky adsorbates such as Alachlor may be made to undergo rapid adsorption with relatively high loading of the reversibly adsorbed species.

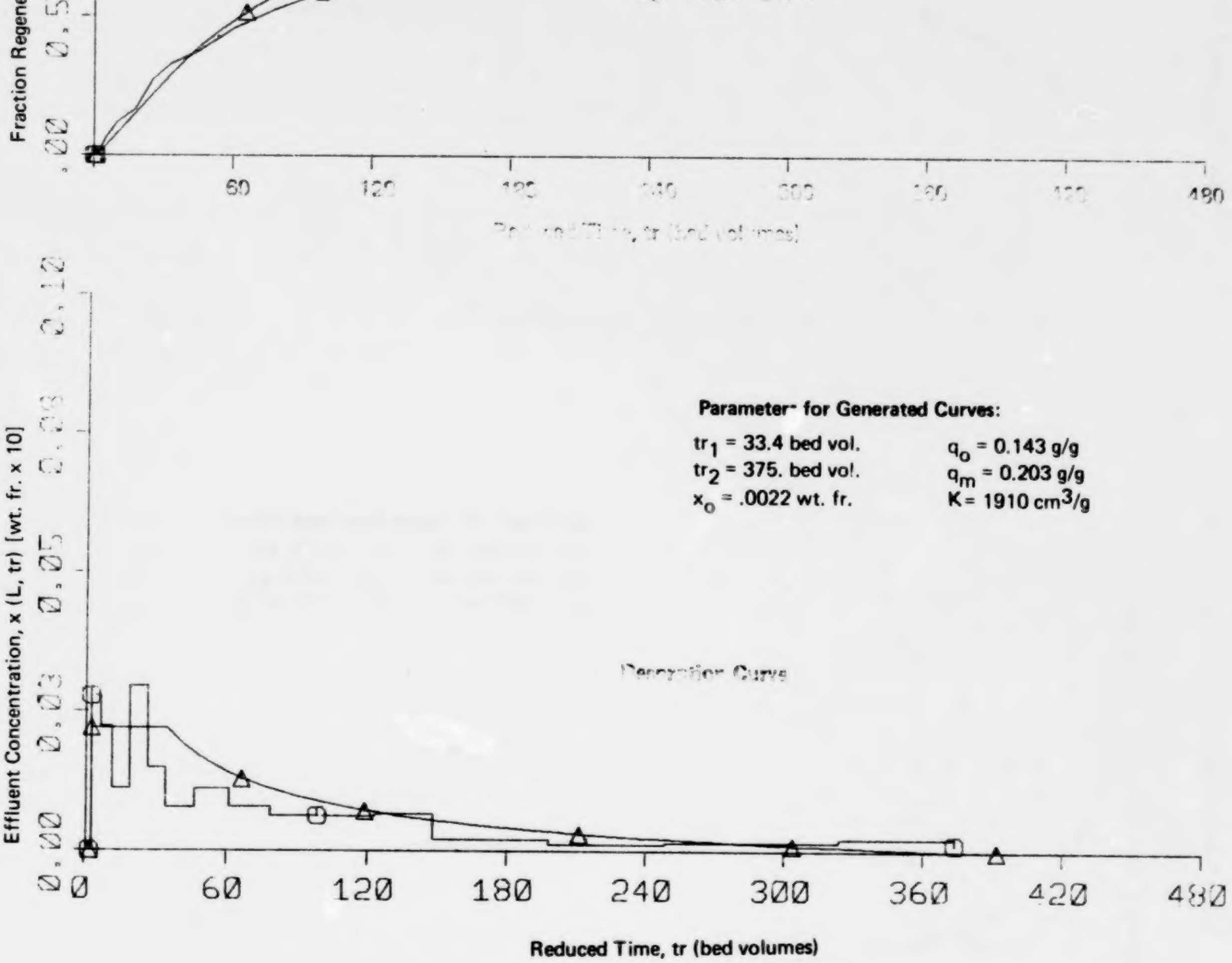

FIGURE VI–13A REGENERATION AND DESORPTION CURVES AFTER ONE-DAY ADSORPTION OF 120 PPM ALACHLOR

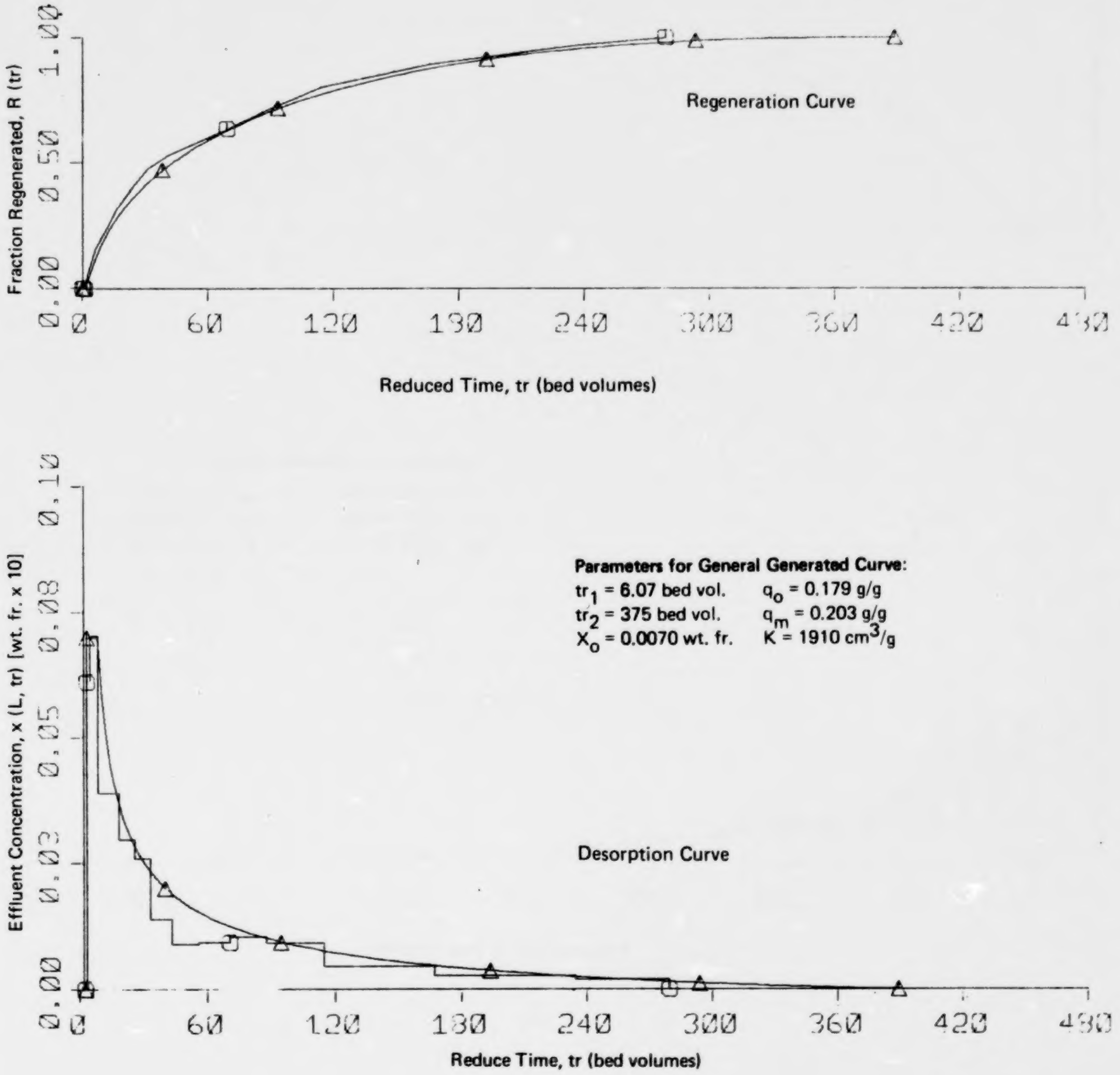

Parameters for General Generated Curve:

tr_1 = 6.07 bed vol. q_o = 0.179 g/g

tr_2 = 375 bed vol. q_m = 0.203 g/g

X_o = 0.0070 wt. fr. K = 1910 cm^3/g

FIGURE VI-13B REGENERATION AND DESORPTION CURVES AFTER THREE-DAY ADSORPTION OF 120 PPM ALACHLOR

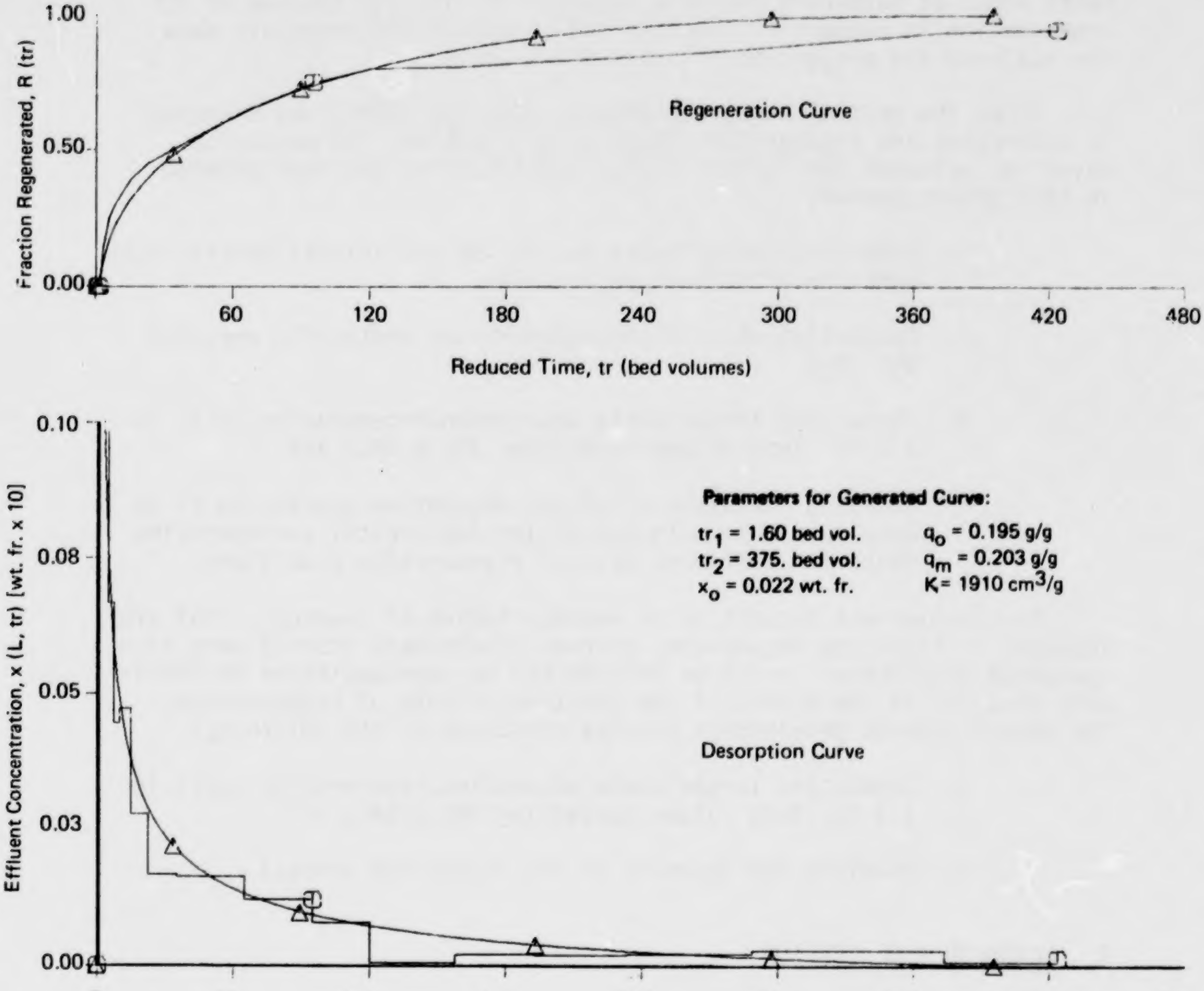

Parameters for Generated Curve:

tr_1 = 1.60 bed vol.

tr_2 = 375. bed vol.

x_o = 0.022 wt. fr.

q_o = 0.195 g/g

q_m = 0.203 g/g

K = 1910 cm^3/g

FIGURE VI-13C REGENERATION AND DESORPTION CURVES AFTER TEN-DAY ADSORPTION OF 120 PPM ALACHLOR

VII. PROCESS DEVELOPMENT STUDIES

The process development studies consisted of a number of experiments aimed at gathering the data required to simulate the use of SCF regeneration in commercial practice and to obtain the necessary data for scale-up and projection of plant-scale costs.

After the initial screening phase, concerted effort was directed to adsorption and regeneration tests using alachlor, the pesticide which was selected for further study; specifically, the test program in this phase covered:

1. Examining the effluent quality by the initial breakthrough behavior of SCF-regenerated GAC;
2. Conducting closed-loop regeneration tests with recycled SCF CO_2;
3. Conducting larger scale adsorption/regeneration tests in a 4-ft.-long column containing 380 g GAC; and
4. Modeling the dynamics of the desorption process so as to develop a rationale for projecting capital and operating costs for different sets of regeneration conditions.

As alachlor was thought to be representative of chemicals that are somewhat difficult to regenerate, process development studies were also conducted with phenol, which we believe may be representative of chemicals that lie in the middle of the spectrum of ease of regeneration. The phenol process development studies consisted of the following:

1. Conducting larger scale adsorption/regeneration tests in a 4 ft. long column containing 380 g GAC; and
2. Modeling the dynamics of the desorption process.

A. ALACHLOR REGENERATION

1. Effluent Quality Tests; Initial Breakthrough Behavior

During the earlier screening phase, the behavior of the total breakthrough curve had been primarily used to characterize the efficiency of regeneration and the capacity recovery during subsequent adsorption. The term "total" connotes the entire effluent concentration-vs-time curve from 0 to the end of the test, where the end point was chosen when the effluent concentration had reached about 85% of the influent; for example, in Figure V-14, which shows a series of adsorption breakthrough curves for Alachlor, the effluent concentration at the end of Al-1-Al is 105 ppm. Although the behavior of the total curve was a reasonable consideration for early regeneration tests in the screening phase, operation of a commercial or municipal adsorber is usually based upon considerations of an effluent quality limit, with "breakthrough" defined as an effluent concentration greater than the allowable limit. For Alachlor, using the source data in EPA 440/1-75/060d, Development Document for Interim Final Effluent Limitations Guidelines for the Pesticide Chemicals Manufacturing Point Source Category (November 1976),an allowable discharge stream concentration of 0.22 ppm was calculated from the following criteria:

Effluent Limitations Guideline = 0.00705 kg/1000 kg of product

Wastewater Flow = 3,840/gal/1000 lb. of product

and based upon the previous information,

Allowable Concentration of Alachlor in Discharge Stream =
$[0.00705/(3840 \times 8.3 \text{ lb/gal})] \times 10^6 = 0.22$ ppm

In order to investigate the ability to achieve the effluent quality with GAC regenerated with CO_2, adsorption breakthrough tests were made at a superficial velocity of about 1 gpm/ft^2 (rather than the 7.5 gpm ft^2 value tested in the previous rapid exhaustion rate runs); the 11" x 3/8" ID column holding 7 g GAC was used in these tests.

Adsorption tests were continued for a total length of time equal to at least twice the time to breakthrough, i.e., if the effluent reached 0.22 ppm in, say, 16 hours, the adsorption was continued for at least another 16 hours or longer. For the analysis of very low concentration levels, 100 mm path-length flow cells were used in the double-beam UV spectrophotometer which was operated at a wavelength of 225 nm, using the long path cells the resulting accuracy in concentration measurement was found to be about 0.02 ppm.

The initial portion of the breakthrough curves are given in Figure VII-1. The figure shows that both on virgin and on regenerated GAC, a 118 ppm influent Alachlor solution can be lowered to below the allowable 0.22 ppm level. Breakthrough curves for two virgin GAC adsorption tests and for two regenerated GAC tests which were carried out at 1.1 and 7.5 gpm/ft^2 respectively, are plotted in Figure VII-2. (as a function of volume throughput, rather than as a function of time) in order to compare the breakthrough curves at the two respective flow rates. As is seen in Figure VII-2,the effect of the higher flow rate is a faster (and in fact, an immediate) breakthrough, in agreement, of course, with all literature data on dynamic adsorption. The 0.22 ppm breakthrough,which is indicated by an arrow at 2.6 liters of solution, equates to about 350 bed volumes of wastewater passed.

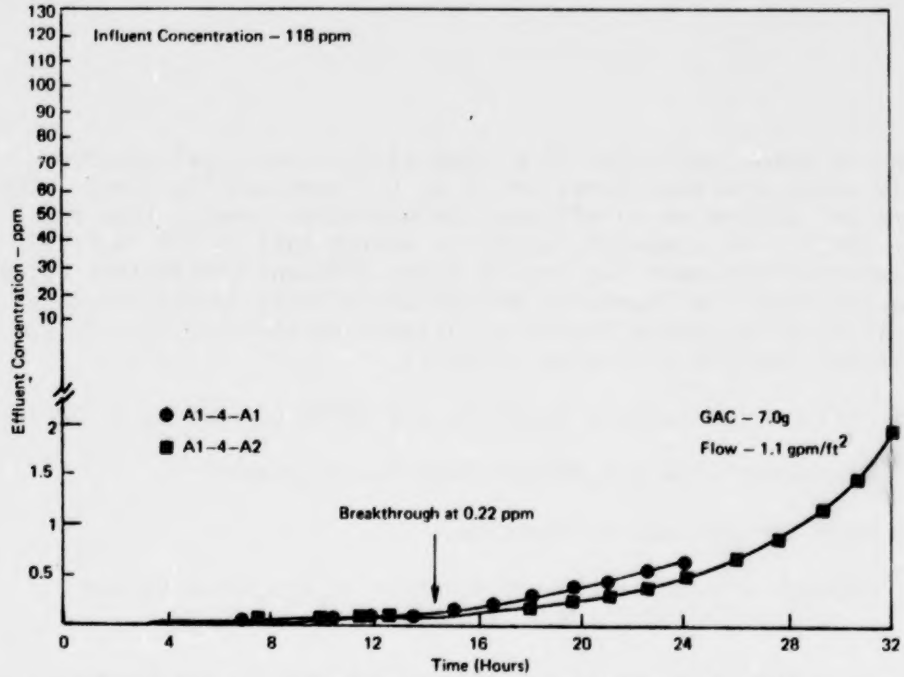

FIGURE VII-1 ALACHLOR ADSORPTION BREAKTHROUGH CURVES (Effluent Quality Series)

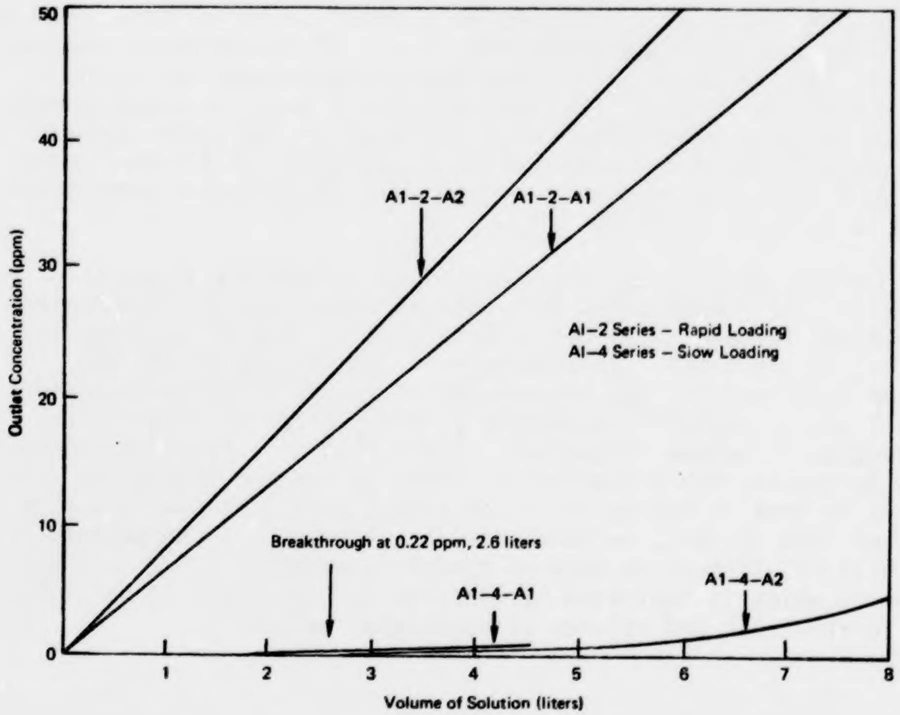

FIGURE VII–2 ALACHLOR ADSORPTION BREAKTHROUGH CURVES COMPARISON OF SLOW AND RAPID LOADING

Two series of adsorption/regeneration tests comparing the behavior of F-300 and F-400 GAC were made. The effluent quality portions of the breakthrough curves are shown in Figures VII-3 and VII-4 respectively, and the data show that the time to reach breakthrough is greater for the F-400 GAC, both on virgin GAC and on SCF-regenerated material. The F-300 material was screened to +20 mesh particle size, wheras the F-400 GAC was used directly for the adsorption tests. For informational purposes, the size characteristics of the two commercial grades are compared in Table VII-1; the differences in the breakthrough characteristics of F-300 (+20 mesh) and F-400 in Figures VII-3 and VII-4 then, are probably attributable to the particle size differences in the two GAC materials.

Two effluent quality tests were next made with F-300 GAC of two different particle size distributions; the +20 mesh cut, and a small size range of -12+30 mesh screened from the commercial grade. The effluent quality portion of the respective breakthrough curves and the total breakthrought curves for the two mesh sizes are compared in Figure VII-5 On the basis of the effluent quality portion of the breakthrough curve, the -12+30 mesh size demonstrated a factor of three improvement in capacity at breakthrough (76 hrs-22 hrs)/22 hrs), compared to the capacity of +20 mesh GAC. Smaller mesh GAC results in sharper breakthrough curves. For data evaluation purposes, a reasonably sharp breakthrough is an optimum situation for studying effects of SCF regeneration on effluent quality,and thus it was concluded that subsequent tests with all pesticides and with phenol were to be carried out using only the smaller particle size fraction, -12+30 mesh, to be obtained by screening standard F-300.

2. Closed-Loop Regeneration Tests of Alachlor-Loaded GAC

The adsorption capacity recovery data that has been reported in previous sections was the result of regeneration of spent GAC carried out with SCF CO_2 in a once-through mode; i.e., CO_2 from a cylinder was passed through the column wherein dissolution of pesticide from the GAC occurred, the CO_2 expanded to 1 atm to precipitate collect the pesticide, and the CO_2 exhausted to the atmosphere.

A closed-loop regeneration train was assembled in order to assess the capacity recovery of spent GAC after contact with recycled CO_2. Preparatory to the start of the closed-loop regeneration series, the efficiency of precipitating and separating pesticide from a stream expanded to some intermediate pressure level that would be operative in a pilot plant or full-scale facility was determined, and along with the separation efficiency tests a more complete "solubility map" for Alachlor was determined so that the pressure level for operating the separator in the closed-loop series could be selected.

Figure VII-6 gives extended solubility data for Alachlor covering a temperature range from 50°C to 120°C and a pressure range from 1300 to 4000 psi. It is seen that at the 1300 psi pressure level the solubility behavior of Alachlor gives a minimum in solubility at about 75°C, somewhat similar to that reported for naphthalene at 80-100 atm shown in Figure IV-6.

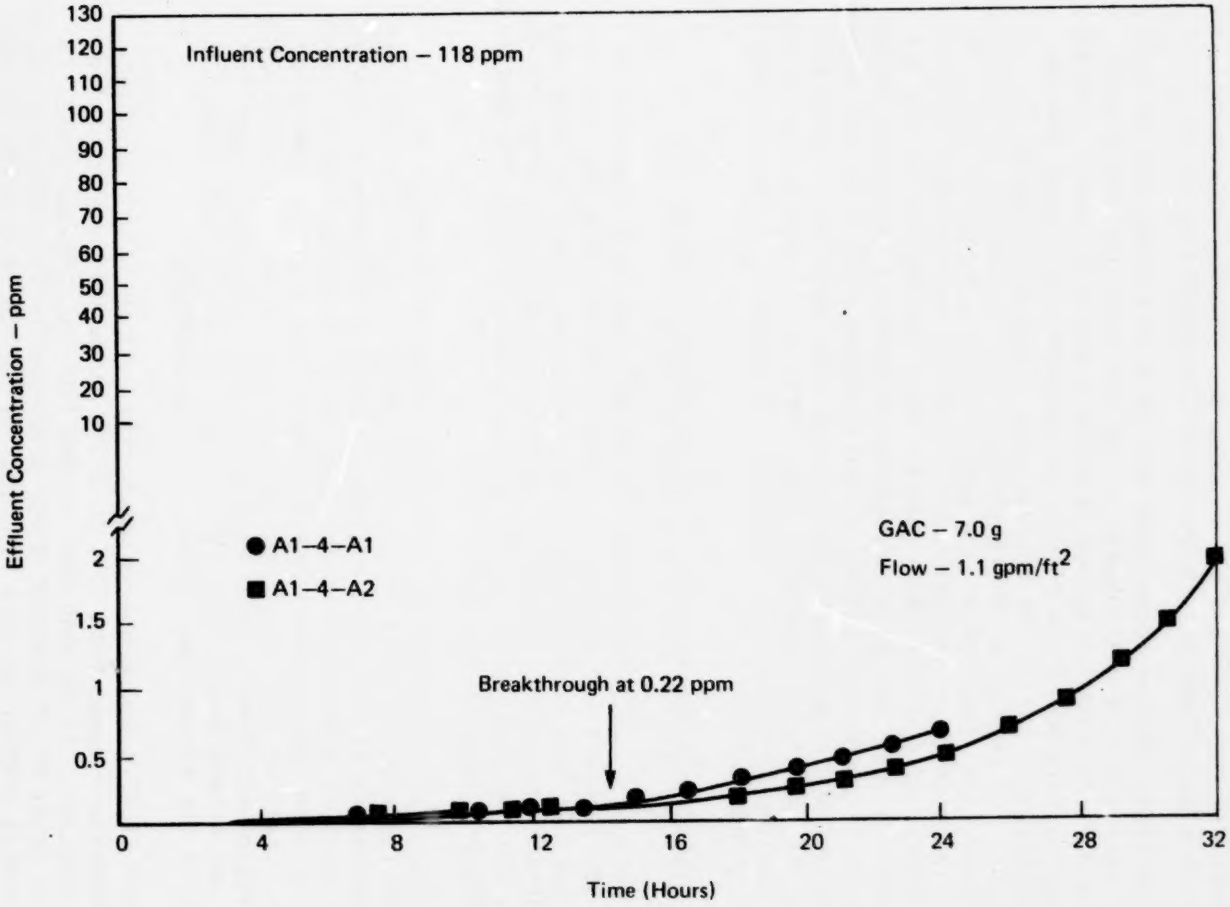

FIGURE VII–3 ALACHLOR ADSORPTION BREAKTHROUGH CURVES WITH F–300
(Effluent Quality Series)

FIGURE VII - 4

ALACHLOR ADSORPTION BREAKTHROUGH CURVES F–400 SERIES

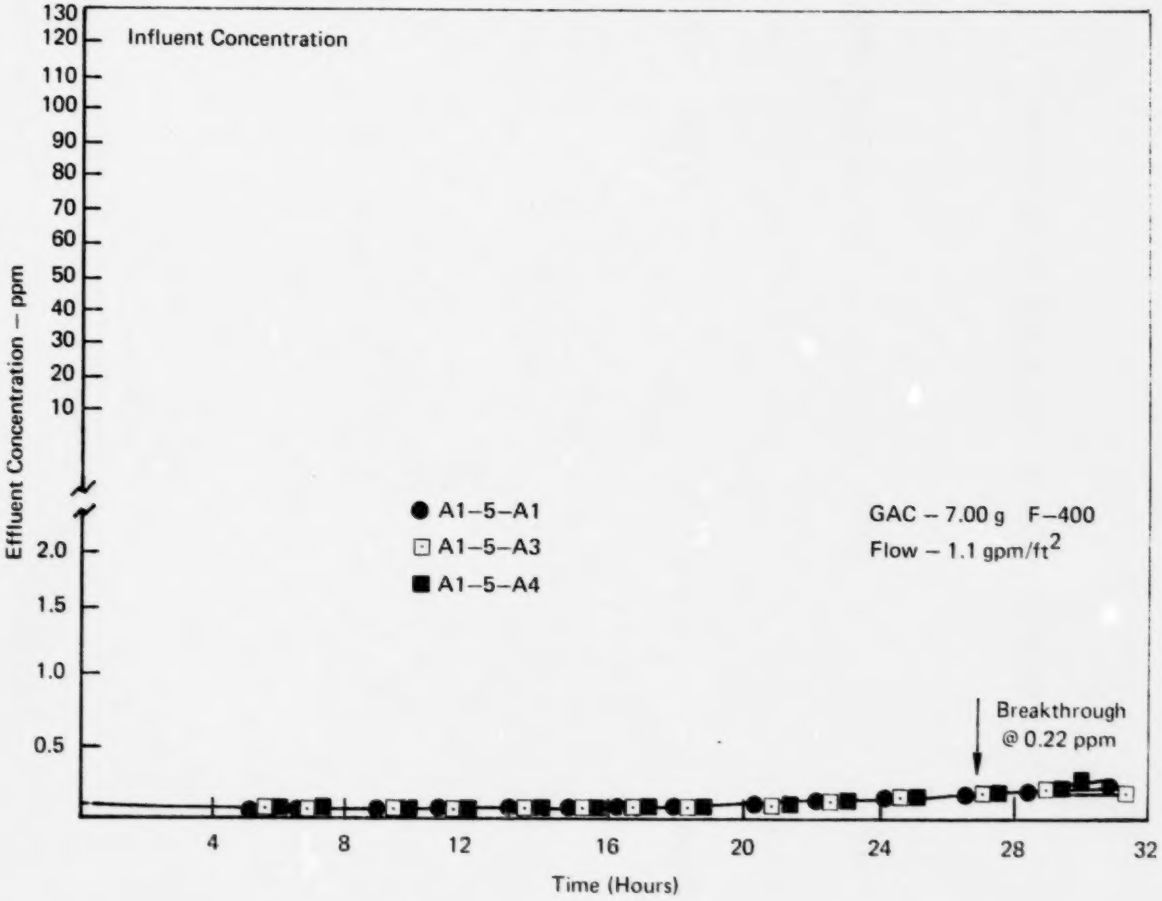

TABLE VII-1

CHARACTERISTICS OF CALGON ACTIVATED CARBONS

TYPE	NORMAL MESH SIZE	SURFACE AREA m^2/g
F-300	+ 20	950 - 1050
F-400	-12 + 40	1050 - 1200

FIGURE VII-5

ALACHLOR ADSORPTION BREAKTHROUGH CURVES EFFECT OF GAC MESH SIZE ON EFFLUENT QUALITY

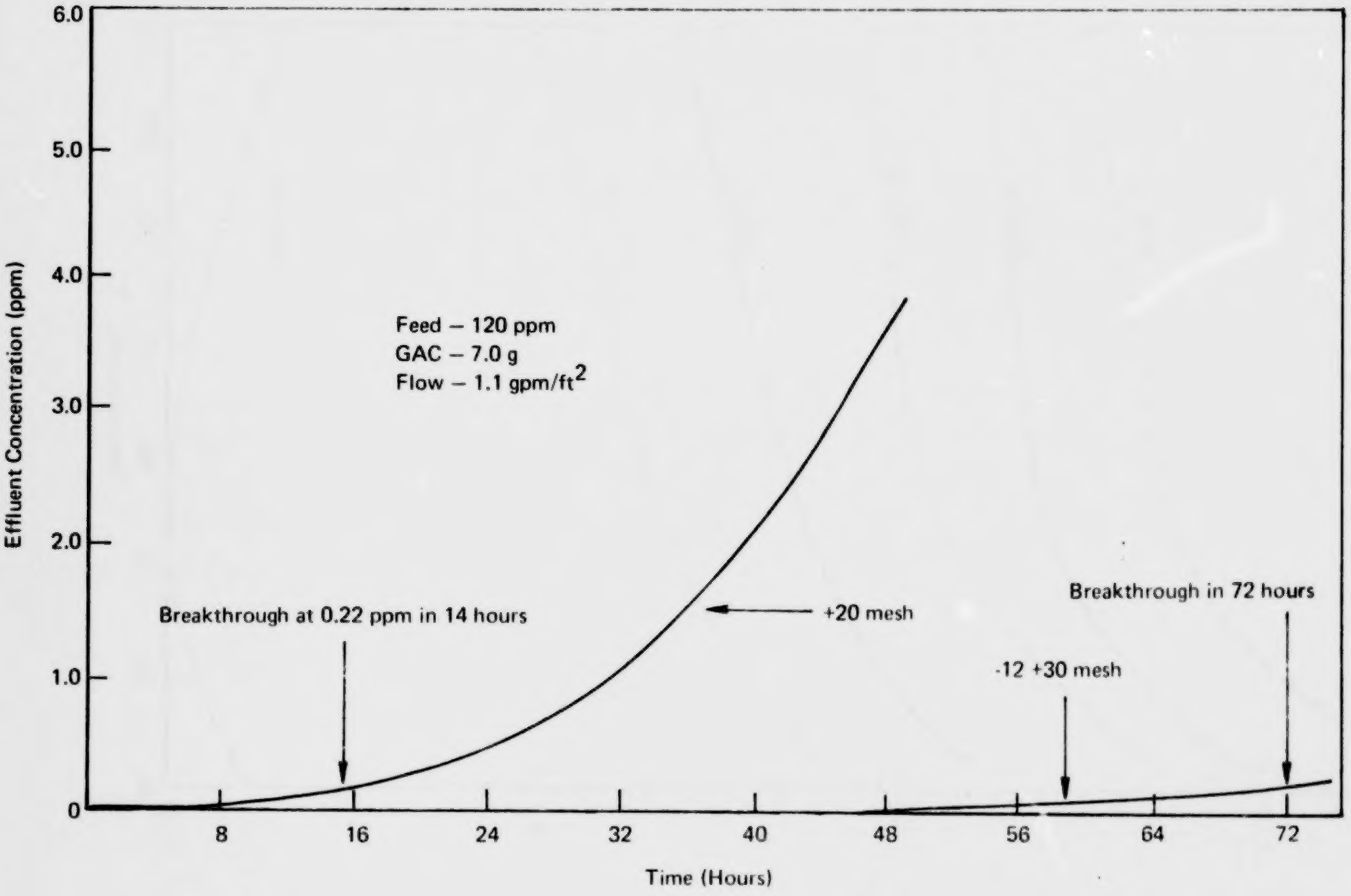

FIGURE VII - 6

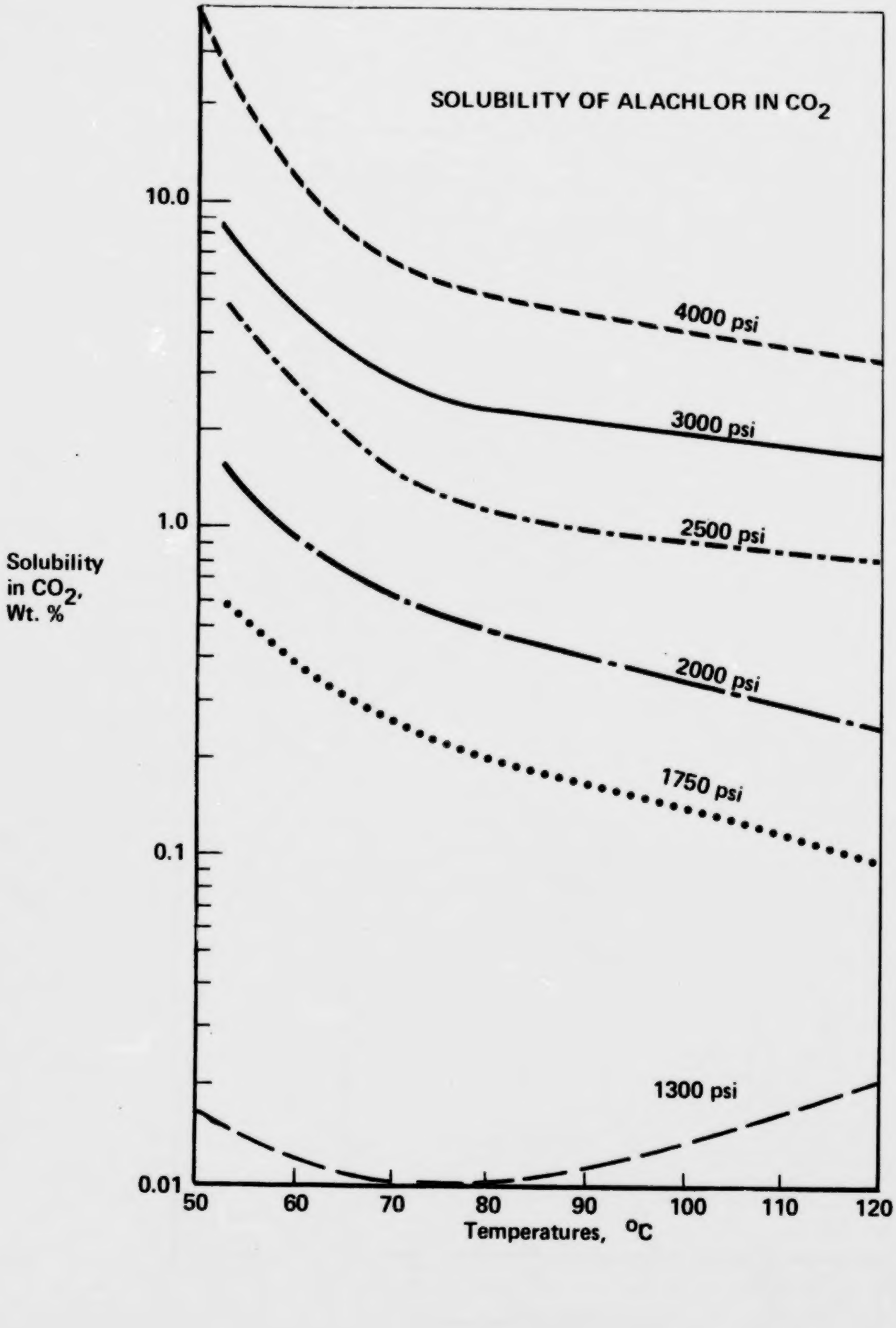
SOLUBILITY OF ALACHLOR IN CO2
Solubility in CO2, Wt. %
10.0
1.0
0.1
0.01
4000 psi
3000 psi
2500 psi
2000 psi
1750 psi
1300 psi
50
60
70
80
90
100
110
120
Temperatures, °C

The pressure level of 1300 psi was selected for closed loop separator operation and for preliminary separation tests. For these tests the apparatus shown schematically in Figure VII-7 was used. To the high pressure solubility set-up previously shown in Figure V-1 there was added another pressure vessel to act as a separator and a back-pressure regulator as indicated. In the determination of separator efficiency the extraction vessel was loaded with Alachlor, and operation of the system to test separation at intermediate pressure was carried out in the following manner: high pressure CO_2 was passed through the Alachlor, the stream expanded to an intermediate level of 1300 psi as controlled by the back-pressure regulator, and the Alachlor which precipitated at that pressure was collected in the separator. The 1300-psi stream was then expanded to 1 atm across the back-pressure regulator and the Alachlor remaining in the CO_2 flow-measured as before with the rotameter and Dry Test Meter. In another test preparatory to closed loop regeneration, a column of Alachlor-loaded GAC was regenerated in the same system shown in Figure VII-8; a material balance on Alachlor removed from the GAC and that collected in both filters was calculated. The pertinent data are shown in Table VII-2 and agreement is reasonably good, the material balances closing within 90%.

The closed-loop regeneration tests were carried out on a 7.7 g column which was loaded using a synthetic 120 ppm Alachlor solution; adsorption breakthrough cruves were obtained in the standard system previously shown in Figure V-4 using on-line UV analysis. Regeneration was carried out in the closed-loop system shown schematically in Figure VII-8 In this system the CO_2 stream leaving the back-pressure regulator is sent to the inlet side of the compressor, recompressed to 4000 psi, and returned to the GAC column.

The complete set of adsorption breakthrough curves for 7 cycles are shown in Figure VII-9 As before, there is a first-cycle capacity loss, but for the second through seventh cycles the total capacity is essentially constant. Figure VII-10 gives the effluent quality portions of the same breakthrough curves on a magnified ordinate scale; loading data are given in Table VII-3. The breakthrough appears to fall into two groupings, but unrelated to the progression of cycles. For example, the second, fourth, and last cycles fall together indicating that there was no monotonic trend in breakthrough behavior. It should be noted that the method of plotting the data in Figure VII-10 magnifies any experimental error; the same data plotted in Figure VII-9 previously showed that cycles 2 through 7 coincided reasonably well.

3. 4-Ft. Column Adsorption/Regeneration

As stated previously, the rationale for using small columns and a high feed flow rate was to obtain rapid loading of GAC in a short time so that many cycles of adsorption/regeneration could be logged on a single charge of GAC. Subsequently, it was found that low flow rate tests on the small columns could provide reasonable breakthrough behavior, but it was desirable to test the finding with a larger scale column. A 1-1/4" ID x 4-ft column adsorption/regeneration system for Alachlor was built for this purpose.

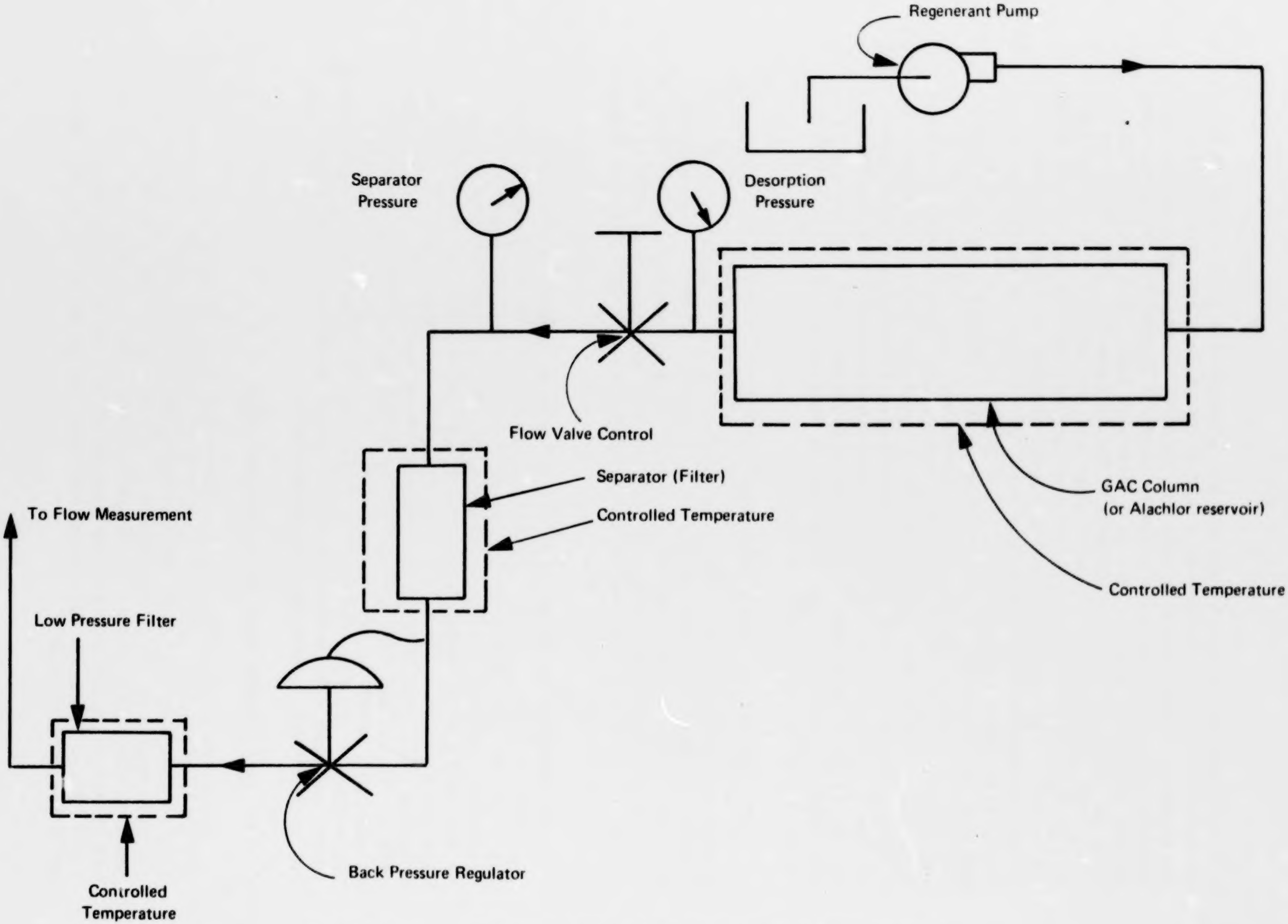
Regenerant Pump
Separator
Pressure
Desorption
Pressure
Flow Valve Control
Separator (Filter)
Controlled Temperature
GAC Column
(or Alachlor reservoir)
Controlled Temperature
To Flow Measurement
Low Pressure Filter
Back Pressure Regulator
Controlled
Temperature

FIGURE VII–7 SCHEMATIC DIAGRAM OF DESORPTION AND SEPARATION

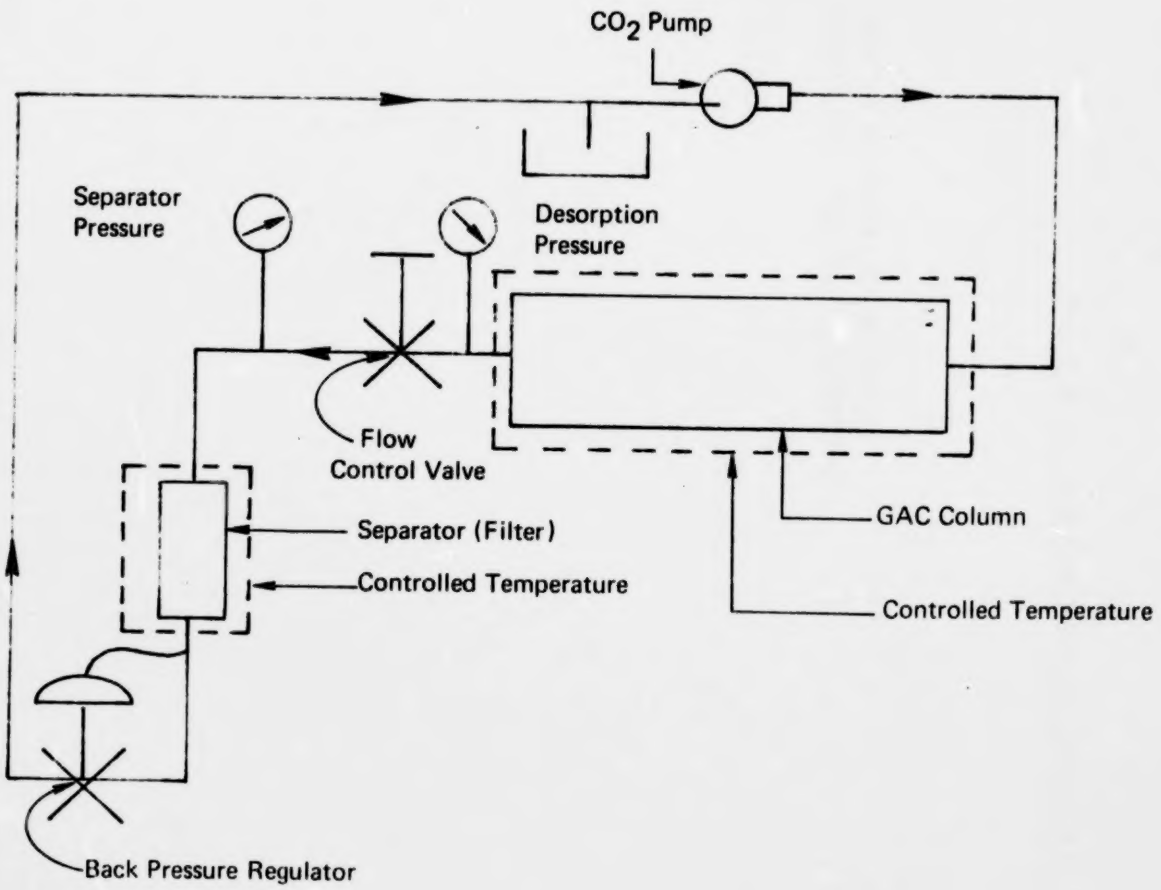

CO_2 Pump
Separator Pressure
Desorption Pressure
Flow Control Valve
Separator (Filter)
Controlled Temperature
GAC Column
Controlled Temperature
Back Pressure Regulator

Figure VII-8 **SCHEMATIC DIAGRAM OF RECYCLE TEST**

TABLE VII-2

ALACHLOR DESORPTION MATERIAL BALANCE DATA

ALACHLOR REMOVED	ALACHLOR COLLECTED IN FILTERS	
	Intermediate Pressure	Low Pressure
0.58 g	0.33 g	0.19 g

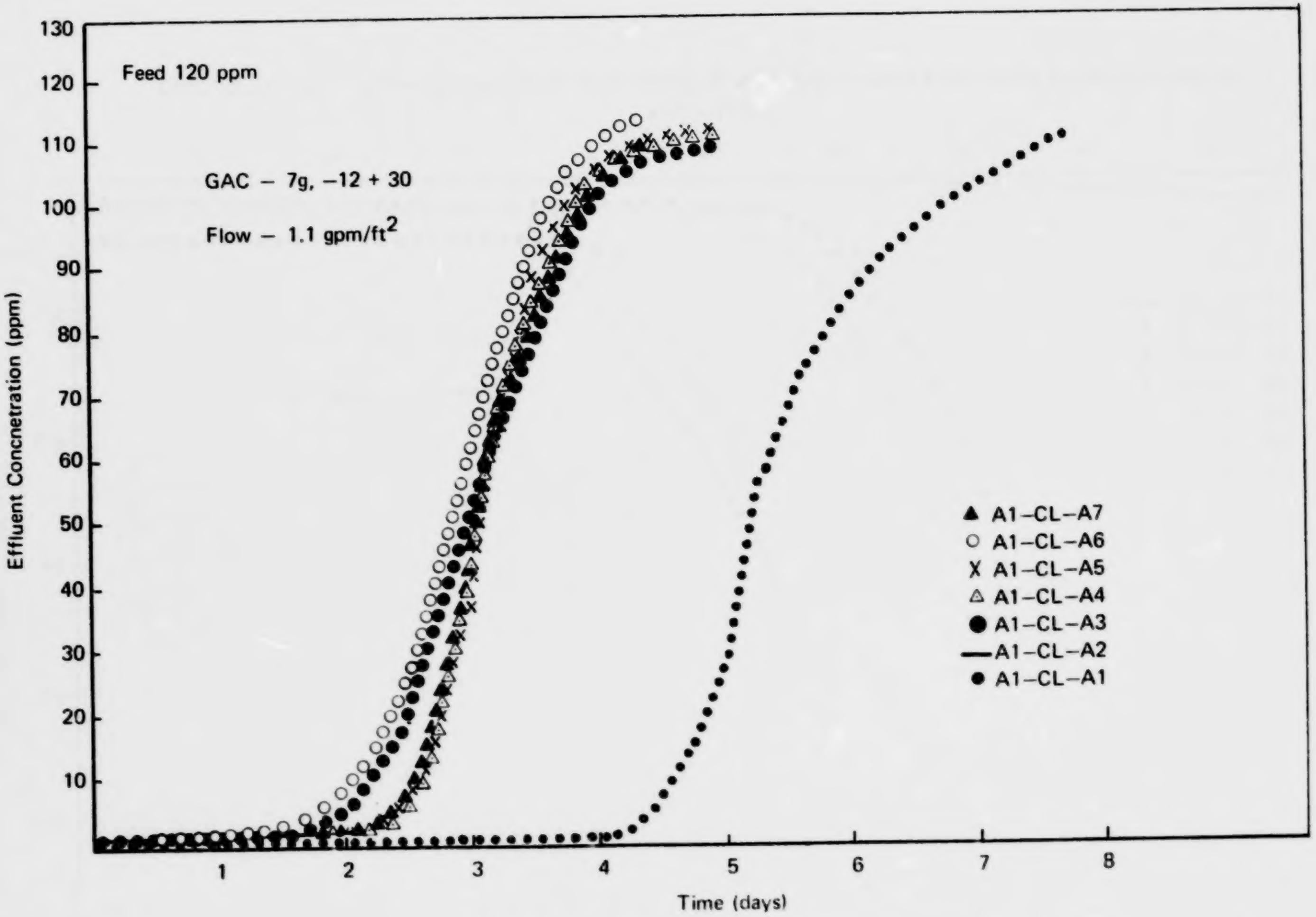

FIGURE VII–9 COMPARISON OF COMPLETE BREAKTHROUGH CURVES FOR ALACHLOR ADSORPTION CLOSED LOOP SERIES

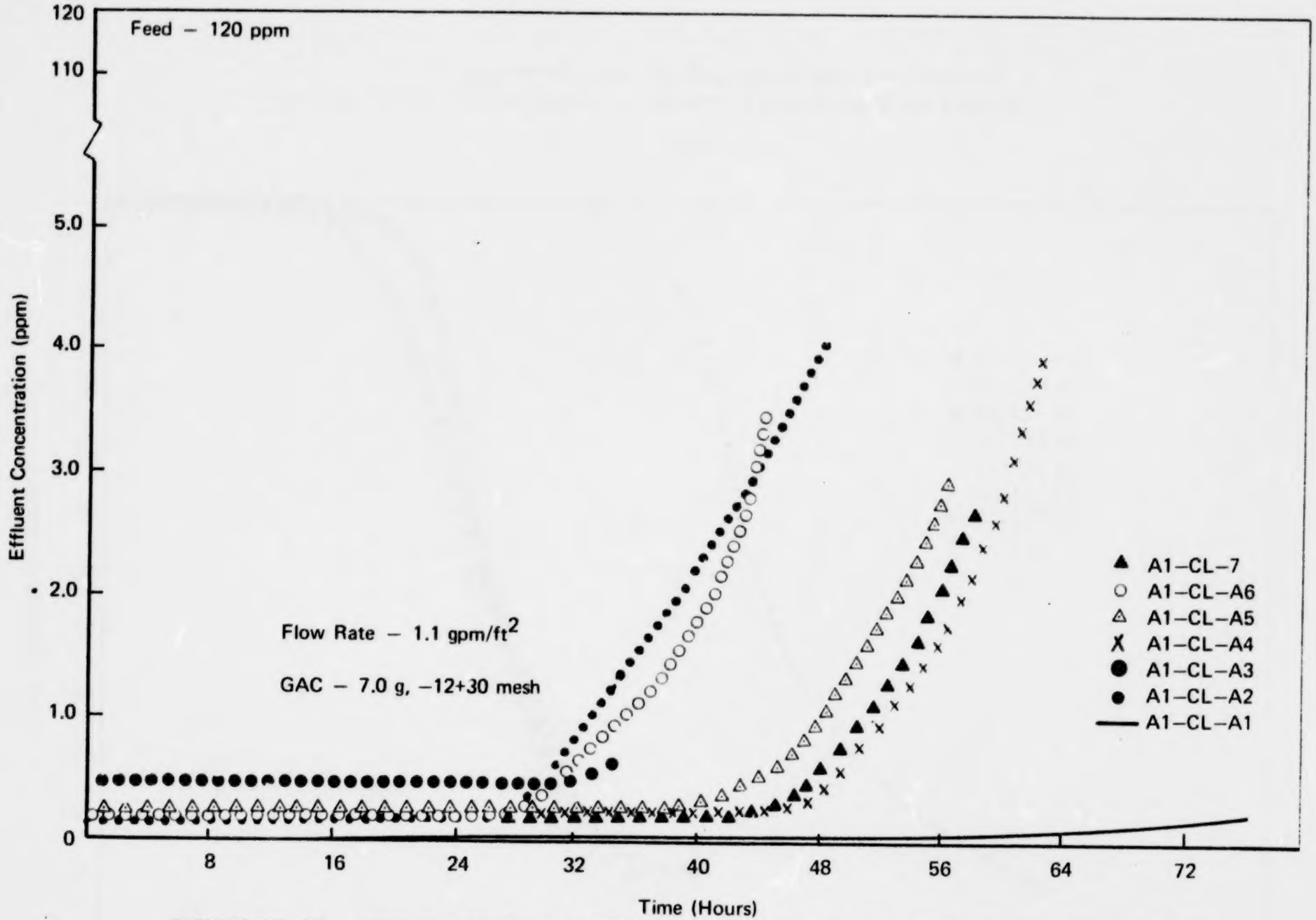

FIGURE VII–10 ADSOPRTION FROM SYNTHETIC ALACHLOR CLOSED LOOP REGENERATION SERIES

TABLE VII-3

ALACHLOR LOADING AND EFFLUENT QUALITY RESULTS AFTER CLOSED-LOOP REGENERATION

Cycle #	Loading After Adsorption	Residual Loading After Regeneration	Initial Effluent Concentration
1	0.38 g/g	0.12 g/g	~ 0
2	0.39 g/g	0.16 g/g	0.1 ppm
3	0.40 g/g	0.14 g/g	0.4 ppm
4	0.40 g/g	0.15 g/g	0.3 ppm
5	0.39 g/g		0.3 ppm

An adsorption test using 120 ppm Alachlor was carried out using the 4-ft. column system, the adsorption continuing until the effluent concentration was essentially equivalent to influent. In order to duplicate the previous fully-loaded tests on small columns, the flow was continued for five days longer. The breakthrough curve for the adsorption is shown in Figure VII-11 and integration of the curve gives an Alachlor loading value of 0.50 g/g GAC. The 4-ft. column was regenerated at the same conditions used for previous Alachlor tests, 275 atm and 120°C. The same SCF supercritical velocity was used for the regeneration, and the desorption curve was obtained described earlier. The desorption curve is shown in Figure VII-12 and the previous desorption curve for a small column is reproduced for comparison; the curves are normalized by the ratio of the GAC charge in the columns, i.e., 380/7. As is evident, the curves are nearly coincident.

4. Modeling Alachlor Desorption; Local Equilibrium Theory

Determining the optimum conditions for regenerating a column by trial-and-error experimentation is a costly, time-consuming process. For each desorption run, the column must be loaded by adsorption prior to desorption. Although desorption with a supercritical regenerant is a relatively fast process, the adsorption step is slow, especially when one wants to attain fully-loaded conditions.

The time required to saturate the adsorbent with solute can be determined either by batch-adsorption testing or by flow testing a column on-line. Batch-testing is easier to do experimentally, but the time required to reach saturation in a batch test has been found to be shorter than that for flow testing. In other words, the batch test vies a lower limit to the time required to saturate a column on-line.

The rate of adsorption of Alachlor from an aqueous solution was determined by batch adsorption tests. The results, shown in Section IV, indicate that more than seven days are required to closely approach equilibrium coverage. In column adsorption flow tests, the time to load the column to near equilibrium coverage is significantly longer: for 7 g-carbon columns (20 cm length by 1 cm i.d.), over ten days were required, while for 380 g-carbon columns (4 ft length by 1.25 inch i.d.) over forty days were required to reach saturation.

Clearly, the number of experimental desorption runs that can be conducted within a given time frame is limited by the slow kinetics of adsorption; the larger the scale, the more severe is the time-constraint. In order to minimize the number of runs required and to develop a rationale for scale-up, an effort was undertaken to develop a theory-based model of the desorption process. With such a theory in hand, one can develop optimization strategies from small-scale tests, extrapolate these results to larger scales, and then perform a small number of large-scale tests to verify the model predictions.

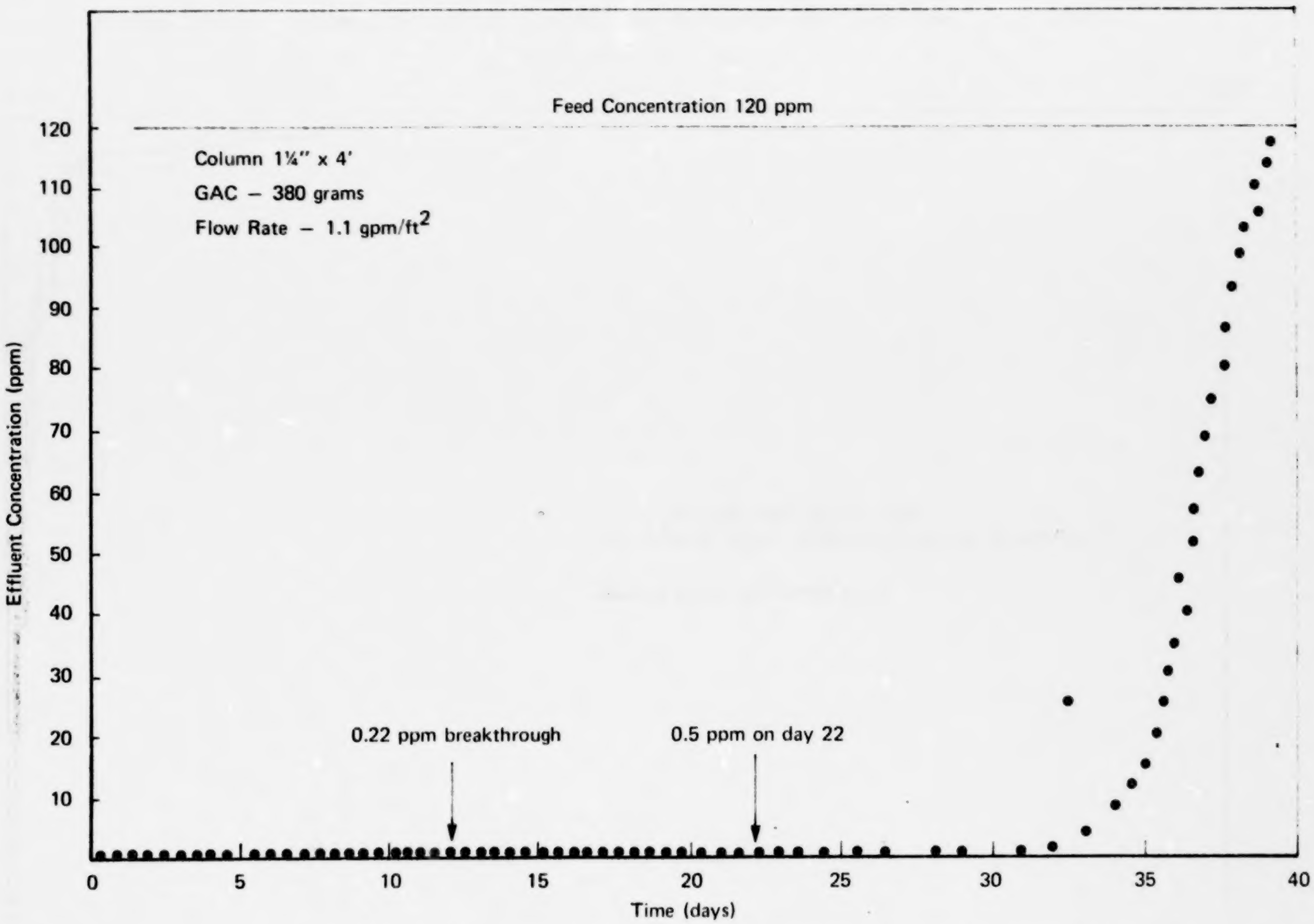

FIGURE VII–11 ADSORPTION FROM SYNTHETIC ALACHLOR SOLUTION IN FOUR FT COLUMN

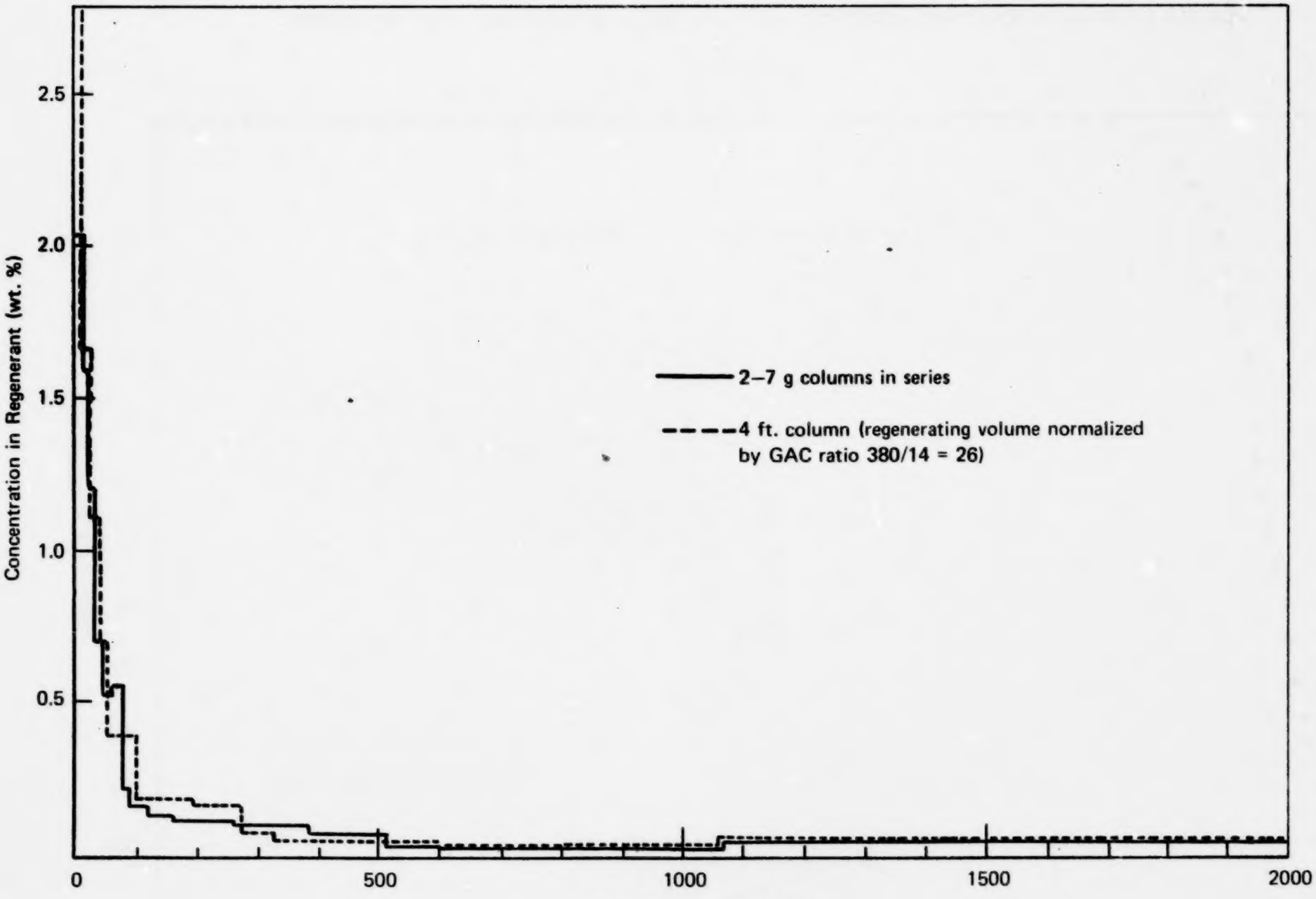

FIGURE VII–12 DESORPTION TRACES OF ALACHLOR REGENERATION CONDITIONS, $120^{o}C$, 4000 psi

The desportion curves for Alachlor (Figure VI-13, Section VI) resemble those predicted by the *local equilibrium theory* (LET) model, which is based on the assumption that equilibrium exists between adsorbent particles and the adjacent fluid at all points within the column (Sherwood, *et al*., 1975). Mass transfer within the SCF phase is rapid and Alachlor solubility in SCF CO_2 is not very high; these two conditions are typical of systems that follow LET behavior. Thus, an effort was undertaken to correlate the Alachlor desorption dynamics by the LET model. A complete description of the LET model is given in Appendix A; a brief outline of the theory along with the significant results are given here.

For a fixed bed wherein longitudinal diffusion is neglected and plug flow is assumed, the material balance on fluid and solid within a differential element is:

$$\varepsilon\left(\frac{\partial c}{\partial t}\right)_z + \rho_B\left(\frac{\partial q}{\partial t}\right)_z + \varepsilon v\left(\frac{\partial c}{\partial z}\right)_t = 0 \qquad (1)$$

where c and q are fluid and solid concentrations, respectively, ε is the fraction of fluid-filled space outside the particles, and ρ_B is the bulk density of the dry adsorbent. The superficial fluid velocity is εv, where v is the average fluid velocity in the interstices between particles.

Before Eq. (1) can be solved, a second equation relating fluid and solid concentrations must be introduced. In the general case, this second equation will take the form of

$$\rho_B\left(\frac{\partial q}{\partial t}\right)_z = kaF(c,q) \qquad (2)$$

which expresses the rate of change of solid phase concentration as a function of the interfacial mass transfer coefficient, ka, and a driving force, F (c,q). Equations (1) and (2) can then be solved simultaneously to obtain the function c (z,t), which is the fluid phase concentration at any position, z, within column as a function of time, t. For example, the effluent concentration curve is c(L, t), where L is the column length.

In the general case, there are two types of mass transfer resistances that are considered in developing Eq. (2): diffusion of solute out of the SCF-filled pores and interfacial mass transfer from the external surface of the adsorbent particle into the bulk of the SCF phase. One of the advantages of a SCF regenerant is that mass transfer is relatively rapid within the SCF phase. In the limiting case where resistance to mass transfer is negligible, Eq. (2) reduces to the equilibrium relationship between solid phase concentration, q, and bulk fluid concentration, c, which is just the adsorption isotherm expression:

$$q = f(c) \qquad (3)$$

For this limiting case, local equilibrium exists at all points within the column and at all times between particles and the adjacent fluid. This, then, is the basis of the local equilibrium theory.

Note that Eq. (3) is the isotherm between GAC and the regenerant, which is SCF CO_2. To avoid confusion with the conventional water-GAC isotherm, the SCF-GAC isotherm will be denoted SCF-isotherm. Also note that Eq. (3) applies to the solute that is desorbed and, hence, it represents only the reversibly-held portion of the solute.

Although we attempted to measure several points on the SCF-isotherm, the data obtained did not cover a wide enough range of concentrations to accurately define the SCF-isotherm (see Appendix A for details). As an alternative, it was assumed that the SCF-isotherm could be described by the Langmuir expression.

$$q = q_m \left(\frac{Kc}{1 + Kc} \right) \qquad (4)$$

where the two contants, q_m and K, were varied to define a set which best fit the desorption and regeneration curves generated by the LET model.

Using a single set of values of q_m and K, desorption and regeneration curves were calculated from the LET model for 10, 3, and 1-day adsorption of Alachlor. The experimentally measured desorption curves were previously given in Fig. VI-13, along with the smooth curve generaged by the LET model. Also shown were the experimental and computed regeneration curves, which are the integrals of the desorption curves.

For the 10-day adsorption experiment, the results of Fig. VI-13C show that the model describes the experimental data moderately well up to 200 bed volumes. Beyond that point, the generated curve goes to zero concentration faster than the experimental desorption trace represents a departure from local equilibrium theory. The regeneration curve accentuates the departure of theory and experiment. It may indicated that pore diffusion out of the particles becomes rate-limiting after a large fraction of the solute is desorbed. The results for the 3- and 1-day adsorption experiments, as shown in Fig. VI-13B and VI-13A agree fairly well with LET-generated curves. Taken as a whole, it appears that the LET model is appropriate for solutes of the Alachlor class.

B. PHENOL REGENERATION

1. Scale-up; Comparison of Small and Large Columns

To gain insight into the dynamics of the desorption process and to develop a rationale for scale-up, several runs were conducted with 380-g (4-ft) columns under conditions similar to those used for 7-g (11-in) columns. Phenol at 2500 ppm was used with F-300. In most cases, the columns were dried prior to desorption. Desorption was conducted at 55°C. The rate of desorption was followed by collecting solute over intervals of time in traps downstream of the pressure letdown valve.

Desorption curves for three 7-g columns on the first regeneration cycle are shown in Fig. VII-13. The total solute collected was 10-20% less than the weight loss of the column; for PB-RI, 0.13 g/g was collected, whereas the column weight loss upon regeneration was 0.16 g/g. Although the desorption curves for the three columns shown in Fig. VII-13 are similar, it was difficult to obtain better accuracy with this procedure because the desorption process is so rapid. The regeneration curves, which are the integrals of the desorption curves, show less scatter (see Fig. VI-13).

The results for regeneration of three 380-g columns are summarized in Table VII-4. Columns P1-48 and P2-48 were adsorbed over moderately prolonged periods and desorbed at 150 atm; these conditions are similar to those of column PB, the results for which were given in Table VI-2 (Section VI). There is relatively good overall agreement between the small and large column behavior.

The regeneration curves for the small and large columns are shown in Fig. VII-14. The difference between the curves for the small and large columns at 150 atm regeneration pressure is related to two factors: the small column curve is lower, in part, due to inefficient collection of solutes in the small column traps. In addition, the large columns contained more transfer units, which tends to enhance the rate of regeneration when plotted on a normalized basis, as in Fig. VII-14.

Column P2-48, which was regenerated at 275 atm, exhibited a faster desorption than the large columns regenerated at 150 atm. This behavior is typical of the effect of pressure on regeneration. In general, higher pressure increases solubility in the supercritical carrier. Since the activity of the adsorbed solute is not appreciably affected by the SCF pressure, the net effect of increasing pressure is to shift the equilibrium adsorption isotherm to lower loading at a given fluid-phase concentration. The desorption rate is quite sensitive to the adsorption equilibrium because mass transfer in the SCF carrier is very rapid. As will be discussed below, the number of transfer units in the 380-g columns is large enough so that the desorption curve approaches that predicted by local equilibrium theory.

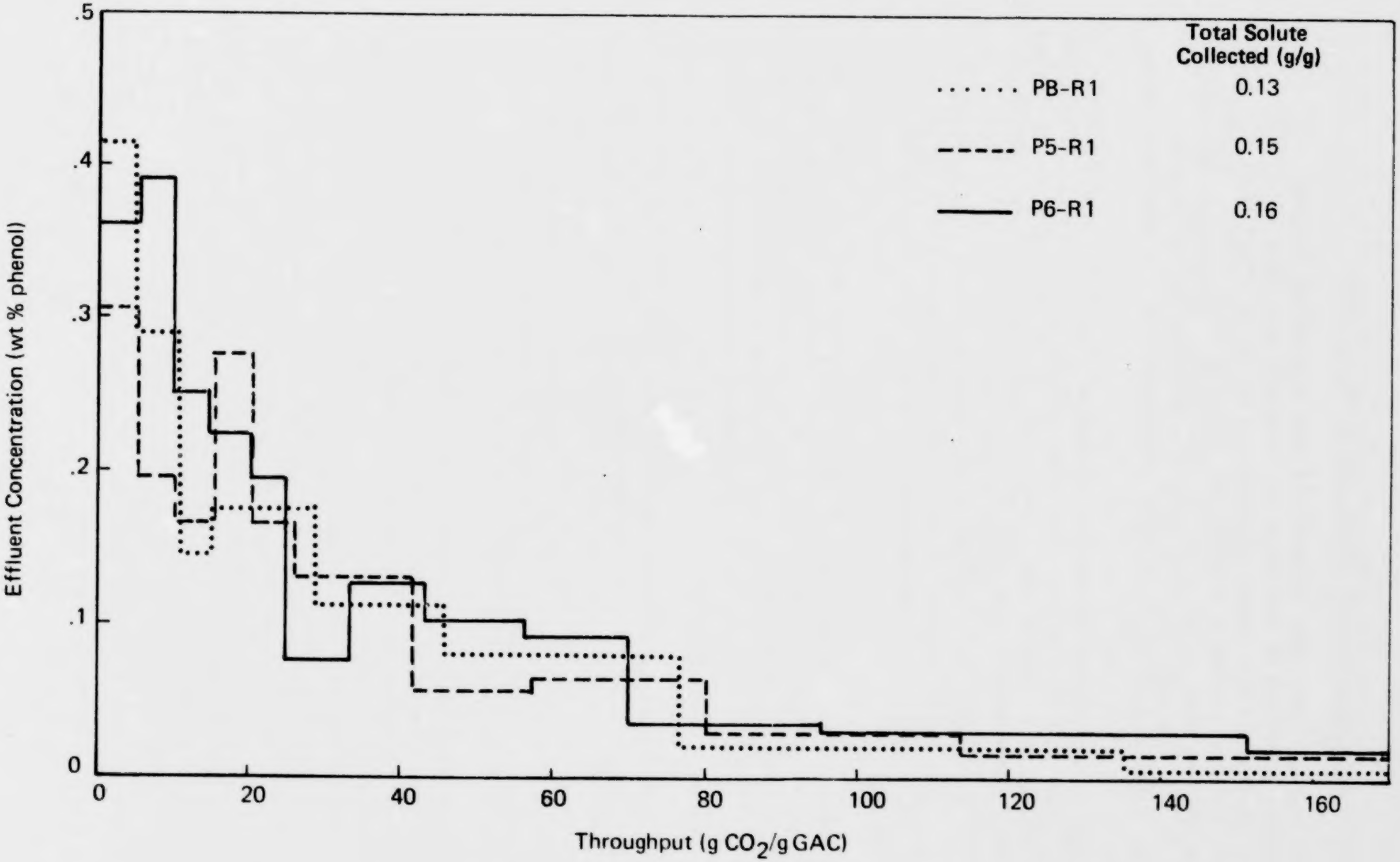

Figure VII-13 **REPRODUCIBILITY OF FIRST CYCLE DESORPTION CURVES; 2500 PPM PHENOL ON 7 g GAC, DESORBED AT 55°C, 15 MPa**

Table VII-4. REGENERATION OF LARGE COLUMNS

2500 ppm Phenol on F-300 Loadings determined by integration of breakthrough curves; desorption at 55^{o}C

Column No.	Desorption Pressure (MPa)	Cycle No.	Adsorption Time (h)	Solute Adsorbed in ith Cycle (g/g)	Solute Desorbed in ith Cycle (g/g)
P1-48	15.0	1	63	0.26	0.17
		2	24	0.25	-wet-
P3-48	15.0	1	52	0.26	0.16
		2	67	0.24	0.12
		3	51	0.19	0.12
P2-48	27.5	1	73	0.26	0.15
		2	56	0.19	0.13
		3	48	0.19	0.13

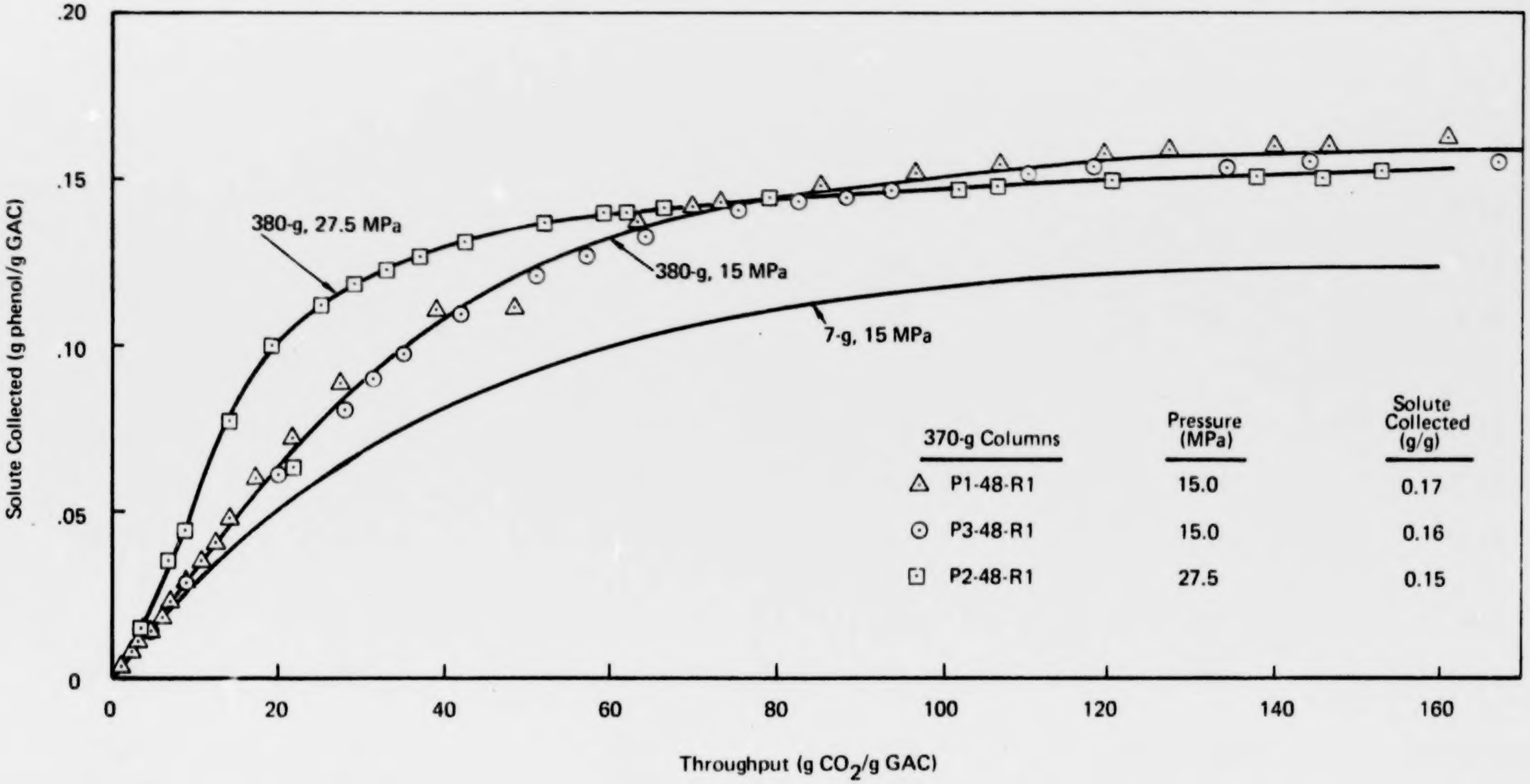

Fig. VII-14 **REGENERATION CURVES FOR SMALL AND LARGE COLUMNS. 2500 ppm PHENOL ON F-300; DESORPTION AT 55° C.**

Column P3-48 underwent three adsorption/desorption cycles; as shown in Table VII-4 , the amount desorbed in the second and third cycles was 0.12 g/g. The regeneration curves for the three cycles are shown in Fig. VII-15. Within the accuracy of the experiment, the desorption curves for the second and third cycles are in good agreement. Note that the regeneration curves for the second and third cycles are shifted down from that of the first cycle. In other words, the fraction of the reversibly adsorbed species is relatively constant with throughput. This results suggests that increased quantities of residual that are present in the second and third cycles do not interfere with the rate of desorption of the reversible species. This result, if it were shown to be true in general, would have broad implications in experimental testing of the applicability of SCF regeneration for other solutes. In the phenol studies we have conducted to date, it appears that the quantity of reversibly-held solute does not change appreciably after the first regeneration (see Figs. VI-3 and VI-7). Since the reversibly-held solute represents the working capacity for SCF regeneration, it is possible to determine the dynamics at the working capacity by measuring the desorption and regeneration curves on the second or third cycles. In other words, there would be no need for conducting a large number of repetitive adsorption/desorption cycles.

2. Modeling the Desorption Process; the Thomas Solution for Fixed-bed Sorbers

As described in the preceeding section, the desorption and regeneration curves for 7-g and 380-g phenol columns are not identical when plotted on a normalized basis (see Fig. VII-14). If the local equilibrium theory were appropriate for phenol desorption, then the normalized curves for large and small columns should be superimposed on one another. The fact that they are not identical implies that mass transfer cannot be neglected in phenol desorption.

For mass transfer in packed beds, the Nusselt number can be expressed as a function of Reynolds number, Re (Gupta and Thodos, 1962):

$$j_D = \frac{1}{\varepsilon}\left[.0100 + \frac{0.863}{Re^{0.58} - 0.483}\right] \qquad (8)$$

where ε is the bed void fraction.

For pore diffusion, the mass transfer coefficient of the solid phase is given by (Sherwood, et al., 1975):

$$k_p = \frac{16.7 D_p}{d_p} \qquad (9)$$

where D_p and d_p are the particle diffusivity and diameter, respectively. The former is expressed as a function of the Knudsen diffusivity, D_k, and the solute diffusivity in regenerant fluid, D_f:

$$\frac{1}{D_p} = \frac{\tau}{\chi}\left(\frac{1}{D_k} + \frac{1}{D_f}\right) \qquad (10)$$

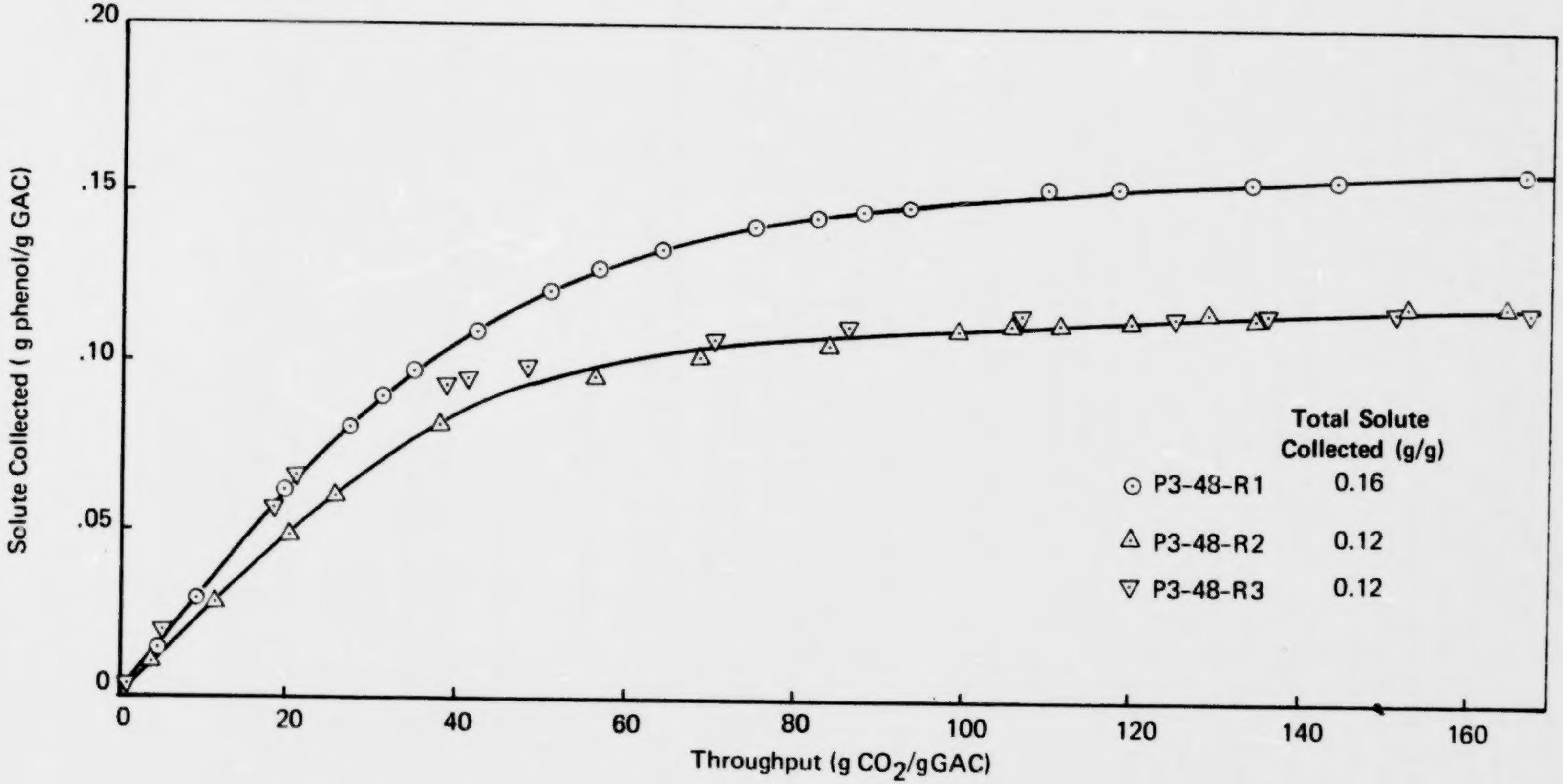

Figure VII-15 **REGENERATION CURVES FOR SUCCESSIVE CYCLES; 2500 PPM PHENOL ON 380 G GAC DESORBED AT 55°C, 1 ATM**

where τ and χ are the tortuosity factor and void fraction within the particle, respectively. The Knudsen diffusivity is a function of particle pore size and mean free path in the fluid-filled pores. It is commonly evaluated by the following correlation (Sherwood, et al., 1975):

$$D_k = \frac{19{,}400\chi}{S_g \rho_p} \sqrt{\frac{T}{M}} \qquad (11)$$

where S_g is adsorbent surface area; ρ_p, particle density; T, temperature; and M, solute molecular weight.

Taken together, Eqs. (7) through (11) provide a means for calculating k_f and k_p which, in turn, allow us to determine κ by Eq. (6). Having evaluated κ, the number of transfer units, N, can be calculated from:

$$N = \frac{\kappa a L}{U} \qquad (12)$$

where L is the bed length and U the superficial velocity.

The Thomas solution provides a prediction of the desorption curve in the following form:

$$X = f(N, R, T) \qquad (13)$$

where X is dimensionless outlet concentration (c/c_0 for adsorption and $1-c/c_0$ for desorption); and T, dimensionless SCF throughput ($Uc_0t/q_0\rho_BL$). The parameter, R, is related to the adsorption equilibrium constant: where ρ_B is adsorbent bulk density; a, solid interfacial area per unit volume of bed; q, adsorbent loading; t, time; and c, fluid concentration. When used to model a fixed-bed desorption process, q_m is the maximum coverage corresponding to a monolayer. C_0 is the fluid concentration at equilibrium with the initial adsorbent loading; and K, the adsorption equilibrium constant. Note that the appropriate adsorption equilibrium is that of reversibly held solute (i.e., the fraction of the solute that desorbs), partitioning between adsorbent and supercritical fluid. Although total GAC adsorption is usually correlated with Freundlich isotherms (see, e.g., Giusti, et al., 1974), we have seen that the Langmuir isotherm is an adequate model of reversible solute isotherms in SCF CO_2 (see Section V-1). Thus, q_m and K were treated as constants in the Langmuir expression:

$$q = q_m \left(\frac{Kc}{1 + Kc}\right) \qquad (4)$$

When mass transfer is not negligible, then an appropriate model of column dynamics should provide for desorption at the surface within the pores, unsteady-state diffusion in the pore volume and/or along the pore walls, and mass transfer to the bulk fluid outside of the particle (Vermeulen, et al., 1973). An approximate solution, based on the mdethod of Thomas, is usually employed for the design of fixed bed adsorbers (Sherwood, et al., 1975). The Thomas solution, which was originally developed for ion exchange, is based on a kinetic driving force of the form:

$$\rho_B \frac{\partial q}{\partial t} = \kappa a \left[c\left(1 - \frac{q}{q_m}\right) - \frac{1}{K}(c_o - c)\frac{q}{q_m}\right] \tag{5}$$

The overall coefficient, κ in Eq. (5), is evaluated from (Sherwood, et al., 1975):

$$\frac{1}{\kappa} = \frac{1}{b}\left(\frac{1}{k_f} + \frac{c_o/q_m\rho_B}{k_p}\right) \tag{6}$$

where k_f and k_p are fluid and solid phase mass transfer coefficients, respectively; b is a correction factor to account for the fact that the solid and fluid phase resistances are not strictly additive. The value of b usually lies between 1 and 2.

Values of k_f, k_p, b and, thence, κ can be evaluated by standard procedures from physical properties of the adsorben and SCF carrier along with the fluid flow conditions in the bed. The fluid phase mass transfer coefficient can be expressed as a function of the Nusselt number, j_D (Sherwood, et al., 1975):

$$k_f = j_D\, U/S_c^{\;2/3} \tag{7}$$

where U is the superficial velocity and S_c is the Schmidt number.

$$R = 1 + Kc_o$$

One form of the solutions to Eq. (13) is given in Fig. VII-16 (from Vermuelen, et al., 1973).

Lacking sufficient data to accurately fit a Langmuir adsorption expression for the reversible adsorbate-SCF CO_2 system, we have attempted to use an experimental desorption curve to back-calculate R. The desorption curve for column P3-48, shown in Fig. VII-17, was used to define the smooth curve given by the dashed line which, in turn, was put in dimensionless form as X vs. T. Points from this curve were then plotted on Fig. VII-16. From these results, it appears that R is the order of 2 for phenol desorption at 55°C and 150 atm. This procedure is not accurate enough to provide a good estimate of the number of transfer units. The central portion of the desorption curve (which is probably the most accurate) suggests that N is greater than 100 for the 380-g column. An independent estimate of N was calculated from EQ. (12) using the procedure outline above (see Appendix B). The value calculated for the 380-g column was between 600 and 1200; the corresponding range of N for the 7-g columns (2500 ppm phenol desorbed at 55°C and 150 atm) was 80 to 160 transfer units.

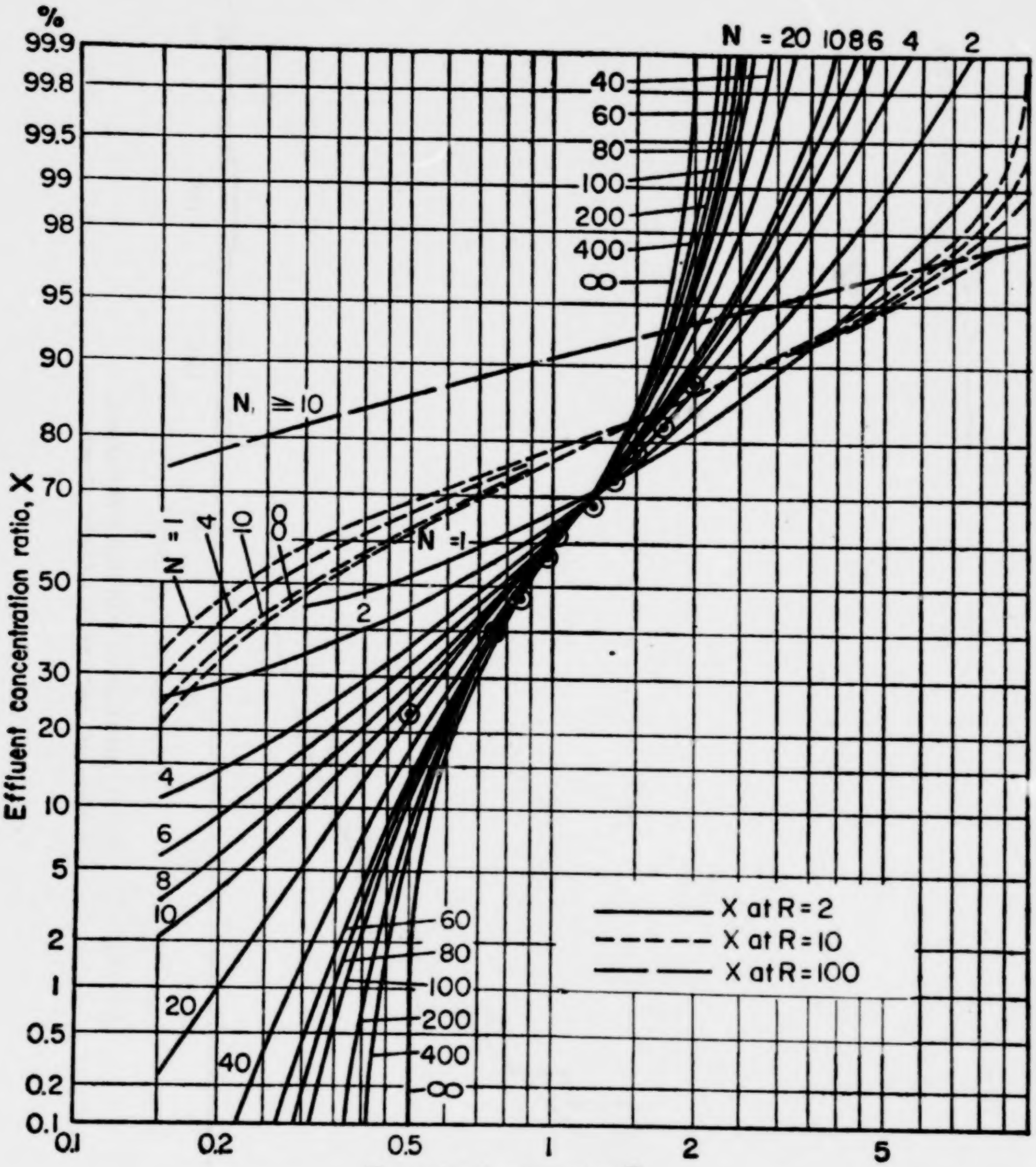

Figure VII-16 **BREAKTHROUGH HISTORIES AT R=2 10 AND 100 (from VERMUELEN et. al., 1973)**
$X = c/c_0$ for adsorption and
$T = c/c_0$ for desorption

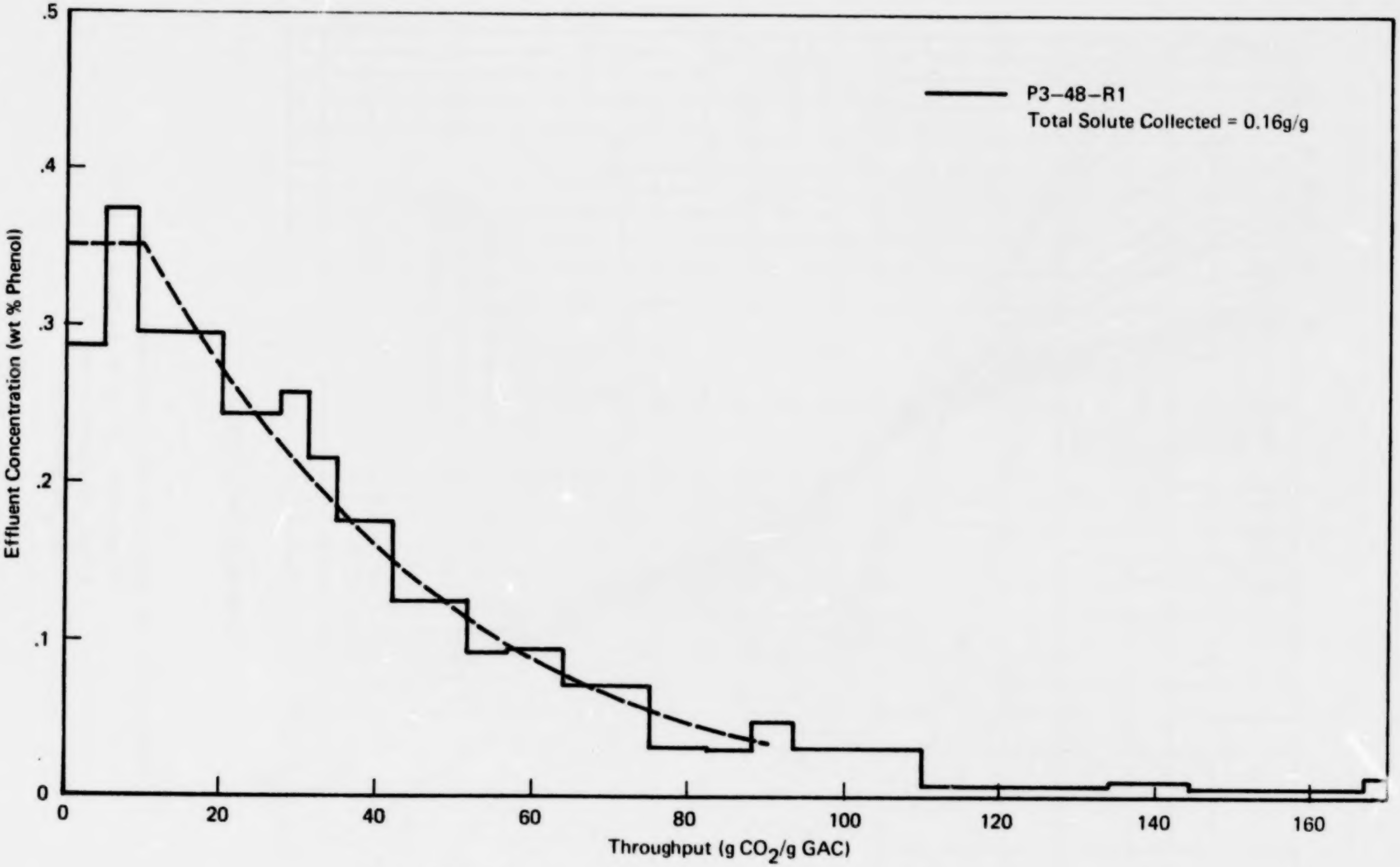

Fig. VII-17 **DESORPTION CURVE FOR 2500 PPM PHENOL ON 380g GAC, DESORBED AT 55°C, 15 MPa**

The family of curves given in Fig. VII-17 illustrates how the desorption curve varies with number of transfer units, N, and strength of adsorption, as measured by R. For R = 2, which is representative of relatively weak adsorption, the family of desorption curves get progressively sharper as N increases; for small N, the change in sharpness with increasing N is rapid, while for large N, the change with increasing N is less severe. To better illustrate this point, the data of Fig. VII-16 were replotted as the normal desorption and regeneration curves. The curves for R = 2 and N = 10, 100, and ∞ are given in Figs. VII-18 and VII-19. The progression of curves with increasing N is what the model would predict when increasing column length at constant superficial velocity, (i.e., constant U and κ). These predictions resemble the experimental results of 7- and 380-g phenol columns, as shown in Fig. VII-18. Note that the experimental curves in Fig. VII-19 were not normalized as in Fig. VII-18; thus, the difference between the 7- and 380-g curves at 150 atm is accentuated.

For R = 2, the difference between N of 100 and is relatively small; that is, the desorption curve is relatively insensitive to the flow conditions within the column. This behavior is indicative of a system wherein mass transfer is not a dominant factor. In the limit of negligible mass transfer resistance (i.e., $N \to \infty$), the desorption dynamics are governed by local equilibrium theory.

The curves for R = 10 and 100 are representative of moderate-to-strong adsorption. As shown in Fig. VII-16, as the strength of adsorption increases, the relative shape of the desorption curve is less sensitive to the number of transfer units; for R = 10, there is little change in X for N = 1 to ∞, up to X = .95. The major impact of changing N occurs in the tail of the desorption curve, for X >.95. For R = 100, a single desorption curve is adequate for describing cases with N above 10.

The Thomas solution for modeling fixed-bed desorption is a powerful tool that greatly simplifies the design procedure for SCF regeneration. The technique has been used to advantage in evaluating alternative desorber designs in conjunction with estimates of process economics. Those results are described in Section IX.

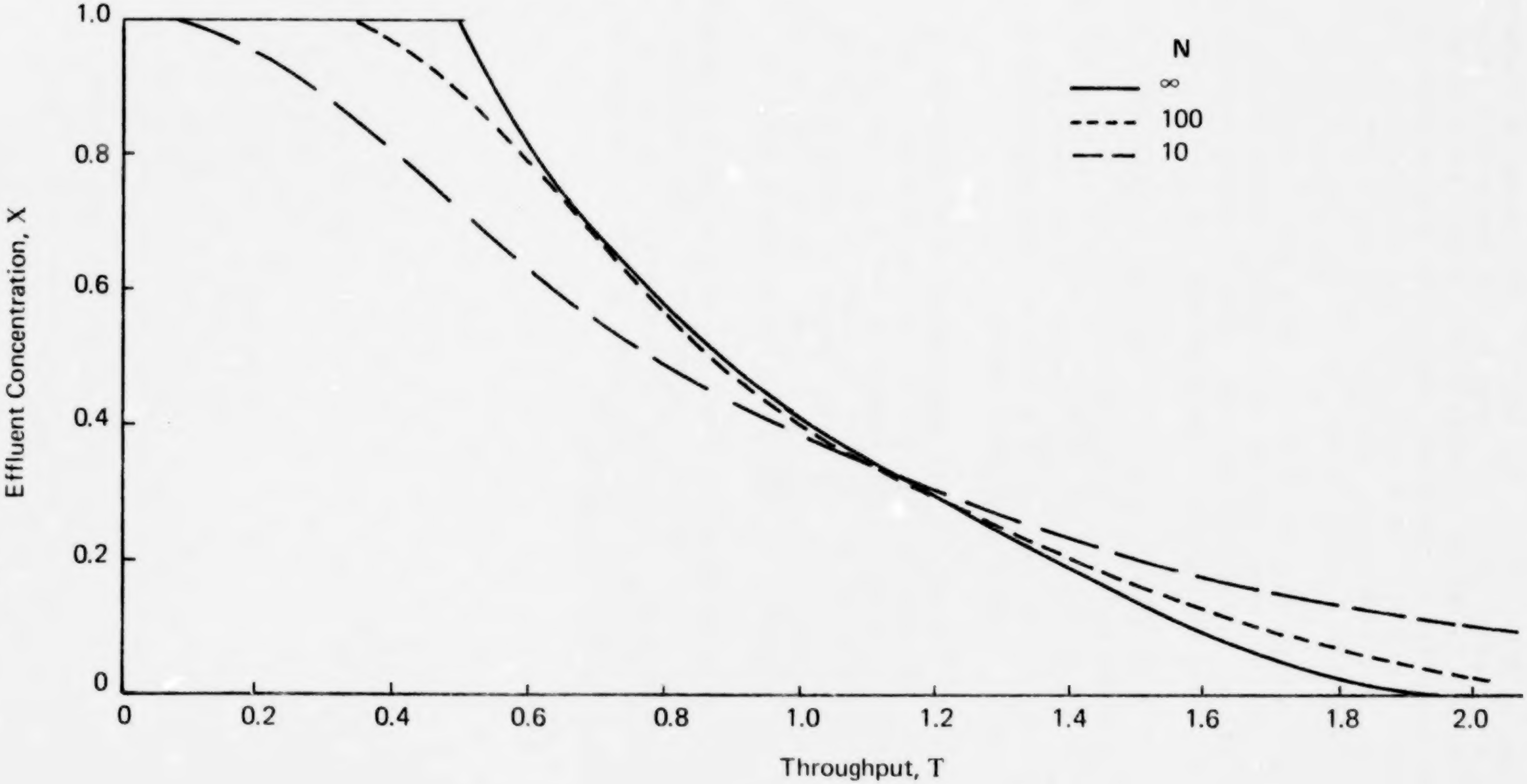

Figure VII-18 **VARIATION OF DESORPTION CURVE WITH NUMBER OF TRANSFER UNITS (for R = 2)**

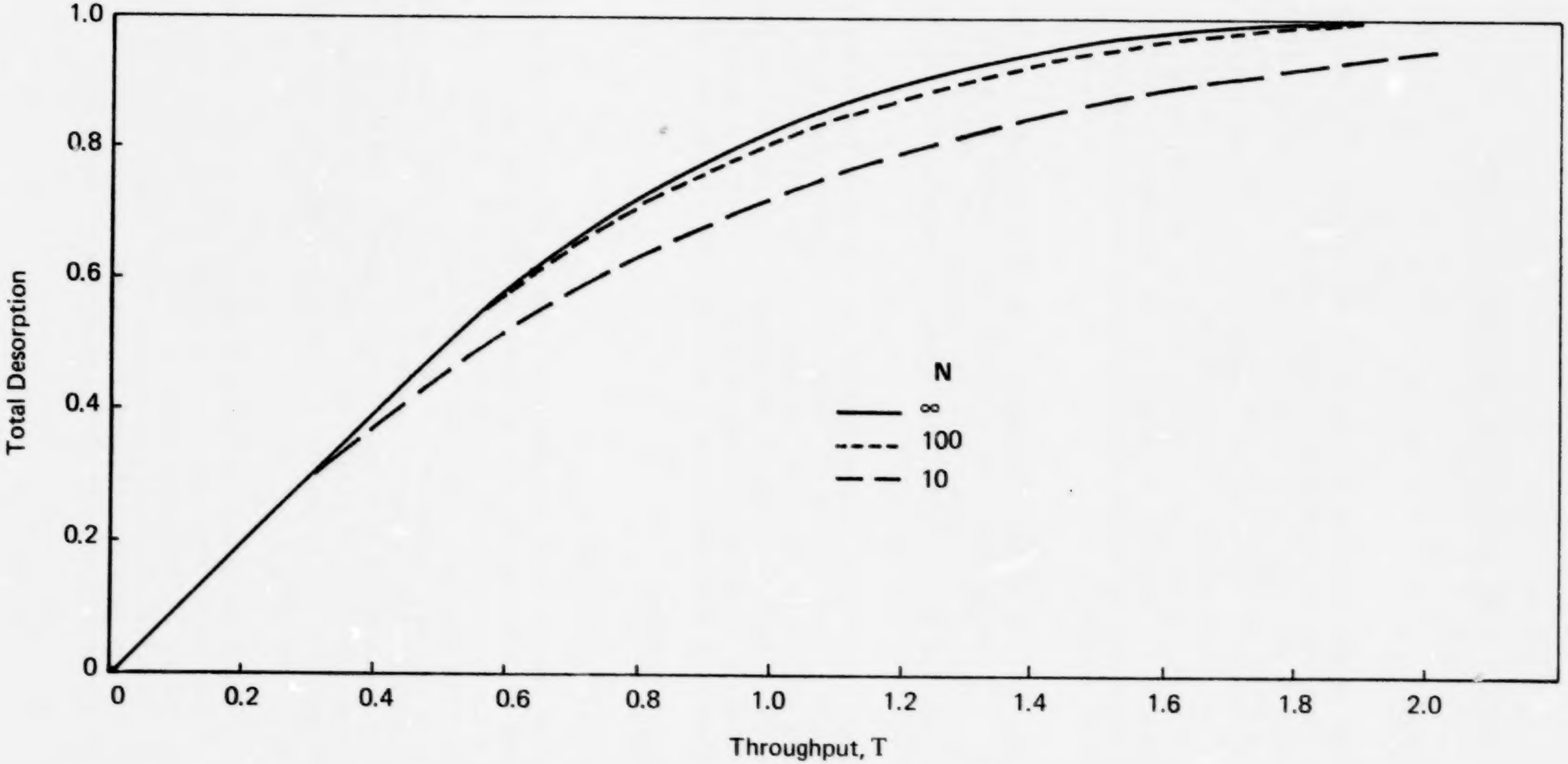

Figure VII-19 **VARIATION OF REGENERATION CURVE WITH NUMBER OF TRANSFER UNITS (for R = 2)**

VIII. PLANT WASTEWATER TREATABILITY STUDY

A. INTRODUCTION

The phase of the program dealing with actual pesticide manufacturing wastewaters used sampled proved by a pesticide manufacturer. This wastewater came from a process manufacturing the herbicide, atrazine. Atrazine is a triazine compound, used to control weeds in corn, sorghum and sugarcane fields. The compound, commercially available for more than twenty years, is nonflammable, noncorrosive, and highly stable. Atrazine is relatively nontoxic with an LD_{50} for rats of 3080 mg/kg with no reported cases of ill effects to humans. The compound is synthesized by reacting cyanuaric chloride with ethylmaine and isopropylamine, in the presence of an acid.

A characterization of the wastewater from this process is shown in Table VIII-1. It can be seen that atrazine contributes only 10% of the total organic carbon (TOC) present in the wastewater. Other possible organics include the starting materials used to manufacture the herbicide as well as other reaction products.

A series of experiments was developed to determine the effectiveness of supercritical carbon dioxide to regenerate granular activated carbon columns loaded with this atrazine wastewater. The plan was similar to that used in the previous synthetic wastewater studies; GAC columns would be cyclically adsorbed and regenerated at various process conditions to determine the steady-state working capacity of the GAC.

B. EXPERIMENTAL METHODS

1. Adsorption Apparatus

A sketch of the adsorption apparatus used is shown in Figure VIII-1. For this phase of the program, the predominant GAC used was Calgon F-400, screened to a particle size of -12+30 mesh. The GAC columns used were the standard, high-pressure, stainless-steel tubes, (0.45 cm id x 22.9 cm long). Each column was loaded with 7.00 gr of GAC with plugs of glass wool in both ends of the column to prevent spillage. The wastewater feed was first pre-treated to remove large suspended solids by filtering through a column packed with glass wool. This filtered feed was then pumped up through the GAC column at a flow of 3.2 ml/min, equivalent to 1.1 GPM/ft^2 of column.

Because of the high concentration and variety of organics in the wastewater, it was found that the concentration of atrazine could not be directly measured by UV spectrophotometry. During earlier studies with pure atrazine dissolved in distilled water, the breakthrough of atrazine could be measured by passing effluent from a GAC column through a spectrophotometer set at 230 nm. In the case of actual wastewater, nonadsorbing

TABLE VIII-1

ATRAZINE

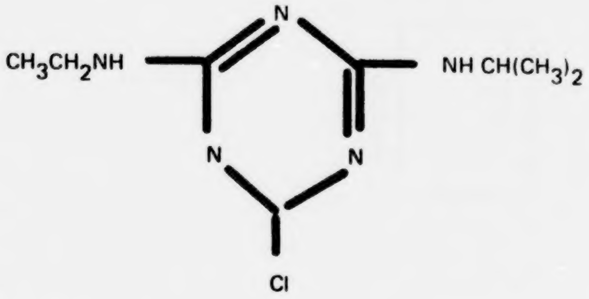

Total Organic Carbon (TOC) Concentration

Total Wastewater	1000 ppm
Atrazine	100 ppm

Other Possible Components of Wastewater

Sodium Chloride	NaCl
Cyanuric Chloride	$C_3N_3Cl_3$
Ethylamine	$C_2H_5NH_2$
Isopropylamine	$(CH_3)_2\ CH\ NH_2$

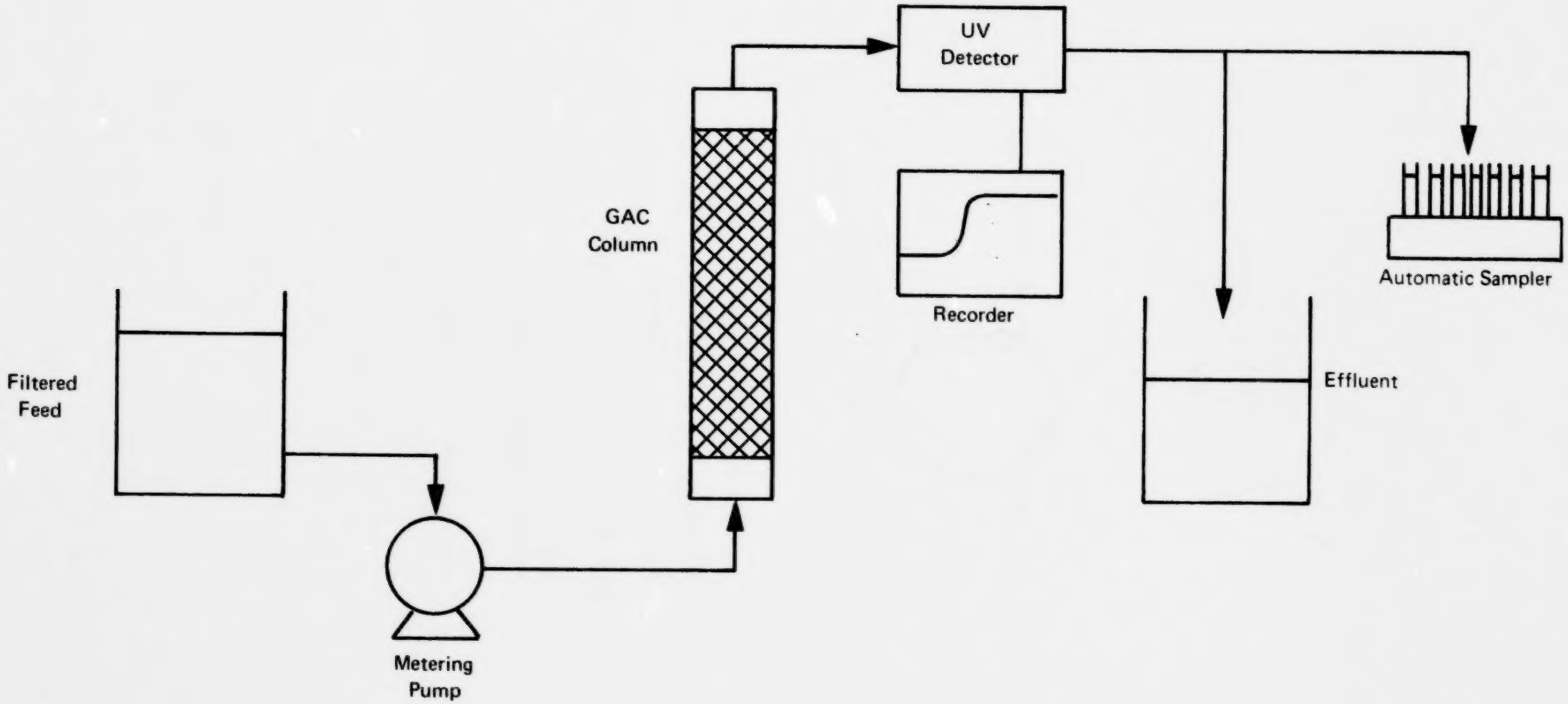
Filtered
Feed
Metering
Pump
GAC
Column
UV
Detector
Recorder
Effluent
Automatic Sampler

FIGURE VIII–1 ATRAZINE WASTEWATER ADSORPTION APPARATUS

species interfered with UV absorbance at this wavelength. UV scans of effluent samples of the wastewater showed that there was a wavelength, 279 nm, where the UV absorbance value rose steadily and leveled off in the shape of a characteristic adsorption breakthrough curve. All GAC adsorptions were monitored at this new wavelength to determine column performance, but this method did not necessarily trace the adsorption of the compound atrazine, rather it indicated the adsorption of some representative organic species in the wastewater. In order to check the loadings on GAC, two additional methods were used. The first, described previously, involved taking a GAC column after adsorption, heating it to 55°C while passing low pressure carbon dioxide over it to dry the GAC, and then weighing the dried column to determine total weight picked up during adsorption. While this method gave a final number for total weight gained during adsorption, it did not give any indication of the initial breakthrough concentration nor did it provide anything like an adsorption breakthrough curve. In order to obtain this data, it was decided to analyze samples of GAC column effluent by means of a Dohrmann/Envirotech DC-52D Total Organic Carbon Analyzer (TOCA).

2. TOCA Description

In the DC-52D analyzer, a combination of oxidative-reductive pyrolysis, and a flame ionization detector are used to determine the carbon content of a solution. The DC-52D also incorporates a carbonate bypass system which eliminates any response to inorganic carbonates that may be present.

A sample to be analyzed is injected onto a bed of granular manganese dioxide (MnO_2) in a platinum boat as shown in Figure VIII-2. During the first step of analysis, the boat is heated to $\sim 115^{\circ}C$ and all volatiles species are swept into a bypass column by a flow of helium. This bypass column selectively traps organics while allowing H_2O and CO_2 to pass through to a vent. In the second step, the helium gas flow to the bypass column is reversed, sweeping the volatiles out to a hydrogen rich reduction zone containing a rhodium catalyst at $\sim 350^{\circ}C$. In this zone, all the volatiles are reduced to methane gas (CH_4) which is then measured directly with a flame ionization detector. In the third and final step of the analysis, the sample boat containing the non-volatile organics is advanced into a zone at $\sim 850^{\circ}C$ where any carbonacous material reacts with the MnO_2 granules, releasing carbon dioxide (CO_2). This CO_2 is then reduced to CH_4 over the rhodium catalyst and detected by the flame ionization detector. Gas flows, temperatures, and timing sequences on the DC-52D are calibrated such that if one injects a $30 \mu l$ sample of solution and starts the analysis, the unit will proceed automatically through all three steps and display the Total Organic Carbon value directly in parts per million (ppm).

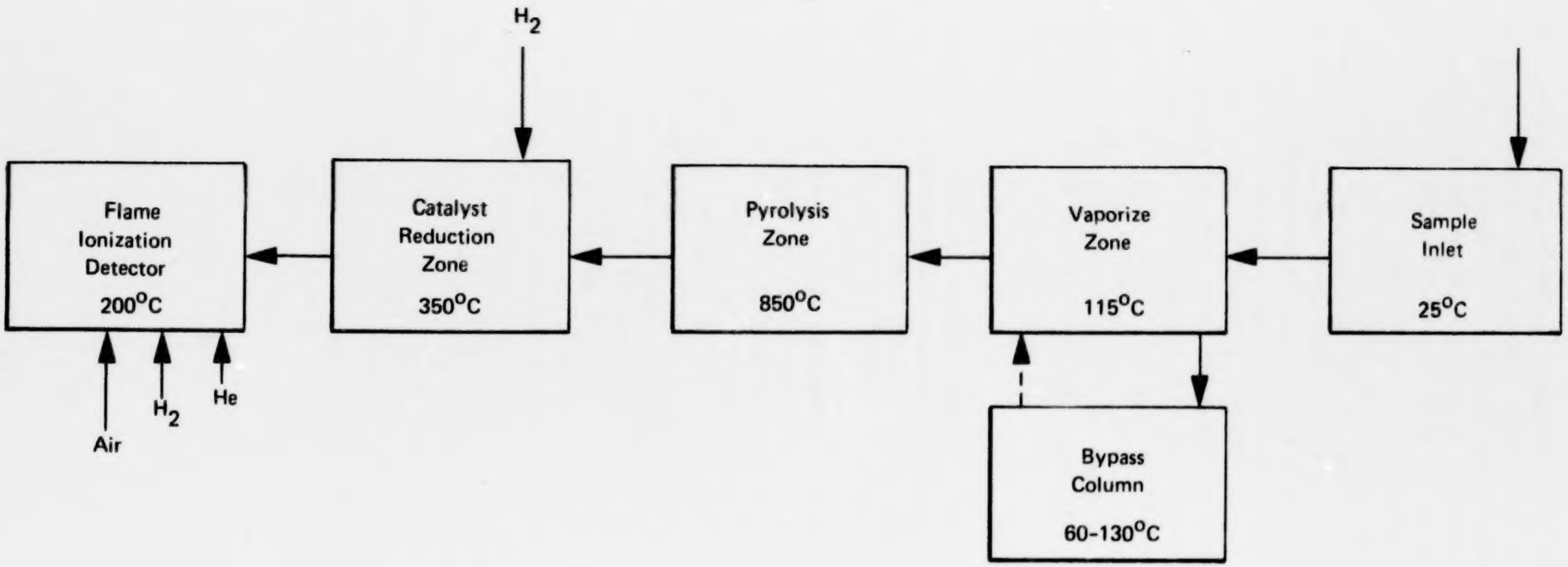
Sample
Inlet
25°C
Vaporize
Zone
115°C
Bypass
Column
60-130°C
Pyrolysis
Zone
850°C
H_2
Catalyst
Reduction
Zone
350°C
Flame
Ionization
Detector
200°C
Air
H_2
He

FIGURE VIII–2 TOTAL ORGANIC CARBON ANALYZER (TOCA)

During a GAC column adsorption, effluent samples would be collected with a fractionator (Gilson, Model #FC-80K) every 30 or 60 minutes. Each of these samples would then be analyzed for its TOC concentration. By plotting these TOC concentrations versus time the sample was taken, one obtains a "TOC adsorption breakthrough curve" giving both initial breakthrough concentrations and the slope of an adsorption breakthrough curve. An example is shown in Figure VIII-3 .

3. Regeneration Apparatus

The apparatus used to regenerate these GAC columns was identical to that used for the synthetic wastewaters as is seen in Figure VIII-4 . Carbon dioxide from high pressure cylinders was compressed at room temperature from a suction pressure of about 1000 psig to an operating pressure in the range of 2250 to 4000 psig by means of a diaphragm compressor (Aminco Cat. No. 46-13421). The carbon dioxide was then heated above its critical temperature, passed down-flow through the GAC column where the organics were dissolved off the carbon and then expanded to atmospheric pressure where desorbed material separated from the carbon dioxide phase. Carbon dioxide flow rates were monitored with a Fisher and Porter flowmeter (FP-1/2-27-G-10/83) and total flow during a regeneration was measured with a Singer (D7M-200), dry test meter. The extent of regeneration was determined by direct weighing of the GAC columns before the after desorption. Initially, the weight of material collected in the low pressure separator was also used to determine regeneration, but due to the volatility of some of the organic species present, this was found not to be effective in measuring regeneration performance.

C. EXPERIMENTAL SERIES

A summary table of all the GAC column work with atrazine wastewater is shown in Table VIII-2. The following gives a brief description of each series, its process conditions, and results obtained.

Series ARW-1: This was the first attempt at working with actual atrazine manufacturing wastewater. The feed for this first adsorption was filtered through a length of glass tubing packed with glass wool. After the first regeneration the column was opened to reveal a brown crust-like solid on the glass wool plugs and on the GAC surface. This glass wool plug was replaced and the column readied for a second adsorption. However, for the second adsorption and all subsequent adsorptions, the feed solution was vacuum filtered through a Whatmann #42 filter paper. Even with this additional filtering, series ARW-1 was stopped after its third adsorption due to plugging in the column from its exposure to inadequately filtered feed.

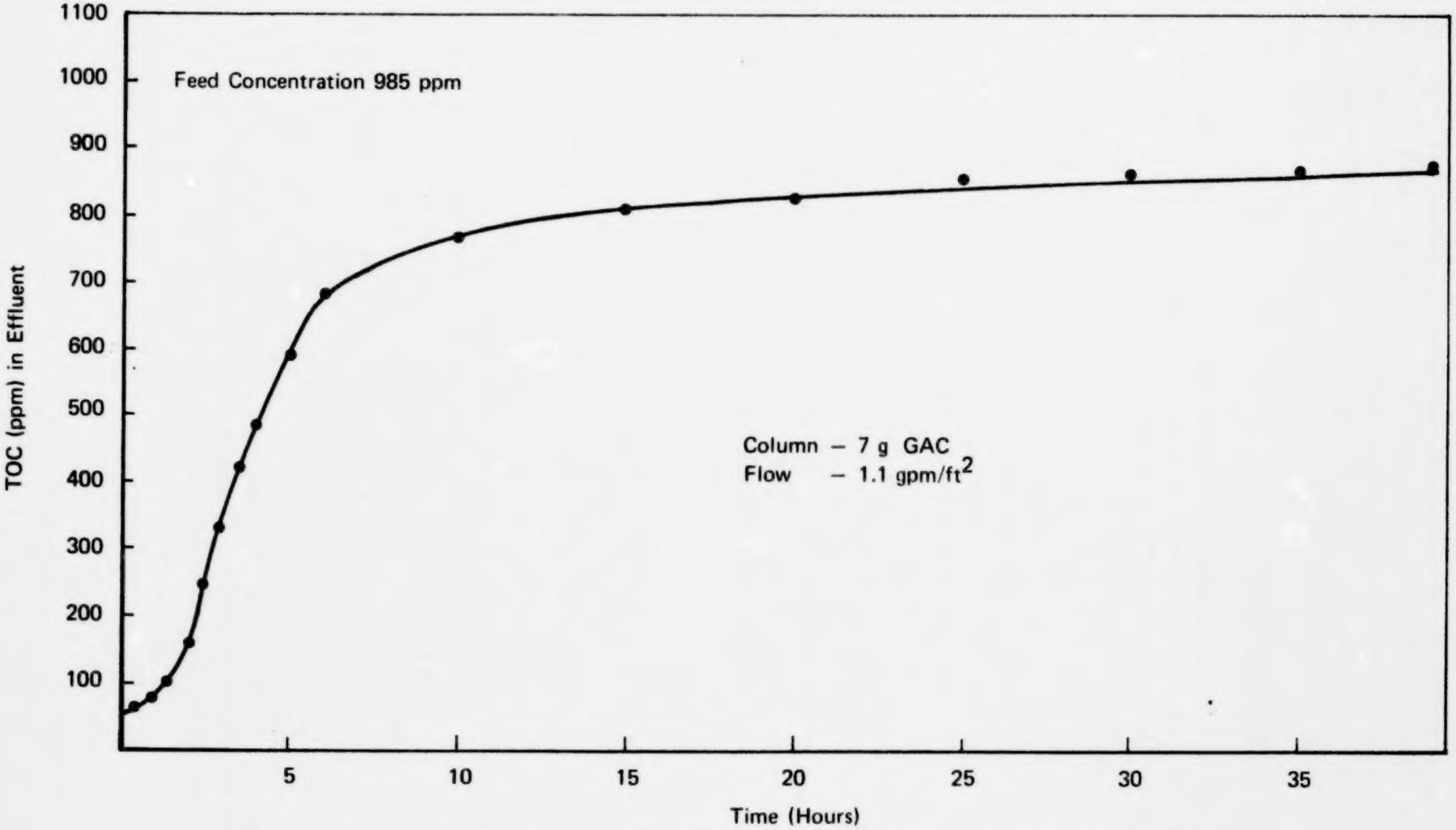

FIGURE VIII–3 ADSORPTION BREAKTHROUGH CURVE FOR TOC IN ATRAZINE REAL WASTEWATER

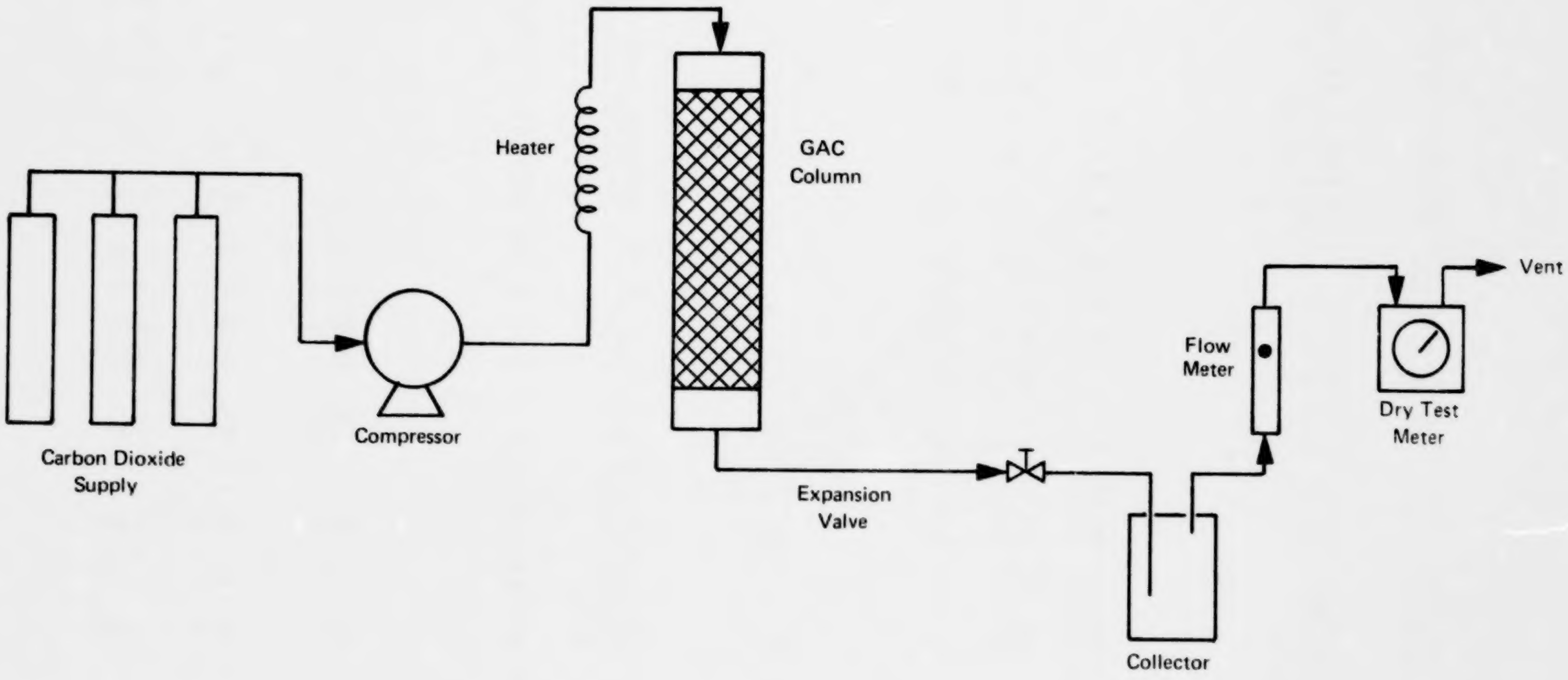
Heater
GAC
Column
Carbon Dioxide
Supply
Compressor
Expansion
Valve
Flow
Meter
Dry Test
Meter
Vent
Collector

FIGURE VIII–4 ATRAZINE WASTEWATER REGENERATION APPARATUS

TABLE VIII–2

COLUMN PARAMETERS				ADSORPTION CONDITIONS AND RESULTS			DESORPTION CONDITIONS AND RESULTS					
Column #	Weight of GAC (g)	Type of GAC	No. of Cycles	Hours on Stream	Loading ΔWt (g/g GAC)	Loading B.T. Curve (g TOC/g GAC)	T (^oC)	P (psig)	Total Flow (SL)	Washed Off (g/g GAC)	Desorbed (g/g GAC)	Residual (g/g GAC)
ARW-1	7.00	F-400	2.5	39	-		55	2,250	7,875		-	0.32
	"	"		40	0.14	0.11	"	"	11,830		0.09	0.05
	"	"		40								
ARW-2	7.00	F-400	5	40	0.39	0.26	135	5,000	8,350		0.14	0.25
	"	"		42	0.19		"	"	7,050		0.12	0.07
	"	"		40	0.11		"	"	5,900		0.07	0.04
	"	"		40	0.12		"	"	5.250		0.09	0.03
	"	"		40	0.05		"	"	4,870	0.07	0.07	-0.09
ARW-3	7.00	F-400	4	40	0.35	0.35	120	4,000	8,400		0.14	0.21
	"	"		40	0.16		"	"	7,650		0.11	0.05
	"	"		40	0.15		"	"	2,420		0.09	0.06
	"	"		40	0.12		"	"	9,680		0.09	0.03
ARW-4	7.00	PCB -40+50	2	40	0.32		135	5,000	7,900		0.09	0.23
	"	"		40	0.06		"	"	12,150		0.04	0.02
ARW-6	7.00	F-400	1	40	0.37		135	5,000	-		0.16	0.21
ARW-7	7.00	F-400	1	40	0.36		250	2,250	750		0.11	0.25
ARW-8	7.00	F-400	1	40	-		250	2,250	2,500		-	0.22
ARW-9	7.00	F-400	2	40	-		250	2,250	3,230		-	0.24
	"	"		40	-		"	"	-		-	0.02
ARW-10	7.00	F-400	5.5	40	0.29		120	4,000	1.800		0.11	0.18
	"	"		40	0.15		"	"	-		0.06	0.09
	"	"		40	0.08		"	"	1,500		0.06	0.02
	"	"		40	0.04		"	"	-		0.02	0.02
	"	"		40	0.08		"	"	-		0.06	0.02
	"	"		40	0.09		"	"	-		-	-
ARW-11	7.00	F-400	6	40	0.32		120	2,250	-		0.04	0.28
	"	"		40	0.05		"	"	2,000		0.06	-0.01
	"	"		40	0.04		"	"			0.04	0.00
	"	"		40	0.07		"	"			0.05	0.02
	"	"		40	0.07		"	"			0.05	-0.01
	"	"		40	0.05		"	"			0.03	0.02

Series ARW-2 and ARW-3: These two series were run simultaneously, ARW-2 at 135°C and 5000 psig, ARW-3 at the somewhat milder conditions of 120°C and 4000 psig. Both of these series used feed solution filtered with Whatmann filter paper, which aided in removing suspended solids. Column ARW-2 was opened after three cycles and no brown material was seen on the GAC or the glass wool. Despite this removal of suspended solids, the loading capacity of these two columns was less than anticipated. About 60% of the material adsorbed in the first cycle was remaining on the GAC after regeneration. An additional 30-40% of the material adsorbed during subsequent adsorption was remaining on the GAC with each additional cycle. These findings were not anticipated from previous work with synthetic solutions. During the fifth adsorption of column ARW-2, severe plugging and pressure drops were found in the column, even though the feed had been pre-filtered. In an effort to remove this plugging material, the column was backwashed with 150 ml of water heated to 55°C. This backwashing step was found to remove a significant amount of material from the column (0.07 gr/gr GAC). The backwashed column was then dried and regenerated, where a normal amount of material (0.07 g/gr GAC) was desorbed.

Series ARW-4: In order to determine the effect of type of carbon on steady-state capacity and residual loading, a column was prepared using a narrow mesh, vapor phase carbon (Calgon PCB, -40+50 mesh). This series was only carried out to two cycles because it was seen that the working capacity of the carbon quickly dropped lower than any value seen for liquid phase carbons.

In order to more fully understand the plugging problem, GAC column studies were temporarily put aside so that more effort could be put into characterizing the wastewater itself. It was first suggested that this solid material forming plugs in the GAC columns was water soluble species that were deposited on the glass wool and GAC during the drying of a GAC column. The general procedure in treating GAC columns was to dry them at 55°C after adsorption so a determination of total weight pick-up could be made. Any dissolved solids would be left on the glass wool and GAC when the water evaporated. To check the nature of these solids, an 1800 ml sample of feed solution was vacuum evaporated at room temperature. Some 40 grams of solid material was collected from this sample and tested for solubility. Measurements of solubility in water and in an organic solvent (acetone) revealed that about half of the solids would dissolve in each solvent. When exposed to supercritical carbon dioxide, (135°C, 5000 psig) the solids were found to have only a 0.006% solubility. This data led to a hypothesis of an SCF-insoluble organic/inorganic mixture of solids. While further tests were being proposed to identify this mixture, information on the characteristics of the atrazine wastewater was received from the manufacturer. This data was collected during research conducted at Research Triangle Institute, Research Triange Park, N.C., and was forwarded by the herbicide manufacturer to ADL. The data included two important pieces of information. First, the wastewater contained ∿ 8500 ppm of chloride, suggesting inorganic chloride salts. This data confirmed a literature search which showed that in some alternative processes to manufacture atrazine, sodium chloride (NaCl) was produced as a byproduct. This chloride could account for the water soluble portion of the solid material. Subsequent analysis detected ∿ 6000 ppm of sodium in the same feed. Secondly, it was reported that the atrazine concentration in the wastewater was ∿ 100 ppm, three times its solubility limit in water. Most of the atrazine was undissolved, present as fine crystalline rods, 5-50μm in length. This atrazine could easily bypass the Whatmann filtration step and account for the organic fraction of the solid material.

In order to alleviate the problems caused by fine particles of atrazine and the chlorides, two changes were made in the experimental procedures. First, Millipore filters (type GS), with a mean pore diameter of 0.22μm were used to pre-filter all wastewater solutions. Secondly, a backwash step, using 150 ml of distilled water, was included after each adsorption and prior to any drying or regeneration. With these steps taken, attention returned to determining multicycle behavior of GAC columns.

Series ARW-6: In addition to being the first column using fine filtered feed and backwashing, ARW-6 was regenerated at a mild temperature and high pressure (135°C, 5000 psig). The results of this regeneration were not significantly different from columns run at lower pressures, so it was decided to halt this series, open the column, and inspect for solids on the surface of the glass wool or GAC. No trace of material was found anywhere in the column.

Series ARW-7, ARW-8, and ARW-9: These three columns were used to test another method of monitoring the desorption behavior of GAC columns. A UV spectrophotometer, identical to that used in adsorption studies, was set up downstream of the desorbing GAC column but upstream of the expansion valve, as shown in Figure VIII-5. With this new configuration it was possible to measure the concentration of organic in the supercritical phase by means of high pressure UV absorption cells. Regeneration of the three columns were run at various flow rates to find the best conditions to operate this new detector. A representative desorption trace is presented in Figure VIII-6. As predicted by Local Equilibrium Theory (LET), the initial concentration of organic in the supercritical phase is quite high, and drops rapidly due to the minimal mass transfer resistance to desorption in the supercritical phase. This high pressure UV technique was used to monitor desorptions for the remainder of the real waste series.

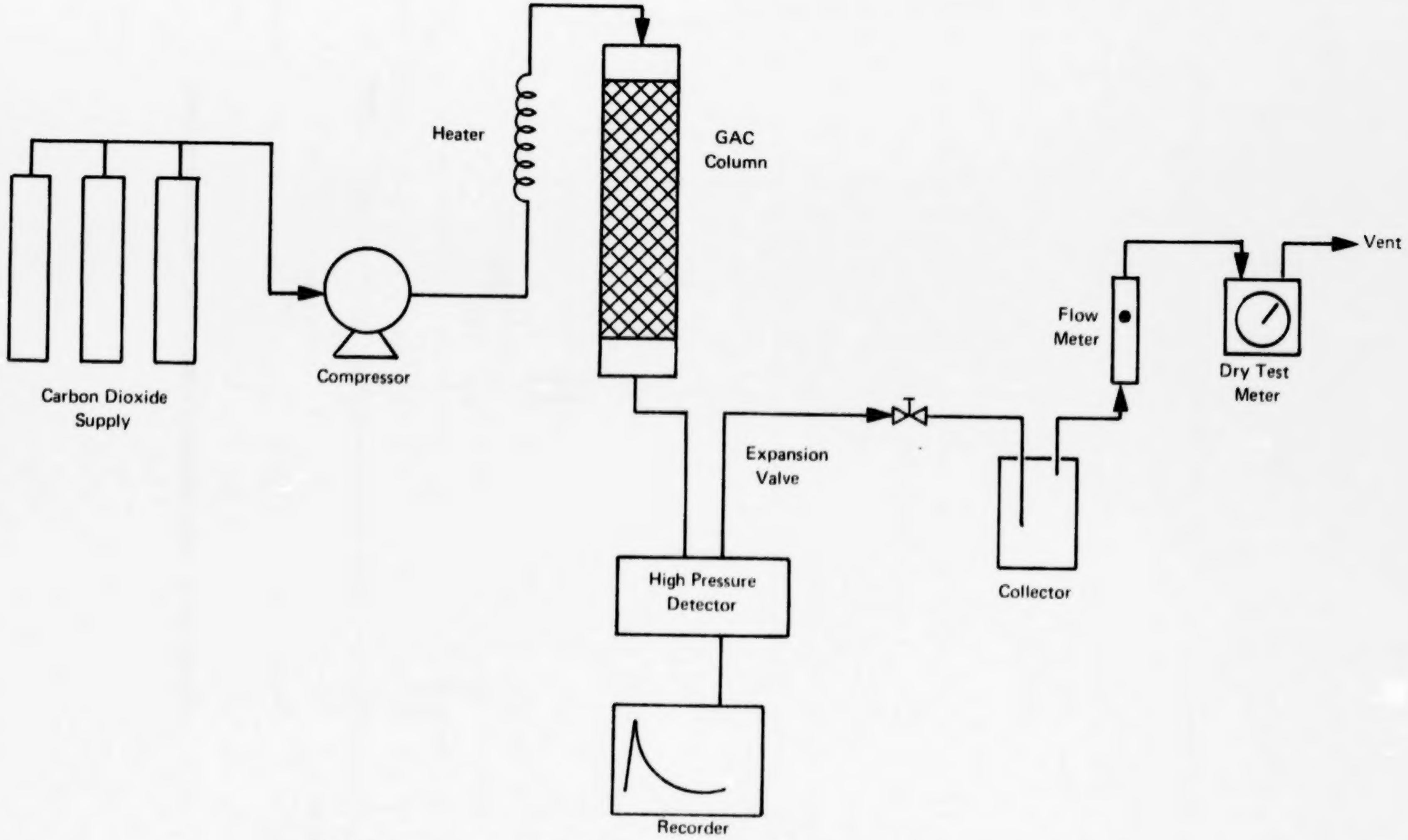
Heater
GAC
Column
Vent
Flow
Meter
Dry Test
Meter
Compressor
Carbon Dioxide
Supply
Expansion
Valve
High Pressure
Detector
Collector
Recorder

FIGURE VIII–5 REGENERATION APPARATUS WITH HIGH PRESSURE UV DETECTOR

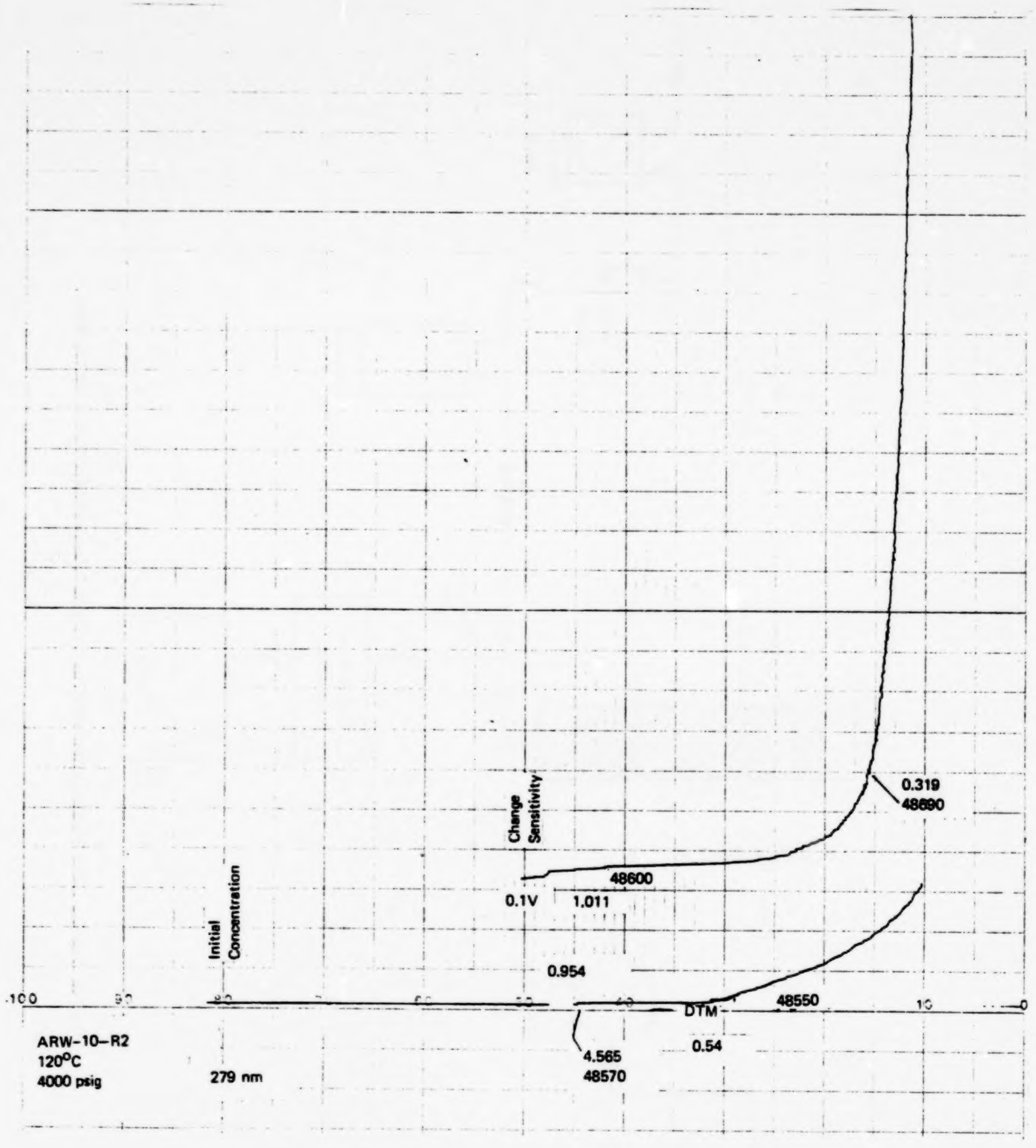

FIGURE VIII–6 HIGH PRESSURE DESORPTION TRACE OF ATRAZINE

Series ARW-10 and ARW-11: After brief excursions of flow rate, temperature, pressure, and the development of the high-pressure UV technique, it was decided to carry out two extended series at conditions representing possible large-scale operating conditions. For series ARW-10, regenerations were done at 120°C, 4000 psig, at a flow rate of 20 SLPM. For series ARW-11, regeneration conditions were 120°C, 2250 psig, and again a flow rate of 20 SLPM. Highlights of the results of these two series are shown in Table VIII-2. The initial loading of column ARW-10 was lower than expected (0.29 gr/gr GAC). Although the residual loading was normal for the first cycle (0.18 gr/gr GAC), it was higher than the norm for the second cycle (0.09 gr/gr GAC). This implied that for some as yet unknown reason, perhaps channeling during the adsorption step, the GAC did not come in contact with the normal volume of wastewater during the first adsorption. The high residual loading of the second cycle of ARW-10 was part of the irreversible loading phenomenon that is usually seen during first cycle adsorptions. The first cycle behavior of column ARW-11 was not unexpected. The loading of 0.32 gr/gr GAC is more typical of the carbon, while the high residual loading (0.28 gr/gr GAC) can be explained by the mild regeneration conditions used. Aside from the anomally in the first two absorptions of ARW-10, the results for both series were encouraging. The residual loadings of both columns quickly dropped to a low level (0.02 gr/gr GAC), a value less than that of early columns. In addition, the amounts desorbed each cycle, which are considered the working capacities of the carbon, leveled off (0.06 gr/gr GAC for ARW-10 and 0.05 gr/gr GAC for ARW-11) rather than continuing to drop, as they did in earlier work.

IX. PROCESS DESIGN AND ECONOMIC ANALYSES

A. PROCESS DESIGN

If a solvent regeneration process is to be economically viable, solute must be readily and efficiently separated from the carrier fluid so that the regenerant can be recycled. One of the major benefits of SCF regeneration is that solutes can be easily separated from the carrier fluid. The solubility of substances in supercritical fluids is very sensitive to the density of the fluid. Since small changes in temperature or pressure have a large effect on density in the critical region, solubility can be altered dramatically by changing operating conditions. A small change in temperature or a modest change in pressure can alter solubility by orders of magnitude. This phenomenon has been used to advantage in SCF extraction applications (see, e.g., Hag, 1973; Maddocks, et al., 1979). In SCF regeneration of adsorbents, such changes in solubility are used to precipitate solutes from the carrier subsequent to desorption. In this manner, the fluid is purified for recycle to the desorption step and the solutes are recovered for reuse or ultimate disposal.

One mode of commercial application of the SCF regeneration process is shown schematically in Fig.IX-1. If adsorption and desorption are not carried out in the same vessel, then the flow of carbon is from the spent carbon drain tank (not shown) to the pressure desorption vessel and then to the regenerated carbon defining and storage tank (not shown). In this mode of operation, regeneration is conducted by batch. The flow of SCF CO_2 proceeds through one of the desorption vessels where it picks up adsorbates, and is then let down in pressure. After expansion, the temperature of the fluid is altered in a heat exchanger to reach the conditions required for solute precipitation. The solute is recovered from the separator and the regenerant is brought back to the conditions required for desorption by heat exchange and recompression.

In batch operation, three high-pressure desorber vessels are used. At any one time, two vessels are off-stream for loading and unloading, while one vessel is on-stream undergoing desorption. In this manner, the regenerant recycle loop is operated continuously.

Early in the development program, preliminary economic analyses were made to define the major cost items so that extra attention could be focused on the dominant factors. The results of those analyses established that there are two major capital costs: the high-pressure desorber vessels and the recirculation compressor. Optimization is simplified somewhat by the fact that the regenerant throughput required per unit of carbon throughput is a rather weak function of column space velocity. As discussed previously, when the mass transfer resistance is small, desorption dynamics approach local equilibrium. When equilibrium prevails within the column, the regenerant throughput per unit of carbon throughput is independent of space velocity. In

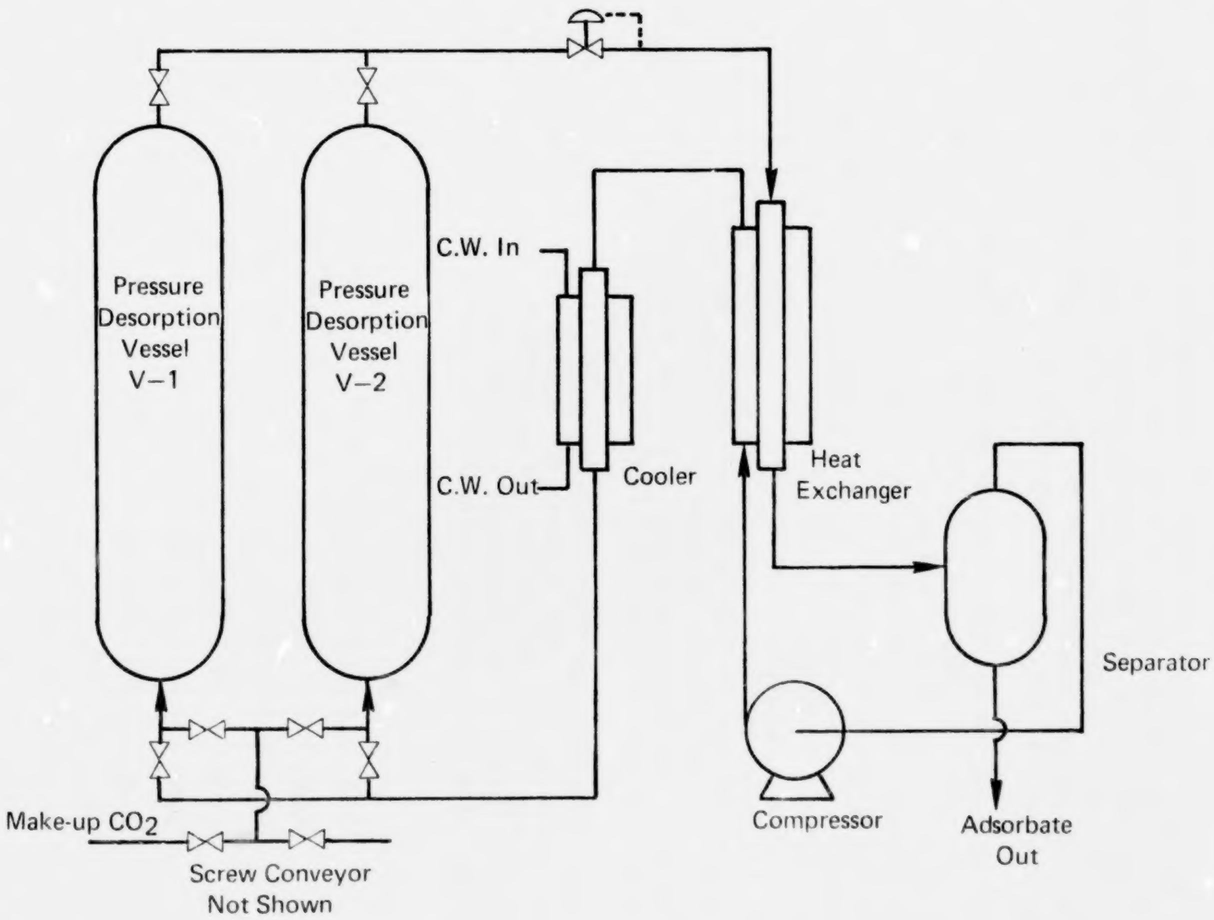
Pressure
Desorption
Vessel
V–1
Pressure
Desorption
Vessel
V–2
C.W. In
C.W. Out
Cooler
Heat
Exchanger
Separator
Compressor
Adsorbate
Out
Make-up CO2
Screw Conveyor
Not Shown

Figure IX-1 **SCHEMATIC OF A SCF ADSORBENT REGENERATION SYSTEM**

actuality, the mass transfer resistance is not negligible, but it is small enough so that column space velocity and regenerant throughput per unit carbon throughput are only weakly coupled. Thus, column space velocity can be chosen to minimize cycle time and, thereby, minimize column volume, while the conditions of the recycle loop can be chosen to minimize compression and heat exchange costs.

The desorber design was based on the method of Thomas, since that method had been shown to adequately describe the dynamics of phenol desorption (see Section VIIB). The method will not be illustrated for the case of regeneration of 10,000 lb/day of GAC, loaded with a solute like phenol and desorbed at 55°C and 150 atm. For these conditons, the isotherm constant, R, was found to be in the range of 2. From the preliminary economic analyses, it was decided that a reasonable design objective was 30 min desorption cycle time, which would conservatively provide for 40 cycles per day. The batch size would then be 10^4 lb GAC/day ÷ 40 cycles/day, or 250 lb GAC per batch. At a bulk GAC density of 0.44 g/cm^3, the volume of a desorber bed is 260 m^3. Two sets of desorber diameter and length were evaluated: case A, diam = 3.6cm (14 in), L = 26 m (8.6 ft); case B, diam = 2cm (7.8 in), L = 85 m (28 ft).

For each case, the superficial SCF CO_2 velocity was treated as an independent variable; the time required for regeneration, the amount of CO_2 passed through the column and the column pressure drop were treated as dependent variables. The procedures will not be illustrated for the case A column, with a superficial velocity of 7 cm/s.

From Eq. (VII-11), $D_k = 3.05 \times 10^{-3}\ cm^2/s$

From Fig. (IX-9), $D_f = 2.5 \times 10^{-4}\ cm^2/s$

From Eq. (VII-10), $D_p = 3.74 \times 10^{-5}\ cm^2/s$

From Eq. (VII-9), $k_p = 6.24 \times 10^{-3}\ cm/s$

From $Re = \underline{dpU}$, $Re = 917$

From Eq. (VII-8), $j_D = 0.062$

From Eq. (VII-7), $k_f = 0.210\ cm/s$

From Eq. (VII-6), $= 0.138\ cm/s$

From $a = \frac{6(1-)}{d_p}$, $a = 34.08\ cm^2/cm^3$

Therefore, $a = 4.70\ s^{-1}$

From Eq. (VII-12), $N = 176$

Having now calculated N for the case under consideration, the throughput of CO_2 required to reach any given degree of regeneration can be determined from the Thomas solution. To aid in determining the CO_2 throughput, the data of Fig VII-16 were replotted in the following manner. For R = 2, the throughput, T, and number of transfer units were read from Fig. VII-16 for outlet concentrations of X = 0.90, 0.95, and 0.98. The results were cross-plotted, as shown in Fig. IX-2. In general, the fraction of the reversible solute remaining on the column is approximately equal to (1-X)/2. In other words, X = 0.90 corresponds to 95% regeneration, X = 0.95 corresponds to 97.5% regeneration and X = 0.98 corresponds to 99% regeneration.

At 97.5% regeneration, with a column containing 176 transfer units, the throughput read from Fig. IX-2 is T = 1.835. The throughput and cycle time are related by the following equation:

$$\hat{t} = \frac{L q_0 \rho_B T}{U c_0} = \qquad (1)$$

where $\hat{t}$ is the time following the arrival of the fluid front at the column exit. The throughput of CO_2 required per unit throughput of carbon regenerated is related to $\hat{t}$, as follows:

$$\frac{gCO_2}{gGAC} = \frac{U \rho_{CO_2} \hat{t}}{L \rho_B} \qquad (2)$$

For the case under consideration,

From Eq. (IX-1), $\hat{t}$ = 30.0 min

From Eq. (IX-2), $gCO_2/gGAC$ = 73.8

The pressure drop of the regenerant through the bed was determined to be 1.4 atm (see Appendix B).

This procedure was used to determine the dependent variables (cycle time, regenerant throughput and pressure drop) at various superficial velocities for each of the two cases, A and B, of column dimensions. The results are given in Tables IX-1 and IX-2. As anticipated, we see that cycle times are roughly inversely proportional to superficial velocity, where the CO_2/GAC ratio is only slightly affected by superficial velocity.

We began this set of calculations by assuming that the desorption cycle time was 30 min. In the subsequent calculations, we treated cycle time as a dependent variable and superficial velocity as the independent variable. We see from Tables A and B that there is only one superficial velocity, for each set of column dimensions, that is consistent with our initial choice of a 30 min cycle. These values are summarized in Table IX-3. We see that the case A column dimensions are clearly superior to those of case B because A has a small pressure drop, whereas the ΔP of B is prohibitive. Thus, we conclude that a 14 in i.d. x 8.6 ft bed of GAC is capable of being regenerated in 30 min cycles for a solute like phenol being desorbed at 55°C and 150 atm. The CO_2 throughput will be in the range of 34,000 to 42,000 lb/hr for a carbon throughput of 10,000 lb/day.

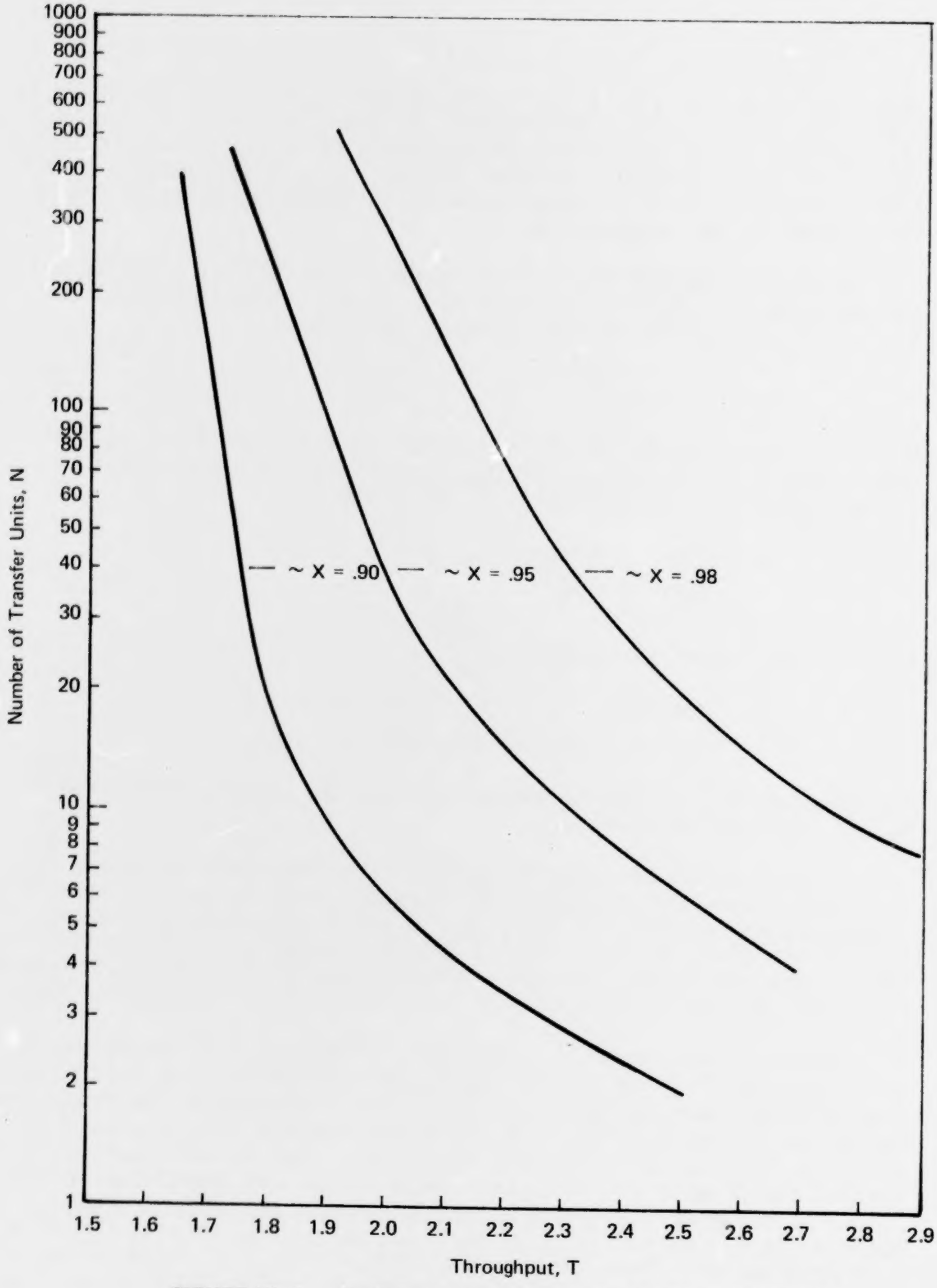

FIGURE IX–2 **NUMBER OF TRANSFER UNITS VS. THROUGHPUT**

Table IX-1

Design Calculations, Small Column Case

Column i.d. = 14", length of fill = 8.58 feet

D = 35.56 cm
Ac.s. = 993.2 cm
V = $2.597 \times 10^5 cm^3$

L = 261.5 cm
T = 55^oC
P = 150 **bar**

U(cm/s) =	5	7	10	20	30	40	50
Re =	655	917	1,310	2,620	3,930	5.256	6.570
j =	.070	.062	.055	.044	.040	.037	.035
K_f(cm/s)=	.167	.210	.267	.419	.571	.705	.833
X (cm/s)=	.124	.138	.152	.176	.191	.199	.205
Xa(S^{-1}) =	4.22	4.70	5.18	6.01	6.50	6.78	6.99
L/U =	52.3	37.4	26.2	13.1	8.72	6.54	5.23
N =	221	176	135	78.6	56.7	44.4	36.6
P(Pa) =	$7.4x10^4$	$1.37x10^5$	$2.73x10^5$	$1.06x10^6$	$2.34x10^6$	$4.05x10^6$	$6.16x10^6$

X = .98

T =	2.06	2.07	2.12	2.19	2.24	2.28	2.325
t(min) =	47.0	33.8	24.3	12.53	8.53	6.51	5.31
gCO_2/gGAC=	82.7	83.2	85.2	88.0	90.0	91.6	93.4

X = .95

T =	1.81	1.835	1.865	1.935	1.960	1.980	2.010
t(min) =	41.3	29.97	21.34	11.07	7.46	5.65	4.59
gCO_2/gGAC=	72.7	73.8	74.9	77.7	78.7	79.5	80.7

X = .90

T =	1.680	1.690	1.700	1.730	1.745	1.755	1.762
t(min) =	38.4	27.60	19.45	9.90	6.64	5.01	4.02
gCO_2/gGAC=	67.5	67.9	68.3	69.5	70.1	70.5	70.8

Table IX-2

Design Calculations, Large Column Case

Column i.d. = 7.75 in., length of fill = 28.0 ft.

D = 19.69 cm
Ac.s. = 304.3 cm^2
V = 2.597 x $10^5 cm^3$

L = 853.4 cm
T = 55^oC
P = 150 bar

U(cm/s)	7	10	20	30	40	50
Re	917	1,310	2,620	3,930	5,256	6,570
j	.062	.055	.044	.040	.037	.035
k_f(cm/s)	.210	.267	.419	.571	.705	.833
X(cm/s)	.138	.152	.176	.191	.199	.205
Xa(s^{-1})	4.70	5.18	6.01	6.50	6.78	6.99
L/U(s)	122	85.3	42.7	28.4	21.3	17.1
N	573	442	257	185	144	120
X = .98						
T		1.931	2.017	2.061	2.100	
t(min)		71.93	37.61	25.56	19.53	
gCO_2/gGAC		77.6	81.0	82.8	84.3	
X = .95						
T		1.740	1.795	1.830	1.858	
t(min)		64.8	33.5	22.7	17.3	
gCO_2/gGAC		69.9	72.1	73.5	74.6	
X = .90						
T		1.645	1.670	1.688	1.700	
t(min)		61.3	31.1	20.9	15.8	
gCO_2/gGAC		66.1	67.1	67.8	68.3	

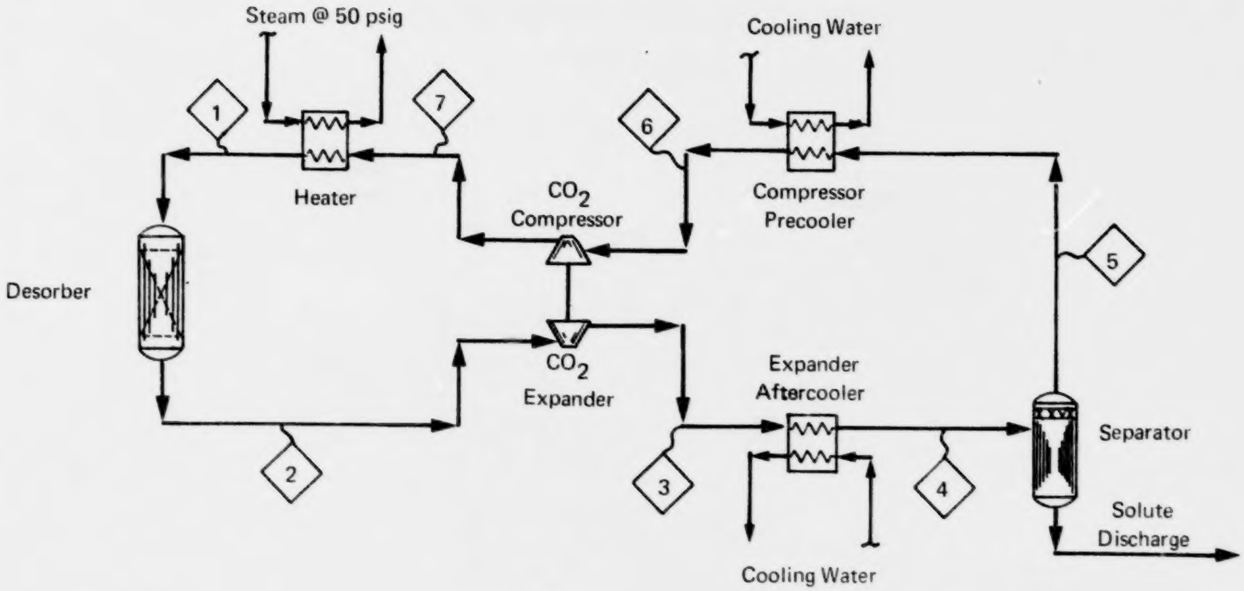
Steam @ 50 psig
Cooling Water
1
7
6
Heater
CO_2 Compressor
Compressor Precooler
Desorber
5
CO_2 Expander
Expander Aftercooler
Separator
2
3
4
Solute Discharge
Cooling Water

State Point	1	2	3	4	5	6	7
Location	Desorber Inlet	Expander Inlet	Expander Outlet	Separator Inlet	Precooler Inlet	Compressor Inlet	Steam Heater Inlet
Pressure PSIA (MPa)	2176 (15)	2176 (15)	1161 (8)	1161 (8)	1161 (8)	1161 (8)	2176 (15)
Temperature °F (°C)	248 (120)	248 (120)	158 (70)	113 (45)	113 (45)	90 (32.2)	140 (60)

Fig. IX-3 PROCESS FLOW DIAGRAM (PHENOL CASE)

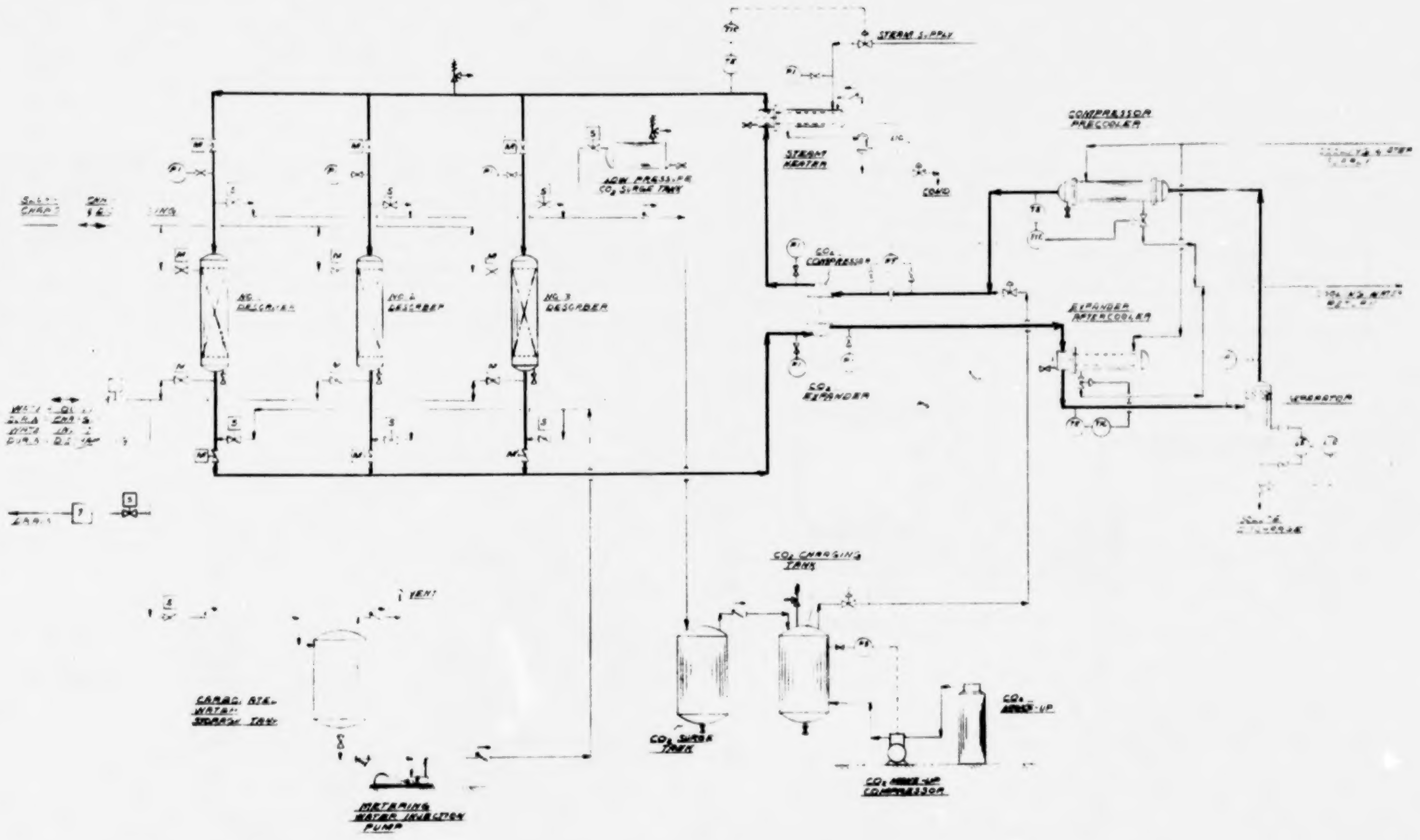
STEAM SUPPLY
TIC
STEAM HEATER
COND
COMPRESSOR PRECOOLER
LOW PRESSURE CO2 SURGE TANK
NO. 1 DESORBER
NO. 2 DESORBER
NO. 3 DESORBER
CO2 COMPRESSOR
CO2 EXPANDER
EXPANDER AFTERCOOLER
SEPARATOR
DRAIN
VENT
CARBONATED WATER STORAGE TANK
METERING WATER INJECTION PUMP
CO2 SURGE TANK
CO2 CHARGING TANK
CO2 MAKE-UP
CO2 MAKE-UP COMPRESSOR

FIGURE IX–4

PIPING AND INSTRUMENTATION DIAGRAM

Table IX-3

Summary of Desorber Analysis

T = 55°C, P = 150 atm

	Case A	Case B
No. of Columns	1	1
Column i.d. (in.)	14	7.75
Length of fill (ft.)	8.6	28.0
Ac.s. (cm^2)	993	304

Calculated values for 30 min. cycles,
40 cycles/day
10^4 lb GAC/day

X = C outlet @ end of cycle/C outlet in equal with loaded column

	Case A	Case B
X = .02		
$U_{superficial}$ (cm/s)	8	25
lb CO_2/hr	42,000	40,950
P (atm)	1.5	49.4
X = .05		
$U_{superficial}$ (cm/s)	7	23
lb CO_2/hr	36,750	36,250
P (atm)	1.2	41.8
X = .10		
$U_{superficial}$	6.5	20
lb CO_2/hr	33,900	33,550
P (atm)	1.0	31.6

B. PLANT DESIGN AND ECONOMICS

1. Overall Plant

These specifications were used as the basis for estimating operating and capital costs for a 10,000 lb/day GAC regeneration system used for phenol. Figure IX-3 gives a process flow diagram with temperature and pressure conditions. CO_2 flows through the desorber at regenerating conditions and then through an expander which directly drives the compressor. The expander replaces the let-down valve indicated in the earlier general process description. Based on discussions with the compressor/expander supplier and internal engineering evaluations, the device is applicable at these higher CO_2 flows, but is uneconomical at the low flows that would be used in small regeneration systems of about 5,000 lbs/day GAC or less.

The expanded CO_2 stream, at 80 atm, is cooled to 45°C to further reduce the phenol solubility for separation. This temperature was chosen as a phenol solubility minimum based on available data. The separator includes a mesh disengagement section to trap entrained water and adsorbate. Solute (adsorbate) is discharged from the separator as a solution or slurry in water which has also been stripped from the GAC pores. CO_2, which is still a condensed phase near critical conditions, is compressed to desorption pressure, heated, and recycled to the desorber.

A piping and instrumentation drawing for a 10,000 lb/day GAC-phenol system is shown in Figure IX-4. Included is the basic CO_2 circulation, plus equipment to provide the following functions:

Charging and discharging spent and
regenerated GAC, respectively;

Transfer of CO_2 between columns;

CO_2 make-up.

2. GAC Charging and Discharging

Spent GAC is transferred from storage as a slurry to the available desorber. The desorber is equipped with a plate or screen assembly to hold the charged GAC and allow drainage of superficial water. It is assumed that no pore water is drained.

After regeneration is complete, GAC is discharged by up-flow of water, providing slurry flow of carbon to the adsorption columns.

The following equipment is off-plot and not included in the cost of the regeneration plant: spent GAC storage tanks; regenerated GAC storage tanks; slurry pump for charging; and high-water flow carbon discharge pump.

3. Transfer of CO_2 Between Columns

The regeneration plant operates with one desorber on stream (for CO_2 circulation), and two desorbers involved in either charging or discharging carbon, or transferring CO_2 between them.

After a 30-minute regeneration cycle is completed in No. 1 desorber, flow is switched from No. 1 to No. 2 desorber. No. 3 desorber has been charged with spent carbon, and is completely filled with water to minimize introduction of air into the system. The high-pressure metering water pump then transfers carbonated water into No. 1 desorber at a low flow rate (sufficiently low to keep the bed from partly fluidizing), and slightly above bed pressure. The high-pressure water flow displaces CO_2 from desorber No. 1 to desorber No. 3, thereby pressurizing No. 3 bed to desorption pressure, and displacing its interstitial water. No. 3 desorber is then ready to accept CO_2 circulation for regeneration.

No. 1 bed, containing regenerated GAC in high-pressure water, and with pores containing high-pressure CO_2, is let down to separator pressure and held to allow expansion and release of a portion of the pore-volume CO_2. That CO_2 is collected in the low-pressure surge tank. No. 1 bed is then vented to atmospheric pressure, and the regenerated carbon is discharged as described above.

The same transfer and venting operation takes place at the completion of regeneration in each of the beds in sequence. Automatic valve operation is anticipated and accounted for in instrumenting the plant.

4. CO_2 Make-Up

CO_2 make-up is provided by cylinder liquid CO_2 at ambient temperature and its vapor pressure. A CO_2 charging tank is maintained at a pressure slightly above the compressor suction pressure. The charging tank is maintained full by flow from the low-pressure surge tank, and on demand by pressure control with flow from the make-up source.

Make-up to the circulation loop is based on flow control at the compressor suction. A short-fall on recycle flow will open the make-up valve to allow CO_2 to be drawn from the make-up CO_2 charging tank.

5. Process Costs

Table IX-4 lists the individual equipment components. For most components, the specification given resulted from discussions with suppliers and identification of specific hardware. Estimates of total system cost were made from summing the component costs, determining assembly costs from structure and piping layout sketches, and using accepted installation factors. The total system cost, including engineering, profits, and contingencies, was estimated at about $800,000.

Table IX-4

PLANT COMPONENT LIST

Regeneration of Activated Charcoal
By Supercritical Carbon Dioxide
Case: Phenol

		List of Major Components
1.	Desorber Assembly	3 x (14" ID x 8') carbon steel vessel lined with 1/8" S.S. 304 interconnected with S.S. 304 piping, mounted with required valves and instruments
2.	Carbonated Water Storage Tank	Carbon steel, 150 #, 100 gal.
3.	Metering Water Injection Pump (for SCF CO_2 transfer)	10 GPM, plunger type, C.S. construction 14.7 psi to 2200 psi Wheatley, 3000 psig design, 200 RPM 20 HP, 20" x 30" base plate, 2" piping
4.	Low Pressure CO_2 Surge Tank	25 ft^3, 250 # design, C.S.
5.	High Pressure CO_2 Surge Tank	16" ID x 8", 1500 # design, C.S.
6.	CO_2 Charging Tank	16" ID x 8', 1500 # design, C.S.
7.	CO_2 Make-up Compressor	Charging 24 lb of CO_2/30 min. into CO_2 charging tank P_1 = 80 bar, P_2 = 100 bar Draw CO_2 from source at 250 psi (min.) PPI
8.	Compressor/Expander Assembly	Rotoflow Skid size: 6' x 9'
9.	Expander Aftercooler	Shell and tube, S.S. 304 tube, 14 BWG, Carbon steel shell, CO_2 in tube side, BEU 12" Ø x 15', 400 ft^2
10.	Separator	S.S. 304 or lined carbon steel tank 3 ft^2, 18" Ø x 2' (Cyclonic type, dimensions are rough, additional design work needed)

Table IX-4 (cont'd.)

Phenol Case

11. Compressor Precooler	-	Shell and tube, S.S. 304 tube, 14 BWG, C.S. shell, CO_2 in tube, BEM 16" Ø x 15', 950 ft^2
12. Steam Heater	-	Shell and tube, S.S. 304 tube, 14 BWG C.S. shell, CO_2 in tube, BEU 12" Ø x 6', 126 ft^2
13. Valves	-	1 lot
14. Instruments	-	1 lot
Total Systems Installed Cost		\$800,000

Table IX-5 gives a summary of operating costs for the plant on a daily basis. Because the plant was designed on the basis of the steady-state GAC working capacity measured after the decline from virgin capacity, carbon capacity losses are not a factor. Negligible destructive losses were assumed.

The estimated operating cost is $0.085 per pound of regenerated carbon.

Table IX-5

ESTIMATED PROCESSING COST OF ACTIVATED CHARCOAL REGENERATION BY SUPERCRITICAL CARBON DIOXIDE PROCESS

Plant Capacity: 10,000 lbs/day Regenerated Charcoal
Case: Phenol
Operating Factor: 330 days/yr
Capital Investment: $812,000

Variable Costs	Unit/Day		$/Unit	$/Day
Electricity	163.5	KWH	.03	4.91
Cooling Water	446.4	MGal	.10	44.64
Steam	43.0	MMBtu	3.50	150.50
CO_2	525	Lbs	.03	15.75
				215.80

Semivariable Costs		
Operating Labor:	1/2 man/shift, 3 shifts/day @ $10/hr	120.00
Supervision:	1/2 man @ $20,000/yr	38.46
Labor Overhead:	40% Labor & Supervision	63.38
Maintenance:	2% of Capital Investment/yr	46.40
		268.24

Fixed Costs		
Plant Overhead:	60% of Labor & Supervision	95.08
Taxes & Insurance:	1.5% of Capital Investment/yr	34.80
Depreciation:	10% of Capital Investment/yr	232.00
		361.88

Direct Processing Costs: $ 845.92 /day
$ .085 /lb of Regenerated Charcoal

REFERENCES

Am. Public Health Assn., "Standard Methods for the Examination of Water and Wastewater," 13th ed., New York, 1971.

Anon, Chemical and Engineering News, June 9, 1975, P. .

Buelow, R. W., J. K. Carswell and J. M. Symons," An Improved Method for Determining Organics by Activated Carbon Adsorption and Solvent Extraction," J. Am. Water Wks. Assn., part I, 65(1):57-72; part II, 65(3):195-199(1973).

Burant, W. and Voelstadt, T. J., Water & Sewage Works, Nov., 1973, p. 42.

Chriswell, C. D., R. I., Ericson, G. A. Junk, K. W. Lee, J. S. Fritz and H. J. Svec, "Comparison of Macroreticular Resin and Activated Carbon as Sorbents," J. Am. Water Works Assn., 69, 669 (1977).

Cohen, J. M. and English, J. N., AIChE Symp. Series No. 144, 70, 326 (1974)

Coughlin, R. W., F. S. Ezra and R. N. Tan, "Influence of Chemisorbed Oxygen in Adsorption onto Carbon from Aqueous Solution," J. Colloid Interface Sci., 28:386(1968).

Francis, A. W., "Ternary Systems of Liquid Carbon Dioxide," J. Phys. Chem., 58, 1099 (1954).

Franck, E. U., "Water and Aqueous Solutions at High Pressures and Temperatures," Pure Appl. Chem., 24, 13 (1970).

Giddings, J. C., M. N. Myers, L. McLaren and R. A. Keller, "High Pressure Gas Chromatography of Nonvolatile Species " Science, 162:67-73(1968).

Gouw, T. H., and R. E. Jentoft, "Physical Aspects in Supercritical Fluid Chromatography," Adv. Chromatogr., 13, 1 (1975).

Grob, K. J. Chromatogr., 84, 255 (1971).

Grob, K., and G. Grob, J. Chromatogr., 90, 303 (1974).

Grob, K., et al, J. Chromatogr., 106, 299 (1975).

Gruber, G., "Assessment of Industrial Hazardous Waste Practices: Organic Chemicals, Pesticides, and Explosives Industry," U. S. Environmental Protection Agency.

REFERENCES (continued)

Hag, A. G."

a. "Extraction of caffeine from coffee," Ger. Offen. 2, 212,281 (Sept. 27, 1973).

b. "Aroma-rich decaffeinated tea," Fr. Demande 2, 140,098 (February 16, 1973).

c. "Cocoa butter," Fr. Demande 2, 140,099 (February 16, 1973).

d. "Aroma Extracts of Natural Composition," Fr. Demande 2, 140,096 (Feb. 16, 1973).

e. "Selective Extraction of Nicotine from Tobacco," Ger. Offen. 2, 142,205 (May 15, 1973).

Himmelstein, K. J., Fox, R. D., Winter, T. H., AIChE Symp. Series No. 144, 70, 310 (1974).

Hutchins, R.A., AIChE Symp. Series No. 144, 70, 296 (1974).

Jentoft, R. E., and T. H. Gouw, "Analysis of Polynuclear Aromatic Hydrocarbons in Automobile Exhaust by Supercritical Fluid Chromatography," Anal. Chem., 48, 2195 (1976).

Kennedy, G. C., "A Portion of the System Silica-Water," Econ. Geol., 45, 629 (1950).

Liphard, K. G., and G. M. Schneider, "Phase Equilibria and Critical Phenomena in Fluid Mixtures of Carbon Dioxide + 2,6,10,15,19,21-hexamethyltetracosane up to 423 K and 100 MPa," J. Chem. Thermodyn., 7, 805 (1975).

Loven, A. W., AIChE Symp. Series No. 144, 70, 285 (1974).

Maddocks, R. R., J. Gibson and D. F. Williams, "Supercritical Extraction of Coal," Chem. Eng. Prog., 75, 49-55 (1979).

Mattson, J. S., H. B. Mark, Jr., M. D. Malbin, W. J. Weber, Jr., and J. C. Crittenden, "Surface Chemistry of Active Carbon:Specific Adsorption of Phenols," J. Colloid Interface Sci., 31:116 (1969).

Middleton, F. M., H. Braus and C. C. Ruchloft, "The Application of the Carbon Filter and Countercurrent Extraction to the Analysis of Organic Industrial Wastes," Proc. 7th Purdue Ind. Waste Conf., 79:439 (1952).

Middleton, F. M., W. Grant and A. A. Rosen, "Drinking Water Taste and Odor-Correlation with Organic Chemical Content," Ind. Eng. Chem., 48:268-74 (1956).

REFERENCES (continued)

Minor, P. S., Env. Sci. & Tech. 8, 620 (1974).

Pahl, R. H., K. G. Mayhan and G. L. Bertrand, "Organic Desorption from Carbon-II. The Effect of Solvent in the Desorption of Phenol from Wet Carbon," Water Research, 7:1309-22 (1973).

Paul, P.F.M., and W. S. Wise, "The Principles of Gas Extraction," Mills and Boon, Ltd., London, 1971.

Peng, D. Y., and D. B. Robinson, "A New Two-Constant Equation of State," Ind. Eng. Chem. Fundam., 15, 59 (1976).

Perrotti, A. E., and C. A. Rodman, AIChE Symp. Series No. 144, 70, 31 (1974).

Quinn, E. L., and C. L. Jones, "Carbon Dioxide," Rheinhold Publ. Corp., N. Y., 1936, pp. 109-10.

Remirez, R., "New Routes Compete for Spent Carbon Recovery," Chemical Engineering, Sept. 12, 1977, P. 95-97.

Rijnders, G.W.A., "Supercritical Fluid Chromatography," in 5th Intern. Symp. on Separation Methods: Column Chromatography, 1969, Chimia Suppl., p. 192.

Rosen, A. A., F. M. Middleton and N. W. Taylor, "Identification of Anionic Synthetic Detergents in Foams and Surface Waters," J. Am. Water Wks, Assn., 48:1321-1330 (1956).

Schneider, G. M., "Phase Equilibria in Fluid Mixtures at High Pressure," Adv. Chem. Phys., 17, 1 (1970).

Schuliger, W. G., and MacCrum, J. M., AIChE Symp. Series No. 144, 70, 352 (1974).

Shell, G. L., AIChE Symp. Series No. 144, 70, 371 (1974).

Shuckrow, A. J., and Culp, G. L., "Appraisal of Powdered Activated Carbon Processes for Municipal Wastewater Treatment," U. S. Environmental Protection Agency Report No. EPA-600/2-77-156, 1977, P. 247.

Sie, S. T., W. Van Beersum and G.W.A. Rijnders, "High-Pressure Gas Chromatography and Chromatograpny with Supercritical Fluids. I. The Effect of Pressure on Particiation Coefficients in Gas-Liquid Chromatography with Carbon Dioxide as a Carrier Gas," Separation Sci., 1, 459 (1966).

Smith, S. B., Chem. Eng. Prog. 71, 87 (1975).

REFERENCES (continued)

Snoeyink, V. L., and W. J. Weber, Jr., "The Surface Chemistry of Active Carbon - A Discussion of Structure and Surface Functional Groups," Environ. Sci. Tech., 1:228 (1967).

Suffet, I. H., and McGuire, M. J., "Activated Carbon Adsorption of Organics from the Aqueous Phase, Vol. 1 and 2, Ann Arbor Science, to be published, 1980.

Tsekhanskaya, Yu. V., M. V. Iomtev, and E. V. Mushkina, "The Solubility of Naphthalene in Ethylene and in Carbon Dioxide Under Pressure," Russ. J. Phys. Chem., 38(9):1173 (1964).

U. S. Department of Health, Education and Welfare, "Public Health Service Drinking Water Standards, 1962."

U. S. Environmental Protection Agency Technology Transfer: "Process Design Manual for Carbon Adsorption," October, 1973.

Wise, W. S., "Solvent Extraction of Coal," Chem. Ind. (London), 1970:950.

Zhuze, T. P., and G. N. Yushkevich, "Compressed Hydrocarbon Gases as Solvents for Crude Oils and Residuums," Izvest. Akad. Nauk SSSR, Otdel. Tekh. Nauk, 1957 (11):63-8.

Zimpro, "Wastewater Reclamation," commercial literature Catalog No. 2700-2.

XI. APPENDIX

A. Local Equilibrium Theory

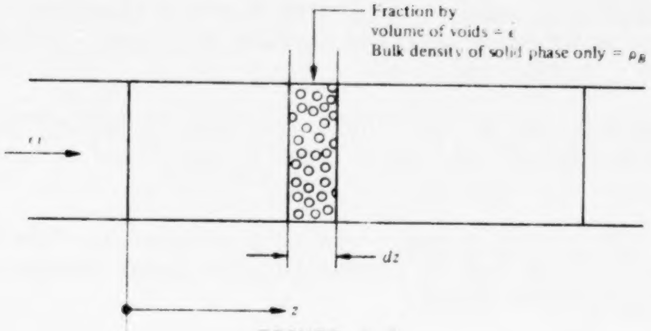
Fraction by volume of voids = ε
Bulk density of solid phase only = ρ_B
v
dz
z

FIGURE A-1

Consider a differential, cylindrical volume element of the bed, of length dz, as shown in Fig. A-1. The material balance on the fluid and solid phases contained within the differential volume element is

$$\varepsilon\left(\frac{\partial c}{\partial t}\right)_z + \rho_B\left(\frac{\partial q}{\partial t_2}\right) + \varepsilon v\left(\frac{\partial c}{\partial z}\right)_t = 0 \qquad (1)$$

where c and q are fluid and solid concentration, respectively, ε is the fraction of fluid-filled space outside the particles, and ρB is the bulk density of the dry adsorbent. The superficial fluid velocity is v, where v is the average fluid velocity in the interstices between particles. For this simple model, longitudinal diffusion is neglected and plug flow is assumed.

Before Eq. (1) can be solved, a second equation relating fluid and solid concentrations must be introduced. In the general case, this second equation will take the form of

$$\rho_B\left(\frac{\partial q}{\partial t}\right)_z = kaF\,(c,q) \qquad (2)$$

which expresses the rate of change of solid phase concentration as a function of the interfacial mass transfer coefficient, ka, and a driving forces, F(c,q). Eqs. (1) and (2) can than be solved simultaneously to obtain the function c(z,t), which is the fluid phase concentration at any position, z, within the column as a function of time. For example, the effluent concentration curve is c(L,t), where L is the column length.

In the general case, there are two types of mass transfer resistances that are considered in developing Eq. (2): diffusion of solute out of the SCF-filled pores and interfacial mass transfer from the external surface of the adsorbent particle into the bulk of the SCF phase. One of the advantages of SCF regenerant is that mass transfer is relatively rapid within the SCF phase. In the limiting case where resistance to mass transfer is negligible, Eq. (2) reduces to the equilibrium relationship between solid phase concentration, q, and bulk fluid concentration, c, which is just the adsorption isotherm expression:

$$q = f(c)$$

For this limiting case, local equilibrium exists at all points within the column and at all times between particles and the adjacent fluid.

When the local equilibrium theory (LET) applies, Eq. (1) is solved simultaneously with Eq. (3). By differentiating Eq. (3) with respect to time, we obtain the following equation:

$$\left(\frac{\partial q}{\partial t} \right)_z = \frac{d[f(c)]}{dc} \left(\frac{\partial c}{\partial t} \right)_z \qquad (4)$$

or

$$\left(\frac{\partial q}{\partial t} \right)_z = f'(c) \left(\frac{\partial c}{\partial t} \right)_z \qquad (5)$$

where f'(c) is d[f(c)]/dc. Substituting Eq. (5) into Eq. (1) and collecting terms, we obtain Eq. (6):

$$\left[1 + \frac{B}{} f'(c)\right] \left(\frac{\partial c}{\partial t} \right)_z + v\left(\frac{\partial c}{\partial z} \right)_t = 0 \qquad (6)$$

Eq. (6) is a first-order partial differential equation that is linear in the derivatives but has a variable coefficient because of the f'(c) term. Such equations have relatively simple geometrical properties as expressed by a solution procedure known as the "method of characteristics" (Sherwood, et al., 1975). In essence, each concentration, c, or coverage, q, moves through the bed at a characteristic velocity, v_c, where

$$v_c = \frac{v}{1 + (\rho_B/\varepsilon)f'(c)} \qquad (7)$$

The characteristic velocities can be appreciated more directly by examining the column profiles during the regeneration process. The column profile may be represented, as shown in Fig. A-2, by the coverage versus distance down the column at various times during the regeneration process. Each curve in Fig. A-2 is a cross-sectional 'snap-shot' of solute remaining on the column at the designated time. At $t = 0$, $q/q_0 = 1$ for all x, where q_0 is the initial loading. At some time, t_1, solute has been removed from the adsorbent near the column inlet, but near the outlet the adsorbent is still loaded to the initial value of q_0. At 10 t_1, a larger region near the inlet has been fully regenerated, while the outlet has been reduced to q/q_0 of .83. At 180 t_1, about 76% of the column has been fully regenerated, while the remaining 24% ($.76 < z/L < 1.0$) has less than 14% of the initial coverage still remaining ($q/q_0 < .14$). At $t = 237t_1$, the regeneration is complete.

Now let us examine the velocity with which a given level of coverage moves through the bed. In Fig. A-2, we have drawn a horizontal line through $q/q_0 = .363$. The corresponding values of t/t_1 and z/L are:

t/t_1	1	10	30	60	90
z/L	.01	.10	.30	.60	.90

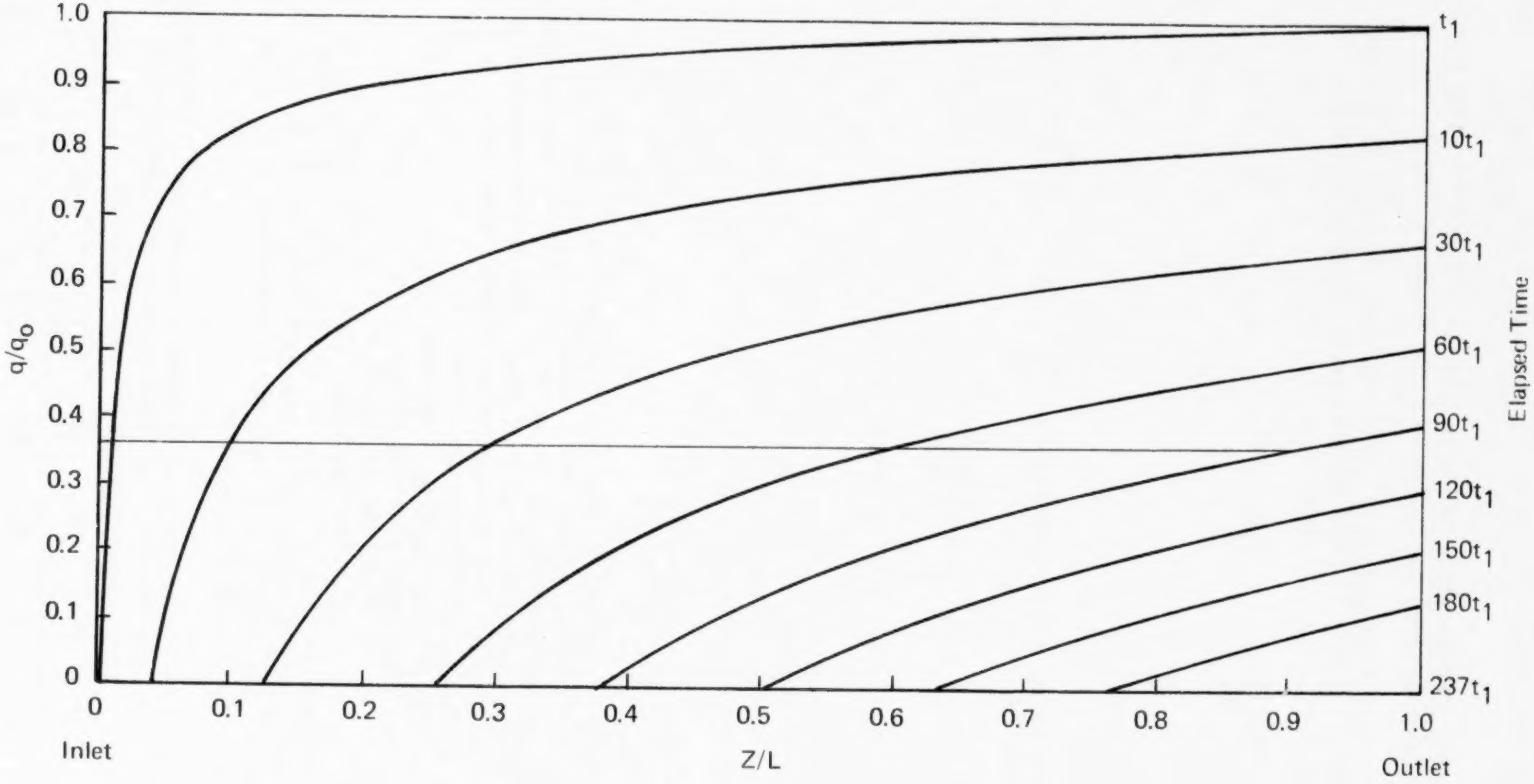

Figure A-2 Column Profiles of Adsorbent Coverage as a Function of Time During Regeneration Under Local Equilibrium Conditions

In other words, this level of coverage moves through the column at a constant velocity of $z/t = .01\ L/t_1$ (where L and t_1 are constants that are fixed by the nature of the adsorbent and adsorbate). A similar analysis at $q/q_o = 0$ shows that the velocity of the fully regenerated "wave" is $.0042\ L/t_1$.

Although Fig. A-2 is given in terms of the coverage profile, q/q_o, we could equally as well have given the profile of solute in regenerant, c/c_o, because fluid concentration and coverage are directly coupled by the adsorption isotherm expression, as represented by Eq. (3). Thus, given the isotherm, we could calculate a c/c_o for every q/q_o, where c_o is the concentration of solute in regenerant in equilibrium with a column at the initial loading, q_o.

In general, higher values of c (or q) move through the column more rapidly than lower concentrations. The analytical relationship between wave velocity and concentration is given by Eq. (7) for the LET model. The term f'(c) increases as c decreases, so that v_c decreases as c decreases.

The desorption curve is the effluent concentration as a function of time, c(L,t). It can be obtained indirectly from the column profile, Fig. A-2, by noting q at the outlet ($z/L = 1$) as a function of time, and then converting q to c using the adsorption isotherm, Eq. (3). Alternatively, it can be found by solving the differential equation, Eq. (1).

A typical desorption curve predicted by the LET model is shown in Fig. A-3. The corresponding regeneration curve, which is the fractional regeneration, R(t), as a function of time, is shown in Fig. A-4. The residence time for the non-adsorbing regenerant fluid to pass through the bed is t_o. Between t_o and t_1, the effluent concentration is constant at c_o because the adsorbent at the column outlet is still loaded with solute at the initial value of q_o (see curve t_1 in Fig. A-2). For times greater than t_1, the effluent concentration decreases with time until the column is fully regenerated at t_2 [in Fig. A-2, $t_2 = 237t_1$]. The tail in the desorption curve between t_1 and t_2 is a consequence of the fact that the characteristic velocity of the concentration wave decreases as concentration decreases.

The regeneration curve, shown in Fig. A-4, is the fraction of the initially adsorbed solute that has been removed from the column up to time, t. If m is the mass of solute left on the column at any time, t, then by material balance at the column exit,

$$-\frac{dm}{dt} = \varepsilon v\ A_{cs} \cdot c(L,t) \qquad (7)$$

Integrating from t_o to any time during desorption, t,

$$m_o - m = \varepsilon v A_{cs} \int_{t_o}^{t} c(L,t)dt \qquad (8)$$

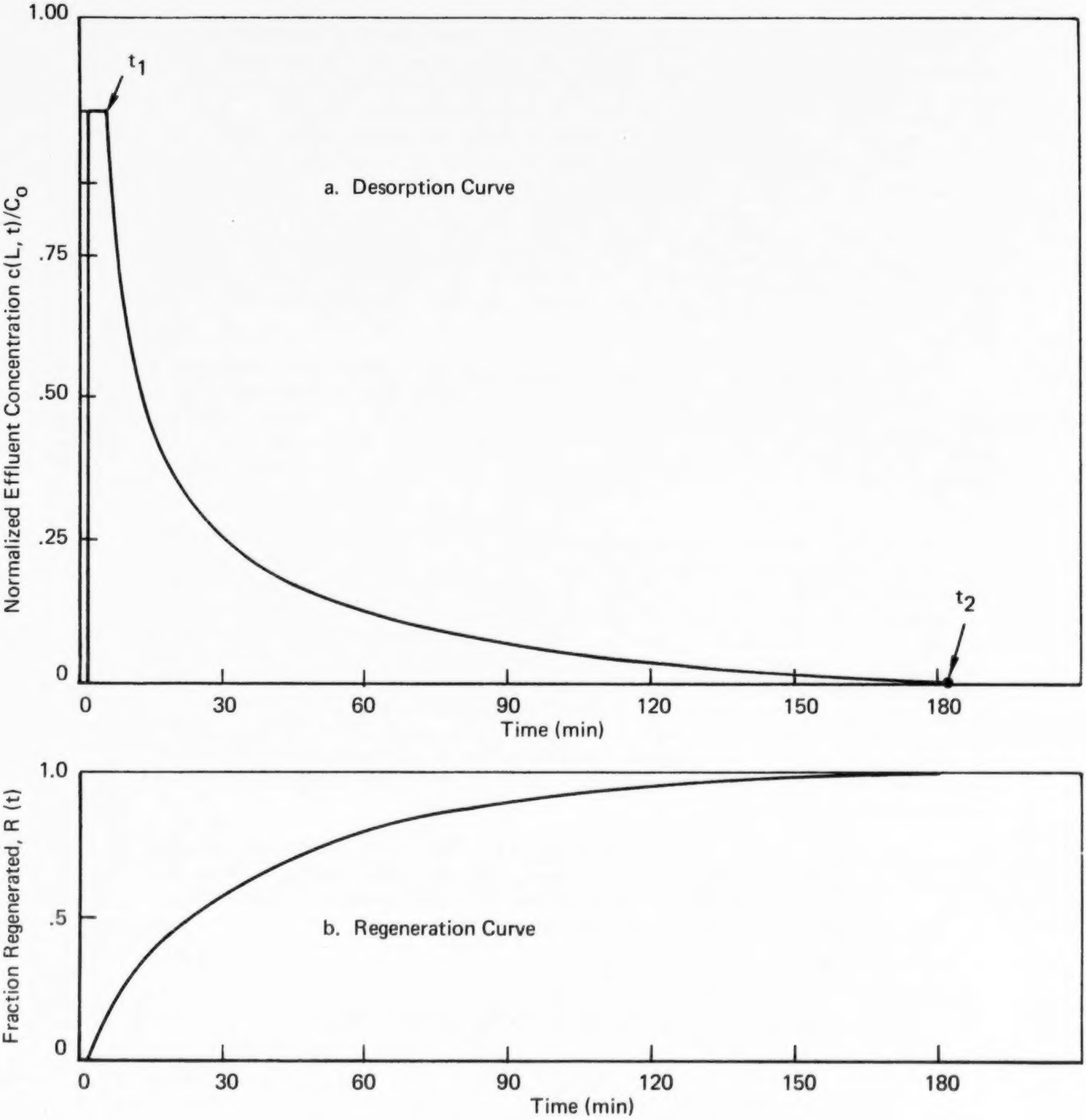

FIGURES A-3 and A-4
L.E.T. DESORPTION AND REGENERATION CURVES

where m_0 is the initial loading:

$$m_o = q_o \rho_B L A_{cs} \tag{9}$$

Defining the fractional regeneration, R(t) as

$$R(t) = \frac{m_o - m}{m_o} \tag{10}$$

from the equations above, it follows that

$$R(t) = \frac{\varepsilon V}{q_o L \rho_B} \int_{t_o}^{t} c(L,t)dt \tag{11}$$

The regeneration curve calculated from the desorption curve of Fig. A-3 is shown in Fig. A-4. It can be seen that the general shape of the desorption and regeneration curves, as predicted by the LET model, looks very similar to the desorption curves obtained experimentally (see Fig. VI-13). In fact, it was this similarity that led us to attempt to develop a quantitative theoretical model to correlate our experimental results.

To apply the LET theory quantitatively, an isotherm of the form of Eq. (3) is required. Note that Eq. (3) is not the conventional water isotherm; rather, it is the isotherm for supercritical fluid with adsorbent. Furthermore, the loading, q, is the surface concentration of mobile adsorbed species rather than the total loading of solute.

Since the SCF adsorption isotherm of mobile species was not available, we attempted to use an assumed isotherm expression for Eq. (3) and then used an experimentally measured desorption curve to determine best-fit isotherm constants. The assumed isotherm was taken to be the Langmuir form,

$$q = q_m \left(\frac{K_c}{1 + K_c}\right) \tag{12}$$

where K and qm are constants and c is solute concentration in the regenerant fluid. Using Eq. (12) for the function in Eq. (3), the method of characteristics leads to the following solution for the desorption curve: [Note that the time variable, t, is given in reduced form, tr = t/t_0, where t_0 is time for regenerant to pass through the fluid space of the bed (i.e., L/v). In other words, t is the number of bed volumes of regenerant passed through the bed in time t.]

$$c(1,tr) = 0 \qquad 0 \leq tr < 1 \tag{13}$$

$$c(L,tr) = c_o \qquad 1 \leq tr \leq tr_1 \tag{14}$$

$$c(L,tr) - \frac{1}{k} \sqrt{\left(\frac{\rho B}{\varepsilon}\right) \frac{q_m K}{(tr - 1)}} - 1 \qquad tr_1 < tr \leq tr_2 \tag{15}$$

$$\text{where } tr_1 = 1 + \left(\frac{\rho_B}{\varepsilon}\right) \frac{q_m K}{(1 + Kc_F)^2} \tag{16}$$

$$\text{and } tr_2 = 1 + \left(\frac{\rho_B}{\varepsilon}\right) \frac{q_m K}{(1 + Kc_F)^2} \tag{17}$$

The parameter tr_1 defines the length of the plateau during the early phase of regeneration and tr_2 is the number of bed volumes of regenerant required to complete the desorption process (see Fig. A-3).

Using Eqs. (16) and (17) to determine tr_1 and tr_2, Eqs. (13) to (15) can then be used to generate the complete desorption curve. The parameters required in these equations are q_m, K (isotherm constants), ρ_B, ε(column parameters), c_F and c_0 (regenerant feed and initial effluent concentrations). The last parameter, c_0, is related to the initial loading, q_0, by the isotherm expression:

$$q_0 = q_m \left(\frac{Kc_0}{1 + Kc_0}\right) \tag{18}$$

$$\text{or} \qquad c_0 = \frac{q_0/q_m}{K(1 - q_0/q_m)} \tag{19}$$

Thus, given knowledge of the isotherm and column parameters and the initial loading, it is possible to generate a predicted desorption curve.

Lacking isotherm data for determining K and q_m, we attempted to choose values of K and q_m that best fit the desorption curve. Fig. A-5 is the desorption curve obtained by collecting solute from SCF CO_2 desorption of alachlor. Desorption followed a ten-day adsorption on fresh Filtrasorb 300. From the total alachlor collected during desorption, q_0 was known to be 0.185 g/g GAC. From Fig. A-5, the weight fraction of alachlor at the beginning of the desorption run, x_0, is seen to be around 0.021. The conversion of weight fraction to concentration is $c_0 = \rho_C x_0$ where ρ_C is the regenerant density at column conditions (0.57 g/cm^3); thus, c_0 is about 0.012 g/cm^3. From Fig.A-5, tr_1 is in the neighborhood of 1.5 to 2 bed volumes. The column parameters for this run were L = 4.09 cm and v = 111 cm/sec.

By varying the Langmuir constants, q_m and K, and the initial loading, q_0, best-fit desorption and regeneration curve were generated, as shown in Fig. A-6. The best-fit desorption curve appears to describe the experimental data moderately well up to about 200 bed volumes. Beyond tr of 200, the generated curves go to x(L,tr) of zero faster than the experimental curve. The generated curve predicts completion of the desorption process in 375 bed volumes, wheras the experimental desorption curve was terminated at 642 bed volumes.* This slow, prolonged tailing

---

* At 642 bed volumes, minute concentrations of alachlor were still detected in the outlet. Subsequent test indicated that close to 1000 bed volumes were necessary to reach constant weight in the U-tube collector.

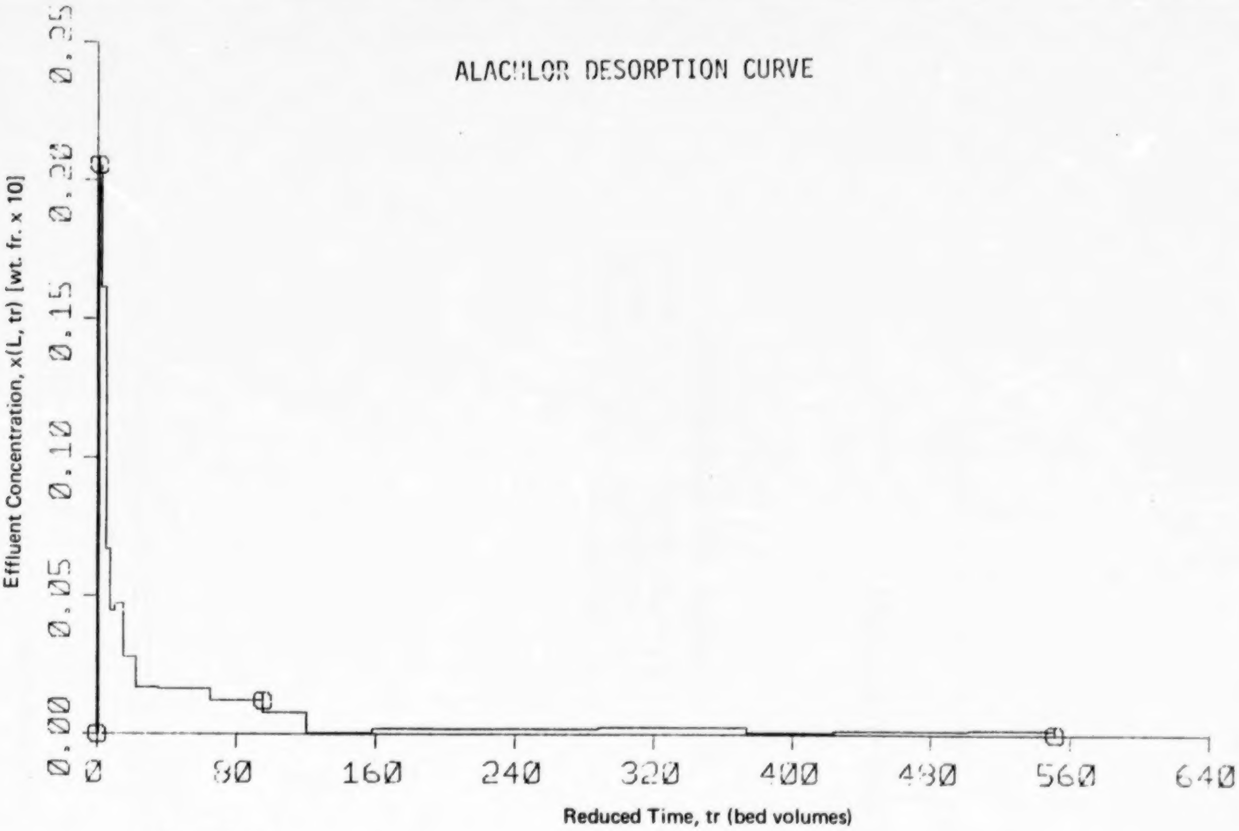

a. Entire Curve

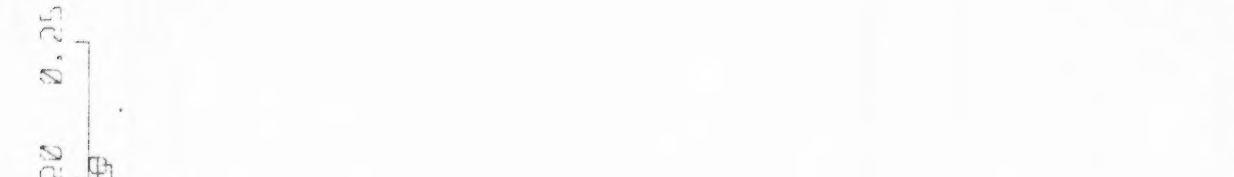

b. Blow-up of 0–120 Bed Volumes)

Figure A-5

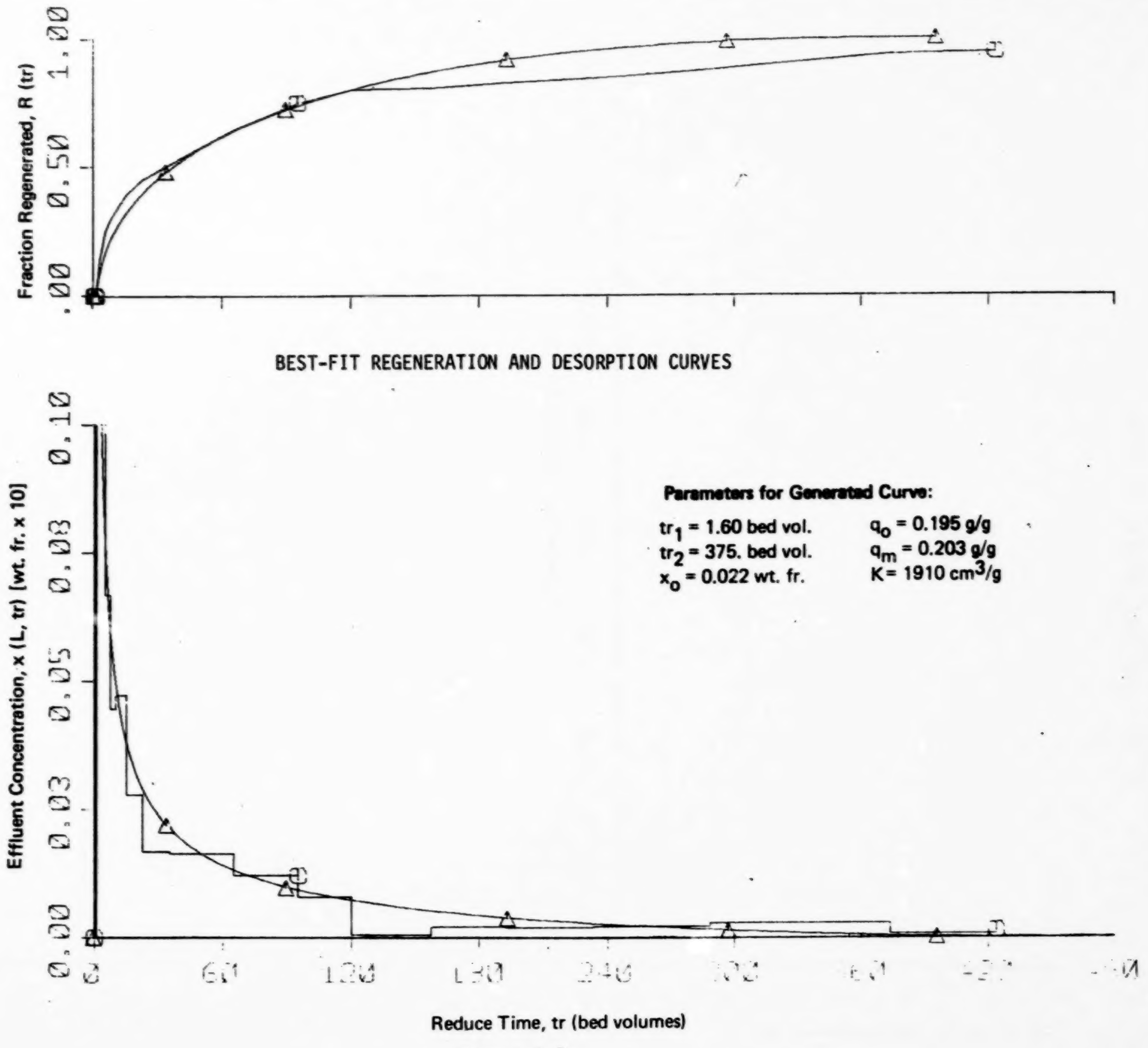
Fraction Regenerated, R (tr)
.00
0.50
1.00
BEST-FIT REGENERATION AND DESORPTION CURVES
Effluent Concentration, x (L, tr) [wt. fr. x 10]
0.00
0.03
0.05
0.08
0.10
Parameters for Generated Curve:
tr_1 = 1.60 bed vol.
tr_2 = 375. bed vol.
x_o = 0.022 wt. fr.
q_o = 0.195 g/g
q_m = 0.203 g/g
K= 1910 cm^3/g
0
60
120
180
240
300
360
420
480
Reduce Time, tr (bed volumes)

Figure A-6

of the experimental desorption trace represent a departure from local equilibrium theory. It may indicate that pore diffusion out of the carbon particles becomes rate-limiting after the pores have been depleted of a large fraction of solute.

We have found that, in general, the regeneration curve is a more sensitive test of the theory than the desorption curve. The regeneration curve shown in Fig. A-6 shows an accentuation of the departure of theory and experiment; beyond about 130 bed volumes, the calculated regeneration curve continues smoothly to completion whereas the experimental curve has a sharp change in slope after about 80% of the adsorbate is removed.

The constants chosen for the best fit in Fig. A-6 are: $tr_1 = 1.6$ bed vol., $x_0 = 0.022$ wt. fr. and $q_0 = 0.195$ g/g. The corresponding calculated values are: $q_m = .203$ g/g, $K = 1910$ cm^3/g and $tr_2 = 375$ bed vol. The initial reversibly adsorbed loading (q_0) used for the best fit was 0.195 g/g whereas the actual amount collected during desorption was 0.185 g/g. In general, it is to be expected that the q_0 used in the model will be equal to or less than the actual amount desorbed. When a column has been on stream during adsorption of a time sufficient to reach adsorption equilibrium, then q_0 should be equal to the actual amount desorbed. In most cases, we stop the adsorption process before the column has reached adsorption equilibrium. The alachlor run under discussion was on stream for 10 days, which is time enough for the front end of the column to approach adsorption equilibrium. Note that the front end of the column for adsorption becomes the column exit for desorption because the direction of flow for desorption is the reverse of adsorption. Therefore, the last adsorbate seen by the regenerant at the start of desorption is the highest loading achieved anywhere in the column during adsorption (i.e., at the entrance during adsorption).

This phenomenon of partial loading during adsorption is best illustrated by examining the predictions of the LET model. For example, the curve generated for the best fit for the 10-day alachlor adsorption is shown as the full curve in Fig. A-7. The initial effluent concentration, x_0, is 0.022 wt. fr. corresponding to $q_0 = .195$ (or $q_0/q_m = .195/.203 = .96$; i.e., the loading is equivalent to 96% of a monolayer.) First, we note from Eq. (17) that tr_2 is independent of the initial loading. Furthermore, from Eq. (15), the effluent concentration between tr_1 and tr_2 is independent of the initial loading. Therefore, the declining portion of the effluent concentration curve is the same for 90% of a monolayer as it is for 95% initial coverage. The only differences between the two curves are the height of the initial plateau, x_0, and the time at the end of the plateau, tr_1. To determine x_0, we use Eq. (19) to determine the value of c_0 in equilibrium with q_0 and then calculate $x_0 = c_0/\rho_c$. By this procedure, we determine that for 90% loading, x_0 is 0.00827 wt. fr. We can then calculate tr_1 from Eq. (16) or, alternatively, draw in the plateau at $x_0 = .00827$ in Fig. A-7 and

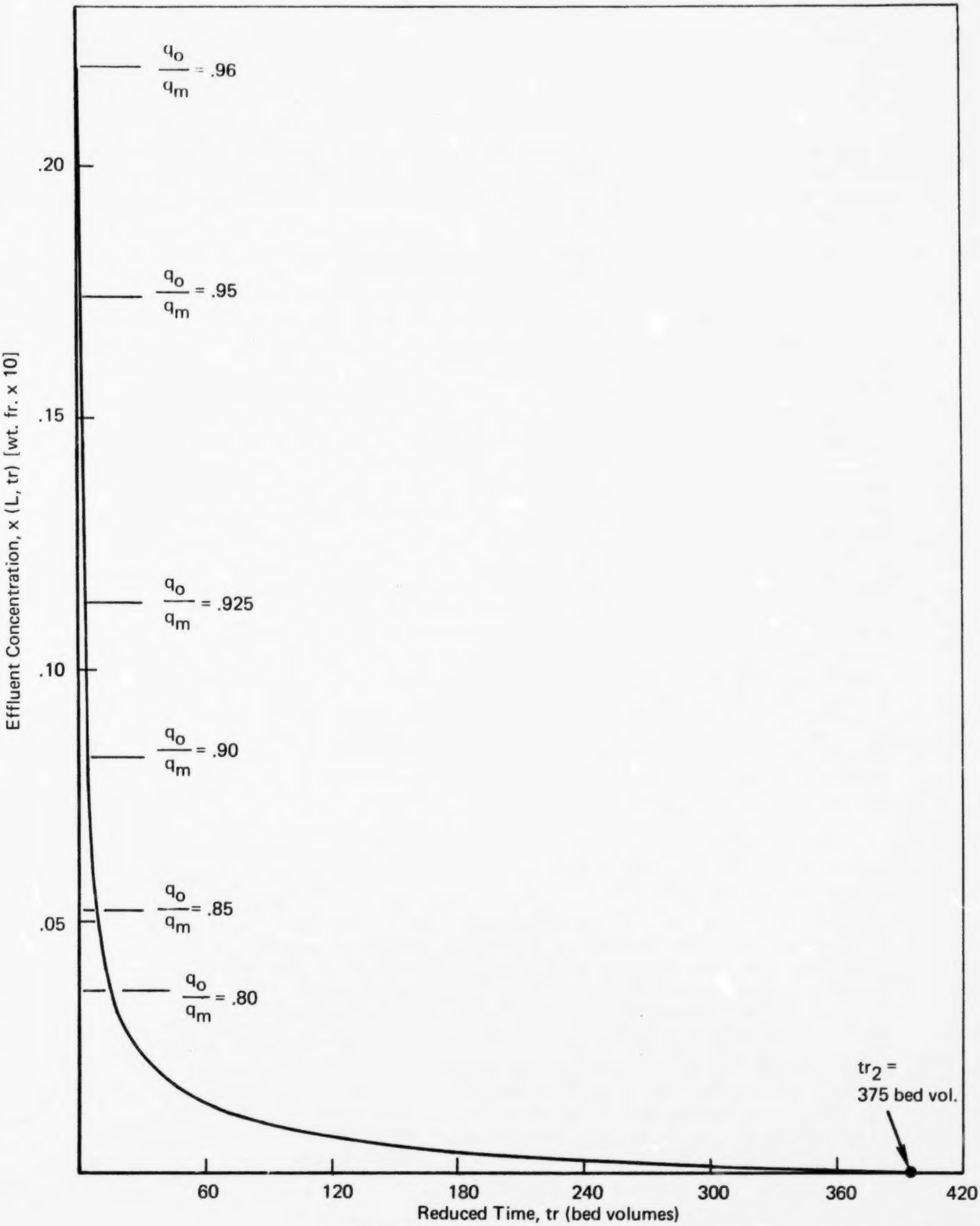

Figure A-7
BEST-FIT FOR 10-DAY ALACHLOR ADSORPTION

read off tr_1 directly. In this manner, the desorption curves for any initial loading can be calculated once we know the isotherm parameters, q_m and K. The results for initial loadings ranging from 80 to 96% are shown in Fig. A-7.

Let us now examine experimental data obtained from relatively short adsorption cycles, wherein the loading was less than that obtained in the 10-day adsorption run. As part of our repeated cycling test series with alachlor, two 7 g GAC columns were loaded in series during a 3-day adsorption, which is insufficient time to reach adsorption equilibrium; we might expect that the loading would be no more than 50 to 70% of the equilibrium value. Indeed, during desorption of these columns, the amount of solute collected was 0.131 g/g GAC.

As a further test of the validity of the LET model, we generated desorption and regeneration curves from the LET model for the 3-day adsorption run. If the model is appropriate, then the same isotherm constants, q_m and K, found for the best fit for the 10-day adsorption experiment should apply to the 3-day adsorption experiment. The difference between the 10-day and 3-day results should lie in the initial loading, q_o, which in turn will lead to different values of x_o and tr_1. Using the best fit values of q_m and K found for the 10-day run and using x_o = .070 wt. fr., which was the value measure experimentally, the desorption and regneration curves shown in Fig. A-8 were generated. The agreement between the experimental and generated curves - both for desorption and regeneration - is excellent! We believe that such agreement is strong evidence of the validity of the LET model.

Note that the initial loading for the regenerated curve in Fig. A-8 is 0.179 g/g. As mentioned previously, only 0.131 g/g was collected during desorption. The higher value of q_o was not chosen to force agreement of theory with experiment; rather, the value of $q_o = q_m$ and K, along with the experimental value of x_o = .0070 wt. fr. (which is equivalent to $c_o = {}_c x_o$ = .0040 g/cm^3), using Eq. (18). In other words, q_o = 0.179 is the loading reached at the inlet during adsorption and, therefore, is the value in equilibrium with the effluent at the start of desorption. During short adsorption cycles, it is expected that the column inlet will reach a higher loading than the average loading of the entire column.

A large number of runs for alachlor had been made using a 1-day adsorption cycle (e.g., the results shown in Table IV). Although adsorption is far from complete after one day, we compared theory and experiment for these data using the same procedure outlined above for the 3-day adsorption run. The results are shown in Fig. A-9. The calculated value of q_o (in equilibrium with x_o = .0022) is 0.143 g/g, where only 0.105 g/g were collected during desorption. The difference is again an indicated of the difference in loading between column inlet and average value for short period of adsorption. It is for this reason that the generated desorption and regeneration curves are somewhat higher than the experimental ones. However, on the whole, the agreement between theory and experiment is remarkably good. These results, taken as a whole, support our contention that supercritical fluids are excellent carriers for repidly desorbing solutes from activated carbon.

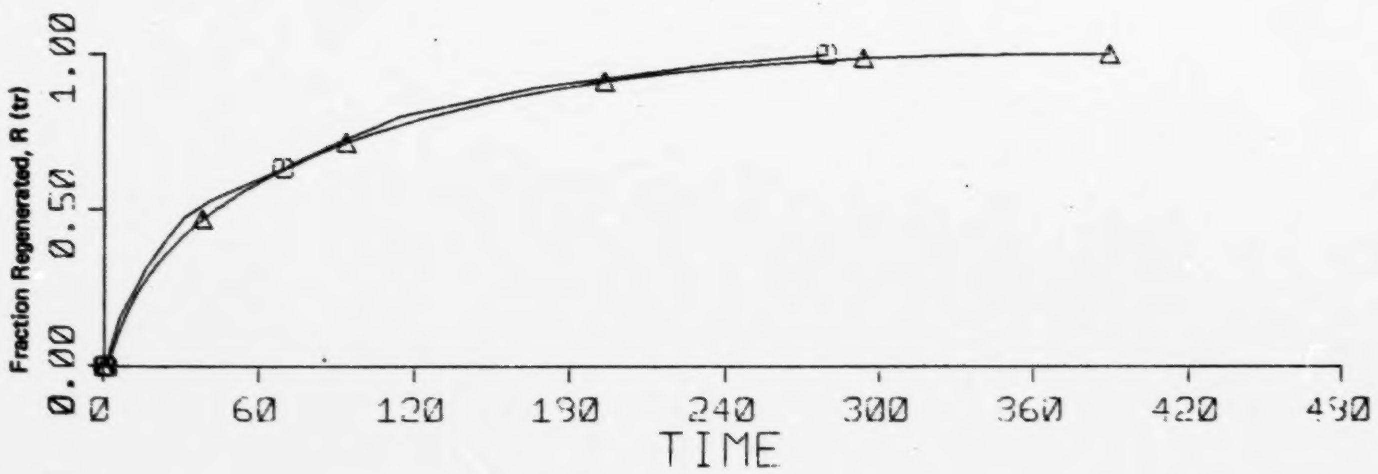

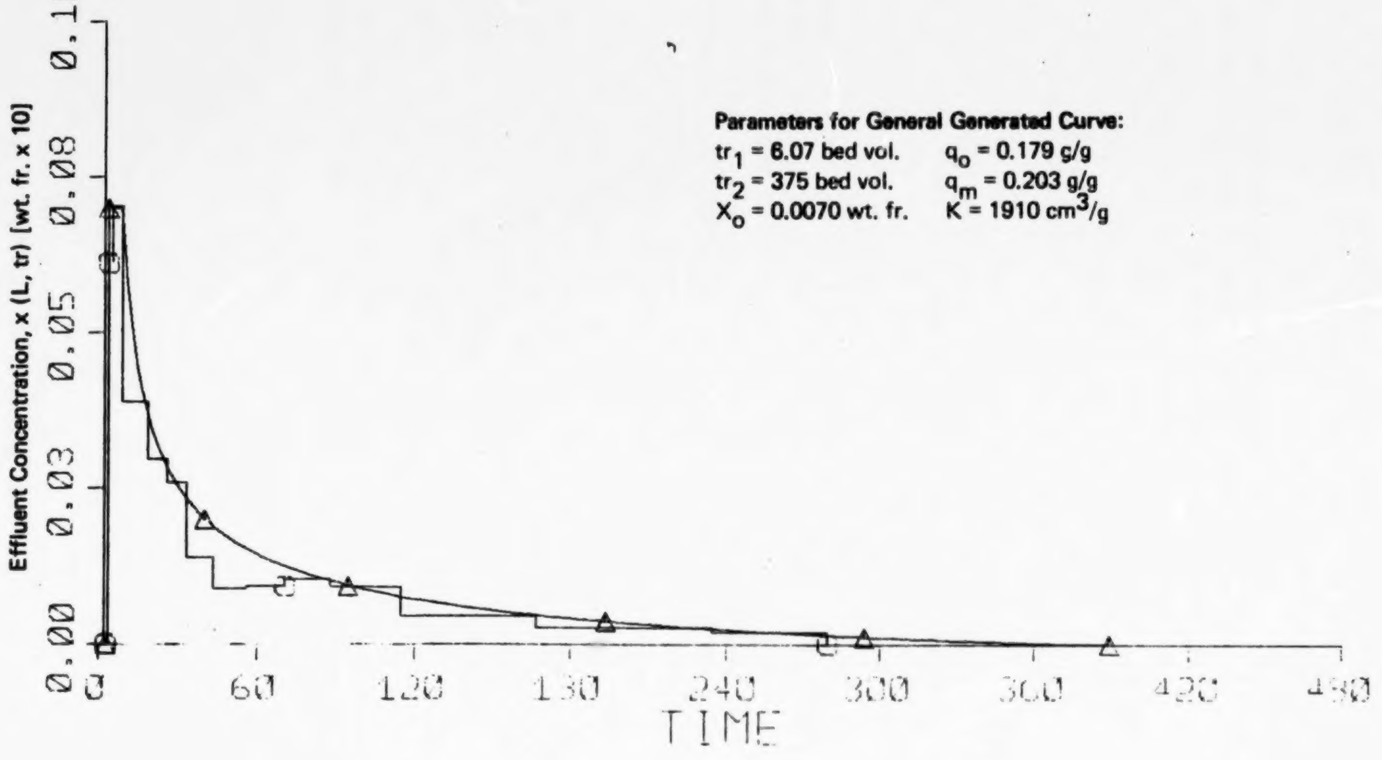

Parameters for General Generated Curve:

tr_1 = 6.07 bed vol. q_o = 0.179 g/g

tr_2 = 375 bed vol. q_m = 0.203 g/g

X_o = 0.0070 wt. fr. K = 1910 cm^3/g

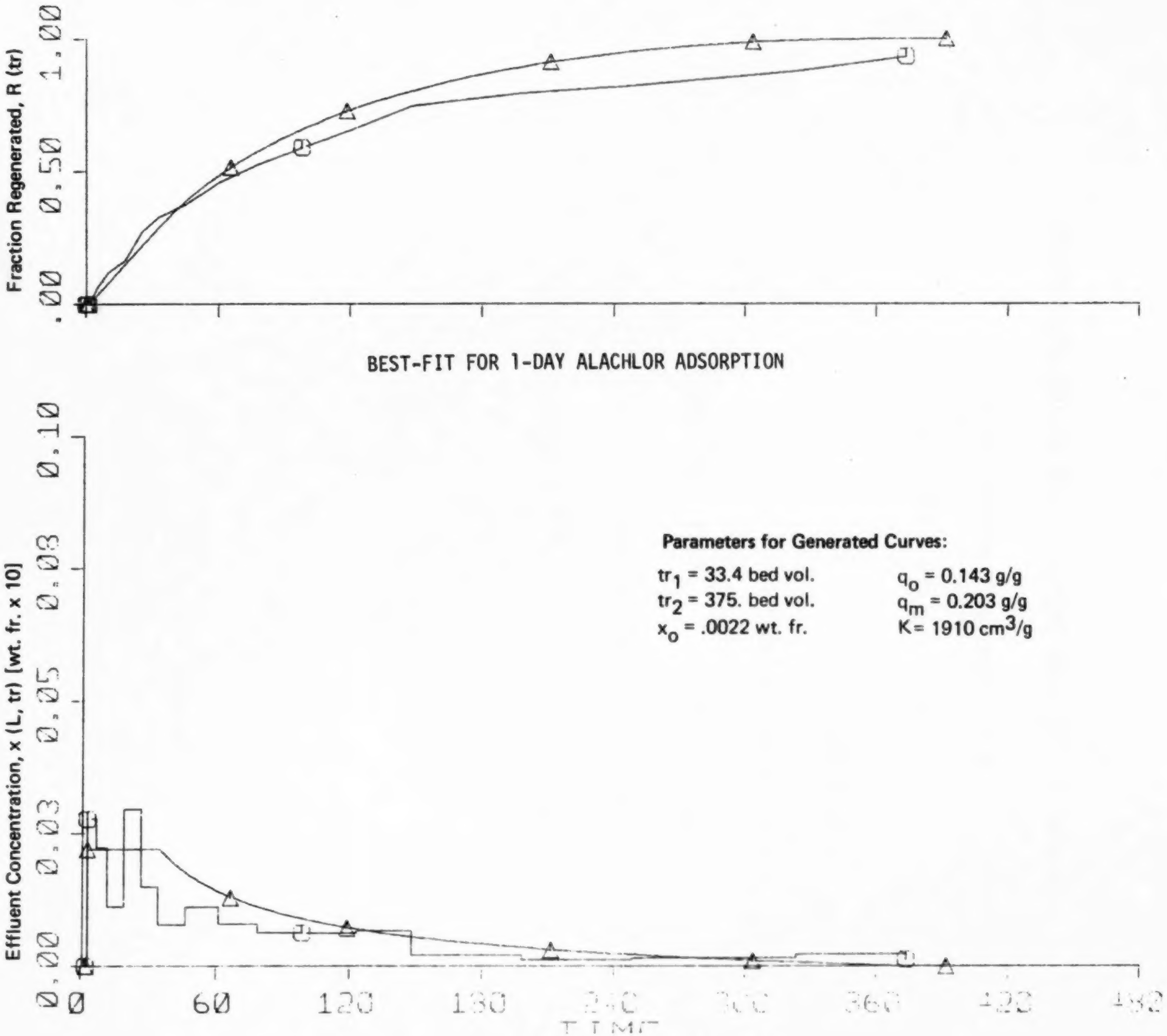
Fraction Regenerated, R (tr)
.00
0.50
1.00
BEST-FIT FOR 1-DAY ALACHLOR ADSORPTION
Effluent Concentration, x (L, tr) [wt. fr. x 10]
0.00
0.03
0.05
0.08
0.10
0
60
120
180
240
300
360
420
480
TIME
Reduced Time, tr (bed volumes)
Parameters for Generated Curves:
tr_1 = 33.4 bed vol.
tr_2 = 375. bed vol.
x_o = .0022 wt. fr.
q_o = 0.143 g/g
q_m = 0.203 g/g
K= 1910 cm^3/g

Figure A-9

APPENDIX B: PHYSICAL PROPERTIES AND DESIGN CALCULATIONS

B-1. Physical Properties of CO_2

55°C, 150 atm (2250 psia)

ρ_{CO_2} = 0.67 g/cm^3

D_f = 2.5×10^{-4} cm^2/S

μ = 5.1×10^{-4} (5.1×10^{-5} NS/m^2)

ν = $\mu/e = 7.61 \times 10^{-4}$ cm^2/sec

Sc = $\nu/D_f = 3.04$ $Sc^{2/3} = 2/10$

B-2. Properties of F-300 GAC

ρ_B (bulk density) = 0.437 g/cm^3

ε (void fraction) = 0.432

ρ_p (particle density) = 0.769 g/cm^3

ρ_c (true carbon density) = 2.18 g/cm^3

χ (void fraction within particle) = 0.647

d_p (particle diameter - an) = 0.10 cm
12 mesh - 0.141 cm
30 mesh = 0.055 cm

$$\varepsilon = \rho_B^{-1} - \rho_p^{-1} \rightarrow \rho_p = \rho_B/(1-\varepsilon)$$

$$\chi = \frac{\rho_p^{-1} - \rho_c^{-1}}{\rho_p^{-1}}$$

B-3. Operating Parameters
(desorption at 55°C, 2250 psia)

	7-g Columns	380 g Columns
L (length of charge-cm)	22.6	101.7
D (i.d., cm)	0.95	3.3
Ac.s. (cross-sectional area cm^2)	0.709	8.55
V_B (bed volume - cm^3)	16.02	869.6
CO_2 flow rate (SLM)	6	40
(g/s)	0.18	1.20
F (superficial volumetric flow rate at column conditions - cm^3/s)	0.27	1.79
U (superficial velocity F/Ac.s. - cm/S)	0.38	0.209

B-4. Adsorption Conditions

For 2500 ppm, take $q_o = 0.41$ g/g 1.5×10^{-3} mol/g

$C_o = (.0035)$ (g/g) (.67) g/cm^3 2.5×10^{-5} mol/cm^3

$$\Lambda = \frac{q_o \quad B}{o} = \frac{\left(1.5 \times 10^{-3} \frac{\text{mol P}}{\text{gGAC}}\right) \left(.437 \frac{\text{g GAC}}{\text{cm}^3 \text{bed}}\right)}{\left(2.5 \times 10^{-5} \frac{\text{mol P}}{\text{cm}^3 \text{ CO}_2}\right)}$$

$$\Lambda = 26.2 \frac{\text{cm}^3 \text{Fluid}}{\text{cm}^3 \text{Bed}}$$

B-5. Mass Transfer Coefficients; Pore Diffusion

(assumes no surface diffusion in pores)

$$\frac{1}{D_p} = \frac{\tau}{\chi} \quad \frac{1}{D_k} + \frac{1}{D_f}$$

$\tau \approx 4$

$$D_k = \frac{19{,}400}{Sg \quad p} \quad \frac{T}{M}$$

$\chi = 0.647$

$p = 0.769$

$Sg = 10^7\ cm^2/g$

$$D_k = \frac{(19400)(.647)}{(10^7)(.769)} \quad \frac{328.2}{94}$$

$T = 328.2°K$

$M = 94$

$$\boxed{D_k = 3.05 \times 10^{-3}\ cm^2/S}$$

$$\boxed{D_f = 2.5 \times 10^{-4}\ cm^2/S}$$

$$\frac{1}{D_p} = \frac{(4)}{(.647)} \left(\frac{1}{3.05 \times 10^{-3}} + \frac{1}{2.5 \times 10^{-4}}\right) = 2.676 \times 10^4$$

$$\frac{1}{D_p} = \left(\frac{4}{.647}\right) \left(\frac{1}{3.05 \times 10^{-3}} + \frac{1}{2.5 \times 10^{-4}}\right) = 2.676 \times 10^4$$

$$\boxed{D_p = 3.74 \times 10^{-5}\ cm^2/S}$$

$$k_p = \frac{16.7\ D_p}{dp}$$

$dp = 0.10\ cm$

$$k_p = \frac{(16.7)(3.74 \times 10^{-5})}{0.10}$$

$$\boxed{k_p = 6.24 \times 10^{-3}\ cm/S}$$

$$a_p = \frac{6(1- \ )}{dp} = \frac{6(1-.432)}{(.1)}$$

$$\boxed{a_p = 34.08\ \mathrm{cm}^2/\mathrm{cm}^3}$$

$$\boxed{k_p a_p = \mathrm{o}.213\ \mathrm{S}\text{-}1}$$

$$\left[\begin{array}{l}\text{Vermuelen-Perry's} \\ k_p a_p = \dfrac{60\ D_p}{d_p{}^2} = 0.230\ \mathrm{S}^{-1}\end{array}\right]$$

B-6. Mass Transfer; Film Coefficients

Film (External mass transfer)

a. 7g carbon columns, 6 SLM

$$Re = \frac{d_p U}{\nu} = 49.9$$

$U = 0.38$ cm/S

$d_p = 0.1$ cm

$\mu = 7.61 \times 10^{-4}$ cm^2/S

From Sherwood, et al., p. 243-4

$$j_p = 0.3$$

$$k_f = j_o \, U/(Sc)^{2/3}$$

$$= \frac{(.3)(.38)}{(2.10)}$$

$Sc = 3.04$

$(Sc)^{2/3} = 2.10$

$$\boxed{k_f = 5.43 \times 10^{-2} \text{ cm/S}}$$

From Sherwood, p. 583, Eq. (10.61)

$$\frac{1}{\kappa} = \frac{1}{b} \left(\frac{1}{k_f} + \frac{1}{\Lambda \, k_p} \right)$$

$$\Lambda = \frac{q_o \rho_\beta}{C_o} = 26.2$$

b ranges between 1 and 2.

$$\frac{1}{k_f} + \frac{1}{\Lambda k_p} = \frac{1}{5.43 \times 10^{-2}} + \frac{1}{(26.2)(6.24 \times 10^{-3})}$$

$$= 24.5$$

$$\therefore \boxed{4.08 \times 10^{-2} < \kappa < 8.14 \times 10^{-2}} \text{ cm/S}$$

$$\boxed{1.39 < \kappa\, \alpha < 2.77 \text{ S}^{-1}}$$

$$N = \frac{\kappa \alpha L}{U} = \frac{L}{U} (\kappa\alpha) = \frac{22.6}{0.38} (\kappa\alpha)$$

$$\boxed{82.7 < N < 165.}$$

7 g column

b. 380 g carbon column, 40 SLM

$$Re = \frac{d_p \mu}{\ } = \frac{(.1)(.209)}{7.61 \times 10^{-4}} \qquad \mu = .209 \text{ cm/S}$$

$$Re = 27.5$$

$$j_D = 0.4 - 0.5 \text{ (take 0.45)}$$

$$k_f = \frac{j_D \mu}{(Sc)^{2/3}} = \frac{(.45)(.209)}{2.10}$$

$$\boxed{k_f = 4.48 \times 10^{-2} \text{ cm/S}}$$

$$\frac{1}{k_f} + \frac{1}{\Lambda k_p} = \frac{1}{4.48 \times 10^{-2}} + \frac{1}{(26.2)(6.24 \times 10^{-3})}$$

$$= 28.44$$

$$\therefore \boxed{3.52 \times 10^{-2} < \kappa < 7.03 \times 10^{-2} \text{ cm/S}}$$

$$\boxed{1.20 < \kappa \, \alpha < 2.40 \ \text{S}^{-1}}$$

$$\frac{L}{\mu} = \frac{101.7}{.209} = 486.7$$

$$\boxed{584 < N < 1168} \quad \underline{\text{380 g column}}$$

c. Extrapolation to Higher Velocities (7 g column)

at 50 SLM, $\mu = 3.17$ cm/S

Re - 416

$j_D = 0.11$

$k_f = \frac{(0.11)(3.17)}{(2.10)} = 0.166$

$$\boxed{k_f = 0.166}$$

$$\frac{1}{k_f} + \frac{1}{\Lambda k_p} = \frac{1}{.166} + \frac{1}{(26.2)(6.24 \times 10^{-2})} = 12.14$$

$$\boxed{8.24 \times 10^{-2} < \chi < 16.48 \times 10^{-2}}$$

$$\boxed{2.81 < \chi\, \alpha < 5.62 \quad S^{-1}}$$

$$\frac{L}{\mu} = \frac{22.6}{3.17} = 7.13$$

$$\boxed{20.0 < N < 40.0}$$

B- 7. Pressure Drop in Packed Beds

(Perry's 4th Ed. pp. 5-50, 51)

$$\Delta p = \frac{2fm\ G^2 L\ (1 - \varepsilon)^{3-n}}{D_p G_c\ \rho\ \phi_s^{3-n}\ \varepsilon^3}$$

Δp lbs/ft^2

L ft

G_c 32.17 lb ft/lbs^2

Dp ft (particle diam)

ε (void fraction)

n defined by Fig. 5-64 = FCN_{Re}1 = GD_p/μ)

G lb/sft^2 (superficial mass velocity)

ρ lb/ft^3 (fluid density)

fm (friction factor) defined by Fig. 5-64 - fCN_{Re}1)

ϕ_s shape factor - .70 (.73 for pulverized coal dust)
(.65 for crushed glass)

Variables: L, μ

$\varepsilon = .432$

$Dp = dp = 0.10\ cm = 3.281 \times 10^{-3}$ ft.

$\rho =_\mu \rho_{co_2} = 0.67\ g/cm^3 = 41.81\ lb/ft^3$

$$G = \rho_{CO_2}^{.67} \left(\frac{g}{cm^2 S}\right) \times \frac{lb}{454\ g} \times (30.48)^2\ \frac{cm^2}{ft^2} = 1.371\ {*}\mu)$$ where μ in cm/S

$$\Delta P = \frac{fm(2)(1.371)^2 \mu^2 L\ (1-.432)^{3-n}}{(3.281 \times 10^{-3})(32.17)(41.81)(.7)^{3-n}\ (.432)^3}$$

$\Delta p = fm\mu^2 L\ (.811)^{3-n}\ (10.566)$

(μ in cm/S)
(L in ft.)
ΔP in lb/ft^2

CASE A

$\mu = 8$, $L = 8.6$

$Re = 1048$

$\eta = 1.93$

$f_m = 0.7$

$$\Delta P = (.7)(8)^2(8.6)(.811)^{3-1.93}(10.566)\ \frac{16}{ft^2} \times \frac{ft^2}{144\ in^2} \times \frac{in^2\ atm}{14.69\ lb}$$

$\Delta P = 1.54$ atm

$\mu = 7$, $L = 8.6$

$Re = 917$

$\eta = 1.93$

$f_m = .7$

$$\Delta P = 1.54\ \frac{(7)^2}{(8)}$$

$\Delta P = 1.18$ atm

$\mu = 6.5$, $L = 8.6$

$Re = 851$

$\eta = 1.92$

$f_m = .7$

$$\Delta P = (1.18)\frac{(6.5)^2}{(7)}$$

$\Delta P = 1.02$ atm

CASE B

$\mu = 25$, L - 28.0

$Re = 3275$

$\eta = 1.98$

$f_m = .7$

$\Delta P = (.7)(25)^2(28.0)(.811)^{3-1.98}(10.566)(4.727 \times 10^{-4})$

$\Delta P = 49.4$ atm

$\mu = 23$

$\Delta P = (49.4)\frac{(23)^2}{(25)} =$

$\Delta P = 4.8$ atm

$\mu = 20$

$Re = 2{,}620$

$\eta = 1.97$

$f_m = .7$

$\Delta P = (41.8)\frac{(20)^2}{(23)} =$

$\Delta P = 31.6$ atm

CASE C

$\mu = 21, L = 46.5$

$Re = 2751$

$\eta = 1.98$

$f_m = .7$

$$\Delta P = (49.4)\frac{(21)^2}{(25)}\frac{(46.5)}{(28.0)} =$$

$\Delta P = 57.9$ atm

$\mu = 20$

$$\Delta P = (31.6)\frac{(46.5)}{(28.0)} =$$

$\Delta P = 52.5$ atm

B-8. Analysis of Breakthrough Curve (380 g Col)

P1 & P2 - 48

$$T \equiv \frac{\mu C_o \hat{t}}{q_o \rho_\beta L} = \frac{\mu \hat{t}}{L\Lambda}$$

$\mu = .209$ cm/S

$L = 101.7$ cm

$\Lambda = 26.2$

$\varepsilon = .432$

$$\hat{t} = t - \frac{L\varepsilon}{\mu} = t = \frac{(101.7)(.432)}{(.209)}$$

$$\boxed{\hat{t} = t - 21.0 \text{ S}}$$

$$T = \frac{(.209)\hat{t}}{(101.7)(26.2)} = 7{:}844 \times 10^{-5}\hat{t}$$

$$\boxed{T = 7.844 \times 10^{-5} (t - 21) \text{ S}}$$

$X \equiv 1 - \frac{c}{C_o}$ where c in mol/cm^3

$X = 1 - \frac{x}{X_o}$ where x in wt fraction